The assessment of flood mitigation measures applied in Cartagena de Indias

A case study approach about investigating types of flood mitigation measures in Cartagena de Indias

Msc Thesis

Gerwin van de Wakker

Delft University of Technology

The assessment of flood mitigation measures applied in Cartagena de Indias

A case study approach about investigating types of flood mitigation measures in Cartagena de Indias

by

Gerwin van de Wakker

G. van de Wakker	
Gerwin	4483529

Instructor TU Delft:	Prof. Dr. Ir. M. Kok, Dr. Ir. G.H.W. Schoups [CEG]
Supervisors Arcadis:	Ir. M. Onderwater, Msc. J. Klooster
Project Duration:	April 2023 - March 2024
Faculty:	Faculty of Civil Engineering and Geosciences, Delft

Cover:
http://tinyurl.com/47z4en93
Style: TU Delft Report Style, with modifications by Gerwin van de Wakker

Preface

Over the past eleven months, I had the privilege to work on my thesis as part of the Water as Leverage Cartagena project at Arcadis. Engaging in this ongoing project provided me with valuable insights into the multifaceted work of an engineering agency. Moreover, the entire graduation process trained me with the skills to guide complicated numerical models and manage limited data availability. This research also allowed me to combine various aspects of my master's degree. Despite its educational value, I must admit that at times, deciphering certain concepts of the graduation process proved to be quite challenging. Thus, I am deeply grateful to the people who supported me throughout this journey.

First and foremost, I extend my sincere appreciation to the members of the graduation committee: Prof. Dr. Ir. M. Kok, along with Dr. Ir. G.H.W. Schoups, Ir. M. Onderwater, and Msc. J. Klooster. Their positive and constructive feedback during the meetings was instrumental in shaping my work, and their encouragement made the expression of my findings a smoother process.

I am particularly obliged to Martijn Onderwater for our weekly brainstorming sessions. Your guidance not only helped me in resolving challenges in modelling but also in structuring my report efficiently and refining my written content. Working with you was a truly rewarding experience.

I also wish to express my gratitude to my fellow graduate interns at Arcadis for their valuable perspectives on the graduation process.

Secondly, I am immensely grateful to my family, partner and friends for their unwavering support during the inevitable ups and downs of this last phase of my master's degree. A special mention goes to Maud, whose endless encouragement sustained me throughout.

With the completion of my thesis, I finished my master's degree in Civil Engineering and say farewell to nine enriching years of academic pursuit. As I embark on a new chapter, I reflect upon the deep impact of these experiences and I am very excited to start a new chapter in my life.

Gerwin van de Wakker
Delft, March 2024

Summary

Urban areas of coastal cities are increasingly susceptible to the consequences of climate change. In particular, the threat of increasing floods due to sea level rise and heavier rainfall is growing. Cartagena de Indias in Colombia is such a coastal city, where flooding is a significant issue, with floods becoming more frequent in recent decades. Arcadis, together with the ConAgua consortium, is currently investigating and designing mitigation strategies for the city's water-related issues. The thesis focuses on defining and quantifying the sources of urban flood problems and assessing the impact of potential mitigation measures for reducing these flooding problems.

The study consists of four parts:

1. Identifying the main causes of floods using a data analysis;
2. Quantifying these findings with a numerical D-Hydro model;
3. Investigating suitable kind of mitigation measures and quantifying the impact of the best feasible mitigation options;
4. Evaluating the investigated mitigation options based on several criteria with the help of a multi-criteria analysis.

Parts 1 and 2 focus on understanding the system. Parts 3 and 4 of the study focus on finding the best option to reduce floods.

The data analysis allows the development of a system description identifying the main causes of flooding. The analysis reveals that the limited capacity of the drainage system, high topographic variations, and extreme rainfall are the main causes of flooding in Cartagena. Extreme rainfall flows quickly from steep upstream areas to milder slope lower-lying areas, particularly those at the edge of the Ciénaga de la Virgen. It is hypothesised that downstream water level plays a role in the accumulation of runoff water, thereby influencing the frequency and intensity of floods in the neighbourhoods at the southern edge of the Ciénaga de la Virgen, especially with a relative sea level increase of approximately half a meter factored in. This hypothesis is checked by quantifying the impact of different scenarios with a numerical model.

A numerical D-Hydro model is used to quantify the impact of different meteorological conditions and downstream water levels on floods. The model's simulation results show that rainfall intensity is a more dominant factor in flood generation than downstream water levels. Even with a return period of two years, rainfall causes significant flooding of almost 25% in the study area. The model also indicates an increasing influence of tidal conditions due to relative sea level rise. Still, the increased influence is mainly visible in the borders of the Ciénaga de la Virgen with minimal residential impact. These conclusions highlight the need for mitigation efforts to focus primarily on improving the areas influenced by the rainfall, especially for short return period rainfall events.

Various flood mitigation measures are considered for the southern border of the Ciénaga de la Virgen to reduce floods caused by the dominant intense rainfall. Wetland creation and evaporation measures are ruled out due to the dominant influence of rainfall-induced floods and the inability to prevent floods caused by extreme rainfall events respectively. After investigating the scale required, considering feasibility, the three types of measures that are converted into mitigation options are:

- Mitigation Option 1: Increasing channel dimensions,
- Mitigation Option 2: Increasing infiltration,
- Mitigation Option 3: Constructing retention areas.

These mitigation options are assessed for their impact on reducing flooded areas and flood levels.

The three mitigation options are evaluated to recommend the best-preferred mitigation design. This evaluation employs a Multi-Criteria Analysis (MCA). The analysis integrates various criteria and scores these criteria on a predetermined scale from 1 to 5. The MCA concludes that Mitigation Option 1 is the most effective and resilient. This Mitigation Option 1 demonstrates superior technical performance and robustness to future scenarios. The construction costs of Mitigation Option 2 are estimated at around 550 million dollars (compared to 10.5 and 6.5 million dollars for Mitigation Options 1 and 3 respectively). Therefore, it is concluded that Mitigating Option 2 is unfeasible. Mitigation Option 3 does not perform well under a 100-year rainfall, but this mitigation option is easily adaptable and the costs are relatively low. Therefore, Mitigation Option 3 outperforms Mitigation Option 2 considering the ultimate MCA scores. The conclusion of the MCA evaluation ultimately results in the recommendation to extend the channels (Mitigation Option 1) and construct the western retention area (partly Mitigation Option 3). The western retention area reduces flooding in parts of the city that the extension of the channels would be unable to.

In response to pressing flooding issues of coastal cities, the approach taken in the case study of Cartagena de Indias, which conducts comprehensive data analyses, quantifies by integrating numerical modelling and utilizes a multi-criteria decision-making tool to develop and investigate functional flood mitigation options that are best preferred, shows effectiveness in establishing the right types of mitigation options for further development.

Contents

Preface i

Summary ii

1 Introduction 1
- 1.1 Background . . . 1
- 1.2 Case Study: Water-related issues in Cartagena de Indias . . . 2
- 1.3 Problem definition . . . 6
- 1.4 Knowledge gap . . . 7
- 1.5 Research goal and objectives . . . 7
- 1.6 Research questions . . . 7
- 1.7 Report structure . . . 8

2 Methodology 9
- 2.1 Data Analysis . . . 9
- 2.2 Modelling Study . . . 9
- 2.3 Investigating possible types of mitigation measures and developing mitigation options . 10
- 2.4 Multi-criteria evaluation of the Mitigation Options . . . 11

3 Data Analysis 12
- 3.1 Study area . . . 12
- 3.2 Available data . . . 13
  - 3.2.1 Channel dimensions . . . 13
  - 3.2.2 Topographic elevation maps . . . 14
  - 3.2.3 Meteorological data . . . 15
  - 3.2.4 Tidal water level . . . 21
  - 3.2.5 Recorded flooding events . . . 24
  - 3.2.6 Relative sea level rise (RSLR) . . . 26
  - 3.2.7 Coastal erosion . . . 26
- 3.3 Data gap analysis . . . 27
- 3.4 System description based on available data . . . 28
- 3.5 Conclusion . . . 29

4 Modelling Study 30
- 4.1 Introduction . . . 30
  - 4.1.1 Model choice . . . 30
  - 4.1.2 D-Hydro . . . 30
- 4.2 Model set-up . . . 33
  - 4.2.1 Computational grids . . . 33
  - 4.2.2 Dimensions and bed levels . . . 34
  - 4.2.3 Hydraulic boundary conditions . . . 37
  - 4.2.4 Schematisation of the model . . . 38
  - 4.2.5 Validation of the model . . . 39
  - 4.2.6 Model-based Assumptions . . . 42
- 4.3 Quantification of Flood Impact . . . 42
  - 4.3.1 Input scenarios . . . 43
  - 4.3.2 Zones of influence for existing situation . . . 44
  - 4.3.3 Future scenarios . . . 50
- 4.4 Conclusion . . . 57

5 Investigating possible types of mitigation measures and developing mitigation options 58
5.1 Introduction . . . 58
5.1.1 Focus zone . . . 58
5.2 Potential types of mitigation measures . . . 59
5.3 Model improvements to assess the technical impact of the mitigation measures . . . 60
5.4 Impact of mitigation measures on flooding . . . 65
5.5 Conclusion . . . 78

6 Multi-criteria evaluation of the Mitigation Options 80
6.1 Set up MCA . . . 80
6.2 Evaluation of criteria . . . 83
6.2.1 Scoring Explanation . . . 83
6.3 Best preferred mitigation option . . . 89
6.3.1 The categories weights . . . 89
6.3.2 Total score . . . 90
6.3.3 Discussion results MCA . . . 90
6.4 Conclusion . . . 91

7 Discussion 92

8 Conclusion 96

9 Recommendations 99
9.1 Recommendations for improving system understanding and quality of model input . . . 99
9.2 Recommendation for the next phase in the project . . . 99
9.2.1 Improvements to the D-Hydro model . . . 100
9.2.2 Further assessment of mitigation options . . . 100
9.2.3 Recommendations regarding public awareness . . . 100

References 102

A Channel dimensions 106
A.1 Channel names . . . 106
A.2 Dimensions per section . . . 107

B Rainfall analysis 109
B.1 Extreme value analysis . . . 109
B.2 Rainfall distribution . . . 116
B.3 Rainfall sequences . . . 118

C Determining of tidal water levels 119
C.1 Santa Marta . . . 119
C.2 14 November 2020 water level . . . 121
C.3 Water level input scenarios . . . 121

D Criteria ConAgua consortium 123

E Mitigation results 125
E.1 Increasing the channel dimensions . . . 125
E.1.1 10 percent channel increase . . . 125
E.1.2 20 percent channel increase . . . 127
E.1.3 30 percent channel increase . . . 128
E.1.4 50 percent channel increase . . . 129
E.1.5 100 percent channel increase . . . 130
E.1.6 200 percent channel increase . . . 131
E.2 Increase the infiltration . . . 132
E.2.1 10 percent infiltration increase . . . 132
E.2.2 20 percent infiltration increase . . . 133
E.2.3 30 percent infiltration increase . . . 134
E.2.4 40 percent infiltration increase . . . 135
E.2.5 50 percent infiltration increase . . . 136

E.3 Establishing retention areas 137
E.3.1 Retention areas 2-meter depth 137
E.3.2 Retention areas 4-meter depth 138
E.3.3 Retention areas 6-meter depth 139
E.3.4 Retention areas 8-meter depth 140

F Future proof scenarios 142
F.1 Extreme rainfall event R=100 years 142
F.1.1 Baseline R=100 142
F.1.2 Mitigating Option 1 R=100 143
F.1.3 Mitigating Option 2 R=100 145
F.1.4 Mitigating Option 3 R=100 146
F.2 Relative sea level rise 148
F.2.1 Baseline Relative Sea Level Rise 148
F.2.2 Mitigating Option 1 RSLR 149
F.2.3 Mitigating Option 2 RSLR 151
F.2.4 Mitigating Option 3 RSLR 152

G Cost estimation 155
G.1 Mitigating Option 1: Extension of the channels 155
G.2 Mitigating Option 2: Increasing infiltration 156
G.3 Mitigating Option 3: Retention areas 156

List of Figures

1.1 Water-related hotspots of Cartagena (Arcadis, 2022). 1) Ciénaga de la Virgen, 2) Drainage channels, 3) Cartgena bay and 4) Coastal seafront. 2
1.2 Population Growth Graph of Cartagena (United Nations Department of Economical and Socaial Affairs, 2018) 3
1.3 The southern border of Ciénaga de la Virgen has witnessed significant urban expansions over the last 37 years (Google Earth, 2023). 4
1.4 Urbanization over the last years. Blue is in 1985, purple after 2005, red after 2015, and orange is the current situation (Google Earth, 2023) 5
1.5 Percentages of disturbances due to named issues (1932-2020) (Bello et al., 2021) . . . 5

3.1 The study area is divided into three zones 12
3.2 The drainage channels of the study area 14
3.3 The used elevation map (resolution size 2x2 m) 15
3.4 The location of the rainfall station in the city (ESCUELA NAVAL CIOH) (IDEAM, 2023) . 16
3.5 The comparison of the different data sets obtained from IDEAM (2023) 16
3.6 Cumulative annual rainfall 1950-2022 17
3.7 The rolling mean for the yearly data set 18
3.8 Cumulative monthly rainfall 1950-2022 19
3.9 The uncertainty of the Weibull and Generalized Pareto distributions using bootstrapping. 20
3.10 The measured water level in Santa Marta on the fourteenth of November 2020 compared with the tidal predictor to observe the phase difference. 22
3.11 The measured water level in Santa Marta in November 2020 compared with the tidal predictor outcome using the tidal constituents measured in Santa Marta. 22
3.12 Water level for a year predicted with the tide predictor software Delft3D 23
3.13 Channel Once de Noviembre 24
3.14 A picture of waste in the channel 24
3.15 Water depths for point in the Edurbe community report and the flooded neighbourhoods during hurricane Iota 25
3.16 a) Boca Grande is seen in the circle. b) Flood map results for a high tide and a wave height of 3 m (Orejarena-Rondon et al., 2019). 26
3.17 Risk on coastal erosion in Cartagena (MIDAS, 2019) 27

4.1 The block scheme of the modelling study. The orange block indicates the input used in the modelling. The black framed box indicates the steps and processes within the modelling study. 32
4.2 Computational grids more in detail. 34
4.3 The 1D channel grid shown overlaid a map of Cartagena. The cross-sections are shown in red 34
4.4 Data for determining catchment areas 35
4.5 The D-Hydro interface including the determined (paved) catchment areas 36
4.6 Interpolated bed level of the grid with relation to sea level. 37
4.7 The line where the water level boundary conditions are imposed. 38
4.8 The schematisation of the D-Hydro model. 39
4.9 The flood map result of the D-Hydro model using the input of the Edurbe study with its validation points. 40
4.10 Flood map when simulating 14-11-2020 with the D-Hydro model. 41
4.11 The input for the scenarios with the tidal water level and cumulative rainfall distribution . 44

4.12 (**a-c**) Rainfall intensity with a return period of 2 years, (**d-f**) Rainfall intensity with a return period of 10 years, (**g-i**) Rainfall intensity with a return period of 100 years. (**Left column**) Extreme low tide, (**Middle column**) Tidal sequence, (**Right column**) Extreme high tide 45
4.13 The influence of the different imposed water levels for every rainfall return period. Green: Extreme low tide, yellow: Tidal sequence, Red: Extreme high tide 46
4.14 The influence of the different imposed water levels including relative sea level rise for every rainfall return period. 47
4.15 The difference in flood levels for extremely high water level and a extremely low water level. The rainfall intensity in this case has a return period of 2 years. 48
4.16 The influence of the different rainfall intensities on the same water level 49
4.17 The different flooding zones of influence. Light blue is the hydraulogical zone which is dependent on the rainfall. Navy blue indicates the tidal zone. 50
4.18 The input for the scenarios including relative sea level rise with the cumulative rainfall distribution 51
4.19 (**a-c**) Rainfall intensity with a return period of 2 years, (**d-f**) Rainfall intensity with a return period of 10 years, (**g-i**) Rainfall intensity with a return period of 100 years. (**Left column**) Extreme low tide + RSLR, (**Middle column**) Tidal sequence + RSLR, (**Right column**) Extreme high tide + RSLR 52
4.20 The influence of the different imposed water levels for every rainfall return period with relative sea level rise in the equation. Green: Extreme low tide, yellow: Tidal sequence, Red: Extreme high tide 53
4.21 The influence of the different imposed water levels including relative sea level rise for every rainfall return period 54
4.22 The difference in flood levels for extremely high water level and extremely low water level in a scenario with a relative sea level rise. The rainfall intensity in this case has a return period of 100 years 55
4.23 The shift in zones of influence. Light blue is the hydraulic zone which is dependent on the rainfall. Navy blue indicates the current tidal zone. Red indicates the increased tidal zone due to relative sea level rise. 56

5.1 The focus area for imposing mitigation measures is subdivided into three zones. 59
5.2 The part of the grid that remains after optimization (red grid) 61
5.3 The difference in grids 62
5.4 The difference between the overall (black field) and the detailed model (red field). 63
5.5 The validation points from the Edurbe community interview 63
5.6 flooded neighbourhoods compared with D-Hydro model including the changes 64
5.7 The baseline of the detailed model used to determine the impact of the mitigation measures 65
5.8 A visual representation of the normative assessment with Google Street View. 68
5.9 The comparison in flood map for the capacity option. The red area is the baseline flood map and the yellow indicates flood for Mitigation Option 1. 69
5.10 The reduced flood levels due to the option of the increased channel dimension. The redder the dots, the greater the reduction in flood levels. 70
5.11 The schematisation of spreading out peak rate by introducing a delay time. 72
5.12 The roads considered for potential modification to permeable surfaces 72
5.13 The comparison in flood map for increasing the infiltration with 20% and introducing a delay time of 30 minutes. The red area is the baseline flood map and the blue indicates flood according to Mitigation Option 2. 73
5.14 The reduced flood levels due to Mitigation Option 2 with a 20% infiltration increase and introducing a delay time of 30 minutes. How redder the dots, how greater the reduction of flood levels. 74
5.15 The indication of areas that will have the highest impact when constructing a retention area. 75
5.16 The two constructed retention areas 76
5.17 The comparison in the flood map for the construction of two retention areas, where the western area has a depth of 4 meters and the eastern area has a depth of 2 meters. The red area is the baseline flood map and the purple area is the flood for Mitigation Option 3. 77

5.18 The reduced flood levels due to Mitigation Option 3. How redder the dots, how greater the reduction of flood levels. 78

6.1 The response to the flooding due to the induced delay time. It creates more evacuation time. 87
6.2 The adjustment to the best preferred mitigation option. The addition of the western retention area will resolve locally for this area. 91

7.1 The overall water system of Cartagena with the points of interest in this research. 95

A.1 1) Canal Bolivar, 2) Canal Maria Auxiliadora,3) Canal San Pablo, 4) Canal Barcelona, 5) Canal Amardor Y Cortes,6) Canal San Martin,7) Canal Libano, 8)Salim Bechara, 9) Tabu, 10) Canal Villa, 11) Canal Papa Negro, 12) Canal Once de Noviembre, 13) Canal El Tigre, 14) Canal Ricaurte, 14a) Chepa + Ricaurte, 14b) Chiquinquirá, 14c) Las Gaviotas, 14d) Bias de Lazo, 14e) San Pedro, 15 Canal Maravilla, 16 Canal Playa Blanca, 17 Canal Arroyo Matute, 17a) Chapundun, 17b) Magdalena, 17c) Matute k3+800–k5+240, 17d) Canal simon Bolivar, 18) Canales de la Cuenca de Arroyo Fredonia, 18a) Calicanto Viejo, 18b) Ciudad Sevilla, 19) Arroyo Tomatal (Límon), 19a) Calicanto, 19b) Canal Limón, 19c) Canal La Carolina, 19d) Isla del León, 19e) San José de los Campanos, 20) Arroyo Chiamaría, 20a) Chiamaria, 20b) Flor de Campo, 20c) Canal Hormiga 106

B.1 The daily data plotted over time with the peaks and threshold (2009-2022) 109
B.2 Histogram of peaks with the different distribution fitted 110
B.3 Data point VS Q 111
B.4 The fitting of the inverse exponential distribution. γ=42.6 and β=31.1 112
B.5 The fitting of the inverse Weibull distribution. γ=42.6 and β=27.7 with α=0.92 112
B.6 The fitting of the inverse Gumbel distribution. γ=60.1 and β=23.4 113
B.7 The fitting of the inverse Generalized Pareto distribution. γ=43.9 and β=28.3 with α=0.05 114
B.8 The daily precipitation rates vs return periods for each distribution. 114
B.9 The uncertainty of the Weibull and GP distributions using bootstrapping. 115

C.1 The location of the Santa Marta water level station. (EPSG:3116[8634826.4,1031199.1: -8087663.7,1349183.7]) 119
C.2 The unfiltered dataset 120
C.3 The cleaned data set 120
C.4 Water level measured in Santa Marta for the whole data set (University of Hawaii Sea Level Center, 2023) 120
C.5 The hurricane track of hurricane Iota (National Oceanic and Atmospheric Administration, 2023). The red circle indicates where Cartagena is located. 121
C.6 The water level on the 14th of November 2020 when Tropical Storm Iota was offshore Cartagena 121
C.7 The tidal sequence used in the input scenarios 122

E.1 The decrease in a flooded area with after the increase of 10 % channel width and height. 126
E.2 The flood level reduction with after the increase of 10 % channel width and height. . . . 126
E.3 The reduction in flooded area after the increase of 20 % channel width and height. . . . 127
E.4 The flood level reduction with after the increase of 20 % channel width and height. . . . 128
E.5 The reduction flooded area with after the increase of 30 % channel width and height. . . 128
E.6 The flood level reduction with after the increase of 30 % channel width and height. . . . 129
E.7 The reduction in flooded area with after the increase of 50 % channel width and height. 129
E.8 The flood level reduction with after the increase of 50 % channel width and height. . . . 130
E.9 The reduction in flooded area with after the increase of 100 % channel width and height. 130
E.10 The flood level reduction after the increase of 100 % channel width and height. 131
E.11 The reduction in flooded area after the increase of 200 % channel width and height. . . 131
E.12 The flood level reduction after the increase of 200 % channel width and height. 132
E.13 The reduction in flooded area after the increase of 10 % of infiltration. 132
E.14 The flood level reduction after the increase of 10 % of infiltration. 133

E.15 The reduction in flooded area after the increase of 20 % of infiltration. 133
E.16 The flood level reduction after the increase of 20 % of infiltration. 134
E.17 The reduction in flooded area after the increase of 30 % of infiltration. 134
E.18 The flood level reduction after the increase of 30 % of infiltration. 135
E.19 The reduction in flooded area after the increase of 40 % of infiltration. 135
E.20 The flood level reduction after the increase of 40 % of infiltration. 136
E.21 The reduction in flooded area after the increase of 50 % of infiltration. 136
E.22 The flood level reduction after the increase of 50 % of infiltration. 137
E.23 The reduction in flooded area after the retention areas with a 2-meter depth 138
E.24 The flood level reduction after the establishment of two retention areas with a 2-meter depth. 138
E.25 The reduction in flooded area after the retention areas with a 4-meter depth 139
E.26 The flood level reduction after the establishment of two retention areas with a 4-meter depth. 139
E.27 The reduction in flooded area after the retention areas with a 6-meter depth 140
E.28 The flood level reduction after the establishment of two retention areas with a 6-meter depth. 140
E.29 The reduction in flooded area after the retention areas with an 8-meter depth 141
E.30 The flood level reduction after the establishment of two retention areas with a 8-meter depth. 141

F.1 The base flood map for an extreme rainfall R=100 years 142
F.2 The increase in flood levels (above 1 mm difference) due to the change of rainfall intensity from R=2 Y to R=100 Y. 143
F.3 The flood map for Mitigating Option 1 under an extreme rainfall (R=100 years) 144
F.4 The reduced flood levels due to Mitigating Option 1 for an extreme rainfall R=100 years 144
F.5 The flood map for Mitigating Option 2 under an extreme rainfall (R=100 years) 145
F.6 The reduced flood levels due to Mitigating Option 2 for an extreme rainfall R=100 years 146
F.7 The flood map for Mitigating Option 3 under an extreme rainfall (R=100 years) 147
F.8 The reduced flood levels due to Mitigating Option 3 for an extreme rainfall R=100 years 147
F.9 The base flood map with an imposed relative sea level rise. 148
F.10 The increase in flood levels (above 1 mm difference) due to the induced RSLR. 149
F.11 The flood map for Mitigating Option 1 with a relative sea level rise imposed. 150
F.12 The reduced flood levels due to Mitigating Option 1 with relative sea level rise imposed 150
F.13 The flood map for Mitigating Option 2 with a relative sea level rise imposed. 151
F.14 The reduced flood levels due to Mitigating Option 2 with relative sea level rise imposed. 152
F.15 The flood map for Mitigating Option 3 with a relative sea level rise imposed. 153
F.16 The reduced flood levels due to Mitigating Option 3 with relative sea level rise imposed. 153

G.1 The calculation of the construction costs for Mitigating Option 1. 155
G.2 The calculation of the costs for Mitigating Option 2 156
G.4 The costs recorded from a calculation of Northen Arizona University () 157
G.3 The calculation of the costs for the retention area design 157

List of Tables

2.1 List of to-be-analysed data 9
2.2 The investigated scenarios to determine the zones of influence 10

3.1 The return values for the Generalized Pareto distribution with the 90% confidence interval after bootstrapping 20
3.2 The return values for the Weibull with the 90% confidence interval after bootstrapping . 20
3.3 A summary of the hourly rainfall distribution of 70% of recorded events (EDURBE, 2022). 21
3.4 The observed tidal constituents for the Santa Marta Bay (Latandret-Solana et al., 2023) 21
3.5 The observed tidal constituents for the Cartagena port (Latandret-Solana et al., 2023) . 23
3.6 Extreme tidal water levels from a year simulation with the tidal predictor. 24
3.7 The water depth per point found with conducting a community interview by Edurbe. . . . 25

4.1 The corresponding size of the catchment areas (Edurbe, 2022). 35
4.2 The imposed conditions to validate the model. 39
4.3 Comparison between the found water depth from the community interview by Edurbe and the output of the D-Hydro model. 40
4.4 The input scenarios for the D-Hydro model determining the different flood zones. 43
4.5 The corresponding percentages (%) of flooded areas for each scenario. 45
4.6 The corresponding percentages (%) of flooded areas for each scenario. 52

5.1 Comparison between the found water depth from the community interview by Edurbe and the computational results of the customized D-Hydro model. model 64
5.2 The computational results for the evaluated baseline scenario. These results consist of flooded area in (m^2 and %) and average flood level. 65
5.3 The computational results increase the channels. The reduction is expressed in flooded areas and the reduction in average flood level. 66
5.4 The categorization of the channels. The possible increase is investigated with Google Street View.*Tabu is deepened as was possible due to the height difference. **No information is found with Google Street View so 100% retained. The channels are ordered from west to east. 67
5.5 The calculated performance of Mitigation Option 1 where the channels are increased. The reduction is expressed in flooded areas and reduction in average flood levels . . . 70
5.6 The calculated performance by increasing the infiltration in the area. The reduction is expressed in flooded areas and the reduction in average flood level. 71
5.7 The calculated performance of the option where the infiltration is increased. The reduction is expressed in flooded areas and the reduction in average flood level. 74
5.8 The computational results by constructing two retention areas with different depths. The reduction is expressed in flooded areas and the reduction in average flood level. 75
5.9 The calculated performance when constructing two retention areas. The reduction is expressed in flooded areas and the reduction in average flood level. 78

6.1 The computational results for the options regarding the technical aspects. This computational output consists of the flooded area in (m^2 and %) and an average reduced flood level. *Average flood level 84
6.2 The weights and scores for each criterion per specific option. 84
6.3 The scores explanations given to the different mitigation options regarding technical aspects. 84

6.4 The computational result for the scenarios using extreme rainfall with a return period of 100 years. These computational results consist of flooded areas in (m^2 and $\%$) and average flood level. *This is the average flood level . . . 85
6.5 The weights and scores for the future proof criteria for a R= 100. . . . 85
6.6 The scores explanations given to the different mitigation options regarding a future-proof scenario of R=100. . . . 85
6.7 The result for the scenarios using relative sea level rise of 47 cm. This output consists of the flooded area in (m^2 and $\%$) and the average reduced flood level. *This is the average flood level . . . 85
6.8 The weights and scores for each criterion per specific option. . . . 85
6.9 The scores explanations that are given to the different mitigation options regarding a future proof scenario of RSLR. . . . 86
6.10 The weights and scores regarding the adaptivity . . . 86
6.11 The scores explanations given to the different mitigation options regarding the adaptivity. 86
6.12 The weights and scores regarding the socio-economic aspect. . . . 87
6.13 The scores explanations given to the different mitigation options regarding the socio-economical aspects. . . . 87
6.14 The weights and scores regarding the costs. . . . 88
6.15 The scores explanations given to the different mitigation options regarding the financial aspects. . . . 88
6.16 The weights and scores regarding the environmental aspects. . . . 88
6.17 The scores explanations given to the different mitigation options regarding the environmental aspects. . . . 89
6.18 The weights of the different categories and the motivation behind these weights. . . . 90
6.19 The performance of the mitigation options in the MCA. The retention area is receiving the highest overall score but the scores are close. . . . 90

A.1 The dimensions of the channels per section. Section indicates the start of the new section (upstream); h= height of cross-section in meters; B= width at the bed level of the cross-section in meters; shift=upwards shift of the cross-section in meters; Btop= width at the top of the cross-section in meters. . . . 108

B.1 Sorted data . . . 110
B.2 Precipitation values [mm/day] per return period for each distribution. . . . 114
B.3 The return values for the GPD with the 90$\%$ confidence interval after bootstrapping . . . 116
B.4 The return values for the Weibull with the 90$\%$ confidence interval after bootstrapping . 116
B.5 The distribution versus the duration of high-intensity rain events (EDURBE, 2022) . . . 117
B.6 Rainfall distributions for the input for the numerical model. . . . 118

F.1 The computational results for the baseline scenario for a R=100 . . . 143
F.2 The computational result for Mitigating Option 1 for a scenario with a R=100. . . . 145
F.3 The computational result for Mitigating Option 2 for a scenario with a R=100. . . . 146
F.4 The computational result for Mitigating Option 3 for a scenario with a R=100. . . . 148
F.5 The computational results for the baseline with a relative sea level rise imposed. . . . 149
F.6 The computational result for Mitigating Option 1 with a relative sea level rise imposed. . 151
F.7 The computational result for Mitigating Option 2 with a relative sea level rise imposed. . 152
F.8 The computational result for Mitigating Option 3 with a relative sea level rise imposed. . 154

List of Abbreviations

D-RR D-Rainfall Runoff. 31

GPD Generalized Pareto Distribution. 113
GUI Graphical User Interface. 33

MCA Multi-Criteria Analysis. 11, 58, 80
MCDM Multi-Criteria Decision Making. 11

RMSE Root Mean Square Error. 19, 115
RSLR Relative Sea Level Rise. 6

SUDS Sustainable Urban Drainage Systems. 60

1
Introduction

1.1. Background

Coastal cities around the world are wrestling with challenges that revolve around water, their livelihood and their vulnerability. 50 % of the population lives in a city located within 100 km of a coastline (Barragán & de Andrés, 2015). The significant threat of rising sea levels and more frequent extreme rainfall casts a shadow of potential disaster in the form of increasing flooding. These threats, as outlined in the Intergovernmental Panel on Climate Change's (IPCC) Sixth Assessment Report by Glavovic (2022), underline an alarming projection: historically rare extreme sea level events, which have occurred sporadically in the past, are expected to be occurring annually in these cities by the year 2100. Furthermore, extreme rainfall is increasing due to the rising global temperature (Fischer & Knutti, 2016). For every degree Celsius increase in temperature, the air can hold more moisture, leading to more intense rainfall events (Centre for Climate and Energy Solution, 2023).

Assessing the severity of this trouble in terms of human populations at risk results in an increasingly bad scenario. A rise in global mean sea level of just 0.15 meters from current levels would increase the population vulnerable to a 100-year coastal flood by around 20%. For sea-level rises of 0.75 meters and 1.4 meters, this vulnerability increases by a factor of two and three, respectively (Glavovic, 2022).

Due to the more extreme rainfall, most of the coastal cities also face therefore more extreme river drainage and domestic stormwater runoff. With increasing heavy rainfall these riverine and pluvial floods will increase in magnitude and frequency. In urban areas, this threat is greater where impermeable built-up areas force water to quickly run off into the city's stormwater drainage system (Centre for Climate and Energy Solution, 2023).

As said above, both high rainfall intensity and rising sea levels pose significant challenges in the context of flood risk. Thus, both pose significant threats to the livelihoods of coastal city inhabitants. It is essential to identify the specific sources of potential flooding to make informed decisions about appropriate mitigation measures. Identifying the areas most vulnerable to flooding allows authorities and communities to prioritise and implement targeted measures to address the specific risks posed by both heavy rainfall and sea level rise. By understanding the different sources of flooding, effective strategies can be developed for the specific vulnerabilities of each location.

With the escalating threat of urban flooding in coastal cities, this report aims to address the pressing issue of assessing types of mitigation measures for these increasing risks of floods projected in a case study. The case study that was chosen for this research is the city of Cartagena. Arcadis along with the ConAgua consortium are in the process of mitigation the above-mentioned flooding issues there during the writing of the report. This research aims to support not only the project in Cartagena but also the broader goal of assessing mitigation measures in coastal cities worldwide.

1.2. Case Study: Water-related issues in Cartagena de Indias

Cartagena is a coastal city in northwestern Colombia on the Caribbean Sea. It holds the distinction of being the fourth-largest industrial city in Colombia and has a population of 1.1 million as of 2023 (United Nations Department of Economical and Socaial Affairs, 2018). Ninety-five per cent of the population lives in the urban areas of the city. The water networks combined make up almost 40% of the city's infrastructure. The water systems are depicted in Figure 1.1.

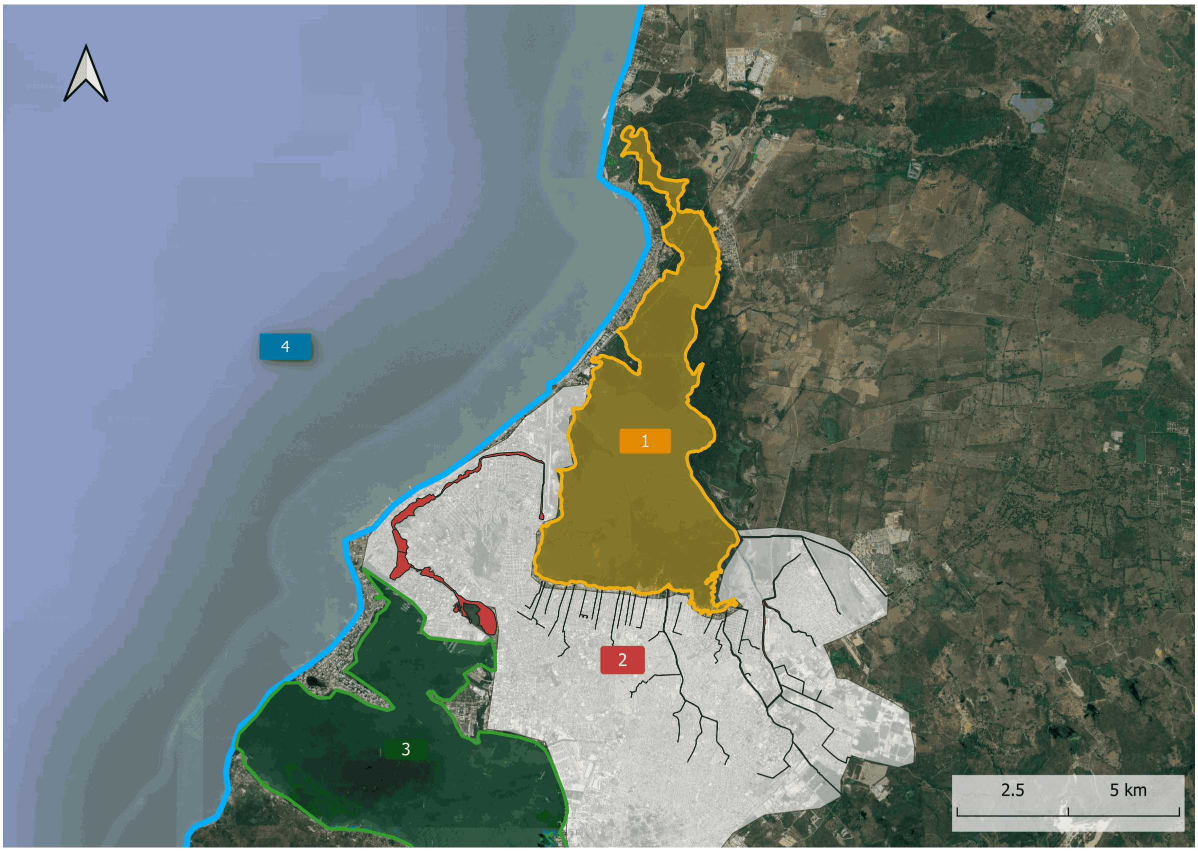

Figure 1.1: Water-related hotspots of Cartagena (Arcadis, 2022). 1) Ciénaga de la Virgen, 2) Drainage channels, 3) Cartgena bay and 4) Coastal seafront.

1. **Ciénaga de la Virgen wetland**: is a marsh area controlled by the tide (Díaz Cuadro, 2011). This marsh collects most of the city's rainwater and wastewater (Díaz Cuadro, 2011). It is serving recreational purposes and is an important ecological asset for the city.
2. **Drainage channels and lakes**: Most of the drainage channels direct rainwater from the city centre to the Ciénaga de la Virgen. The lakes on the western side of the city connect the Ciénaga de la Virgen with the bay.
3. **Cartagena's bay**: The bay contains one of the largest harbours of the Caribbean Sea (Insight, 2023). The bay's water system is primarily influenced by the seasonal discharge of Canal del Dique, a Colombian river, and the tide (Serna et al., 2019).
4. **Coastal seafront**: The beaches are one of the main tourist attractions for the city. The beaches have a dissipative nature and are composed of sandy sediments (Rangel-Buitrago et al., 2015). Due to significant erosion, these beaches have frequently been subject to tidal floods.

The existence of a diverse water system has rendered Cartagena a highly influential city in terms of industry, ecology, and tourism. These attractions resulted in the city's growth and becoming more densely populated. According to Figure 1.2, the city's population has grown from approximately 0.5 million to 1.2 million inhabitants. This led to a surge in population density from 1020 ppl/km^2 (people per square kilometre) to 1561 ppl/km^2 between 1990 and 2015, respectively (European Commission's

Joint Research Centre, 2015).

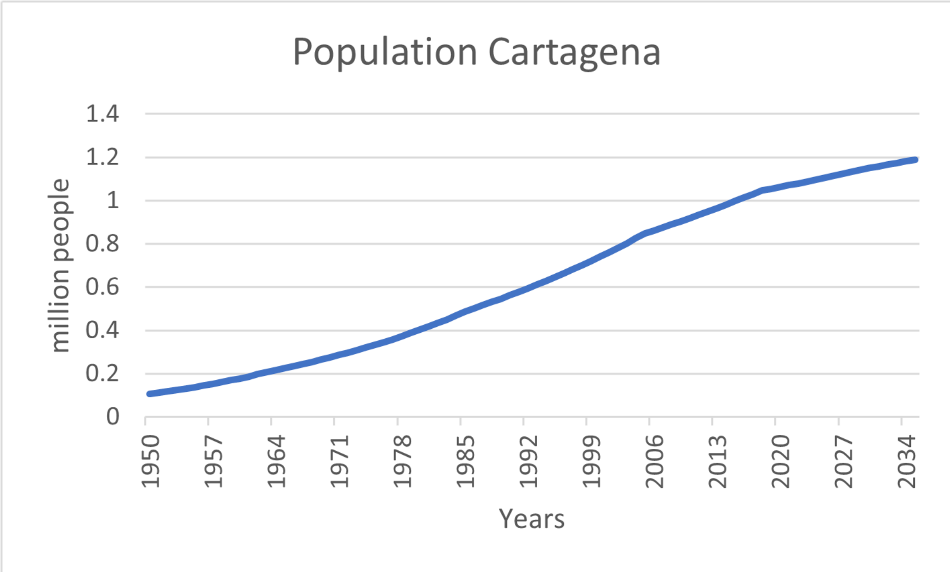

Figure 1.2: Population Growth Graph of Cartagena (United Nations Department of Economical and Socaial Affairs, 2018)

As the city grew massively over the last three decades, the urban expansions at the edge of the Ciénaga de la Virgen took place without prior urban planning regulation (Flórez, 2015). This led to the construction of illegal settlements (Villate Daza et al., 2020). Similar to other cities worldwide, residents of Cartagena tend to live close to the waterline which resulted in the citys expansion towards the waterfront and rural areas outside the city, as illustrated in Figure 1.3 and Figure 1.4.

(a) 1985

(b) 2022

Figure 1.3: The southern border of Ciénaga de la Virgen has witnessed significant urban expansions over the last 37 years (Google Earth, 2023).

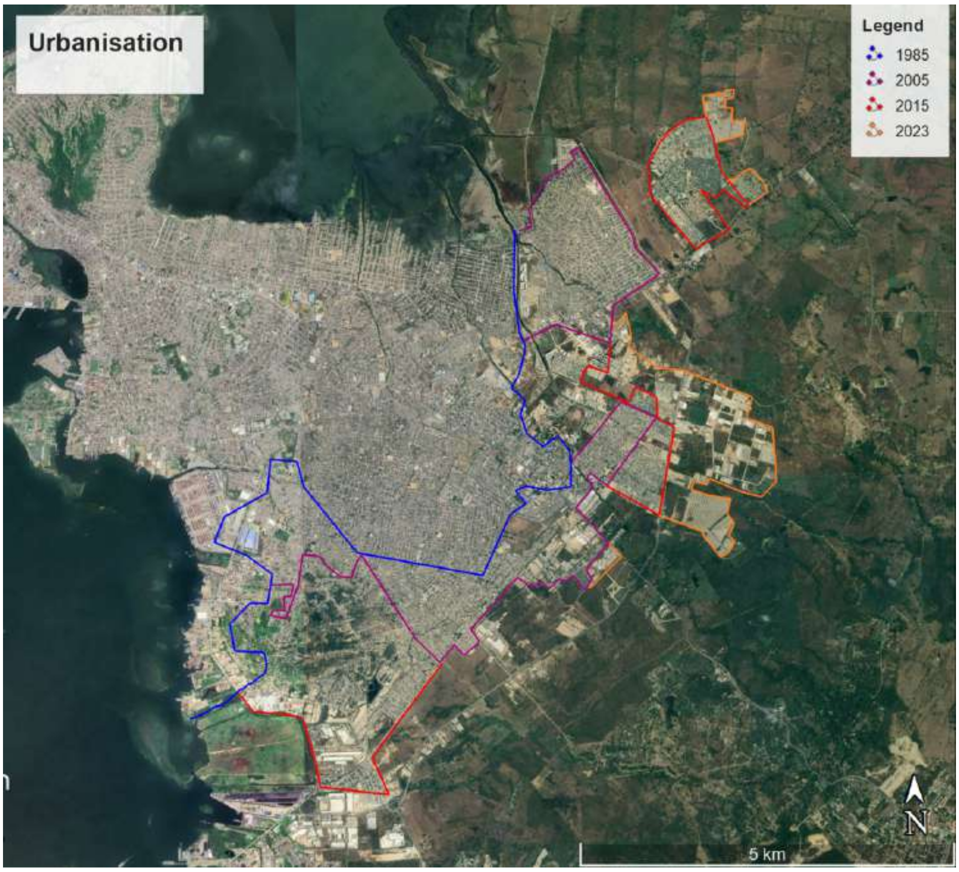

Figure 1.4: Urbanization over the last years. Blue is in 1985, purple after 2005, red after 2015, and orange is the current situation (Google Earth, 2023)

Water-related issues

According to Figure 1.5 floods account for 35% of the disturbances, making them the most pressing issue in the area.

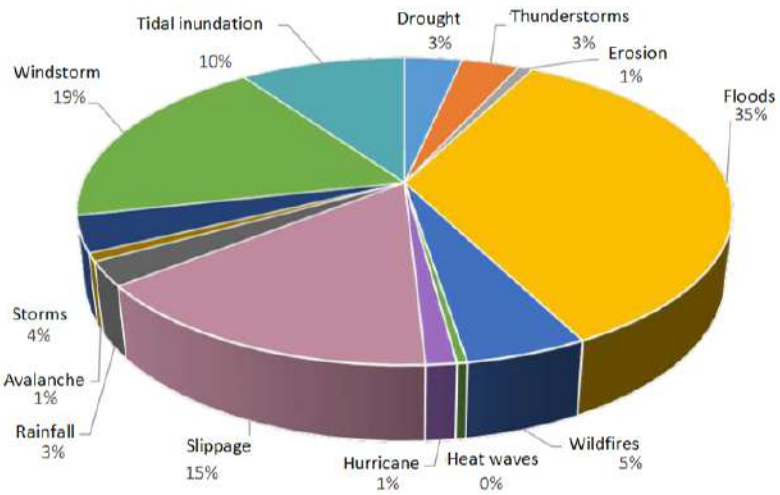

Figure 1.5: Percentages of disturbances due to named issues (1932-2020) (Bello et al., 2021)

Since 2000, there has been an increase in extreme rainfall, leading to the following numerous disasters (Bello et al., 2021):

- **2004**: Above-average rainfall claimed the property of almost 600 households.
- **2007**: A record total yearly rainfall of approximately 2000 mm/year was recorded. This led to significant flooding issues along the southern bank of the Ciénaga de la Virgen.
- **2010**: The record for the total amount of rainfall was once again surpassed. This time the total yearly rainfall reached approximately 2500 mm/year. This heavy rainfall resulted in significant flooding along the southern bank of the Ciénaga de la Virgen.
- **2016**: Hurricane Matthew's rainfall and gusts caused flooding in six channels and floods along the banks of the Ciénaga de la Virgen. The subsequent storm surge led to flooding at the connection between the coastal seafront and the Ciénaga de la Virgen.
- **2020**: On November 14 2020, Tropical Storm Iota raged on. This led to a recorded 12-hour rainfall that surpassed the normal rainfall of 8 months. This extreme weather event resulted in flooding that affected more than half of the city and around 20,000 households (Puello & Martelo, 2021).

The list above shows that the city has become more frequently subjected to flooding in the last two decades. Considering these extreme rainfall events in combination with a worrying sea level rise, the risk that these floods will concentrate along the banks of the Ciénaga de la Virgen is very likely. Given that the poorest citizens live close to the waterfronts, this vulnerability to flooding could have disastrous consequences for numerous lives (Camacho & Rodríguez, 2021).

1.3. Problem definition

As mentioned in Section 1.2, the most prominent water-related problem in Cartagena is flooding. The banks of the Ciénaga de la Virgen are prone to flooding caused by heavy rainfall and tidal water levels. In many cases, even moderate rainfall results in flooding of streets. Urbanisation has significantly increased the volume of run-off. The connecting channels suffer from poor maintenance and are insufficient in number and capacity to cope with the increased water flow. The drainage channels are often blocked in both width and length (Utria et al., 2017).

Almost all of the city's rainwater is directed towards the Ciénaga de la Virgen (Díaz Cuadro, 2011). In addition, it is not known how much the level of the Ciénaga de la Virgen affects the flooding of the neighbourhoods on the south bank, not to mention the effects of the expected rise in sea level. This ignorance poses a significant threat to the people living on the Ciénaga's edge. These inhabitants are some of the most impoverished communities in the city and already face difficult living conditions. The increased risk includes potential loss of property, an increased likelihood of waterborne diseases, injuries, and, tragically, loss of life.

The lack of a comprehensive understanding of the interactions between different influence flood drivers makes it difficult to mitigate flooding along the Ciénaga border. Currently, rainfall flooding and tidal flooding are often studied independently. This separated approach makes it difficult to determine a mitigation measure, especially in areas such as the banks of Ciénaga de la Virgen. These border areas, are or will become due to Relative Sea Level Rise (RSLR), zones of interaction between the water level boundary and the rainfall run-off upstream. As a result, it remains unclear how best to mitigate the southern edge of the Ciénaga.

Numerical modelling could be considered to determine the extent to which different types of mitigation could have an impact. However, existing flood modelling tools have limitations in accurately representing urban flooding processes (Fan et al., 2017). Traditional models often treat urban and coastal/lake processes independently, neglecting the complex feedback mechanisms within the system. This compromises the accuracy of the models, particularly in zones of interaction where both urban and coastal/lake processes come into play (Twigt et al., 2009).

D-Hydro is promising as it combines urban/rural and tidal flow models, allowing the coupling of 1D rainfall drainage models with a 2D flood flow model (Deltares, 2023a). However, the software is still at an early stage of application in the area of work, and there is a lack of comprehensive studies analysing its accuracy and performance in evaluating proposed mitigation measures for complex water-related problems such as those in Cartagena.

In summary, the problem definition revolves around the need for a holistic understanding of the flood dynamics in Cartagena, taking into account the interaction between different driving forces, to devise suitable types of mitigation measures. If the source of the flood can be linked to an area, the suitable types of mitigation measures can be determined. The integration of advanced modelling tools such as D-Hydro could potentially address these challenges, but its real-world applicability and performance remain uncertain. Therefore, there is an urgent need for thorough assessments and studies to couple the flood source with the suitable types of mitigation measures that are evaluated.

1.4. Knowledge gap

The following knowledge gaps will be explored in this thesis:

1. **The influence of the Ciénaga de la Virgen water level and different rainfall intensities on the floods of the southern bank**: It is crucial to determine the extent to which source will affect the severity and location of floods to devise a suitable mitigation plan.
2. **The performance of a complex integrated urban model**: Current approaches typically treat urban drainage models and tidal-induced models separately. Integrating these models should lead to improved accuracy.
3. **The Evaluation of D-Hydro Software's performance on mitigation measures**: Despite the D-Hydro software's ability to combine urban/rural flow and tidal flow models, its usage in assessing flood mitigation measures in this specific area has not been extensively studied or documented. Understanding how well D-Hydro software resolves the technical evaluation of the proposed measures is essential for making informed decisions.

By addressing these knowledge gaps, this thesis aims to fill in certain gaps and provide a starting point for further studies.

1.5. Research goal and objectives

The goal of this research is to define and quantify the source of the flood problems and assess the impact of potential mitigation measures aimed at reducing flooding problems. To achieve this goal, the following objectives are established:

1. Understanding the current interrelated water system of Cartagena.
2. Development of a numerical model that comprehensively captures the current water system and flood issues.
3. Utilizing the numerical model to formulate and investigate types of flood mitigation measures.
4. To assist the project, the most appropriate mitigation option is recommended by weighing up different criteria.

1.6. Research questions

From the goal stated in Section 1.5 the following research question can be stated:

> *How can an integrated approach, after effectively investigating different types of flood sources along the edge of Ciénaga de la Virgen, recommend the best-preferred mitigation design?*

To address this question, the research was divided into two parts. The first part involves understanding the system and identifying the causes of flooding in the study area. The second part focuses on identifying mitigation measures and evaluating their effectiveness. In line with the research objectives, the following sub-questions will provide additional support for the main inquiry.

Sub-question 1: What are the key reasons for flooding which can be supported by available data?

Sub-question 2: How do various meteorological conditions and downstream water levels quantitatively impact flooded areas when analyzed using a numerical model?

These two sub-questions will underline the first part of the research since an analysis is made of the current system. This provides the necessary knowledge to understand the system. After the analysis, the second part of the research can be executed. For this second part, the aim is to investigate different types of mitigation measures and recommend the best preferred mitigation design based on different criteria. Therefore, the two remaining sub-questions are defined as follows:

Sub-question 3: What types of mitigation measures are possible to develop into a mitigation option to reduce floods in urgent zones?

Sub-question 4: Which mitigation option is most preferred in this study area?

Going through these 4 sub-questions step by step ultimately determines the answer to the main question.

1.7. Report structure

in Chapter 2 the methodology that was used to answer all the sub-questions is laid out. In Chapter 3 the data analysis provides a system description. Chapter 4 describes the set-up of the numerical model and the results in flooding for the different scenarios. In Chapter 5 the different mitigation measures are explored and their reduction impact is simulated. From there, suitable mitigation options are set up. These designs are assessed based on various criteria in Chapter 6. The discussion in Chapter 7 describes assumptions and uncertainties that could potentially change the conclusion, this conclusion is written in Chapter 8. Lastly, the thesis gives recommendations for improving system understanding and quality of model input and recommendations for the next phase in the project in Chapter 9,

2
Methodology

In this chapter, each section describes the methodology for answering a subsequent sub-question. Each answer to a sub-question is used as input for answering the following sub-question. Answering the sub-questions incrementally, ultimately determines the answer to the main question.

2.1. Data Analysis

To answer Sub-question 1, data regarding the study area is collected and evaluated to analyze the system and determine the factors that contribute to the area's flood risks. Table 2.1 provides a concise summary of the data that is collected and analyzed

Table 2.1: List of to-be-analysed data

Type of data	Needed for
Drainage channel dimensions	Investigating capacity and flow of the channels
Topographic data	Determines altitude variations and Run-off directions
Meteorological data	Analysing the extreme rainfall and their return periods
(Tidal) Water levels	Determines the boundary conditions downstream
Flood levels	To indicate the hazards and validate the model study

Based on the assessment of this data, as well as relevant literature, an analysis is conducted to evaluate the current drainage system. The data analysis and the subsequent system description addresses Sub-question 1. This step is crucial for answering the subsequent sub-questions as it establishes a hypothesis regarding the sources of flooding. Furthermore, it provides valuable insights before establishing a numerical model, the results of which validate and quantify the proposed hypothesis.

2.2. Modelling Study

To address Sub-question 2, a numerical model is developed to quantitatively assess the sources of flooding in the study area. The D-Hydro software is utilized for this evaluation of the flood-prone sections of the city's drainage system. The D-Hydro model is newly constructed and validated as thoroughly as possible with the available data from Chapter 3. The analysis involves studying the impact of water levels in combination with different rainfall intensities, categorized by their return period, on the flooded area and flood levels. The objective is to identify which zone in the study area is influenced by which source of flooding, and whether this influence would change due to relative sea level rise. The findings from these investigations are divided into three distinct zones, as introduced by Shen et al. (2019):

1. The rain-induced zone (hydraulic zone)
2. The high-water zone (tidal zone)
3. The transition zone

The dividing into zones of influence and the quantification of flooded areas and levels is done by investigating the scenarios shown in Table 2.2:

Table 2.2: The investigated scenarios to determine the zones of influence

1	A rainfall intensity with a return period of 2 years in combination with an extra low tide
2	A rainfall intensity with a return period of 2 years in combination with a tidal sequence
3	A rainfall intensity with a return period of 2 years in combination with an extra high tide
4	A rainfall intensity with a return period of 10 years in combination with an extra low tide
5	A rainfall intensity with a return period of 10 years in combination with a tidal sequence
6	A rainfall intensity with a return period of 10 years in combination with an extra high tide
7	A rainfall intensity with a return period of 100 years in combination with an extra low tide
8	A rainfall intensity with a return period of 100 years in combination with a tidal sequence
9	A rainfall intensity with a return period of 100 years in combination with an extra high tide

For these scenarios, one full day is simulated because the extreme rainfall intensity is determined daily. In the computational results, a flood is defined as the water level in a grid cell being greater than 1 mm ($\geq$0.001 m). This threshold is chosen to exclude very small outliers, as a millimeter of water can be defined as a wet surface.

To investigate the impact of the water level, the rainfall is kept at the same intensity while the water levels vary. This approach highlighted differences in flooded areas and flood levels, indicating where the water level influences flooding. This influence is also examined under different rainfall intensities to determine if the impact of the water level changes with a greater volume being drained.

Similarly, to investigate the impact of rainfall intensity, the water level conditions are therefore kept constant across different rainfall intensities. This analysis reveals differences in flooded areas, indicating where rainfall intensity influenced flooding. The influence of water level conditions is also examined to see if their impact changes with a greater volume being drained.

The computational results of the numerical model concluded that the transition zone could be excluded from the analysis as it is not significant. This divides the area into two zones with different driving forces behind flooding. After establishing these zones, the shift between them is examined in the context of relative sea level rise, as recommended by Shen et al. (2019) and because relative sea level rise doubles the tidal range. The same scenarios are simulated but with an adjusted water level. Ultimately, new influence zones are determined, and the shift is observed.

The computational results are used to prioritize a specific area within the study area to investigate under which conditions the most effective types of mitigation measures should be explored.

2.3. Investigating possible types of mitigation measures and developing mitigation options

The conclusions drawn from the modelling study will significantly influence the development of mitigation strategies. The answer to Sub-question 2 will guide the direction of these strategies. If the tidal zone is identified as having a greater influence on flooding, the focus would shift towards identifying measures that can control water levels downstream. Conversely, if the hydraulic zone is identified as the primary concern, efforts will be concentrated on improving there.

To determine the effectiveness of mitigation strategies, relevant types of mitigation measures are examined. The developed numerical model is used to assess the impact of these strategies on a specific part of the study area. The computational results evaluate the reduction in the flooded area and flood levels. This combination of reduced values provides a comprehensive indication of the mitigation measure's effectiveness. The area indicates the quantity of the impact, and the reduced levels reflect the quality of the impact. If assessed independently, the flooded area alone could provide misleading information about the significance of the reduction, addressing only the total reduction. Conversely, assessing only reduced flood levels could be misleading because the average reduction could be high but over a minimal area. The combination provides insight into both aspects, ensuring a fair comparative assessment

Different scales of application investigate the optimal effect of the chosen types of mitigation measures. Based on this analysis covering the scales, functionally and technically feasible mitigation options are proposed for each type of chosen mitigation measure. These mitigation options are tested with the D-Hydro model, and their technical performance is evaluated. This process will provide the answer to Sub-question 3.

2.4. Multi-criteria evaluation of the Mitigation Options

To address Sub-question 4, the mitigation options are evaluated. The evaluation process utilizes a Multi-Criteria Decision Making (MCDM) tool, which is widely recognized as an effective method for assessing flood risk measures (Brito & Evers, 2016)

The use of Multi-Criteria Analysis (MCA) plays a key role in evaluating different flood mitigation measures, providing a systematic approach to decision-making. This approach allows for a focus not only on technical aspects but also on other factors. The MCA incorporates these different criteria into the evaluation process, ensuring a comprehensive assessment. The MCA also provides a structured framework for weighing the pros and cons of each option. Predetermining a clear scale and quantifying where possible offers a transparent comparison of different mitigation options. The ultimate score serves as a tool for making a recommendation.

The categories used for the assessment are carefully selected to provide a comprehensive perspective on the implementation of each measure. Input from the consortium Con Agua, which includes Arcadis and is involved in the design process of the project, is considered. This consortium has already established a framework of objectives and criteria, which are relevant to the project. While it is not possible to assess all specific criteria within this study, the following categories are selected for evaluation:

1. Technical aspects
2. Future proofness
3. Adaptivity
4. Socio-economic aspects
5. Financial aspects
6. Environmental aspects

Each category incorporates various criteria, with some categories capturing more criteria than others. Each criterion is assigned a weight ranging from 1 to 5, reflecting its importance in the assessment within the category. For the technical criteria and costs (1, 2, and 5), specific quantifiable distinctions are linked to the scoring factors. The remaining criteria are assessed qualitatively.

To determine the best-preferred mitigation option, the weights and scores are multiplied, resulting in a total score for each measure. The mitigation option with the highest total score is identified as the best-preferred option. The results of this analysis subsequently will lead to a discussion on which design is best-preferred for implementation in this area.

By addressing all sub-questions, the main research question can be answered, which results in the overall conclusion and recommendations for this thesis.

3 Data Analysis

A thorough data analysis of the research area is conducted to understand the system dynamics fully. This chapter introduces readers to the study area, clarifies its common water-related problems, and leads to the identification and collection of various types of important data. This approach provides insights into potential drivers for current problems, and describes and answers Sub-question 1: *What are the key reasons for flooding which can be supported by available data?*

3.1. Study area

The study concentrates on the urban residential city area as shown in Figure 3.1. The reasons for the concentration upon this area is the area's interaction with various water bodies in and around Cartagena making it very dynamic. Also, almost all rainwater was directed to the banks of the Ciénaga, making it highly susceptible to floods in poor residential areas. The study area is split into three sections to develop knowledge of the elements at play. The different areas are discussed further in detail below.

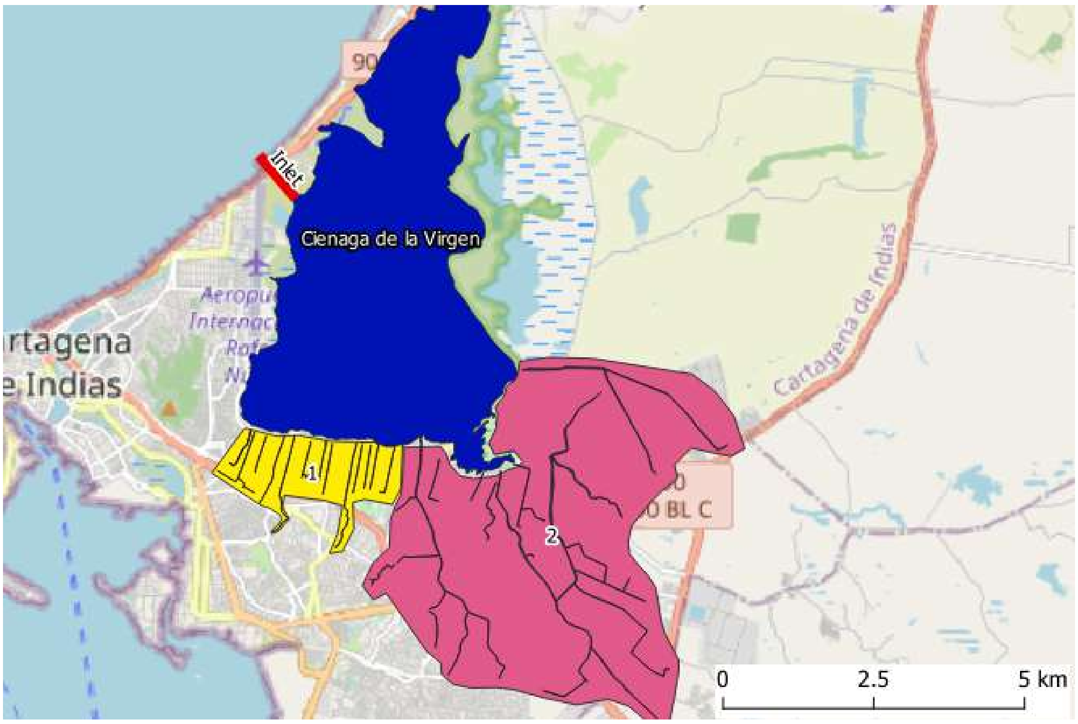

Figure 3.1: The study area is divided into three zones

1. **Southern drainage system:** The urban drainage system directs rainfall water and domestic wastewater from the city towards the southern banks of the Ciénaga de la Virgen. Thirteen drainage channels are present in this section. The average size of these drainage channels is typically smaller than the average size of all the city's channels (see Section 3.2.1). Low drainage capacity is identified as the main issue Local authorities (2009). Almost all of the thirteen channels contain sections that experience inundation more frequently than every two years (Local authorities, 2009a). Domestic waste is deposited into the channels, exacerbating the situation (Local authorities, 2009b).
2. **South-eastern drainage system:** In this area, seven large drainage channels discharge towards the southeastern banks of the Ciénaga de la Virgen. Four of those channels have numerous side channels and are larger drainage channels than the average dimensions of the channels. Water from the rural area at the southeast side of the Ciénaga de la Virgen is drained through the three most eastern channels. The catchment areas in this area are noticeably larger than the catchments of the southern drainage system as a result (Brakel et al., 2017). The maximum drainage capacity is exceeded mainly in the side channels of the four large channels. Flooding occurs here more frequently than every two years and is primarily in urban areas (Local authorities, 2009a). The urbanisation increased rapidly in this part of the city. Run-off water increases and flooding becomes more severe due to this growth and unauthorized construction initiatives (also described in Section 1.2).
3. **Ciénaga de la Virgen:** Water from the drainage system discharges onto the Ciénaga de la Virgen. This marsh area is connected to the sea with an inlet point: La Bocana (The red inlet point indicated in Figure 3.1). A network of inflow and outlet gates controls the water flow. A few kilometers north of this gate, two natural inlet points are present. However, these inlet points are not connected to the lake all year round. This is why La Bocana was created in 2001. It was designed to oxygenate the lake, as it was almost completely cut off from the tide before. The cut resulted in the deterioration of the water quality, causing a loss in biodiversity (Díaz Cuadro, 2011). The tide gates have never seen any maintenance and therefore became non-functional (Yuca-Pelá, 2016). The gates remain open, causing an uncontrolled tidal influence in the Ciénaga de la Virgen. Sediment is brought in via the sand trap in front of the gates (Tinoco Devia, 2006). This can cause a lower water storage capacity.

3.2. Available data

To address Sub-question 1, a comprehensive data analysis of the study area is conducted. Various types of literature and data sets are examined to quantify the diverse flood issues within the water system.

3.2.1. Channel dimensions

The considered channels are depicted inFigure 3.2. The dimensions of these channels were documented in a hydraulic report conducted by the municipality of Cartagena (Local authorities, 2009a).

Figure 3.2: The drainage channels of the study area

In this extensive report of Local authorities (2009), the urban channels have been examined in terms of the following:

- Hydraulic Study
  - Geometrical dimensions of the channels per section
  - Discharge exceeding probability
- Hydrological Study
  - Morphometry;
  - Synthetic Hydrographs

According to the views of local experts, the research carried out in 2007, as part of a plan to enhance the existing channels, did not result in any improvements. Hence, the dimensions provided in the report are assumed as representative of the current situation.

The morphometry per section of the report includes the average slope, form and contraction coefficients, and the maximum/minimum height relative to the sea level per channel. Based on this report, the crucial data is compiled into a single Excel sheet for further processing, as illustrated in Appendix A.

3.2.2. Topographic elevation maps

The company EDURBE (Empresa de Desarrollo Urbano de Bolívar), in collaboration with the local authorities, created a high-resolution topographic height map using the local cadastre (Hawkins & Quintero Banda, 2022). This Tag Image File (TIF) has a resolution of 2 by 2 meters, enabling a clear distinction between streets and houses. No clear reference level (relative to a 0 value) is given for this topographic map. Therefore, the assumption is made that the reference level is the mean water level of the Ciénaga. This map is further utilized in the numerical model. The topographic height map is presented in Figure 3.3.

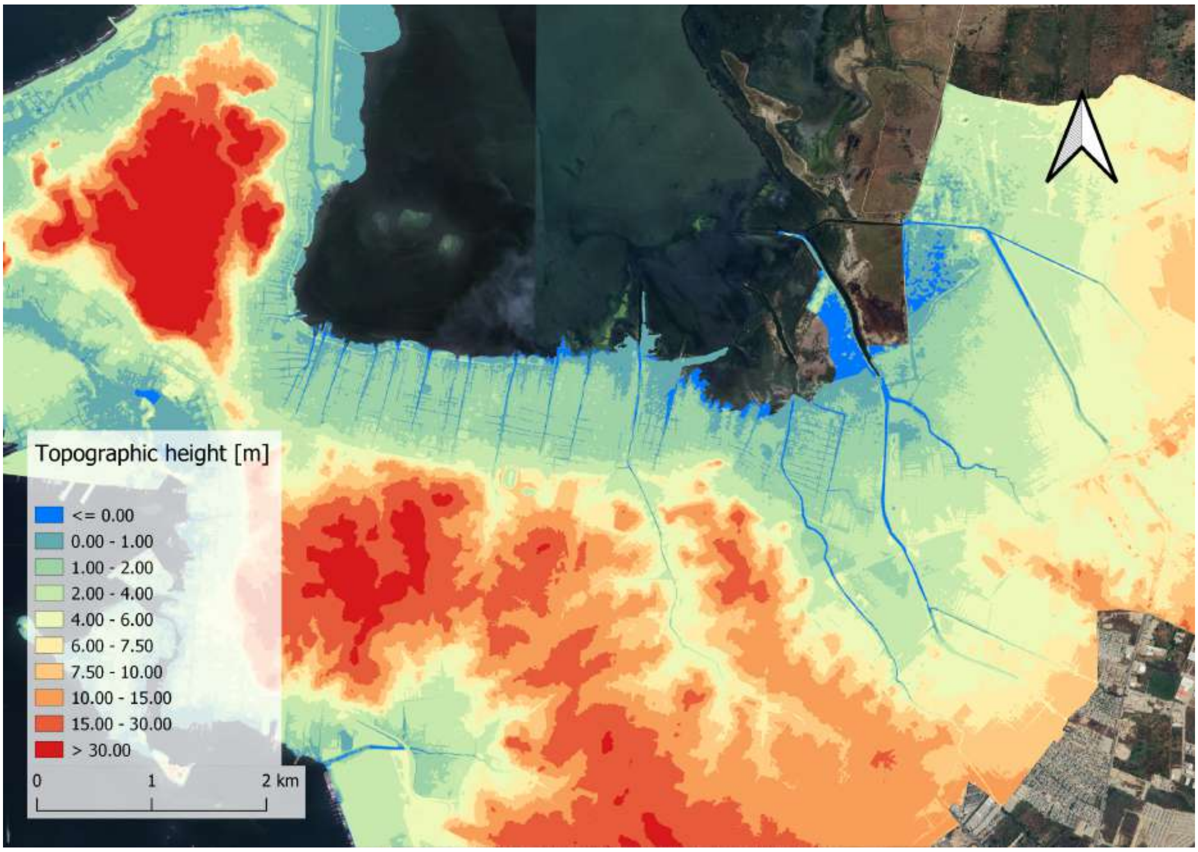

Figure 3.3: The used elevation map (resolution size 2x2 m)

The following points stand out about the topographic elevation of the study area.

- Most bed levels of channels downstream are situated below the mean water line. This indicates that the channels are (partially) filled in general conditions.
- The banks of the Ciénaga are relatively flat.
- The most of residents in the downstream area live within 2 meters of the mean water line.
- The significantly high-altitude upstream areas indicate that the run-off water flows very quickly towards the flat areas where the velocity will stagnate due to the small slope.

3.2.3. Meteorological data

In almost all of Colombia, an increasing trend of rainfall intensity and frequency is observed (Cerón et al., 2022). Along the Caribbean coastline, the number of days that are experiencing more than 30 mm of rain increases for September, October and November. Zooming in on the study area, the extreme rainfall is evaluated with found data from IDEAM (2023). It is crucial to identify the frequency and intensity of the rainfall to determine the run-off water to the Ciénaga. The rainfall data is obtained from the rainfall station ESCUELA NAVAL CIOH, depicted in Figure 3.4. This station, located near the airport, is selected because it has the most extensive data available.

Figure 3.4: The location of the rainfall station in the city (ESCUELA NAVAL CIOH) (IDEAM, 2023)

This study conducts a temporal analysis of the available data. This is deemed necessary because previous studies had only covered rainfall data up to 2009 or 2016 (Arrieta-Pastrana et al., 2023; Local authorities, 2009a). The most recent analysis was conducted by Mouthon-Bello et al. (2023) but focused primarily on spatial variability. The various sets of data that could be obtained from the database of IDEAM (2023) include:

1. Annual rainfall (1950-2022)
2. Monthly rainfall (1950-2022)
3. Daily rainfall (1970-2022)
4. Hourly rainfall (2009-2022)

The four different data sets are examined for significant irregularities. The examination compares the cumulative annual rainfall for output consistency from the years 2009 to 2022. As depicted in Figure 3.5, data sets 1 to 3 exhibit consistency, while set 4 demonstrates irregularities.

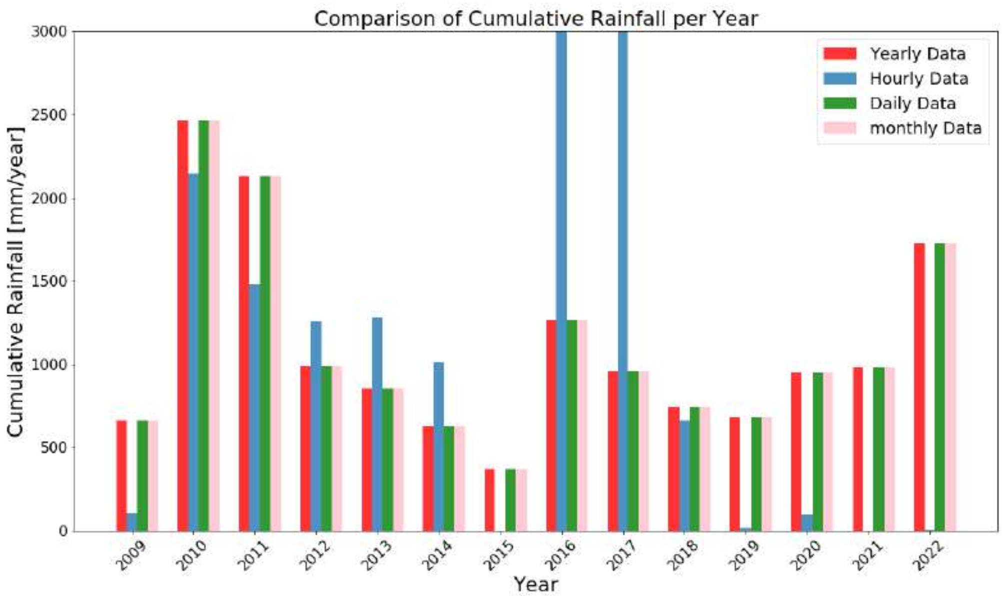

Figure 3.5: The comparison of the different data sets obtained from IDEAM (2023)

Between 2010 and 2014, data set 4 exhibits reasonable similarities, despite some deviations. However, significant disparities emerge in 2009 and after 2014, concluding that the data set is unusable.

The annual data set is utilized to examine whether an increasing trend in rainfall over the years could be identified. The monthly data set determines the wettest months. The daily set is used for an extreme value analysis to find extreme rainfall intensities with their corresponding return periods. Since the hourly data set is deemed unreliable, an alternate survey from EDURBE (2022) is used to recreate the distribution of a rainfall event.

Annual rainfall

The cumulative annual rainfall has been recorded from 1950 to 2022. As depicted in Figure 3.6, the average yearly rainfall over the last 72 years is 1011 mm. Notably, extreme events have become increasingly recurring over the last 20 years, and these extreme years have also witnessed intensifying rainfall. For instance, the highest rainfall values were recorded in 2010 and 2011, measuring 2469 mm/year and 2130 mm/year, respectively, representing a doubling compared to the average.

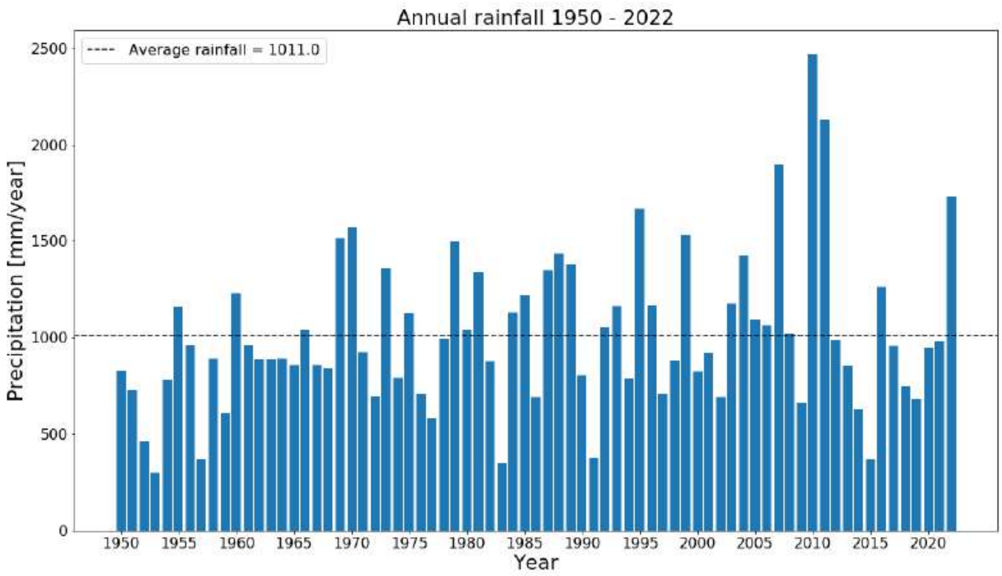

Figure 3.6: Cumulative annual rainfall 1950-2022

A rolling mean test shows the data set's stationarity. Figure 3.7 shows that there is no significant increase in the rolling mean, which indicates that the data set is indeed stationary. Therefore, it is concluded that there is no direct increase in annual rainfall.

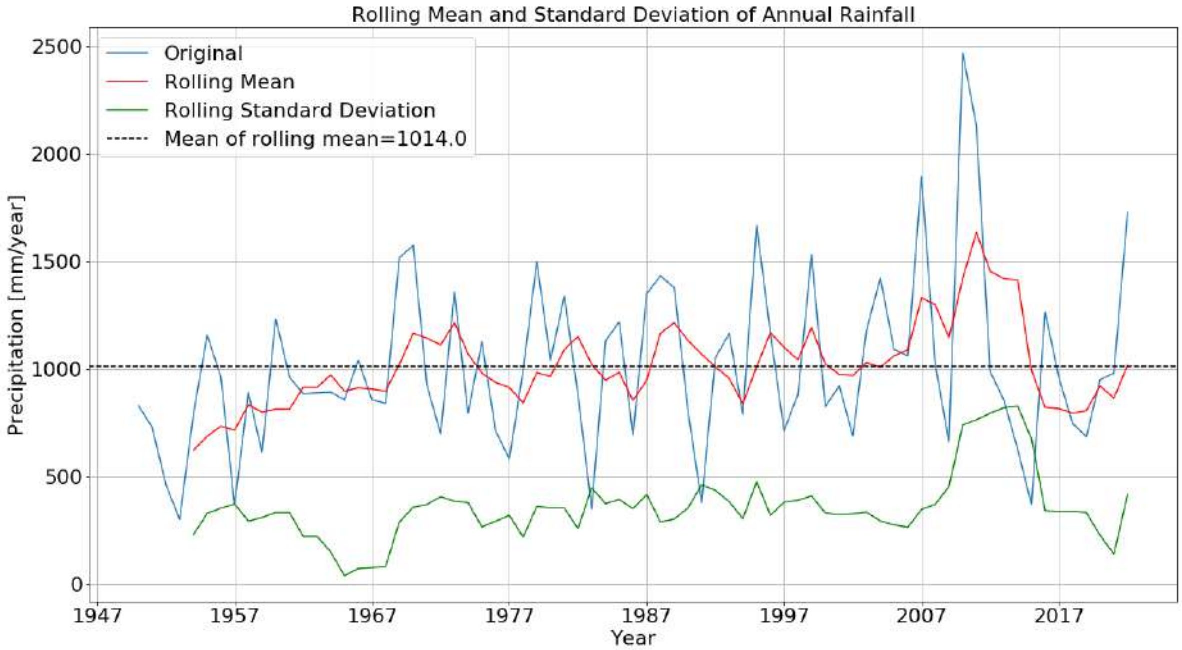

Figure 3.7: The rolling mean for the yearly data set

Monthly rainfall

With this data, an analysis of the monthly rainfall data set identifies distinct dry and wet seasons and any potential changes. The cumulative rainfall data for each month is illustrated in Figure 3.8, with each bar representing the total rainfall for that month in the respective year. The findings consistently highlighted October and November as the wettest period of the year on average, indicating the presence of a distinct rainy season during these months. Moreover, recent years have exhibited significantly higher peaks of cumulative rainfall during October and November, suggesting a possible intensification of the rainy season during this period. This observation aligns with the historical records of disasters throughout the last century, as discussed in Section 1.2.

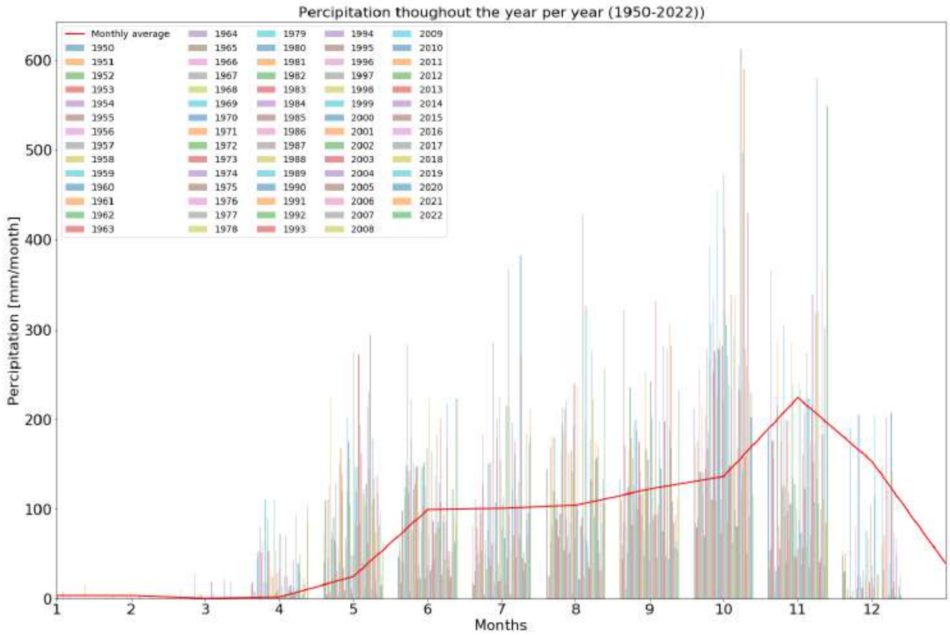

Figure 3.8: Cumulative monthly rainfall 1950-2022

Daily rainfall

A data set covering the period from the 1st of January 1970 to the 31st of December 2022 was examined for daily rainfall analysis. With this data, an evaluation of daily rainfall intensities identifies representative values for days with flooding occurrences. The highest cumulative rainfall value was recorded on October 2nd, 2016, reaching 222 mm/day. This corresponds with the passing of Hurricane Matthew as talked about in Section 1.2.

An extreme value analysis determines the return periods associated with rainfall intensities. These determined return values help to understand the recurrence of such extreme events. The daily data set is used for this purpose.

Extreme value fit

An extreme value analysis is conducted with a peak-over threshold method on the daily rainfall set. The following four distributions are checked:

- Exponential Distribution
- Weibull Distribution
- Gumbel Distribution
- Generalized Pareto

Linear regression is conducted for different distributions, and prediction curves (return period vs. daily cumulative rainfall) are generated. By defining the Root Mean Square Error (RMSE), the two best prediction curves are determined, identified as the Weibull distribution and the Generalized Pareto Distribution. For both distributions, the bootstrap method is employed to calculate a 90$\%$ uncertainty (+/- 1.64 standard deviation). The final extreme value curves along with their corresponding values are presented in Figure 3.9, Table 3.2, and 3.1. Further details of the entire extreme value analysis can be found in Appendix B.1.

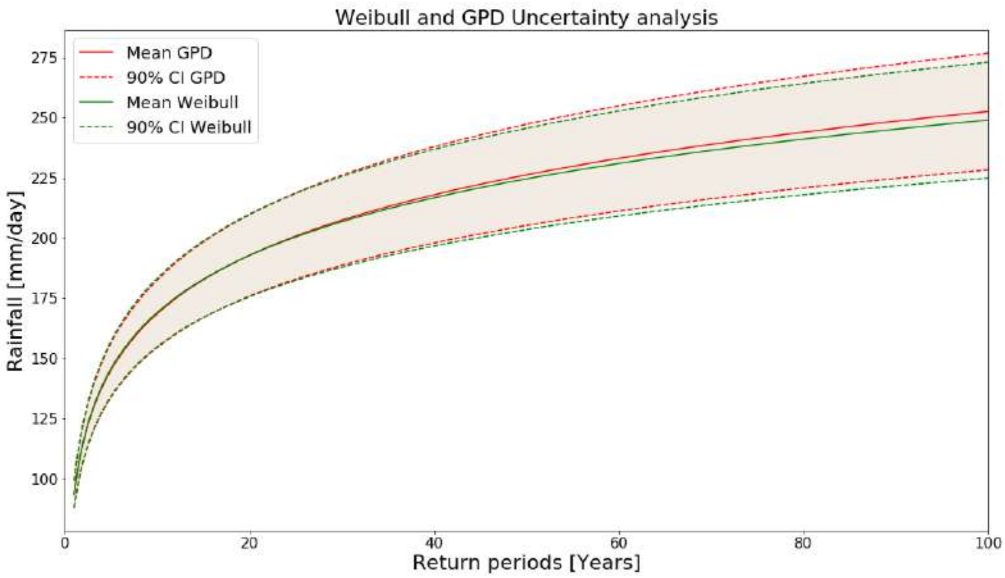

Figure 3.9: The uncertainty of the Weibull and Generalized Pareto distributions using bootstrapping.

Table 3.1: The return values for the Generalized Pareto distribution with the 90% confidence interval after bootstrapping

R [years]	**1**	**2**	**5**	**10**	**20**	**50**	**75**	**100**
GPD [mm/day]	94	115	145	169	193	226	242	253
σ_{gpd} [+/-]	3	5	7	8	10	13	14	15
Max R	99	123	156	**183**	**210**	**247**	**265**	**277**

Table 3.2: The return values for the Weibull with the 90% confidence interval after bootstrapping

R [years]	**1**	**2**	**5**	**10**	**20**	**50**	**75**	**100**
Wei [mm/day]	94	116	146	169	193	225	239	249
σ_{gpd} [+/-]	3	5	7	9	10	13	14	15
Max R	**99**	**124**	**157**	**183**	**210**	246	262	273

For application further in the study, the maximum values are used to address the most negative scenario possible (shown in bold in Table B.3 and Table B.4).

Rainfall distribution

It was expected in advance that hourly data would provide the rainfall distribution for the extreme events. However, due to its non-usability, a rainfall distribution will be reproduced based on the findings of EDURBE (2022). The conclusions drawn from this research were the following:

1. 70% of all daily cumulative rainfall records have fallen within eight hours.
2. 80% of the recorded rainfall per event fell within two and a half hours

From these statements, an hourly distribution can be mimicked shown in Table 3.3.

Table 3.3: A summary of the hourly rainfall distribution of 70% of recorded events (EDURBE, 2022).

Time [h:mm]	Dist [%]
0:00	0.0
0:30	20.4
1:00	53.2
1:30	71.0
2:00	76.8
2:30	81.6
3:00	83.8
3:30	87.2
4:00	89.2
4:30	91.5
5:00	92.9
5:30	94.4
6:00	95.6
6:30	97.2
7:00	98.4
7:30	99.6
8:00	100

This distribution is used to simulate rainfall events of the extreme value analysis in the input of the model. The other cumulative distributions that cover different duration times can be consulted in Appendix B.2

3.2.4. Tidal water level

Cartagena experiences a semi-diurnal tide, with one high tide, one relatively lower high tide, and two low tides in a day. With the use of the tidal constituents, a tidal harmonic cycle can be simulated. This was facilitated by the tidal predictor that is incorporated in Delft3D. To verify the accuracy of the tidal predictor, November 2020 was analyzed, considering the flood event during that month, which was triggered by Hurricane Iota (see Section 1.2).

Since no historical water level data from Cartagena is available, historical water level data from Santa Marta, located approximately 170 km northeast of Cartagena, is utilized to verify the water levels of the predictor. The data is acquired from the University of Hawaii Sea Level Center (2023). Outliers are removed and set to 0.00 meters. To ensure reference water levels were used, the data set was normalized to +0.00 m above local sea level, resulting in an offset deduction of 1.38 meters from the initial data set. For additional information regarding the Santa Marta measured data, please refer to Appendix C.1. The constituents in Santa Marta, as measured by Latandret-Solana et al. (2023), are presented in Table 3.4.

Table 3.4: The observed tidal constituents for the Santa Marta Bay (Latandret-Solana et al., 2023)

Santa Marta	**K_1**	**O_1**	**P_1**	**M_2**	**N_2**	**S_2**	**M_f**
Amplitude [cm]	9.6	5.6	3.1	6.4	2.4	1.8	1.2
Phase lag [degree]	241	237	243	128	107	49	44

Validation of the predictor compares the amplitudes and the phase differences of the predictor.

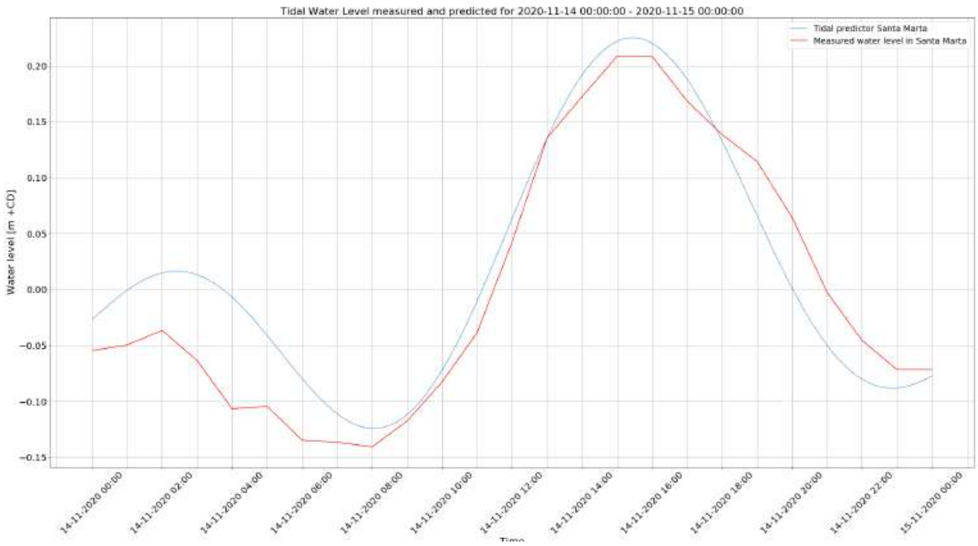

Figure 3.10: The measured water level in Santa Marta on the fourteenth of November 2020 compared with the tidal predictor to observe the phase difference.

Regarding Figure 3.10 no real phase difference is observed. In Figure 3.11 the amplitude difference is plotted and the deviations are highlighted.

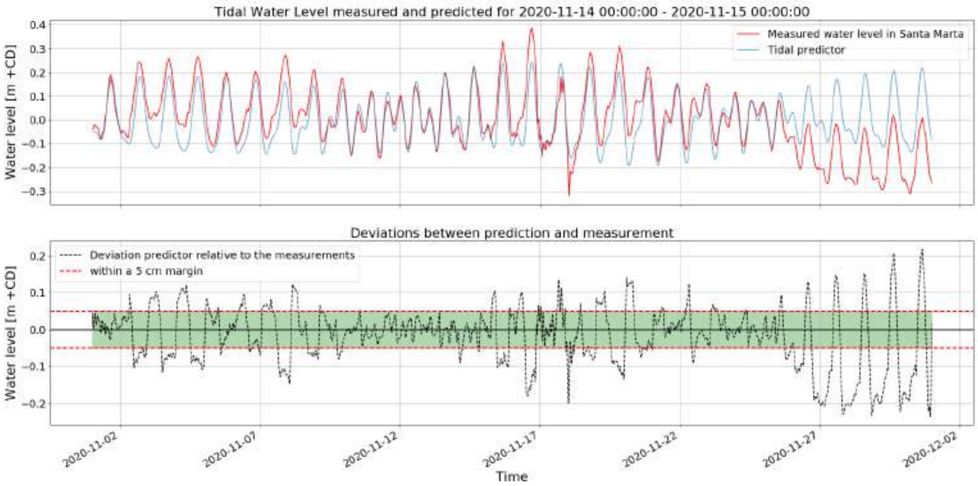

Figure 3.11: The measured water level in Santa Marta in November 2020 compared with the tidal predictor outcome using the tidal constituents measured in Santa Marta.

The following statements can be made:

1. The shape is fairly similar.
2. The amplitude deviation remains below the 5 cm range for most of the month.
3. The difference lies mainly at the end of the month. Here very low water level values were observed concerning the rest of the data set.

The differences lay mainly at the end of the month. The reasons for the differences can be explained as follows::

1. The predictor makes a perfect harmonic tidal sequence. Natural additional factors, such as wind set-up or set-down, are not taken into account.
2. Not all 60 constituents could be included. The majority of the constituents should be insignificant, but this might clarify the minor variations.
3. Regarding the end of the month, it can be concluded that there is an error in the measured water level. These values were amongst the lowest of the whole data set. A sudden drop of 20 cm would be very unlikely.

Overall, the differences in the shape and values of the tidal predictor are not significant. Therefore, the tidal predictor performs sufficiently well to be considered reliable for assessing water levels in Cartagena. The amplitudes and phase lags of the observed Cartagena constituents are presented in Table 3.5.

Table 3.5: The observed tidal constituents for the Cartagena port (Latandret-Solana et al., 2023)

Cartagena port	K_1	O_1	P_1	M_2	N_2	S_2
Amplitude [cm]	9.8	5.8	3.1	7.4	2.9	1.6
Phase lag [degree]	242	243	243	133	110	46

Figure 3.12 used the constituents and predicted the water level for a whole year.

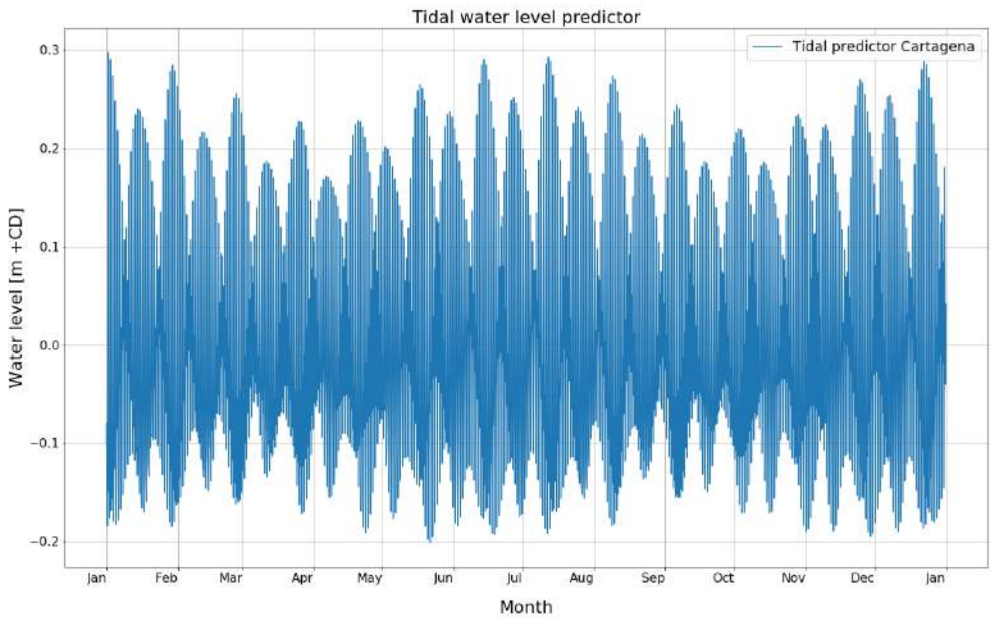

Figure 3.12: Water level for a year predicted with the tide predictor software Delft3D

The extremely high and low tidal water levels are considered for a full-year simulation. The exterme water levels give insight into the total tidal range. In Table 3.6 these extreme tidal water levels are shown. The maximum tidal range in a year that can be anticipated is 0.50 meters. Other physical processes that could increase or decrease the water level are not considered for this prediction.

Table 3.6: Extreme tidal water levels from a year simulation with the tidal predictor.

	Water level [m]
Extreme high tide (EHT)	0.30
Extreme low tide (ELT)	-0.20

This is also used as water level input for the boundary conditions in the modelling study (Chapter 4).

3.2.5. Recorded flooding events

Pluvial flooding

As mentioned in Section 3.2.1, the city's drainage system is incapable of handling significant rainfall volumes due to inadequate maintenance and the constriction or obstruction of channels (Utria et al., 2017). This issue is illustrated in Figure 3.14

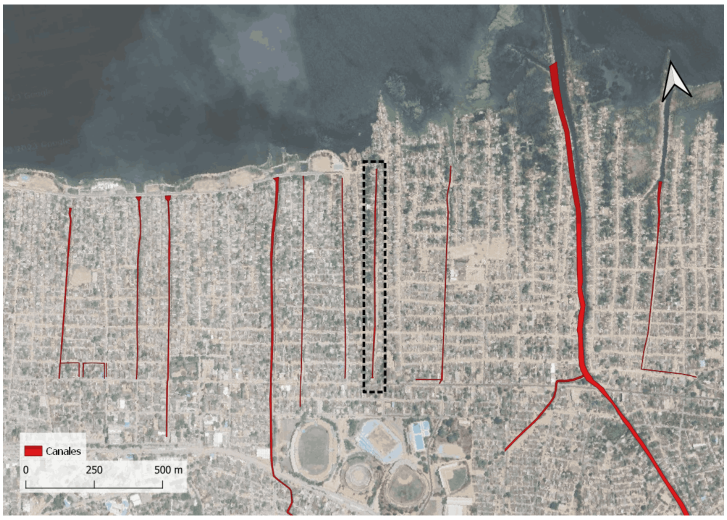

Figure 3.13: Channel Once de Noviembre

Figure 3.14: A picture of waste in the channel

The southern borders of the wetland face the highest risk of pluvial flooding, predominantly affecting the poorest inhabitants of the area (Camacho & Rodríguez, 2021). The consequences of these floods for those living in these neighbourhoods are severe. The economic impact of the floods is estimated to be around 40 billion dollars (Flórez, 2015). As discussed in Section 3.2.3, there is no clear indication of an increasing trend in annual rainfall. Additionally, a study by Arrieta-Pastrana et al. (2023) found no observable trend in the daily maximum from 1970 to 2016. This reconfirms the rainfall analysis in Section 3.2.3.

The available flood level data for Cartagena is limited. An article by Caracol Radio (2020) identified flooded neighbourhoods due to Hurricane Iota. No flood levels are mentioned but it gave an arbitrary indication about the flooded area due to these conditions. The only flood levels that were available, are found in an overview of a community interview conducted by the Edurbe company. These flood level values come from the same study where the rainfall distribution is used from Section 3.2.3. However, the report did not specify the type of storm these values were based on. As no other data is available, these values are to be utilized in the assessment.

The flood data points are displayed in Figure 3.15, with the yellow points representing the neighbourhoods that were flooded during Hurricane Iota on 14 November 2020 and the green point representing the data from the community interview.

According to the daily rainfall data set discussed in Section 3.2.3, the recorded rainfall intensity on 20 November was 83.18 mm/day, with rainfall occurring from 6:00 am to 6:00 pm (Time and Data AS, 2023).

The flood depth found for each point number in the community interview is presented in Table 3.7. Unfortunately, no additional context about this interview is available.

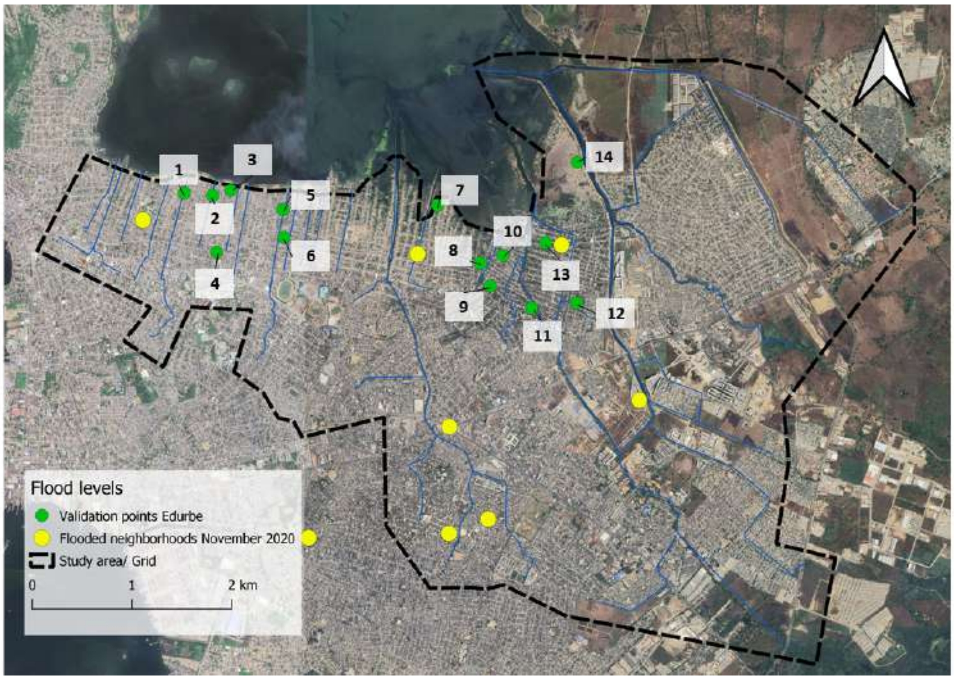

Figure 3.15: Water depths for point in the Edurbe community report and the flooded neighbourhoods during hurricane Iota

Table 3.7: The water depth per point found with conducting a community interview by Edurbe.

Point number	**1**	**2**	**3**	**4**	**5**	**6**	**7**	**8**	**9**	**10**	**11**	**12**	**13**	**14**
Water depth [cm]	70	80	30	60	50	80	90	80	70	90	60	50	30	65

Surge flooding

Due to its location on sandbars, Cartagena is susceptible to coastal and surge flooding. Storm surges can lead to annual overflow levels of 0.22 meters relative to sea level (Andrade et al., 2013). The area most affected by the rising tides is Boca Grande, the city's business district. Orejarena-Rondon et al. (2019) explored various scenarios for coastal flooding and demonstrated that under a scenario with a high tide of 0.2 m relative to the current mean sea level and an offshore significant wave height (H_s) of 3 m, the flooded area in Boca Grande already confines 9.9% of the region (indicated by the red circle in Figure 3.16). These floods typically disrupt traffic, with more severe scenarios rendering the infrastructure impassable or damaged (Andrade et al., 2013). Over the period from 1970 to the present, twenty disasters have been recorded as a result of high tides (Cote & Rodríguez, 2015).

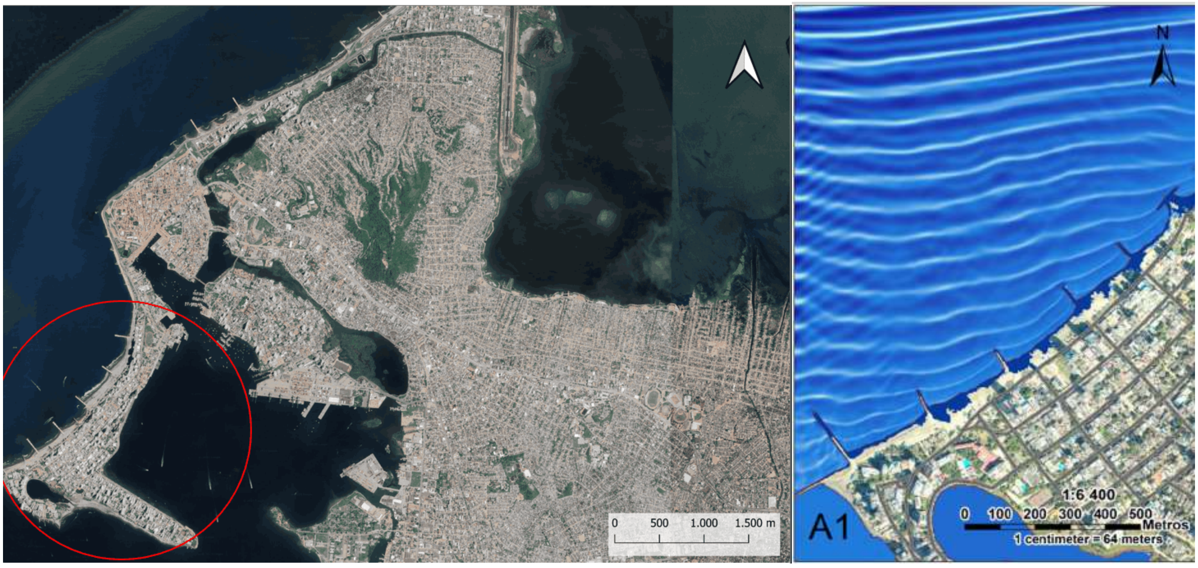

(a) (b)

Figure 3.16: a) Boca Grande is seen in the circle. b) Flood map results for a high tide and a wave height of 3 m (Orejarena-Rondon et al., 2019).

Wave upset is not considered a significant issue in the study area, primarily because the Ciénaga de la Virgen is sheltered from coastal waves. Water levels in this study area are correlated with the tidal water levels described in Section 3.2.4, as further elaborated.

3.2.6. Relative sea level rise (RSLR)

Sea level rise

The current existing flooding problems are anticipated to exacerbate due to climate change. In Cartagena, the sea level rise (SLR) has averaged 5.6 mm/year over the last century, surpassing the global average of 3.4 mm/year (NASA, 2023b; Torres & Tsimplis, 2012). Presently, under the SSP2-4.5 scenario, a rate of 8.7 mm/year is projected (NASA, 2023a). This SSP2-4.5 scenario is classified as the 'middle of the road' scenario. The scenario expects an estimated maximum temperature rise of 2.7 °C by 2100 (Januta, 2021). According to this scenario, the sea level is expected to rise by 34 cm by 2050.

Subsidence

Subsidence is also a significant concern in the city. In Restrepo-Angel et al. (2021), subsidence rates were determined using various methods, with average rates ranging between -5.70 mm/yr ± 2.18 mm/yr and -2.85 ± 0.84 mm/yr. The highest rate of subsidence, -12.87 mm/yr, is found in the Ciénaga de la Virgen area.

In conclusion, the combination of sea level rise with subsidence indicates a RSLR of 46 cm by 2050 (Restrepo-Angel et al., 2021). This value is utilized to examine the resilience of the proposed mitigation measures against the projected increase.

3.2.7. Coastal erosion

Cartagena's appeal for tourism is significantly attributed to its beaches. However, the tourism sector is facing the challenge of beach erosion. In the Cartagena area, maximum erosion rates of 2 m/year have been observed for the Playetas area, 3 m/year for the Tierrabomba island, and 1.7 m/year for the urban city centre of Cartagena. The erosion is attributed to a combination of factors, including wave energy concentrations and propagation patterns, sea level rise, tectonic movement, and human interventions (Rangel-Buitrago et al., 2015). The coastal erosion of the area is visualized in Figure 3.17.

Figure 3.17: Risk on coastal erosion in Cartagena (MIDAS, 2019)

The thin area connecting the Ciénaga with the sea is not very susceptible to erosion. So a breach from the sea to the Ciénaga is not likely to happen. Therefore, for completeness, this has been investigated but does not have an affection for the study area and this will not be further elaborated.

3.3. Data gap analysis

While searching for the data described Section 2.1, some data appeared to be incomplete and therefore cannot be included in the analysis of the system. This consists of the following:

- The flood levels per certain events were desired. This allowed something to be said about the consequences of flooding for which condition. There is searched extensively, but the only sources to be found, are pictures of floods and a community interview from Edurbe missing context (also see Section 3.2.5). The pictures lack unfortunately location or dates. This can say something about the order of magnitude of the floods but cannot describe under which conditions these floods occurred. The community interview of Edurbe included flood depths. Unfortunately, no context is given for these water depths. These values were used in some sort of validation for the computational modelling study of Edube. The boundary conditions under which the Edurbe modelling study was a rainfall intensity of 185 mm/day (a 100-year extreme rainfall event). It is assumed that the computational results were validated with these green data points in Figure 3.15. The results fromSection 4.2.5 shows good resemblance between the flood levels and the results of the model, making the assumption about the conditions of the Edurbe study to be likely. This uncertainty makes it difficult to verify the numerical model against a historical event but it is done as well as possible. Consequently, the model will always have to be treated as conceptual.

- The short-time rainfall interval data is deemed unusable. As the rainfall events in Cartagena can be very short and very intense, this research lacks that information. To work around this problem the rainfall distribution from Edurbe (also see Section 3.2.3 and Appendix B.2) is used to analyse a realistic rainfall distribution.
- The last big data gap was water levels in the Ciénaga de la Virgen. No water level time series could be found inside the wetland. Therefore it is assumed that the tide inside the bay acts the same on the Ciénaga de la Virgen.

Considering these workarounds, the system description can be made in Section 3.4.

3.4. System description based on available data

The analysis reveals challenges for the study area's water system, requiring a comprehensive approach to effectively design mitigation measures that can address the problems. The key findings help in understanding the current system within the study area.

Most of the identified channel dimensions indicate an insufficient drainage capacity, leading to the conclusion that a rainfall event with a return period of 2 years would cause flooding, particularly in region #1 of Figure 3.1.

The study area exhibits significant variations in altitude, contributing to the demand for high drainage capacity. The rapid runoff to the channels is influenced by these substantial differences in elevation. Furthermore, these significant elevation differences suggest that rainfall is likely the predominant factor. Rainwater naturally seeks the path of least resistance, flowing to the low-lying areas as quickly as possible. However, water flow tends to stagnate downstream in the areas with milder slopes at the banks of the Ciénaga. The tidal range is limited to around 30 cm above sea level. Nonetheless, most residents on the banks of the Ciénaga live, on average, only 2 meters above the water line, and most downstream ends of the channels are below the water line, thus filled throughout the year. The filled cross-sections make it difficult for rainwater to flow out into the Ciénaga, leading to the hypothesis that the water level downstream significantly influences floods around the Ciénaga banks. Sea level rise could therefore increase the influence of the water level on the floods and impact the residents living at the border of the Ciénaga.

The data does not distinctly support a trend of increasing annual cumulative precipitation. The analysis reveals that October and November have emerged as the wettest periods, indicating an increased occurrence of both intense rainfall and prolonged droughts in recent years. Notably, the record-breaking daily rainfall of 222 mm/day, documented on 02-10-2016, underlines the potential for extreme precipitation events. Thus, the extreme value distribution for rainfall intensities provides insights into the occurrence of these intense precipitation events. Yearly reoccurring rainfall events of approximately 100 mm/day were found. About 70% of the extreme rainfall events have a minimum duration of 7 hours, and approximately 71% of the precipitation occurs within the first 1.5 hours, suggesting that the intensity and duration of the rainfall play crucial roles in the occurrence of flooding (Hawkins & Quintero Banda, 2022).

Given that the most extreme rainfall typically occurs between October and November, the tidal predictor is configured to these water level variations. The maximum observed water level variations within the predicted data are approximately 40 cm in a single day. The extreme high and low tides projected for an annual cycle are found to be 0.30 meters above and -0.20 meters below sea level, respectively. The influence of the tide is expected to extend toward the whole bank area if the projected relative sea level rise is realized by 2050. An additional 47 cm rise could permanently flood a portion of the southern border of the Ciénaga de la Virgen, exacerbating drainage issues during storm events.

3.5. Conclusion

After conducting the system description outlined above, Sub-question 1 can be addressed through the formulation of a hypothesis. The drainage capacity is anticipated to pose a significant challenge for most parts of the drainage system. The high altitude variations upstream would indicate that the flooded areas would be predominately on the downstream end of the channels where the slope stagnates. The rainfall intensity is so significant that it alone is expected to have a huge impact on the floods. However, the lower-lying areas, which have small elevation differences, are likely to become more reliant on water levels, as the projected that a relative sea level rise of 47 cm will have a significant impact on the drainage system overall. These hypothesized conclusions will be verified against the model study in Chapter 4.

4

Modelling Study

4.1. Introduction

Chapter 3 addresses various types of flooding-related issues. The assessment concluded that drainage capacity and the water level downstream are identified as the main sources in the study area. The relatively low-laying neighbourhoods at the edge of the Ciénaga are highlighted to be increasingly influenced by the relative sea level rise. The data analysis of Chapter 3 provided qualitative insights into the sources of flooding. This chapter validates the conclusion quantitatively. The impact of meteorological conditions and downstream water levels on flooded areas is investigated using a D-Hydro model. By simulating different scenarios, the model quantifies for areas what are the dominant factors influencing flooding. Knowing the most influential source of flooding for each area proves to be crucial for developing effective mitigation measures.

4.1.1. Model choice

A numerical model is set up to quantify the impact of the different flood situations. The software used for the numerical modelling is D-Hydro 1D2D, which was developed by Deltares. D-Hydro is the successor of Delft3D and SOBEK. It combines the two into one integrated model. This model is chosen over HEC-RAS since it can be 6 to 10 times faster. Moreover, when atmospheric forcing is considered, D-Hydro demonstrates significantly higher accuracy (Munoz et al., 2021). This aspect is crucial as the majority of catastrophic floods since the 1990s have been attributed to atmospheric pressure changes (Bharwani, 2020). These types of floods are to be investigated in this study. Additionally, another reason for using D-Hydro software is the application history of D-Hydro. By combining Delft3D and SOBEK in D-Hydro, this new software can be used for new purposes. Using this combination of models maximizes their strengths by complementing (Teng et al., 2017).

Multiple numerical studies have been done in the city of Cartagena with other types of numerical software. For instance Cañate and Guzmán (2017) used MIKE to determine the flood levels at the system of lakes and channels on the west side of the city. Another study is conducted by Edurbe (2022), a local company committed to the Bolivàr region's urban development. The Edurbe study investigated the flood hazard through hydraulic and hydrological analyses with the HEC-RAS software. However, further research would be useful to further explore the possibilities of numerical modelling (Teng et al., 2017).

As far as known, D-Hydro software has not been used in previous studies for modelling mitigation measures. This also applies to the studies mentioned above using different numerical software. Thus, evaluating the application of mitigation measures and the performance of the D-Hydro software software would be beneficial for studies in the future.

4.1.2. D-Hydro

D-Hydro is a software developed by the Dutch company Deltares. It integrates former separate software Delft3D 4 and SOBEK 2 (Deltares, 2023a). The modules that will be used for setting up the model with this software are the D-Flow and the D-Rainfall Runoff modules.

D-Flow 1D/2D

This module works in a 2D depth average way and resolves the continuity (Equation (4.1)) and the Navier-Stokes (Equation (4.2) and Equation (4.3)) implicitly in the D-FLOW module (Munoz et al., 2021). This contains the 1DFLOW and 2DFLOW of the previously used SOBEK suite (Deltares, 2023d).

$$\frac{\partial h}{\partial t} + \frac{\partial (uh)}{\partial x} + \frac{\partial (vh)}{\partial y} = 0 \tag{4.1}$$

$$\begin{aligned} \frac{\partial u}{\partial t} + u\frac{\partial u}{\partial x} + v\frac{\partial u}{\partial y} + fu \\ = \frac{\rho_a C_d \left(U_{10} - u\right)}{\rho(d+h)} \left(\left(U_{10} - u\right)^2 + \left(V_{10} - v\right)^2\right)^{\frac{1}{2}} - \frac{\rho g n^2}{d^{\frac{1}{3}}} u \left(u^2 + v^2\right)^{\frac{1}{2}} \\ + v_H \left|\frac{\partial^2 u}{\partial x^2} + \frac{\partial^2 u}{\partial y^2}\right| - g\frac{\delta h}{\delta x} \end{aligned} \tag{4.2}$$

$$\begin{aligned} \frac{\partial v}{\partial t} + u\frac{\partial v}{\partial x} + v\frac{\partial v}{\partial y} + fu \\ = \frac{\rho_a C_d \left(U_{10} - v\right)}{\rho(d+h)} \left(\left(U_{10} - u\right)^2 + \left(U_{10} - u\right)^2\right)^{\frac{1}{2}} - \frac{\rho g n^2}{d^{\frac{1}{3}}} v \left(u^2 + v^2\right)^{\frac{1}{2}} \\ + v_H \left|\frac{\partial^2 u}{\partial x^2} + \frac{\partial^2 u}{\partial y^2}\right| - g\frac{\delta h}{\delta x} \end{aligned} \tag{4.3}$$

D-Rainfall Runoff

The D-Rainfall Runoff (D-RR) module is a component of the old SOBEK suite used for modelling rainfall runoff in rural and urban areas. The D-RR module is designed to simulate the hydraulic processes that occur in catchments, including infiltration, evapotranspiration and surface runoff (Deltares, 2023b). The module can be used to predict the effects of land use change, climate change and other factors on the water cycle.

When combined, the D-RR and the D-Flow modules can provide a comprehensive picture of the hydrological cycle and the impact of water flow on the environment and infrastructure. In Figure 4.1 the steps in the modelling process of D-Hydro are shown that are used in this research.

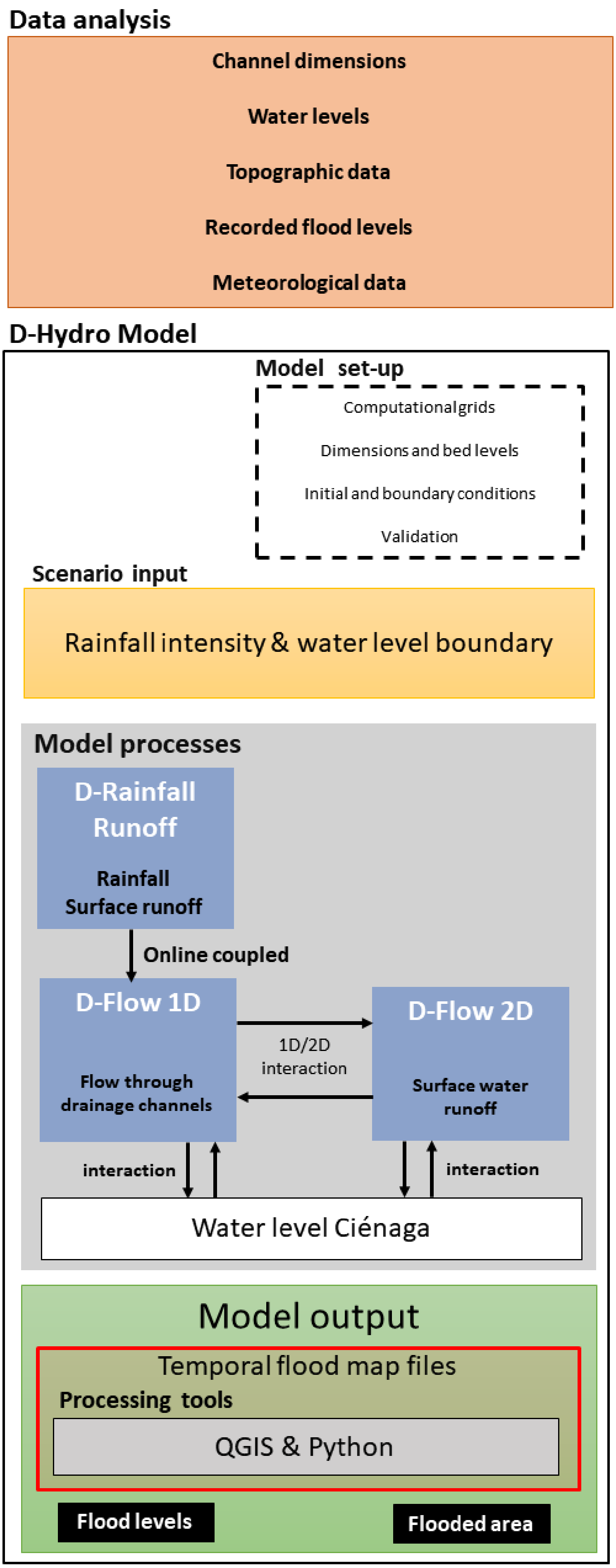

Figure 4.1: The block scheme of the modelling study. The orange block indicates the input used in the modelling. The black framed box indicates the steps and processes within the modelling study.

Setting up the model is discussed in Section 4.2 after which the model output is discussed in Section 4.3.

4.2. Model set-up

The setup of the model contains the following steps:

1. Computational grids
2. Dimensions and bed levels
3. hydraulic boundary conditions

The following paragraphs will describe the steps briefly to explain certain assumptions.

4.2.1. Computational grids

Computational 1D grid

A shapefile (.shp) containing the channels, obtained from GIS data, indicates the outlines of the channels into the D-Hydro Graphical User Interface (GUI). This shapefile facilitated the depiction of every channel within the study area in D-Hydro. Grid points are generated along the water branches to enable computations on the one-dimensional grid. These computational grid points were spaced at intervals of 50 meters.

Creating 2D grid

A rectangular grid is generated from a polygon. To minimize the computational time without compromising accuracy, the grid size is set at 10 by 10 meters. The grid is cut off underneath the end nodes of the branches. This configuration of the grid ensures that the water is effectively drained into the Ciénaga de la Virgen, preventing the accumulation of excess water within the network.

Creating 1D and 2D embedded links

To simulate the interaction between the 1D and the 2D grid, embedded links are established between the 1D grid and the 2D grid. These links check whether the water level in the channel of the 1D grid is higher than the cross-section height. If this threshold is exceeded, the water will flow from the 1D grid to the 2D grid. In the 2D grid, the water will flow according to the imposed bed level.

Figure 4.2 shows the generated grids and links. In Figure 4.2a the 1D branches and their computational grid are shown in more detail and in Figure 4.2b the 2D grid and the 1D and 2D links are shown in more detail.

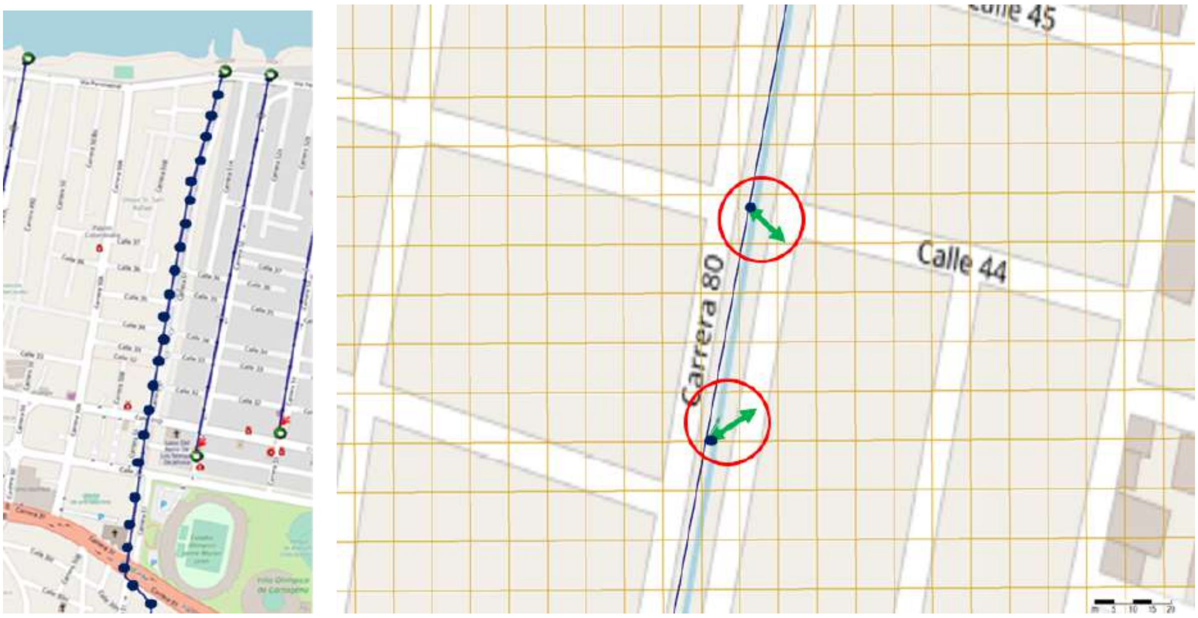

(a) Channel branches and 1D computational grid point

(b) 2D grid with 1D and 2D links

Figure 4.2: Computational grids more in detail.

4.2.2. Dimensions and bed levels

To apply the correct channel dimensions for each channel section, the channel overview presented in Appendix A is utilized. The cross-sections are shown in red in Figure 4.3. To ensure the right slope per section, cross-sections are added at the end at the beginning of a section with the right vertical shifts.

Figure 4.3: The 1D channel grid shown overlaid a map of Cartagena. The cross-sections are shown in red

Catchment areas

The catchment areas are determined with the help of the study of Edurbe (2022) and a catchment shapefile. This shapefile was provided by the company One Architecture & Urbanism. The shapefile's catchment areas approximately matched the values provided in the study of Edurbe. In Figure 4.4a the size of catchment areas that are used for the model are shown.

Only urban catchments are defined in this model. By defining all catchments as paved, all the water has to run off and nothing will infiltrate. This simplification represents therefore the worst-case scenario.

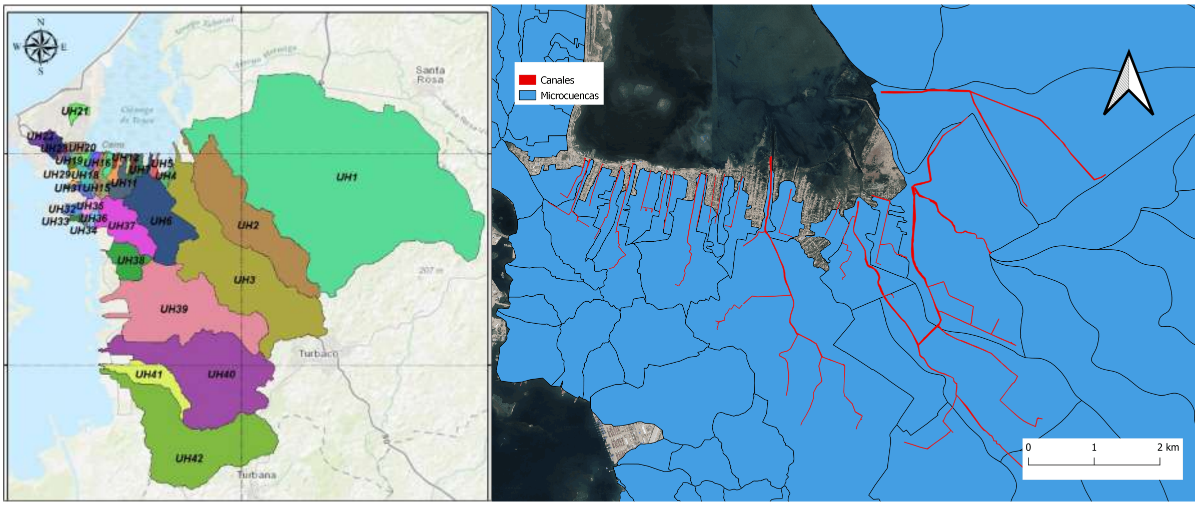

(a) The catchment areas correspond to the different channels (Edurbe, 2022).

(b) Catchment areas based on the microcuencas shape file.

Figure 4.4: Data for determining catchment areas

Table 4.1: The corresponding size of the catchment areas (Edurbe, 2022).

Id	Channel	Area $[km^2]$
UH1	Chiamaria - Flor del Campo	76.77
UH2	Calicanto	14.66
UH3	Matute - Chapundum	22.57
UH4	Playa Blanca	0.41
UH5	Maravilla	0.26
UH6	Ricaurte	7.35
UH7	El Tigre	0.48
UH8	Once de Noviembre	0.18
UH9	Paranegro	0.08
UHI0	El Villa	0.13
UHI1	Tabú	1.28
UHI2	Salim Bechara	0.4
UHI3	El Líbano	0.13
UHI4	San Martin	0.35
UHI5	Amador Auxiliadora	0.67
UHI6	Barbacoa	0.48
UHI7	San Pablo	0.27
UHI8	María Auxiliadora	0.82
UHI9	Bolívar	0.38

To define catchment areas, the regions listed in Table 4.1 are utilized. The lateral inlet point for collected water is strategically positioned upstream, to account for the worst-case scenario wherein all water flows through the entire channel.

The shapefile, which depicts the microcuencas, determines the inlet points per ramifications for the large channels. The inlet point for the ramifications was also chosen, whenever possible, at the upstream starting point.

In Figure 4.5 the final input of the catchment areas is visualized.

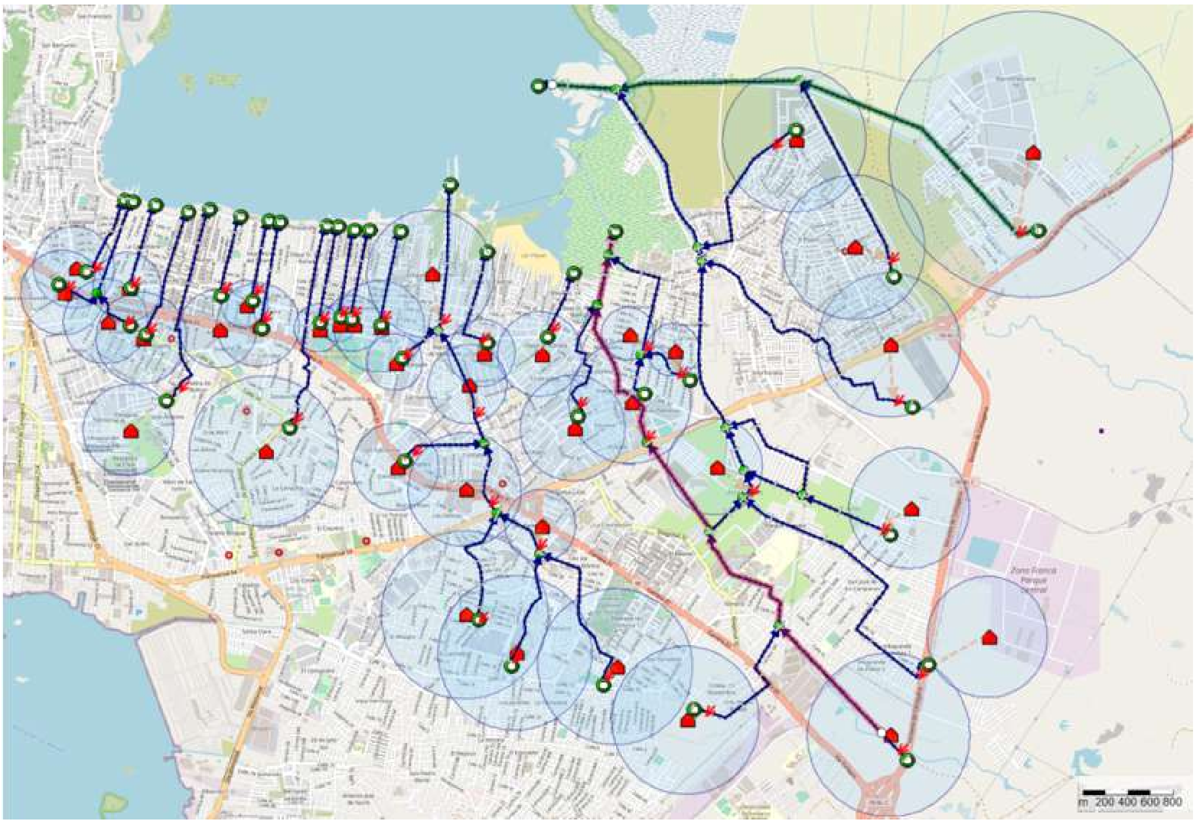

Figure 4.5: The D-Hydro interface including the determined (paved) catchment areas

Bed level

The bed level is determined by the topographic height map discussed in Section 3.2.2. This TIF file is converted to a *.xyz* file to meet the requirements of D-Hydro. The *.xyz* file is then interpolated to obtain the bed level per grid cell. Since the topographic height map has a higher resolution than the generated grid, the height is averaged over one grid cell. The lower eastern part of the grid lacks height information, this was solved by supplementing an additional DEM file. This secondary DEM file has a far lower resolution, so the average bed level was determined to be 13 m above sea level. The resulting bed level map is depicted in Figure 4.6.

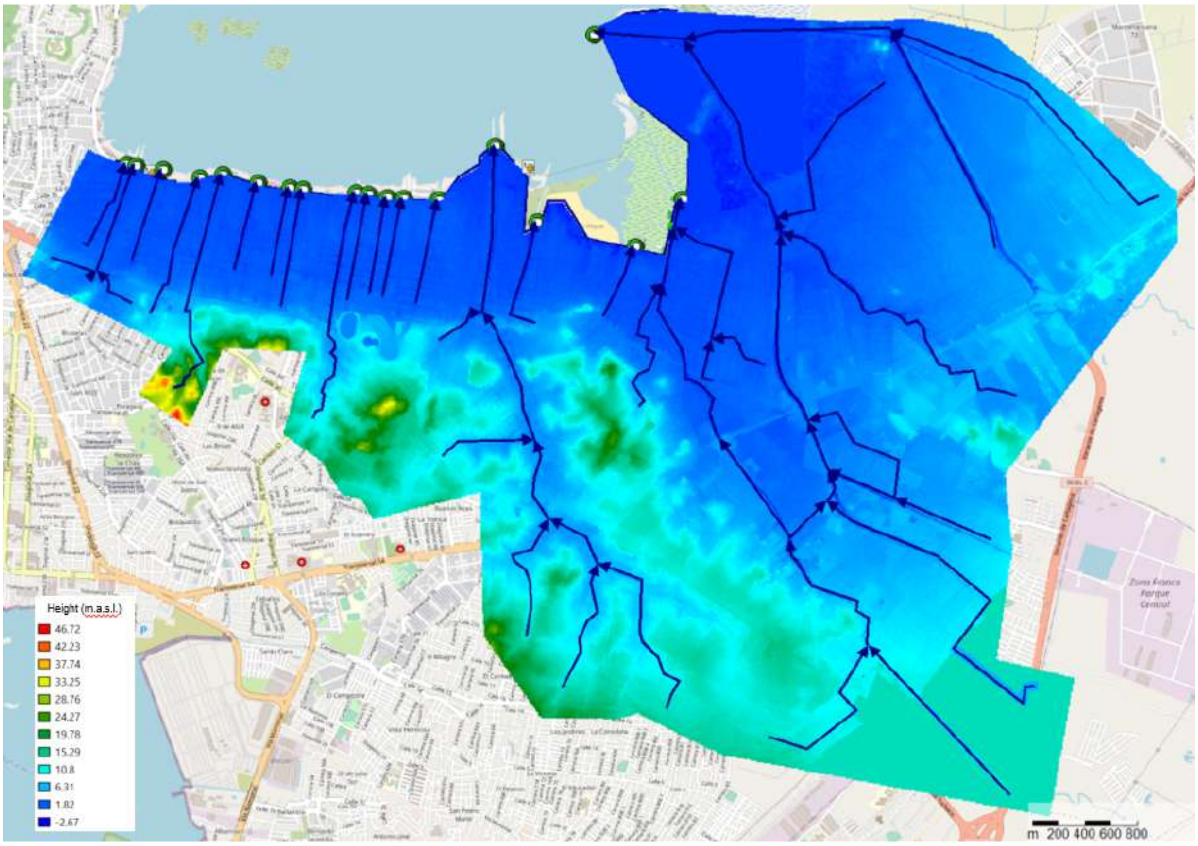

Figure 4.6: Interpolated bed level of the grid with relation to sea level.

4.2.3. Hydraulic boundary conditions

Add Boundary conditions

A boundary condition is applied to the border of the Ciénaga de la Virgen. For this side, a water level boundary is selected to allow the flooded water to flow out of the grid and simulate tidal conditions. The line indicating where the boundary conditions were imposed, is depicted as the black line in Figure 4.7. A more detailed description of the specific boundary conditions for each scenario is provided in Section 4.3.1.

Figure 4.7: The line where the water level boundary conditions are imposed.

Initial conditions

The initial conditions set in the numerical model are a water level of +0 m for both the 1D and 2D computational grids. This is the reference level assumed in the topographic map. This choice enables also the channels that are below sea level to be consistently partially filled with water, reflecting the real-life scenario.

The average Manning's roughness coefficient for the area is set at 0.023 to account for different channel conditions such as excavated sand channels and poorly maintained sections with vegetation (see Section 3.2.1). This coefficient takes into account channels with different characteristics, ranging from concrete construction (0.012-0.018) to sand-dominated areas (0.020-0.035) (Aldridge & Garrett, 1973). The choice of 0.023 strikes a balance and corresponds to the dominant sand roughness, as blockage by waste is common in both concrete channels and sandy areas.

4.2.4. Schematisation of the model

In Figure 4.8 a schematisation of the cooperate functions between the different D-Hydro modules is depicted. The D-RR module induces rainfall on a specific set area and flows using an inlet point on a one-dimensional grid (1D grid) through the set cross-sections. If the threshold of the cross-section is exceeded the water will flow onto the two-dimensional grid (2D Grid) using the 1D/2D links (1D/2D interaction). On the 2D grid, the water will flow according to the bed level. Also shown in Figure 4.1 the 1D grid and the 2D grid have an interaction with water levels downstream.

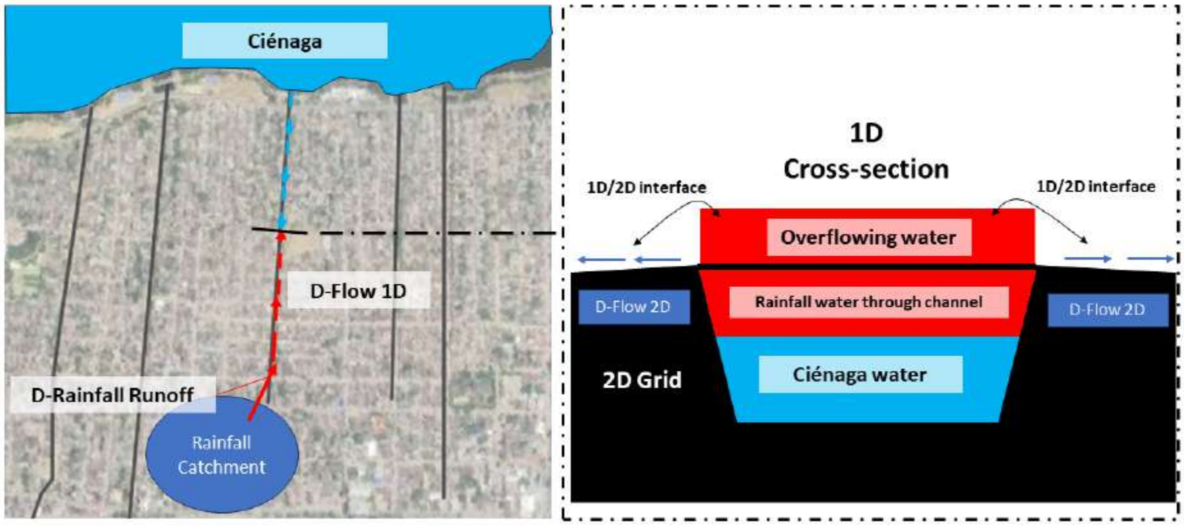

Figure 4.8: The schematisation of the D-Hydro model.

4.2.5. Validation of the model

As detailed in Section 3.3, accurate flood levels were not found during the data analysis. Consequently, the validation of the numerical model relies on the interpretation of results from the Edurbe HEC-RAS study (2022) and information gathered from news articles outlining the impacts of Tropical Storm Iota in November 2020. Given the absence of explicit details regarding the conditions of the community interviews conducted by Edurbe, the assumption is made that the values correspond to a 100-year Edurbe rainfall intensity.

Input calibration scenarios

The following boundary conditions are imposed for the following validations.

Table 4.2: The imposed conditions to validate the model.

Event	Rainfall [mm/day]	Water level [m]
Edurbe Tr 100 years	185	0.52
Edurbe Tr 500 years	195	0.52
14 November 2020 [Hurricane Iota]	83	Tidal sequence

The Edurbe studies employs an eight-hour rainfall duration, leading to the utilization of the distribution outlined in Table 3.3 for these intensities.

The rainfall intensity for the hurricane Iota scenario is obtained from the data detailed in Section 3.2.5. To recreate the conditions during Hurricane Iota, information from Time and Data AS (2023) is consulted, revealing that continuous rainfall occurred for 12 hours on November 14, 2020, from 6:00 am to 6:00 pm. The 12-hour rainfall distribution provided by EDURBE (2022) is therefore used (for more information see section B.2). Both distributions are presented more explicitly in Table B.6.

The water level input in the Edurbe HEC-RAS studies area was set to 0.82 meters above sea level (Edurbe, 2022). Because this study does not specify the reference level, it is assumed that the mean sea level was +0.30 meters for this study (EDURBE, 2022). To compare the water level in the Edurbe study, the water level in the D-Hydro model has to be set at +0.52 meters. This is because the reference level in this study was chosen as 0.00 meters. The water level boundary condition that is imposed for the Hurricane Iota scenario is the tidal sequence for that day. This was generated by the tidal predictor, shown in Section 3.2.4. This predictor generated a tidal water level every 10 minutes. For more information about the tidal water level sequence section C.2 can be consulted.

Results comparison Edurbe scenario

The results of the models are compared with the floodwater levels documented in Edurbe (2022) (refer to Section 3.2.5). Using the Crayfish plugin in QGIS, the water level time series are visualized for the verification points. The maximum flood levels for these validation points are depicted in Figure 4.9. Including the values from Table 3.7 in the comparison yields the results presented in Table 4.3.

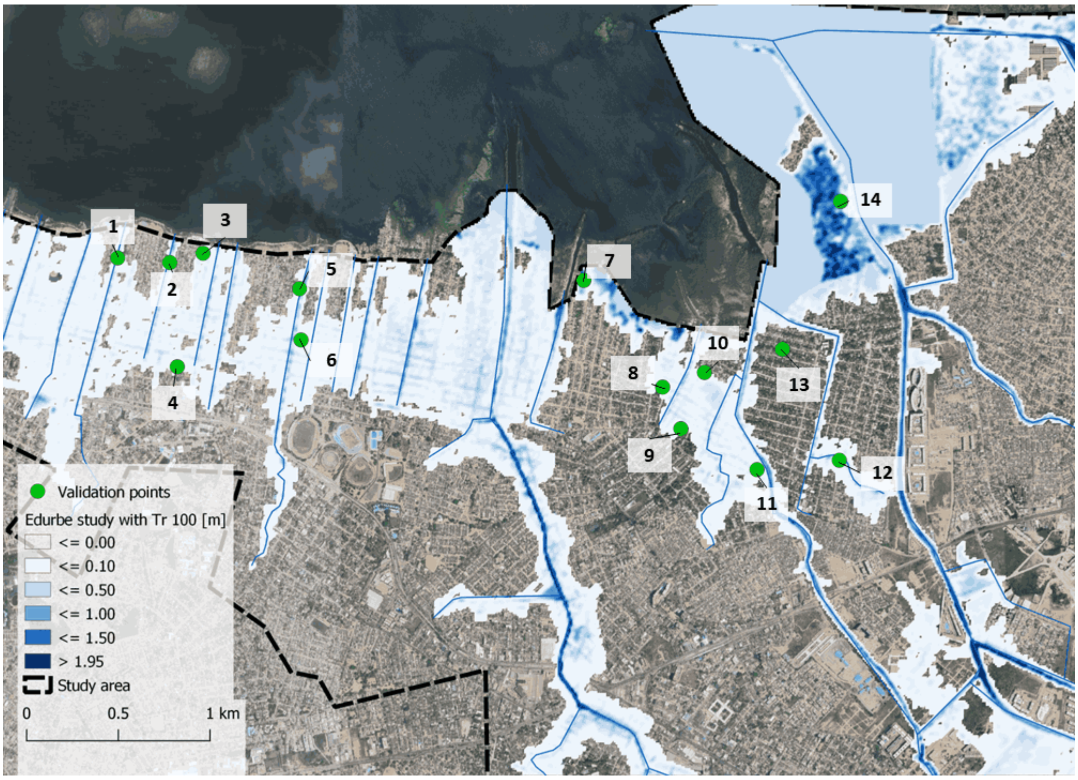

Figure 4.9: The flood map result of the D-Hydro model using the input of the Edurbe study with its validation points.

Table 4.3: Comparison between the found water depth from the community interview by Edurbe and the output of the D-Hydro model.

Point number	**1**	**2**	**3**	**4**	**5**	**6**	**7**	**8**	**9**	**10**	**11**	**12**	**13**	**14**
Edurbe flood level [cm]	70	80	30	60	50	80	90	80	70	90	60	50	30	65
D-Hydro flood level [cm]	74	76	24	53	48	77	87	54	60	44	57	43	0	65
Difference [cm]	+4	-4	-6	-7	-2	-3	-3	-26	-10	-46	-3	-7	-30	0

Only significant differences are observed in points 8, 10, and 13 compared to the results of the community interview. The average difference across all points is approximately 11 cm. Points 10 and 13 did stand out as the severe outliers. Interestingly, point 13 remains unaffected by flooding in the model. However, a reported depth of 30 cm was recorded. Points 1 to 7 are largely consistent with the reference values used for comparison. Point 14 did show even no difference at all.

The following can be concluded about the model's performance:

- The west part of the model shows better overall performance.
- The model produces slightly lower values.
- The model performs adequately overall.
- At point 13 large differences are found as there is no flooding visible at this point.

Results comparison hurricane Iota scenario

The flood levels are not available for this scenario. The neighbourhoods that experienced flooding are stated (Caracol Radio, 2020). The results of simulating this scenario are shown in Figure 4.10.

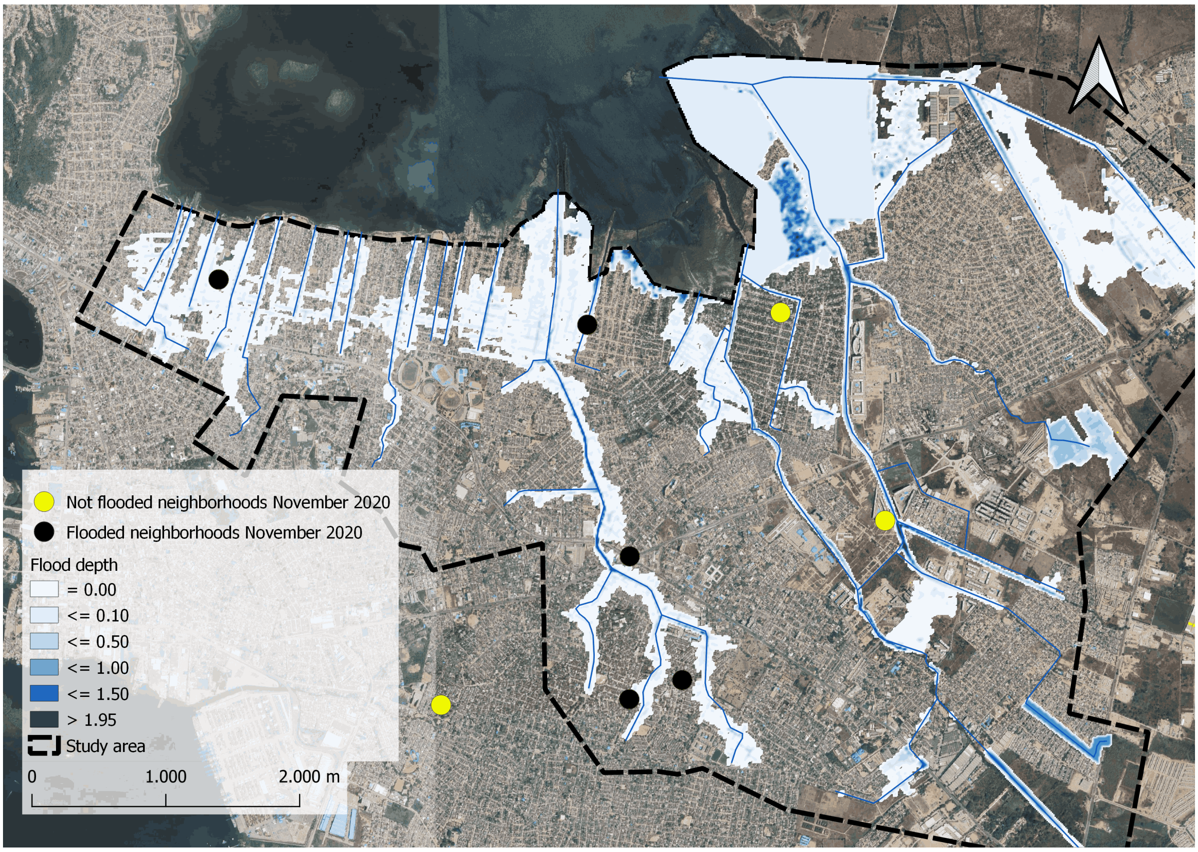

Figure 4.10: Flood map when simulating 14-11-2020 with the D-Hydro model.

In the end, 5 out of the 7 districts are indeed affected by flooding. Only the neighbourhoods of Vila Rosita (southern yellow dot) and Fredonia (northern yellow dot) do not show flooding in the model, despite previous news reports suggesting otherwise. Furthermore, the areas upstream only show minor cases of flooding. The area does not show a pattern of structural flooding.

The following can be concluded about the performance of this scenario:

- The neighbourhood of Fredonia (also point 13 of the Edurbe validation points) is again showing different results than expected. One of the reasons could be the assumption of clean channels. Another reason could be, perhaps due to land subsidence, the height of the topographic map no longer matches exactly.
- The flooding upstream is lower than would be expected from a disaster. A reason for these small flooded areas would be the relatively low rainfall intensity of the hurricane. This could already be an indication that these areas are dependent on their hydraulic capacity.

Based on the available information on the two validation scenarios, the conclusion is that the model performs sufficiently well for the purposes of this research. Despite some discrepancies in the areas around the bigger channels, the model's output generally aligns with the reference values and previous reports. This indicates that the model can capture and simulate flood events to a satisfactory extent.

The area around the east side of the Ciénaga's bank requires further attention when relying on the model's outcome. However, the model's performance can still be considered reliable and suitable for further use in this research. The model serves for addressing flooded areas and predicting flood levels, which can contribute to ultimately indicate the impact of a mitigation measure. By acknowledging its limitations and/or terminating specific areas of concern, the model can be further used. Furthermore, when more flood data is available more validations can be made, ultimately improving the model.

4.2.6. Model-based Assumptions

Although the model performs sufficiently well, the set-up of the model has used assumptions that have to be taken into account when interpreting the results. These assumptions are listed below.

1. The catchment areas are defined by a predetermined area. This means that the topographic DEM file is not used to determine the catchments within the model. Therefore are two reasons. The first reason is to ensure that the water is entering the 1D grid. The second reason is to ensure the full run-off area of catchments that extend further than the borders of the topographic DEM file.
2. The rainwater from the defined catchment area is collected at a single lateral inlet point at the start of the channel. In reality, the water from the catchment flows into the channel along the entire length of the channel. The reason for schematising the model in this way is to investigate the response to peak flows through the full channel. However, for the large channels with very large catchments (which include rural drainage) and side arms, the catchment is divided into smaller sections with more lateral entry points. This is done to increase realism for these channels.
3. The model lacks detailed calibration and validation. Ideally, more information should be collected about the flooded areas and their flood levels. However, the model has been validated as well as possible. Should more data become available in the future, it could be used for better calibration and validation.
4. The overlapping 2D grid is linked to the 1D grid. The embedded links used for this could result in so-called double storage. Double storage happens because the water can be stored within the cross-section and also in grid cells with a lower bed level. The west side of the model has relatively small cross-sections. This extra storage in the 1D model is significantly small compared to the storage in the grid. For the east side of the model, where the cross sections are much larger, this double storage could result in lower flooding values when compared to reality. This could explain the lower generated values shown by the model in the validation (Section 4.2.5). The bed levels of downstream channels are below the water line as imposed by the initial conditions. As the cross-sections are initially filled double storage is not possible in these sections. However, a better representation would be to terminate the 2D grid around the channels and create lateral links towards the banks. This would require a lot of set-up time as D-Hydro's interface does not support creating lateral links inside the grid but places them towards the outer edges of the grid. The links would have to be placed manually. Furthermore, fixed weirs should be installed on both sides of the channel to establish the right threshold. These fixed weirs would have to be laid through the links; this would be a difficult procedure for such a small distance. Lastly, the grid has to be more refined toward the banks to get a good representation of the flow of the excess water. This would increase the computational time. As a result of these arguments, the double storage is taken into account in the evaluation.
5. No hydraulic structures are included in the model This choice was made to simplify the model and reduce setup time.
6. Although Section 3.2.5 shows that the channels are blocked by domestic waste, it assumes that the channels are clean and have a clear cross-section. For a small part, this is accounted for by the chosen Manning's coefficient. However, this will only partly delay the flow velocity and not decrease the capacity of the channels. This assumption should lead to an underestimation of the results. This could be one of the main reasons that the validation of the model also leads to an underestimation. The overall assumption for clear cross-sections was made because a drainage system will have no impact if it is not cleaned. So this should be set as the highest priority as also already mentioned in Local authorities (2009).

4.3. Quantification of Flood Impact

The objective is to quantify the current occurring floods and identify the influence of Ciénaga's water level and the influence of rainfall. The areas that are influenced by the two sources are expressed within three types of different zones of influence (Shen et al., 2019);

1. Tidal zone
2. Transitional zone
3. Hydraulic zone

Defining these zones clarifies which types of mitigation measures could be suitable to explore for certain areas.

Nine different scenarios are simulated with the D-Hydro model to provide information about the influence of downstream water levels and extreme rainfall events. After simulating these scenarios, Sub-question 2 is answered.

4.3.1. Input scenarios

Table 4.4 shows the nine input scenarios that were simulated with the D-hydro model. The simulation times are set at 24 hours because these extreme rainfall intensities are used (mm/day). Also from Section 3.4 it became clear that short intense rainfall is one of the main reasons for flooding.

To investigate the influence of the water level, an extreme high tide (EHT), extreme low tide (ELT) and a tidal sequence (TS) are used as boundary conditions on the downstream side (see Section 4.2.3). The extreme high tide is the highest predicted tidal water level for a year. The extremely low tide is the lowest value found for an annual prediction (also shown in Section 3.2.4). The tidal sequence is chosen with a large daily inequality. Figure 4.11 gives a visualisation of the water levels and the cumulative rainfall distribution as input for the scenarios. The rainfall distribution shown in Figure 4.11 is taken from the 8-hour distribution discussed in Section 3.2.3 (for further details about the distribution Appendix B.2 can be consulted).

Table 4.4: The input scenarios for the D-Hydro model determining the different flood zones.

#	**Scenarios**	**Water level [m]**	**Rainfall [mm/day]**
1	Extreme Low Tide + Rainfall intensity with return period 2y	-0.20	124
2	Extreme Low Tide + Rainfall intensity with return period 10y	-0.20	183
3	Extreme Low Tide + Rainfall intensity with return period 100y	-0.20	277
4	Tidal Sequence + Rainfall intensity with return period 2y	Tidal sequence	124
5	Tidal Sequence + Rainfall intensity with return period 10y	Tidal sequence	183
6	Tidal Sequence + Rainfall intensity with return period 100y	Tidal sequence	277
7	Extreme High Tide + Rainfall intensity with return period 2y	0.30	124
8	Extreme High Tide + Rainfall intensity with return period 10y	0.30	183
9	Extreme High Tide + Rainfall intensity with return period 100y	0.30	277

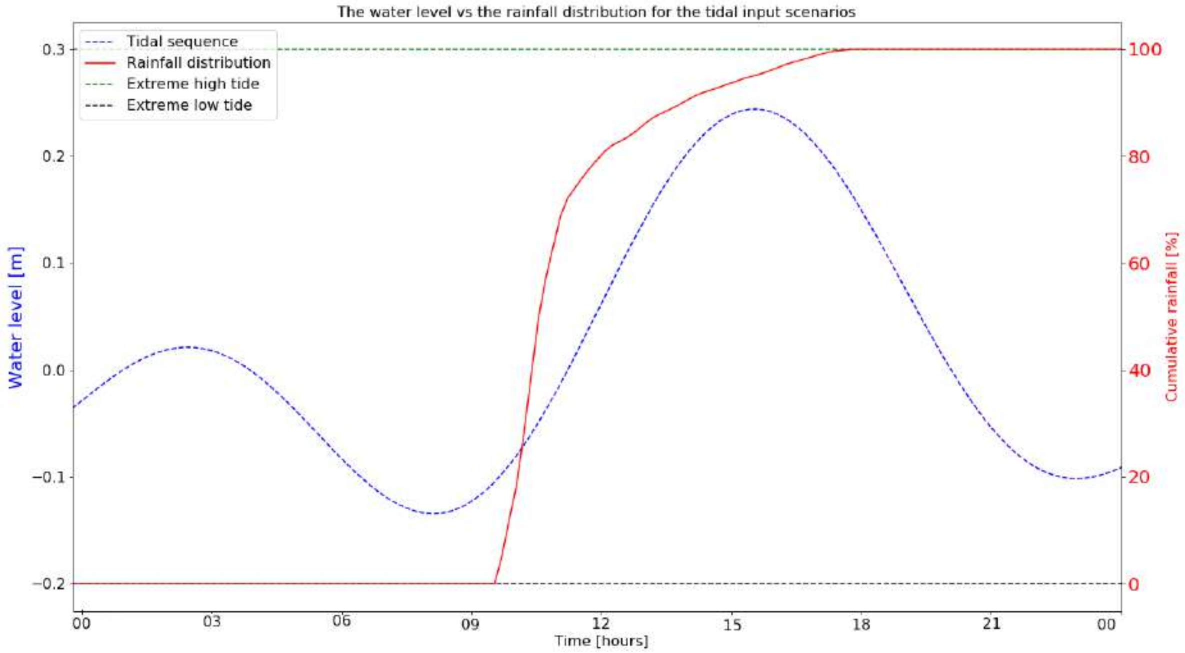

Figure 4.11: The input for the scenarios with the tidal water level and cumulative rainfall distribution

The reasons for using these scenarios are explained below:

1. The maximum water level difference will show the influence of Ciénaga's water level on the flooding. Using these extreme values maximises the visual difference.
2. Examining the influence of water levels under varying rainfall intensities could reveal differences in the influence of Ciénaga's water levels on runoff volume.
3. The tidal sequence scenario has been simulated to observe a more realistic scenario in outflow capacity.
4. Rainfall is distributed between 10:00 and 18:00. This time is chosen in combination with the water level to show the impact on the infrastructure and logistics chain during the peak hours of the day.
5. As stated in Section 3.2.1, most of the channels do not have the capacity for extreme rainfall with a return period of 2 years. This statement was verified.
6. The 10-year extreme rainfall event scenario is chosen to check a medium extreme event. This gives insight into the drainage capacity of the near future.
7. The 100 extreme rainfall event scenario is chosen to check the heavy extreme events and what would be the impact of such rainfall. This is done because the frequency of extreme rainfall events was higher in the last decades.

4.3.2. Zones of influence for existing situation

The results for these scenarios are shown in Figure 4.12. Here all the flood maps are combined into one matrix. The blue parts of the map indicate flooded areas. For the left column, the water levels are held at extreme low tide. The middle columns all have the induced tidal sequence and the right column experiences extreme high tide. The rows all experience the same rainfall. So the top row experiences rainfall with a return period of 2 years and so on.

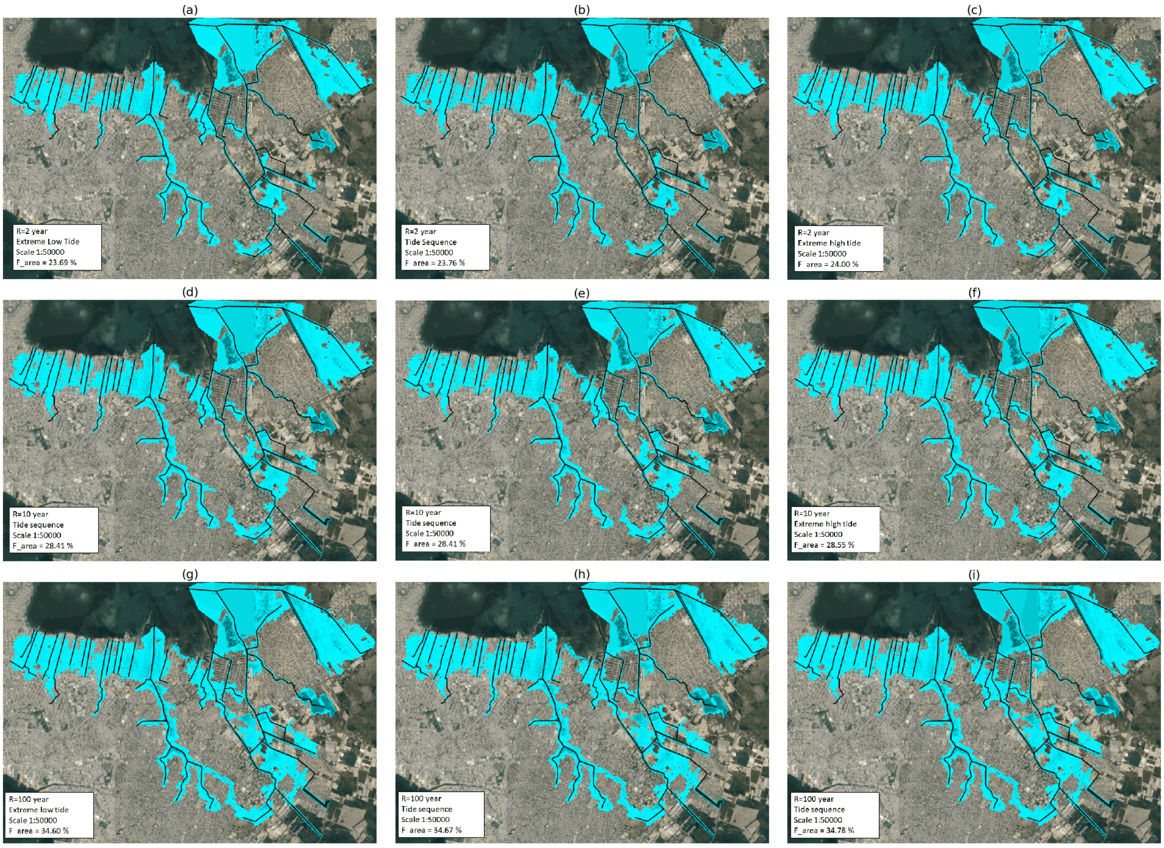

Figure 4.12: (**a-c**) Rainfall intensity with a return period of 2 years, (**d-f**) Rainfall intensity with a return period of 10 years, (**g-i**) Rainfall intensity with a return period of 100 years. (**Left column**) Extreme low tide, (**Middle column**) Tidal sequence, (**Right column**) Extreme high tide

Table 4.5: The corresponding percentages (%) of flooded areas for each scenario.

Flooded area [%]	Extreme Low Tide	Tidal Sequence	Extreme High Tide	Max. Δ
R = 2 years	23.7	23.8	24.0	0.3
R = 10 years	28.3	28.4	28.6	0.3
R = 100 years	34.6	34.7	34.8	0.2
Max. Δ	10.9	10.9	10.8	

Table 4.5 shows the flooded area per flood scenario. It can be seen that the influence of increasing rainfall is much more dominant than the influence of Ciénaga's water levels.

Water level difference

In Figure 4.13, the rainfall intensity is kept the same for each sub-figure to observe the influence of water levels visually. The coloured parts of the map indicate that there is flooding. The green colour shows the extreme low water scenario. Underneath this top layer are the other two scenarios. The yellow colour shows the tidal sequence scenarios and the red colour shows the extreme high water scenarios.

(a) The rainfall intensity has a return period of 2 years

(b) The rainfall intensity has a return period of 10 years

(c) The rainfall intensity has a return period of 100 years

Figure 4.13: The influence of the different imposed water levels for every rainfall return period. Green: Extreme low tide, yellow: Tidal sequence, Red: Extreme high tide

The increase in flooded areas due to the water level difference is around 0.22% (see Table 4.5). Figure 4.13, the difference is concentrated on the southeastern bank of the Ciénaga de la Virgen. This difference is very hard to see in the full overview figure, therefore Figure 4.14 zoomed in to this area

(a) The rainfall intensity has a return period of 2 years

(b) The rainfall intensity has a return period of 10 years

(c) The rainfall intensity has a return period of 100 years

Figure 4.14: The influence of the different imposed water levels including relative sea level rise for every rainfall return period.

In Figure 4.14a the difference is most visible. For the rainfall intensity with a return period of 100 years, two small spills at channels are visible but nothing significant. The difference in rainfall intensities does not show significant water level influence differences.

The difference in flooded levels is also examined for the study area. The flood level difference is calculated by subtracting the flood levels of scenario 1 from the values of scenario 7. The return period of 2 years is taken as this showed the most visual difference. Again only the southeastern border shows a difference. Therefore Figure 4.15 is zoomed in for this area.

Figure 4.15: The difference in flood levels for extremely high water level and a extremely low water level. The rainfall intensity in this case has a return period of 2 years.

The difference is measured in the flood level between the high-water scenario and the low-water scenario. The maximum differences lay at the edge and are around 1.5 m. These differences increase slightly towards the inland. This is where the difference is greatest.

Rainfall intensity difference

To investigate the increasing influence of the rainfall intensity, the water level boundary for each subfigure is kept the same to observe the influence of the rainfall in Figure 4.16. The coloured parts of the map indicate again that there is flooding there. The green colour shows the scenario for which the rainfall intensity had a return period of two years. Underneath that layer the two other scenarios are present. The colour yellow shows the scenarios with a 10-year rainfall intensity and the red colour represents the scenario with a 100-year rainfall intensity.

(a) Extra low tide

(b) Tidal sequence

(c) Extra high tide

Figure 4.16: The influence of the different rainfall intensities on the same water level

Regarding Figure 4.16 in general, there are many differences between the rainfall intensities visible. Especially in the upstream sector of the study area, this is noticeable. An increase in rainfall intensity from a return period of 2 to 100 years, results in an increase in flood area of 10.8%. So the influence of rainfall intensity is very present. For the lowest rainfall intensity, a flooded area of 24 % is already seen. This verifies the analysis of Section 3.5, the drainage system of the city has already too low a capacity for an extreme rainfall event with a return period of 2 years.

Zones of influence for the current situation

An extreme rainfall event with a return period of 2 years provides the ideal scenario to highlight tidal influence. To illustrate the different zones of influence Figure 4.17 is made. Within the tidal zone, flood levels depend on the water level at the boundary of Cienaga de la Virgen. In making Figure 4.17, the differences in flood levels are taken into account. The hydraulic zone includes the rest of the area affected by rainfall-induced flooding. In particular, the hydraulic zone is much bigger than the tidal zone. The tidal zone is mainly concentrated on the southeastern side of the Ciénaga boundary with less residencies.

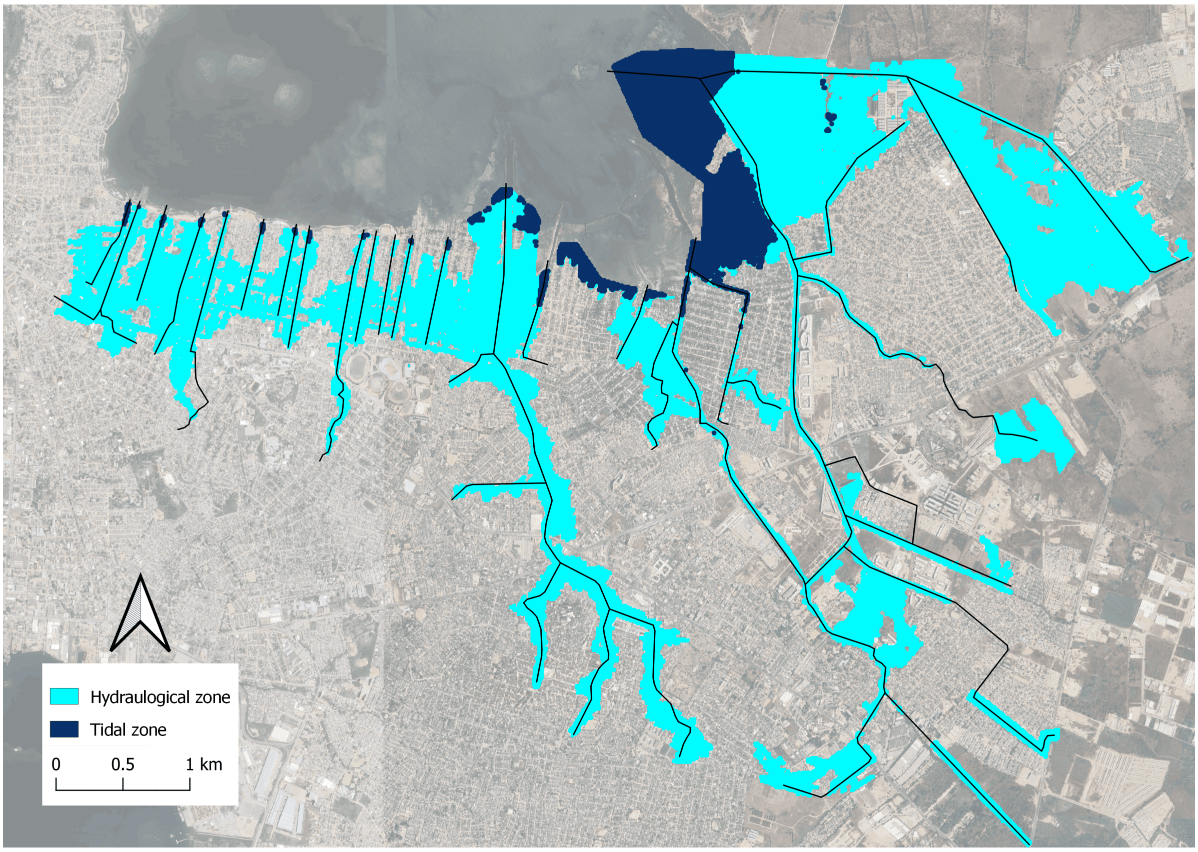

Figure 4.17: The different flooding zones of influence. Light blue is the hydraulogical zone which is dependent on the rainfall. Navy blue indicates the tidal zone.

4.3.3. Future scenarios

For future scenarios, relative sea level rise will double the tidal water level compared to the current situation and this could potentially change the classification of zones. Therefore, the scenarios are also simulated for the year 2050. Section 3.2.6 indicates that the relative sea level rise for this year is expected to be 47 cm. Therefore, this value is added to the water level input. This is shown in the new input graph in Figure 4.18.

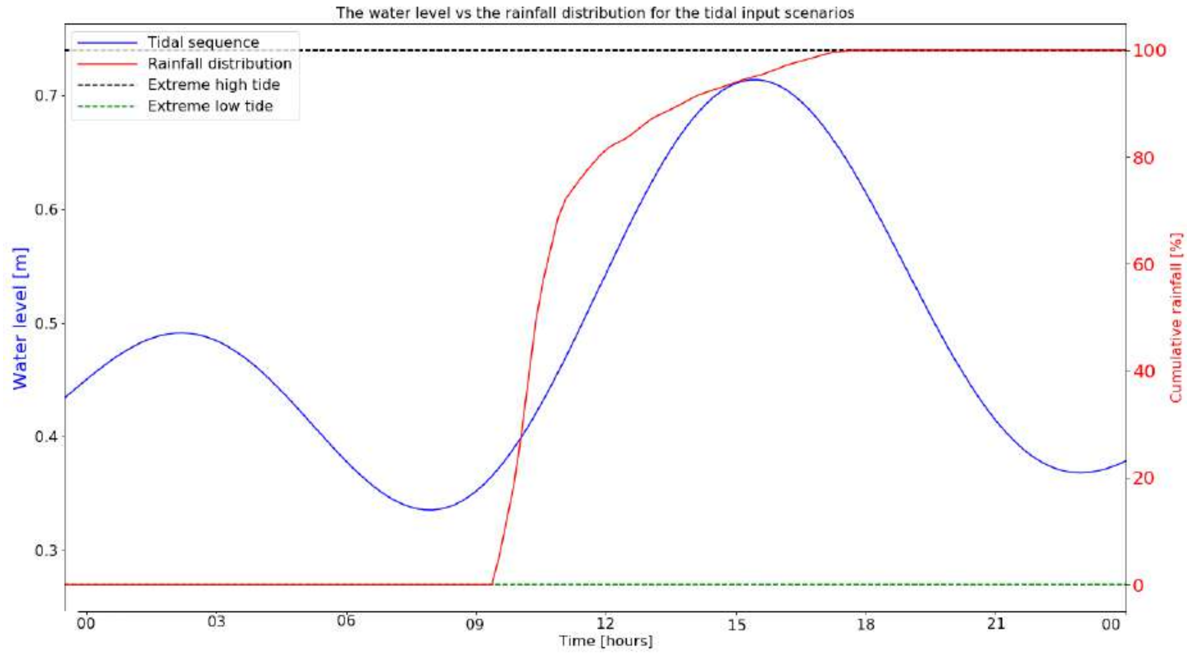

Figure 4.18: The input for the scenarios including relative sea level rise with the cumulative rainfall distribution

Future flood map results including relative sea level rise

To make a clear comparison with the current situation, the same scenarios are calculated. The resulting flood maps are shown in Figure 4.19. The corresponding percentage of flooded areas is shown in Table 4.6.

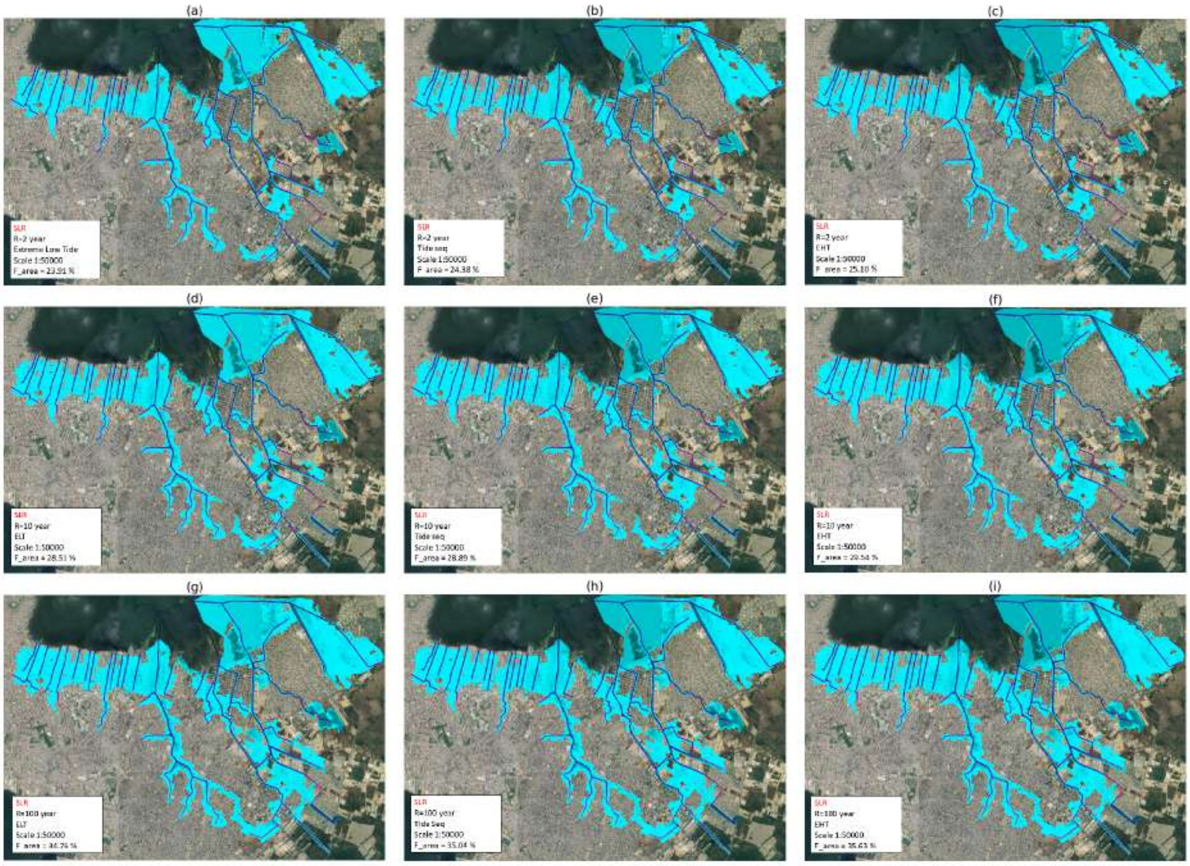

Figure 4.19: (**a-c**) Rainfall intensity with a return period of 2 years, (**d-f**) Rainfall intensity with a return period of 10 years, (**g-i**) Rainfall intensity with a return period of 100 years. (**Left column**) Extreme low tide + RSLR, (**Middle column**) Tidal sequence + RSLR, (**Right column**) Extreme high tide + RSLR

Table 4.6: The corresponding percentages (%) of flooded areas for each scenario.

Flooded area [%]	Extreme Low Tide	Tidal Sequence	Extreme High Tide	Max. Δ	Diff RSLR +/-
R = 2 years	23.9	24.4	25.1	1.2	**+0.9 (↑ 300 %)**
R = 10 years	28.5	28.9	29.5	1.0	**+0.7 (↑ 233 %)**
R = 100 years	34.8	35.0	35.6	0.8	**+0.6 (↑ 300 %)**
Max. Δ	10.9	10.6	10.5		
Diff RSLR +/-	**-0.0 (↓ 0.0 %)**	**-0.3 (↓ 3 %)**	**-0.3 (↓ 3.0 %)**		

In Table 4.6 the extra row is added as a comparison to Table 4.5. This extra information shows the increase or decrease in maximum differences between the scenarios.

The decrease in the differences between the rainfall scenarios is not significant (3% relative difference). One reason for this could be the size of the highly influential hydraulic zone. On the other hand, the increase in the influence of sea level is very significant (00% relative increase). The 47 cm sea level rise shifts the tidal influence from about 0.2 % to about 1.0 %. This is a shift towards tidal influence for the lower-lying areas.

Water level difference with RSLR

To show the influence more clearly in Figure 4.20 again the three different rainfall intensity scenarios are depicted per figure. Again the difference is made clear by the different colors.

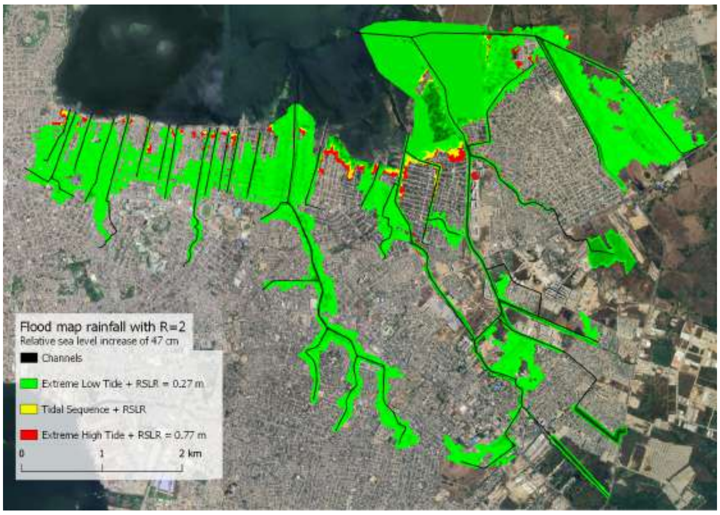

(a) The rainfall intensity has a return period of 2 years

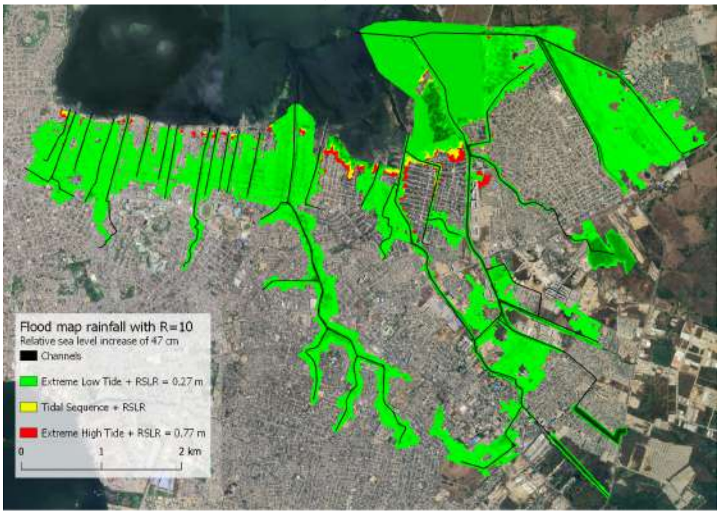

(b) The rainfall intensity has a return period of 10 years

(c) The rainfall intensity has a return period of 100 years

Figure 4.20: The influence of the different imposed water levels for every rainfall return period with relative sea level rise in the equation. Green: Extreme low tide, yellow: Tidal sequence, Red: Extreme high tide

Figure 4.21 zooms in on the area where the difference in zones is most visible. Taking the relative sea level rise into account, it becomes clear that the tidal zone now further extends to parts of the neighbourhood.

(a) The rainfall intensity has a return period of 2 years

(b) The rainfall intensity has a return period of 10 years

(c) The rainfall intensity has a return period of 100 years

Figure 4.21: The influence of the different imposed water levels including relative sea level rise for every rainfall return period

In the situation with relative sea level rise, there are more differences visible for the situation with the highest rainfall intensity. For this situation, flooding can now also be found in the middle of the neighbourhood. To observe the quantifiable differences in flood levels, Figure 4.22 is shown.

Figure 4.22: The difference in flood levels for extremely high water level and extremely low water level in a scenario with a relative sea level rise. The rainfall intensity in this case has a return period of 100 years

The zone influenced by the tide, is increasing land inwards. It is clear that the extension has increased, but also that the difference in high water levels has increased. The tidal influence zone has increased as seen in Figure 4.23. This threatens mainly the inhabitants of the southeastern neighbourhoods part of the Ciénaga's border. The biggest increase in influence is seen at the far east side of the border. Here the rural area between the three channels changed from only rainfall influence to be influenced by the water levels. These newly influenced tidal areas do not contain many residents. The change of influence of the increasing water level is significantly lower than was expected regarding the conclusion in Section 3.5. For the west side of the study area, only a small increase in tidal influence is seen. This small increase in water level influence there concludes that the topographic position of southwestern banks is not important regarding the influence of the raised water levels.

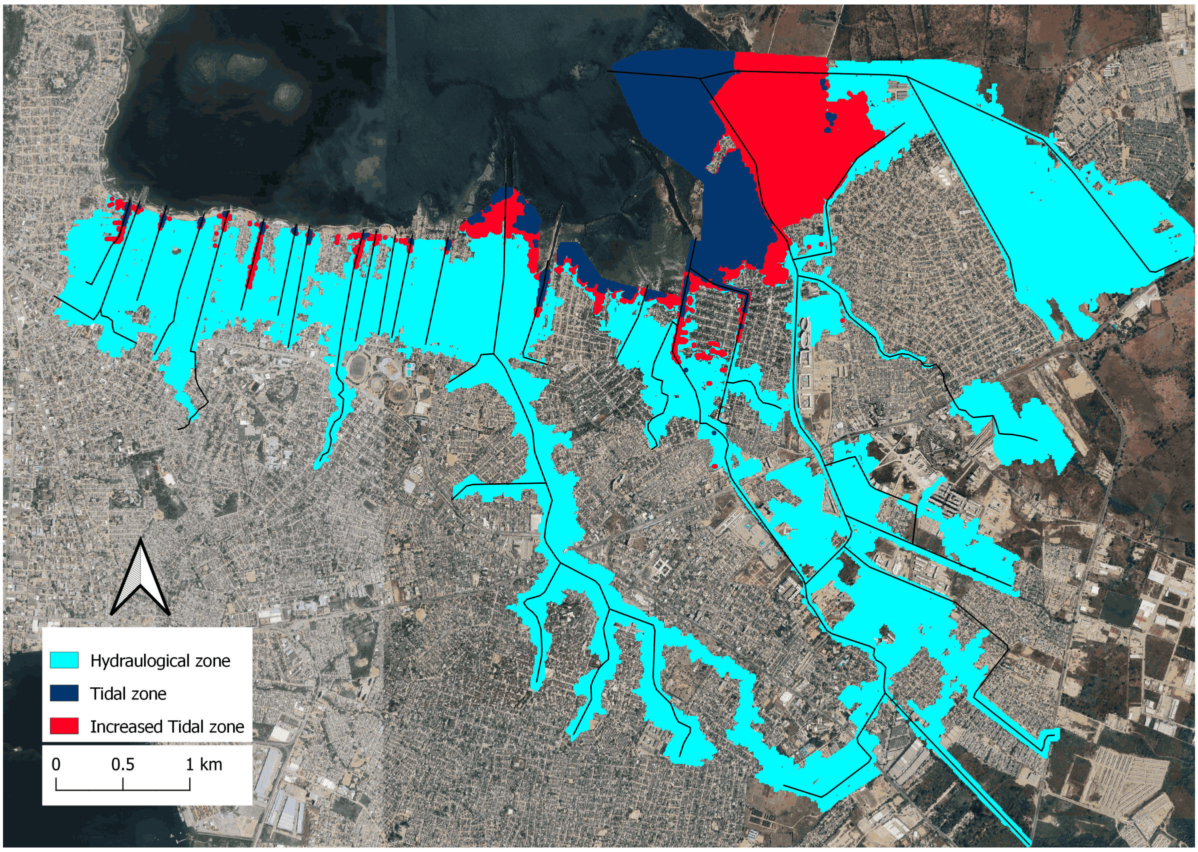

Figure 4.23: The shift in zones of influence. Light blue is the hydraulic zone which is dependent on the rainfall. Navy blue indicates the current tidal zone. Red indicates the increased tidal zone due to relative sea level rise.

4.4. Conclusion

Sub-question 2 of this study is to quantify the impact on flooded areas under different meteorological conditions and downstream water levels using a numerical model. The chosen methodology involves simulating different scenarios, including various extreme rainfall intensities and varying downstream water levels, to provide a comprehensive assessment of flooding.

The computational results obtained from the numerical model demonstrate the impact of flood sources. By systematically changing meteorological conditions such as rainfall return periods and downstream water levels, the model generates flood maps highlighting flooded areas for each scenario. Through quantitative analysis of these maps, it is possible to determine the percentage of flooded areas corresponding to different combinations of meteorological conditions and water levels and the differences in flood levels between the scenarios.

The results of this study show that rainfall intensity plays a more significant role in influencing flooded areas compared to downstream water level variations. The influence of Ciénaga's water level on the flood map is limited to a maximum of 0.27%. In comparison, the influence of rainfall intensity deviates with a maximum of 10.94%. The influence of the downstream water level is far less than expected.

By incorporating relative sea level rise as a future projection, this assessment is extended to predict potential changes in influence for the flood areas. The inclusion of these projections highlights the increasing influence of tidal conditions on the southeastern border due to sea level rise. The relative sea level rise shifts the border of the tidal zone inland into further-reaching parts of border neighbourhoods. The affected area is mainly on the eastern side. The south-western side of the banks is not as affected by the RSLR as hypothesized in the conclusion of Section 3.5.

These computational results ultimately conclude, for the current situation, a critical bottleneck in the capacity of drainage channels, evident even for rainfall events with a return period of 2 years. This underscores the need to focus on improving safety measures in the hydraulic zone, as it is a far bigger influence.

The results of this research have significant implications for applying mitigation measures. In the areas indicated as hydraulic, suitable types of measures can be explored. In addition, the incorporation of future projections also shows that the hydraulic zone should still have more priority over the tidal zone. The increase in the influence of the water level that was less than expected underlines this statement. However, the increasing tidal zone can be used to identify areas of importance for mitigating the rising sea level.

Based on the results, it is recommended that priority should be given to the improvement of the hydraulic zone for a rainfall event with a return period of 2 years. This leads to considering types of mitigation measures that should focus on the hydraulic zone.

5

Investigating possible types of mitigation measures and developing mitigation options

5.1. Introduction

After addressing Sub-question 2, the first part of the research has been completed. Now the second part of the research focuses on different types of mitigation measures that can be applied to the study area and evaluating their performance.

The first step is to select a specific focus area based on the conclusions drawn from Chapter 4. This allows for a more detailed analysis of the performance of a particular mitigation measure and ensures that the types of mitigation measures are applied in a more uniform area. It makes sure that the mitigation options can be compared to each other in the eventual MCA.

Next, the adaptation of the model to incorporate the selected mitigation measures is described. This includes modifications to the model to simulate the effects of the measures accurately.

Furthermore, a description of the different types of mitigation measures that were chosen is provided, along with the motivation for their selection. The impact of each type of measure is evaluated pragmatically, considering effectiveness and feasibility. Subsequently, the best feasible mitigation option for each type of measure is derived as an input for the MCA.

All this information serves as the basis for answering Sub-question 3: *"What type of mitigation measures are possible to develop into a mitigation option to reduce floods in urgent zones?"*

5.1.1. Focus zone

Figure 5.1 shows the focus area. The focus area is divided into three zones for clarity when addressing comments in this area.

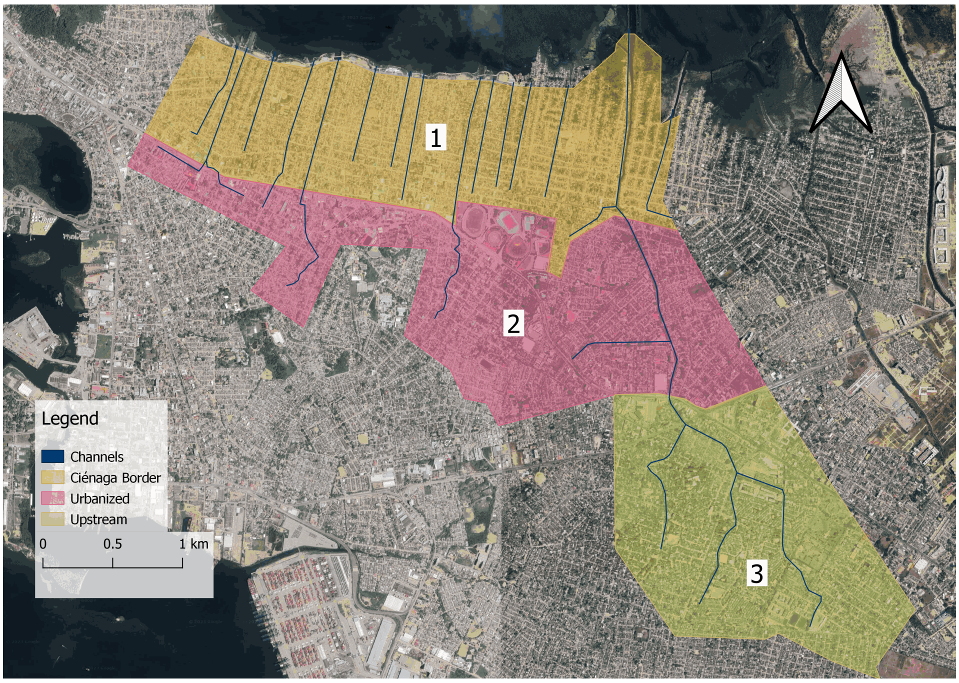

Figure 5.1: The focus area for imposing mitigation measures is subdivided into three zones.

Based on the conclusions drawn in Section 4.4, the focus for implementing mitigation measures is shifted to the west side of the study area. This decision is based on the following reasons:

1. The houses located on the banks of the channels in this area are very vulnerable and densely packed (#1). Therefore, it is crucial to prioritize this area for mitigation measures.
2. The west side of the study area is solely dependent on urban drainage water and does not have to handle the additional discharge of rural drainage water from outside the study area (#2 & #3). This simplifies the analysis and allows for a more focused assessment of the impact of different mitigation measures.
3. The numerical model performs better in this area compared to the eastern part of the study area. This makes it more suitable for analyzing the effects of different types of mitigation measures, as the model's performance is more reliable in this region.
4. The system on the west side is more simplistic, consisting mainly of short, straight channels without intertwined bottlenecks. This further contributes to the confidence in assessing the impact of mitigation measures in this area.

The chosen conditions for evaluating the impact of mitigation measures is a tidal sequence combined with an extreme rainfall event with a return period of two years (R=2y). These conditions are selected because it is evident from Section 4.4 that approximately 25% of the study area already experienced flooding under such conditions. While the flooded area increases to about 35% for a 100-year extreme rainfall event, this difference is primarily observed on the eastern side of the study area. As the focus is on the west side, addressing more frequent rainfall events is deemed a more urgent matter.

The resilience of the mitigation options in the future is ultimately also tested. However, this will be one of the criteria in the MCA. This ensures that the selected options can effectively mitigate flood risks under changing conditions.

5.2. Potential types of mitigation measures

It has come up more than once, that the capacity of the channels is the main issue for floods. Based on this conclusion, the first potential mitigation measure considered is increasing the dimensions of the channels. This would enhance the capacity of the drainage network and potentially reduce the flooded area and flood levels. However, this type of mitigation measure has its limitations. It is a conventional approach that may not be feasible in all areas due to limited available space. Additionally, it is reactive, addressing peak flows rather than preventing them altogether.

Considering these factors, it is important to explore and evaluate other types of mitigation measures that can provide more sustainable and proactive types of mitigation measures. Alternative measures that focus on prevention, such as green infrastructure, retention basins, or improved land use planning, should be considered. These measures aim to manage stormwater at its source, reduce runoff, and promote infiltration, thereby minimizing the risk of flooding.

These mitigation measures considered are part of the so-called Sustainable Urban Drainage Systems (SUDS). The SUDS provides various components for infiltration, retention, evaporation and restoration/preservation of natural features to reduce the amount of runoff entering the system (Yazdanfar & Sharma, 2015). The extended list of detailed measures mentioned in Davis and Naumann (2017) and Poleto and Tassi (2012) focuses mainly on those that improve these processes. These mitigation measures are seen as appropriate for the hydraulic zone.

The remark has to be made, that evaporation is not considered in the D-Hydro model, as it focuses on extreme rainfall events over a short period. Therefore, measures that rely on evaporation may not be incorporated into the model analysis.

Additionally, the preservation or restoration of wetland-like areas is not considered an option in this study. This is because, as demonstrated in Section 4.3.2, the tidal water level does not directly impact the flooded area in the current situation. The primary cause of flooding in the focus area is upstream runoff. Furthermore, the creation of wetlands in densely populated areas may lead to concerns related to health risks associated with insects (Poleto & Tassi, 2012).

For these reasons, the three types of mitigation measures analysed are:

1. Mitigation measure 1: Increasing channel dimensions
2. Mitigation measure 2: Increasing infiltration
3. Mitigation measure 3: Construction retention areas

First, the impact of each measure is considered pragmatically in Section 5.4. Different scales of the mitigation measure are tested with the D-Hydro model to see the impact. Next, a feasible mitigation option is drawn from each type of mitigation measure.

5.3. Model improvements to assess the technical impact of the mitigation measures

As the focus of the mitigation approach shifts to the western part of the Ciénaga border, the model is modified to minimise computation time. The eastern side is removed from the model, resulting in Figure 5.2.

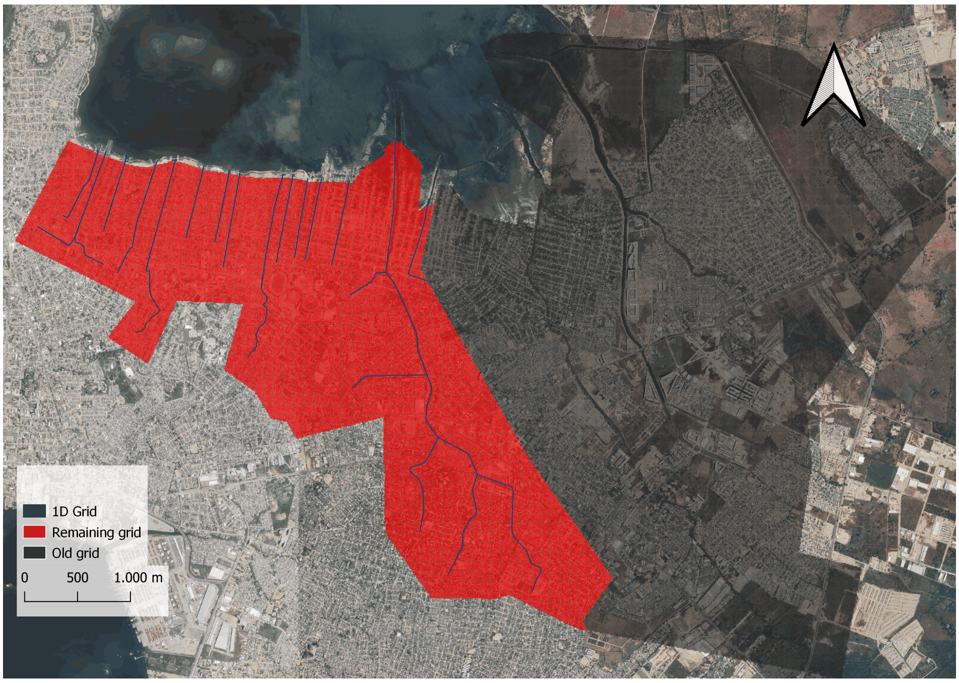

Figure 5.2: The part of the grid that remains after optimization (red grid)

Model error

During the improvement phase of this model, an error was discovered in the physical functioning of the model. Initially, when the model was created, the first step involved generating the 1D computational grid (see Section 4.2.1). This process utilized dimensions and slopes recorded in a hydraulic survey (refer to Section 3.2.1 and Section 4.2.2) (Local authorities, 2009a). These slopes were used in determining the bed levels for the cross-sections of the 1D computational grid. This task was completed months before the creation of the bed-level 2D grid, as the necessary information was received at a later stage. Due to the delayed implementation of this information, the bed levels of the 1D grid did not align with the bed levels of the 2D computational grid. Consequently, the bed levels of the 1D grid were higher than those of the 2D grid.

It was assumed that only the excess water (which would no longer fit within the cross-section) would be deposited on the 2D grid. This would mean that the water could not flow back to the 1D grid. This was not considered a problem as only maximum flood values were considered. However, the assumption about the linkage of the model works was wrong. Namely, if the bed level of the 1D network is higher than that of the 2D network, all the water from the cross-section will be deposited on the 2D network. So to speak, the 1D channels start to 'leak' onto the 2D grid. The 1D grid is only used in this way to deposit the rainwater on the 2D grid. The rainwater follows the bed-level profile of the 2D grid. As the bed level is averaged over a grid size of 10 by 10 meters, the dimensions of the channels in the 2D did not match the imposed cross-section values. The water flow followed largely the channels because the channels are visible in the bed level profile. It corrects the double storage capacity upstream (as discussed in Section 4.2.6). However, most of the correct dimensions of the cross sections are lost due to the averaging per 100 m^2.

The rainwater will follow the bed level of the 2D grid. The 10 x 10 resolution was fine enough to obtain a flow that followed the pattern of the channels towards the Ciénaga border. As the water level boundary condition is also induced at the edges of the 2D grid, the drained water will experience the same influence of the tide. For this reason, and because of the large variation in elevation discussed above, the conclusion about zones of influence from Section 4.4 will not change. However, the error will have a large impact on the hydraulic zone as not the right cross-sections are examined. Therefore, changes had to be made to the model when analysing the impact of mitigation measures.

Improvement to the model

The following two changes are made to the model:

1. The resolution of the mesh is refined around the channels.
2. The bed level of the channel cross-section is set to the bed level of the 2D mesh.

The first enhancement improves the channel dimensions within the 2D grid. The resolution around the channels goes from 10 x 10 meters to 5 x 5 meters with a Casulli refinement (Deltares, 2023c). The change can be seen in Figure 5.3. This improvement gives more detail to flowing of the excess water around the channels. The second improvement fixes the leakage of the channels to the underlying grid. With this improvement, only the excess water will cause flooding in the hydraulic zone.

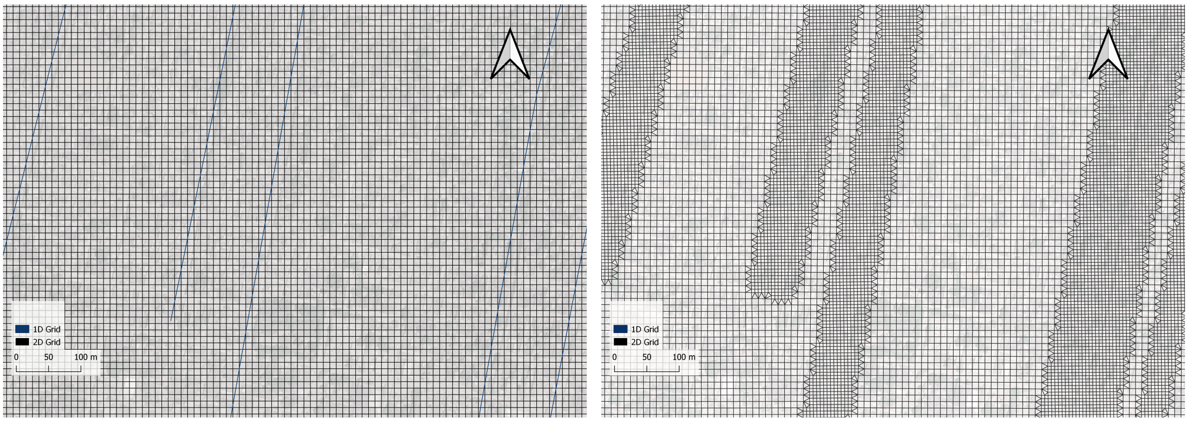

(a) The uniform 2D grid

(b) The improved refined 2D grid

Figure 5.3: The difference in grids

Revalidation of the model

A comparison is made between the overall model and the detailed model. The situation that is compared is a tidal situation with an extreme rainfall event with a return period of 2 years. Where the overall model has a flooded area of 17%, in the detailed model this decreases to 10%. The reason for the decrease is most probably that the capacity of the 1D channels is used and therefore less flooding is recorded. This statement is supported by the fact that the flooded area from the overall model is an extension of the flooded areas already seen in the detailed model. The difference is made visual in Figure 5.4.

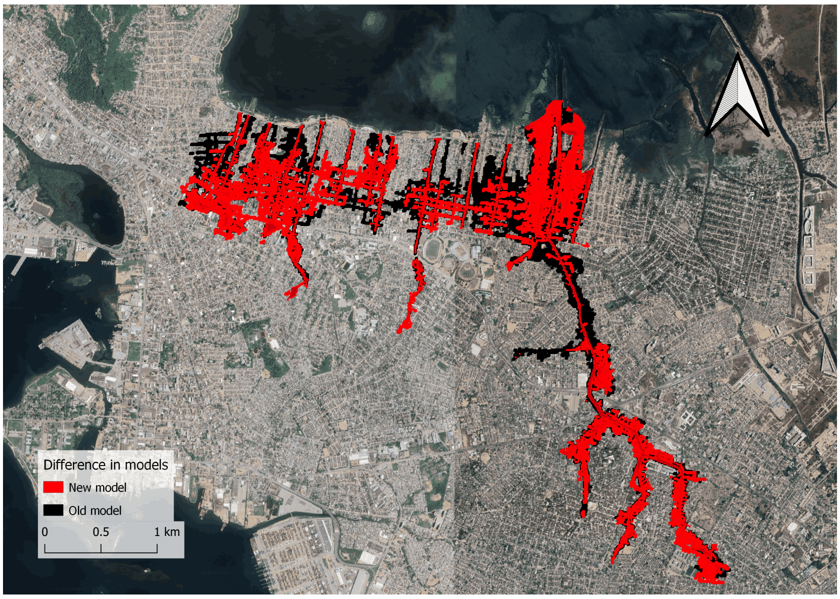

Figure 5.4: The difference between the overall (black field) and the detailed model (red field).

The detailed model is again validated against the same two validation sources as in Section 4.2.5. A good performance is seen from the Edurbe community survey. Although the values have a slightly larger average offset than in Section 4.2.5. The flooded area is shown in Figure 5.5 and the corresponding values with the validation point are shown in Table 5.1.

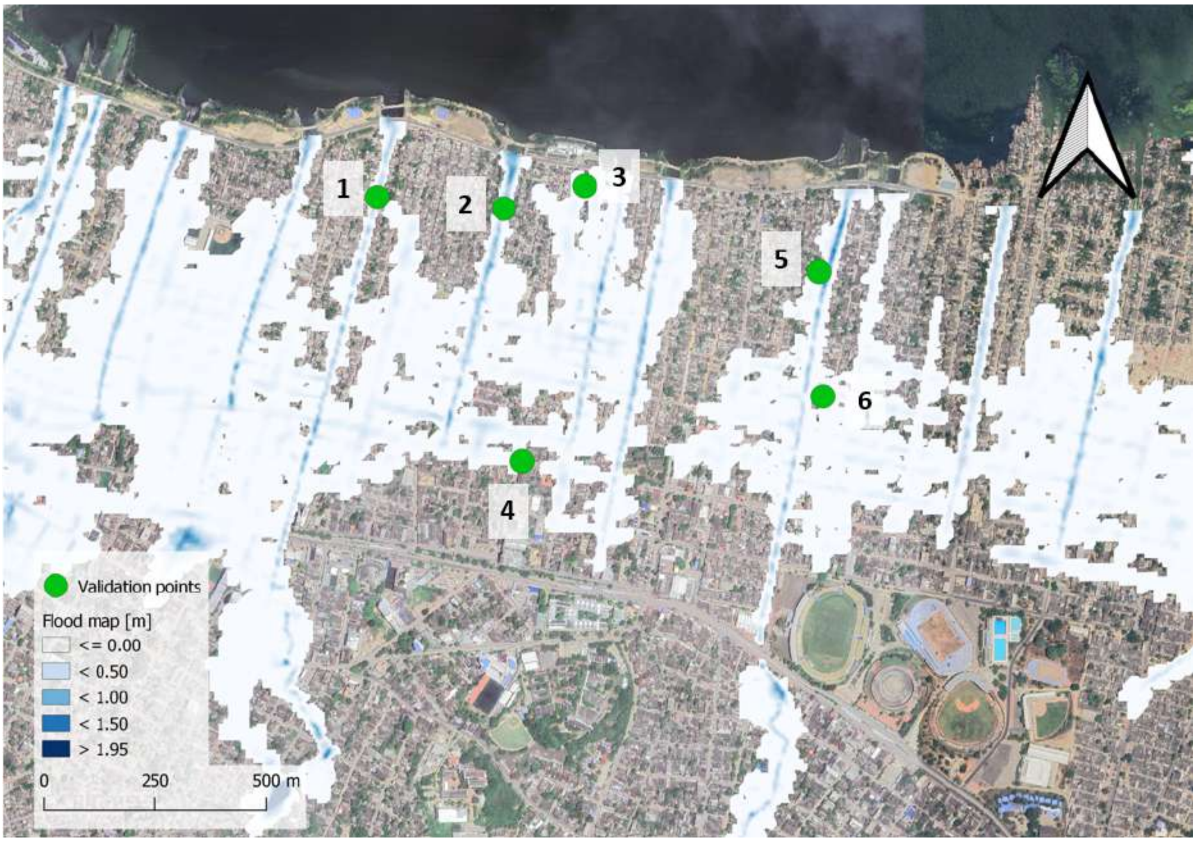

Figure 5.5: The validation points from the Edurbe community interview

Table 5.1: Comparison between the found water depth from the community interview by Edurbe and the computational results of the customized D-Hydro model. model

Validation Points	1	2	3	4	5	6
Edurbe [cm]	70	80	30	60	50	80
D-Hydro model [cm]	69	81	30	48	56	68
Difference [cm]	-1	+1	0	-12	4	-12

The Hurricane Iota situation of November 2020 is also simulated for the detailed model. The flooded area of the model is compared with the known neighbourhoods that experienced flooding as described in the article of Caracol Radio (2020). In Figure 5.6 the flooded neighbourhoods and the flooded area due to the hurricane conditions are shown. In this figure can be seen that all but one of the neighbourhoods experienced some kind of flooding. The upstream part of the model shows no significant differences from Figure 4.10 in Section 4.2.5.

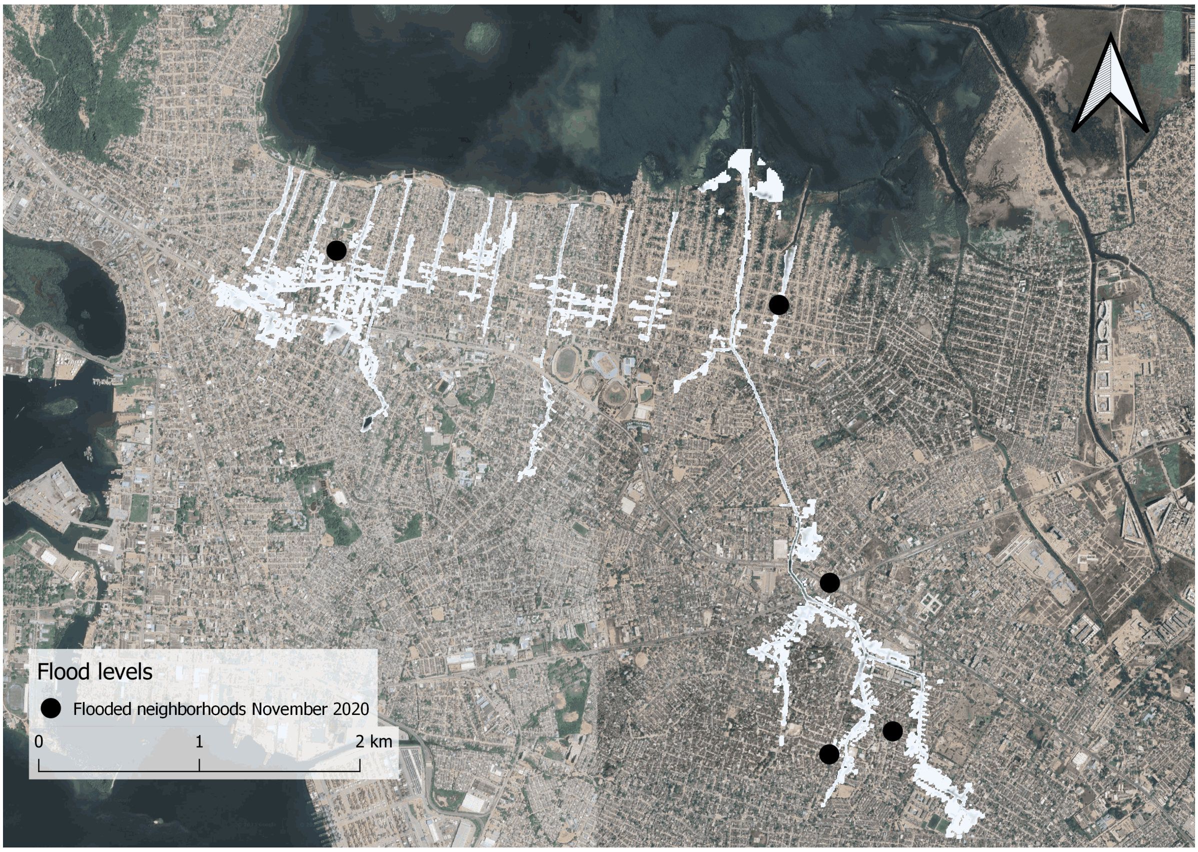

Figure 5.6: flooded neighbourhoods compared with D-Hydro model including the changes

Detailed model

The comparison and validation of the model conclude that the detailed model has a better physical representation of reality, as only the excess water is shown in the 2D grid instead of all the water. Furthermore, the comparison of the detailed model with the same validation sources does not show any significant changes in the model's results. The inundation levels compared with the Edurbe community survey agree quite well, as do the flooded neighbourhoods. The model is therefore referred to as the detailed model and is used to determine the impact of the different types of mitigation measures. The flood map of the detailed model is shown in Figure 5.7.

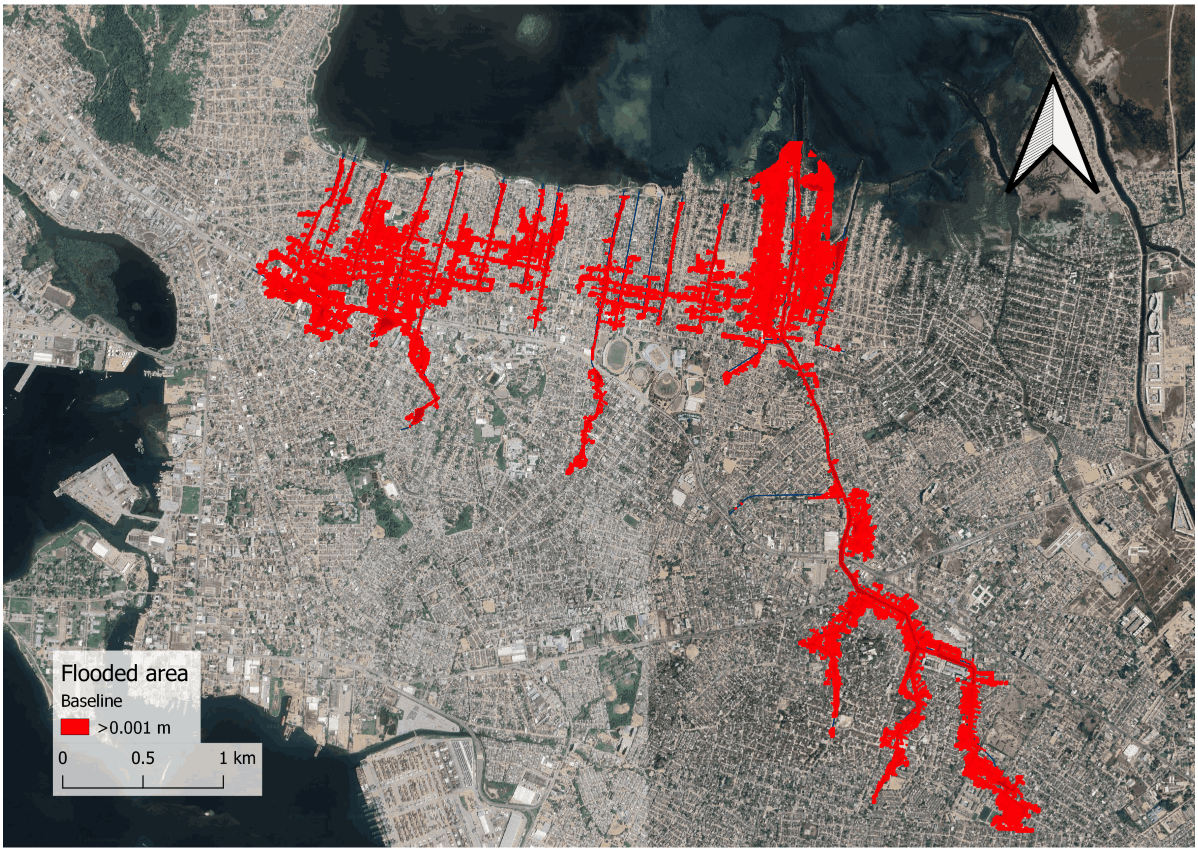

Figure 5.7: The baseline of the detailed model used to determine the impact of the mitigation measures

Table 5.2: The computational results for the evaluated baseline scenario. These results consist of flooded area in (m^2 and %) and average flood level.

	Flooded Area [km^2]	%	Average Flood Level [cm]
Baseline	0.98	10 %	30.0

The results of the model shown in Table 5.2 are used to calculate the flooded area and average flood depth. This is referred to as the baseline scenario. The types of mitigation measures aim to reduce these numbers either overall or locally.

5.4. Impact of mitigation measures on flooding

The impact of the three types of mitigation measures selected will be examined. Firstly, this examination is done broadly to examine the different impacts of the scale of the measures themselves. Scaling up a particular measure provides insight into the required impact. This approach indicates the best functioning scale for each of the measures. To provide a final option for each type of mitigation measure, this optimal scale is considered in combination with the feasibility of the measure.

For each type of mitigation measure the impact of the different scales are investigated. For each scale step the following relative reductions are calculated with Equation (5.1) [%]:

1. Reduction of the total flooded area ($\geq$1 mm)
2. Reduction in average flood level ($\geq$1 mm)

$$Reduction \quad [\%] \quad = \frac{baseline - measure}{baseline} \cdot 100\% \tag{5.1}$$

The total flood area covers only the areas where flooding is prevented. The reduction can be any grid point with an initial flood level over 1 mm that became dry. The average reduction in reduced flood levels will show the average impact on all the flood levels that are reduced by more than 1 mm.

Mitigation measure 1: Increase channel dimensions

Mitigation measure 1 examines the expansion of the dimensions of the channels. To assess the impact, the flooded area and flood depths are evaluated for various percentage increases in channel dimensions. The final D-Hydro model tests six different types of dimension expansion. These types of extensions are as follows:

1. 10 % Increase in dimensions
2. 20 % Increase in dimensions
3. 30 % Increase in dimensions
4. 50 % Increase in dimensions
5. 100 % Increase in dimensions
6. 200 % Increase in dimensions

The increase is conducted for widening and deepening of the channel with the specified percentage.Table 5.3 presents the computational results for the different extensions of channel dimensions. The simulation results indicate that a 200% increase in dimensions performs the best, effectively reducing the flooded area and depths. For a more detailed visual representation and a comparison of flood depths for each type of extension, please refer to Appendix E.1 which includes flood maps and depth differences.

Table 5.3: The computational results increase the channels. The reduction is expressed in flooded areas and the reduction in average flood level.

Channel increase	Flooded Area [km^2]	%	Average FL Reduction [cm]	%
10 %	0.87	11	3.6	12
20 %	0.79	19	6.1	20
30 %	0.71	27	7.6	25
50 %	0.63	35	9.4	31
100 %	0.47	52	15.0	50
200 %	0.28	71	20.0	67

Each extension results in significantly better and better reductions. Compared to the other measures, this is the best performer for both categories of reduction.

Based on the different computational results the preferable capacity increase is determined for each channel. The channels are present in densely populated areas at the Ciénaga border. This means that for some of the channels, the preferable increase in capacity would result in the relocation of houses. The computation results show that significant reduction can already be achieved in most places without relocation. Therefore, the decision is made that in the case of Mitigation Option 1, it is assumed that relocation is not allowed. The maximum allowable increase in the channel's width is determined by Google Street View. In Table 5.4 maximum allowable increase of capacity and the preferable capacity increase are put next to each other. The selected increase in capacity is determined based on the normative value.

Table 5.4: The categorization of the channels. The possible increase is investigated with Google Street View.*Tabu is deepened as was possible due to the height difference. **No information is found with Google Street View so 100% retained. The channels are ordered from west to east.

Channel	Increase possible [%]	Increase needed [%]	Option increase [%]
Bolivar	0	50	0
Maria Auxiliadora	200	100	100
San Pablo	200	200	200
Barcelona	200	200	200
Amador y Cortes	100	>200	0
San Martin	200	100	100
Libano	0	200	0
Salim-Bechara	0	200	0
Tabu*	20	100	100*
Villa**	100	100	100
Papa Negro**	100	100	100
11 November	50	50	50
El Tigre	0	200	0
Ricaurte	30	50	30
Chiquinquirá	30	50	30
Chepa	200	200	200
Las Gaviotas	200	50	50
San Pedro	200	200	200
Bias de Lazo	200	200	200
Canal Maravilla	20	20	20

In Figure 5.8, two examples are provided regarding the assessment of Google Street View. One illustrates when a required increase is considered possible (Figure 5.8a), while the other demonstrates when it is deemed not possible (Figure 5.8b).

(a) For the Barcelona channel the required increase deemed possible

(b) For the Bolivar channel the required increase is not deemed possible

Figure 5.8: A visual representation of the normative assessment with Google Street View.

Mitigation Option 1

The assessment results in a feasible Mitigation Option 1 for Mitigation Measure 1. The flood area and flood level reduction of Mitigation Option 1 are shown in Figure 5.9 and Figure 5.10.

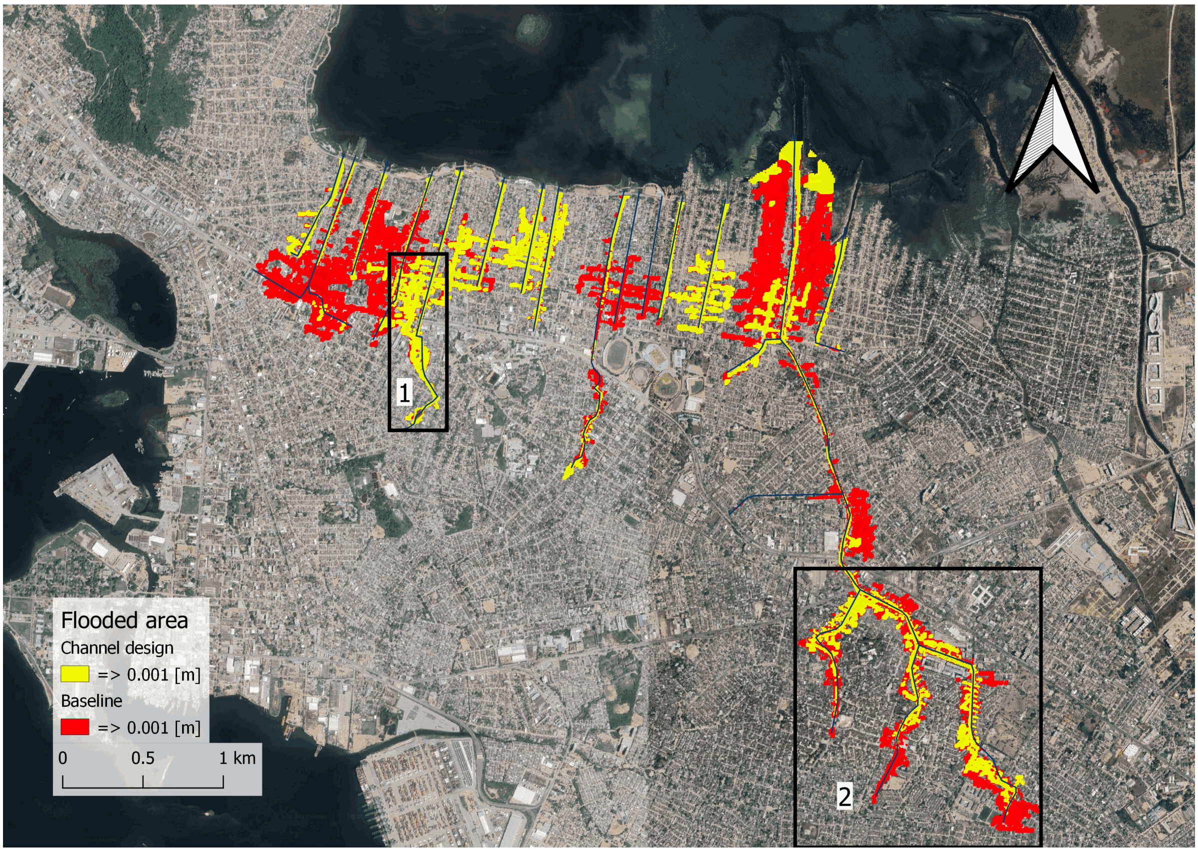

Figure 5.9: The comparison in flood map for the capacity option. The red area is the baseline flood map and the yellow indicates flood for Mitigation Option 1.

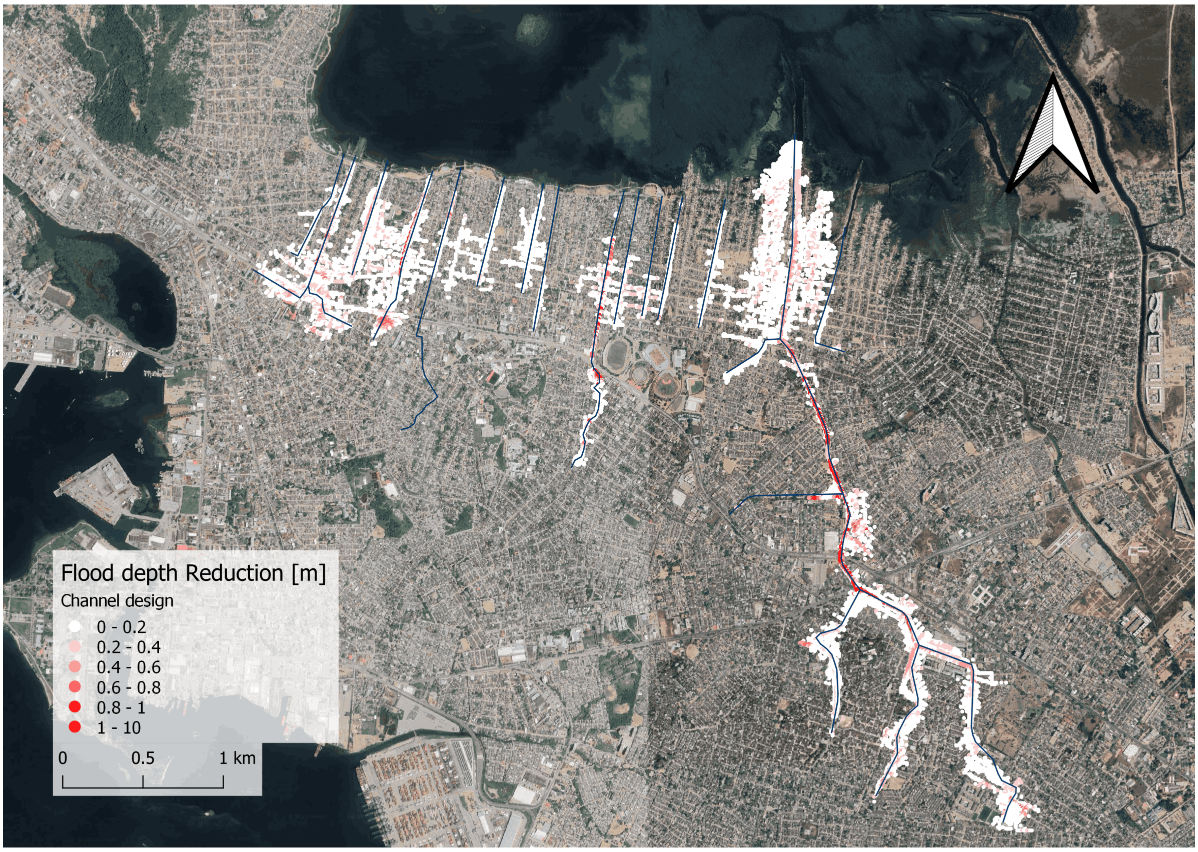

Figure 5.10: The reduced flood levels due to the option of the increased channel dimension. The redder the dots, the greater the reduction in flood levels.

Table 5.5: The calculated performance of Mitigation Option 1 where the channels are increased. The reduction is expressed in flooded areas and reduction in average flood levels

Channels	Flooded Area [km^2]	%	Average FL Reduction [cm]	%
Option 1	0.43	56	18	59

Mitigation Option 1 performs very well in both reducing the flood area and the average flood level. These values are shown in Table 5.5. Both values are reduced by more than half and a large part of the focus area is simulated to become dry. Two comments need to be made when looking at Figure 5.9.

1. The Amador y Cortes channel shows no reduction. For this channel became clear that an increase of 200% still does not change the flood map for this section of the channel. An increase of less than 200% does not even reduce the flood levels. Due to the limited space in this area, the decision is made not to widen the channel. For this section, the conclusion can be drawn that other types of mitigation measures would be more effective in terms of impact and feasibility.
2. For this section, the channel dimensions are all raised by 200% as space allows it. The area still experiences flooding, although the flood levels have been significantly reduced when looking at Figure 5.10. As this catchment is very large, these upstream channels have to drain a large volume. This is represented in the model by dividing the remaining catchment area for these three channels. These values of to-be-drained volume could be higher than in reality. Therefore, very large dimensions are required to drain without flooding.

Overall, this option has a great effect in reducing the flood area and average flood levels, particularly in certain parts of the area. However, it is important to note that the effectiveness of the option may vary depending on the specific characteristics of the channels and catchment areas.

Mitigation measure 2: Enhancing infiltration

Mitigation measure 2 tested the increasing infiltration thereby reducing the amount of runoff in the drainage system. This measure is modelled by reducing the catchment areas in steps of percentages. The different steps considered in this study are 10%, 20%, 30%, 40% and 50%. The maximum increase is set to 50% because this would imply that infiltration measures could be constructed in 100% of the area, assuming the average outflow rate of permeable pavement (Poleto & Tassi, 2012). The computational results of the different percentage steps are shown in Table 5.6.

Table 5.6: The calculated performance by increasing the infiltration in the area. The reduction is expressed in flooded areas and the reduction in average flood level.

Increase Infiltration	Flooded Area [km^2]	% reduced	Average FL Reduction [cm]	% reduced
10 %	0.90	11	1.5	5.
20 %	0.80	18	2.9	10
30 %	0.71	27	4.3	14
40 %	0.64	34	5.7	19
50 %	0.60	39	6.9	23

Increasing the infiltration is not as ultimately effective in reducing the flood area as Mitigation Measure 1. However, for the first three scaling steps, it has roughly the same performance. The extreme increases in dimensions outperform these infiltration methods in terms of flood area reduction. To achieve a significant reduction in both flooded area and depth, an infiltration increase of at least 30 % should be ideal.

The measures to increase the infiltration during extreme rainfall events consist of the following (Poleto & Tassi, 2012):

1. (Semi)Permeable pavement;
2. Infiltration retention areas;
   (a) Trenches;
   (b) Gullies;
   (c) Wells
3. Green roofs
4. Trees/Grass strips

Permeable pavements should be considered as an option to increase infiltration in the focus areas. The run-off reduction for permeable pavements is estimated to be between 60 -75 % (Lee et al., 2023). So for an extreme rainfall event, a maximum reduction of 60 % could be considered when the whole area is paved. Permeable pavements also introduce a delay time of 30 minutes for extreme events (Tirpak et al., 2021). The delay time causes the channels not to be exposed to high peaks in flow rate but spreads these peaks out to a more prolonged manageable lower flow rate. A schematisation of how this spread in a hydrograph works is shown in Figure 5.11

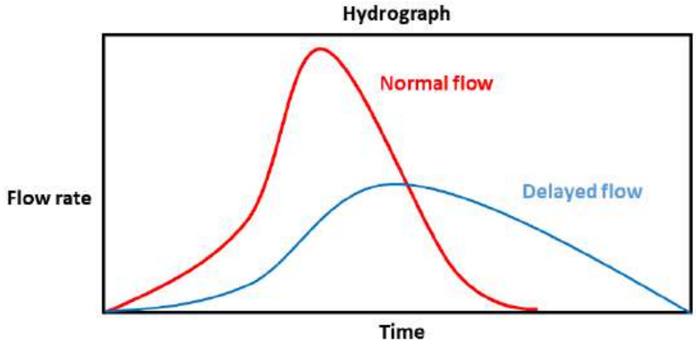

Figure 5.11: The schematisation of spreading out peak rate by introducing a delay time.

Analysing the focus area clarifies that the area consists of 24 % of roads and pavements. Adjusting this total paved area would mean that this measure could increase infiltration by a maximum of 14 %. In terms of feasibility, making all these roads permeable will be far too expensive and not feasible in the narrow streets at the Ciénaga border. Therefore, only the main roads and roads in the upstream areas (#2 in Figure 5.1) could be modified in this way. These considered roads are shown in Figure 5.12.

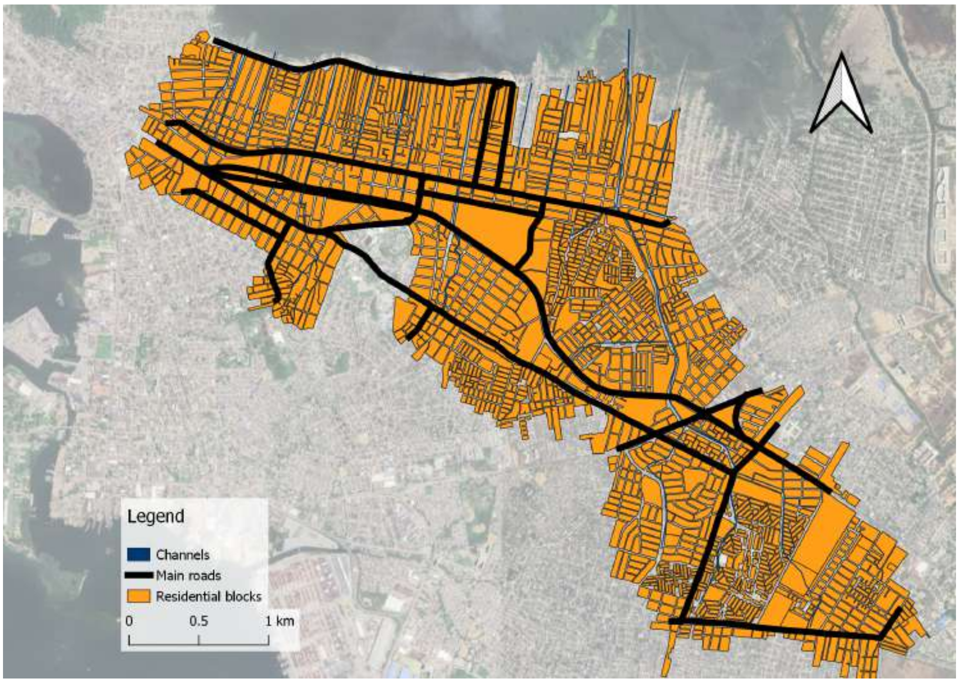

Figure 5.12: The roads considered for potential modification to permeable surfaces

Assuming this feasibility, the maximum percentage of the focus area that could be tiled with permeable pavement would be 10%. This would only increase infiltration by 6%.

Infiltration retention areas are areas that collect rainwater and allow it to slowly infiltrate. As the main focus should be on reducing high peak flows, the effect of this type of measure will mainly be similar to that of normal retention areas (see Section 5.4).

The third option is to incorporate green roofs. These roofs are constructed with layers of soil on roofs in urban areas (Davis & Naumann, 2017). Green roofs reduce peak flows and also improve water quality and thermal and acoustic insulation (Poleto & Tassi, 2012). "Green roofs" can be divided into two categories; vegetative and non-vegetative. Vegetative is the construction of a layer of soil covered with vegetation. This measure has an average retention of run-off water of 57% and can have delay times between 30 minutes and 2 hours (Qin, 2020). The non-vegetative measures consist of permeable roofing material. Gravel can store small amounts of rainwater and can have delay times between 15 and 30 minutes. Stone ballast can capture up to 50% of the rainfall volume. As shown in the calculation for permeable pavement, the amount of built-up area is about 76%. Installing green roofs over the entire area would result in a maximum increase in infiltration of 43% and a run-off time of 30 minutes for peak events. In terms of feasibility, the houses at the edge of the Ciénaga (see #1 in Figure 5.1) are not considered suitable for green roofs. The houses in this area are of too poor a quality to support the weight of infiltrating rainwater. Looking further upstream, the houses appear to be much stronger. Also considering the non-vegetative option, it is assumed that 30% of the urbanised and upstream area (see #2 and 3 in Figure 5.1) in the focus zone should be able to achieve green roofs. This would increase infiltration by about 15% (considering the lowest value for non-vegetative "green" roofs).

The final measure is to establish more grass and trees within the area. This is not suitable for infiltration of extreme rainfall, but will slightly increase the delay time (Susdrain, 2022). As the focus area is very densely populated, it is difficult to create enough grass/trees to have an impact in terms of increasing infiltration.

Considering the arguments presented above, the best feasible Mitigation Option is an increase in infiltration of 20% in combination with a delay time of 30 minutes for Mitigation Option 2.

Mitigation Option 2
Implementing Mitigation Measure 2 results in the following flood map and flood level reduction shown in Figure 5.13 and Figure 5.14.

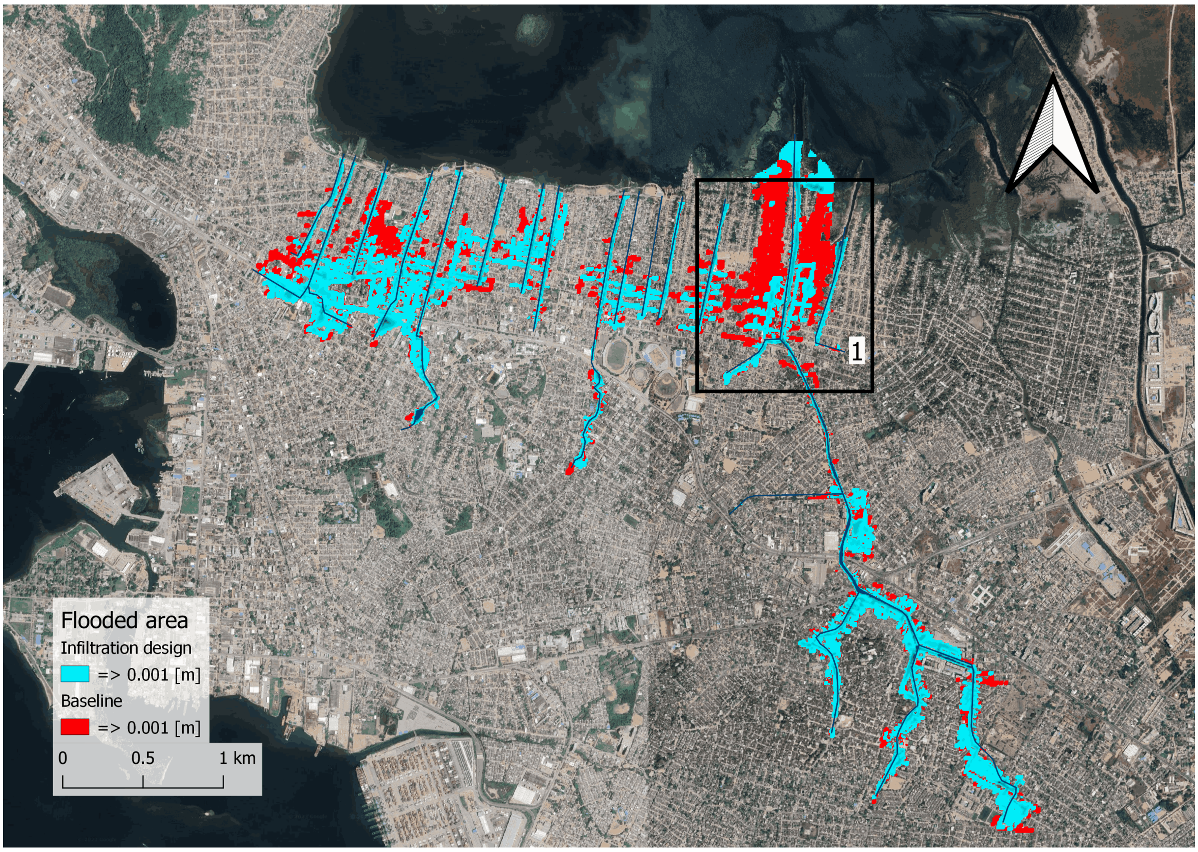

Figure 5.13: The comparison in flood map for increasing the infiltration with 20% and introducing a delay time of 30 minutes. The red area is the baseline flood map and the blue indicates flood according to Mitigation Option 2.

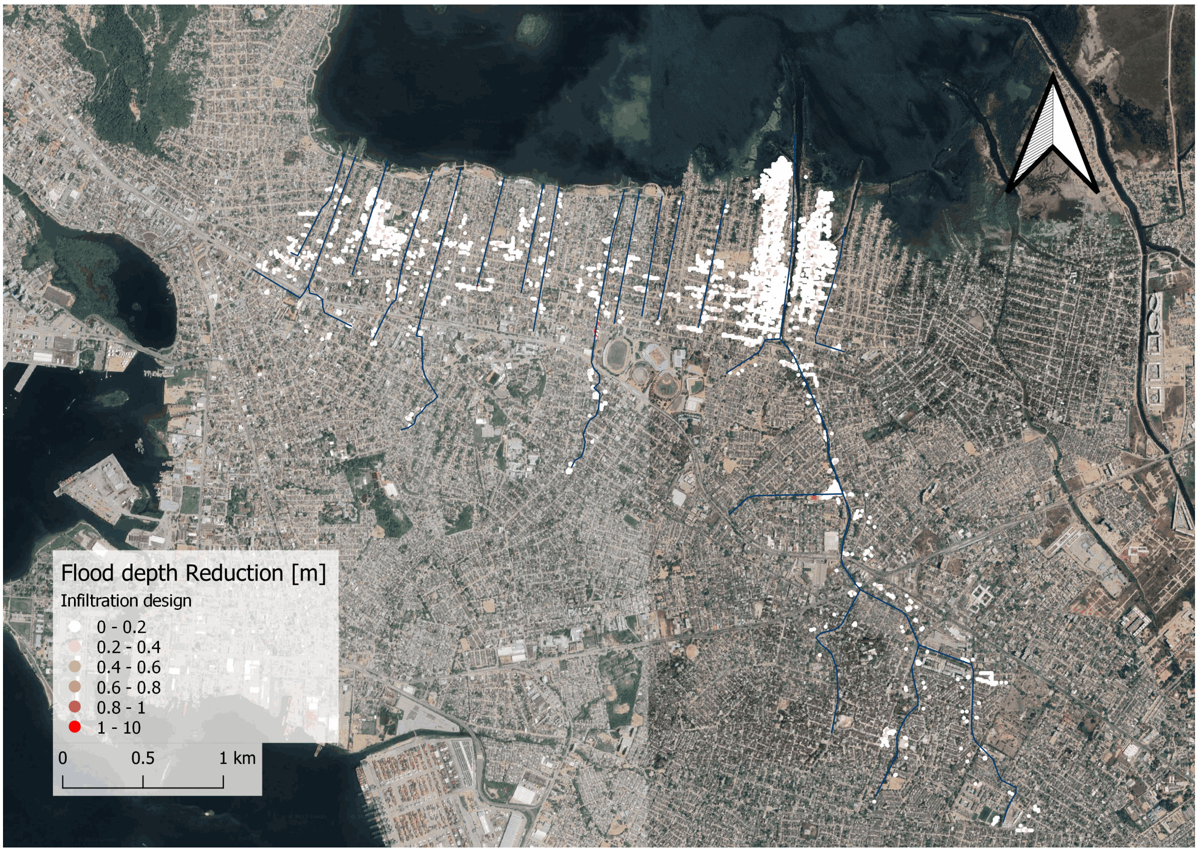

Figure 5.14: The reduced flood levels due to Mitigation Option 2 with a 20% infiltration increase and introducing a delay time of 30 minutes. How redder the dots, how greater the reduction of flood levels.

Table 5.7: The calculated performance of the option where the infiltration is increased. The reduction is expressed in flooded areas and the reduction in average flood level.

Infiltration	Flooded Area [km^2]	%	Average FL Reduction [cm]	% reduced
Option 2	797018	19	8.8	29

The infiltration design results in a reduction of almost 20% in the flooded area and on average reduces the flood levels by almost 9 cm. These values are shown in Table 5.7. A comment can be made on the highlighted section in Figure 5.13:

1. Section 1 shows the most significant reduction. It also shows a greater reduction in flood area and flood level due to the introduction of delay time. The scale-up approach shows less reduction and a smaller reduction in flood levels. The conclusion can be drawn that the delay time was a beneficial difference for this section.

Overall, some comments can be made. In general, the reduction does not cause some parts to be completely dry, but it does make the borders of the baseline flooded area retreat. It is noticeable that the water levels in the channels are not reduced during floods. The reason for this is probably the introduction of the delay time. The water is drained more slowly so that high water levels remain in the channels for a longer period. The average reduction in flood levels is decreased by 8.8 cm. This reduction corresponded with an infiltration increase of more than 50% with no lag time (see Table 5.6). As there was no reduction in the channels, this average reduction lay much higher. The border area of Ciénaga (see #1 of Figure 5.1) benefits most from this option. In the upstream part (#3) the flood level has been reduced, but for the middle zone (#2) the smallest difference can be seen.

Mitigation measure 3: Retention areas

Mitigation Measure 3 consists of constructing retention areas. Retention areas are considered not only because of their flood reduction properties but also because of their positive impact on water planning processes, biodiversity protection, climate change adaptation and urban planning (Zeleňáková et al., 2017). There are two types of retention areas: natural and artificial. Natural retention areas retain water on natural soils and use infiltration. As peak discharges are observed, the basins are being studied for their storage capacity.

The measure can only be applied locally, so the right place has to be found. This space must have an impact on the downstream flooded area and be feasible to build. Ideally, no housing would have to be removed. Unfortunately, the space available for retention areas cannot be found in this densely populated area. Therefore, if housing has to be removed, the areas with the greatest impact are sought. Looking closely at the baseline flood maps (Figure 5.7), two high-impact areas are selected. These are areas where the retention areas would have the greatest impact in reducing flooded areas. This was investigated by looking at the velocity vectors shown in Figure 5.15.

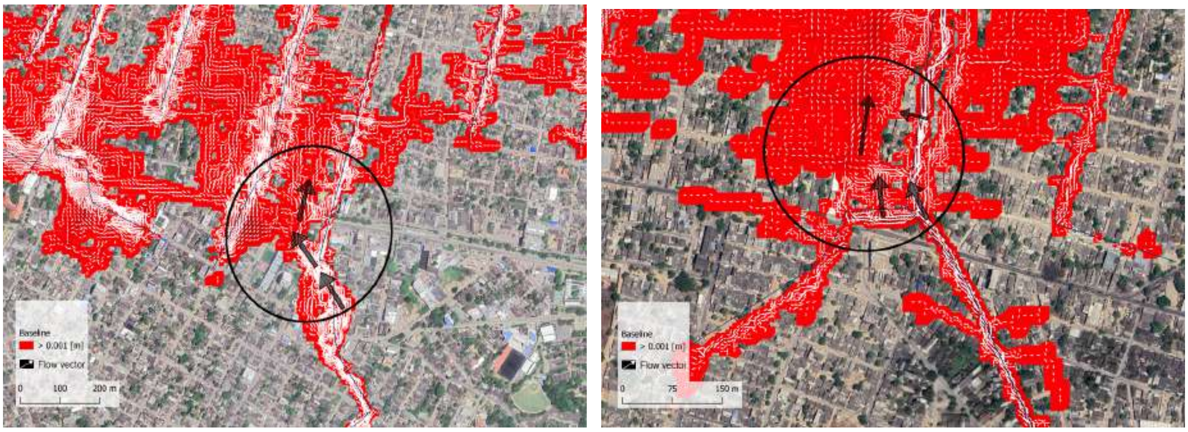

(a) The Amador y Cortes shows flooding directed into the streets resulting in a high impact zone.

(b) The converging channels resulted in a flood directed to the west side of the Rincaute channel. This is indicated as the other high-impact zone.

Figure 5.15: The indication of areas that will have the highest impact when constructing a retention area.

These areas are subjected to extensive flooding. This is due to large volumes of water flowing out of the channel junctions and being diverted through the streets. The two locations for the retention areas are visualised in Figure 5.16. The western retention area is 37016 m^2 and the eastern area is 47313 m^2.

The influence of different depths was tested; 2, 4, 6 and 8 meters. The results are shown in Table 5.8.

Table 5.8: The computational results by constructing two retention areas with different depths. The reduction is expressed in flooded areas and the reduction in average flood level.

Retention area	Flooded Area [km^2]	% reduced	Average FL Reduction [cm]	% reduced
2 m	0.89	9	6.4	21
4 m	0.85	13	8.7	29
6 m	0.85	13	8.7	29
8 m	0.85	13	8.8	29

Being a locally applied measure, it was expected that this type of mitigation measure would not have the same impact on reducing the flooded area as the other two measures. However, two retention areas of 2 meters depth can compete with the two lowest scales of the other measures. For the higher scales, the other measures outperform the retention area in terms of flood area reduction. Again, this is because this measure is applied locally. However, in terms of an average flood level reduction, an excellent performance can be seen. When comparing this flood level reduction with the other two

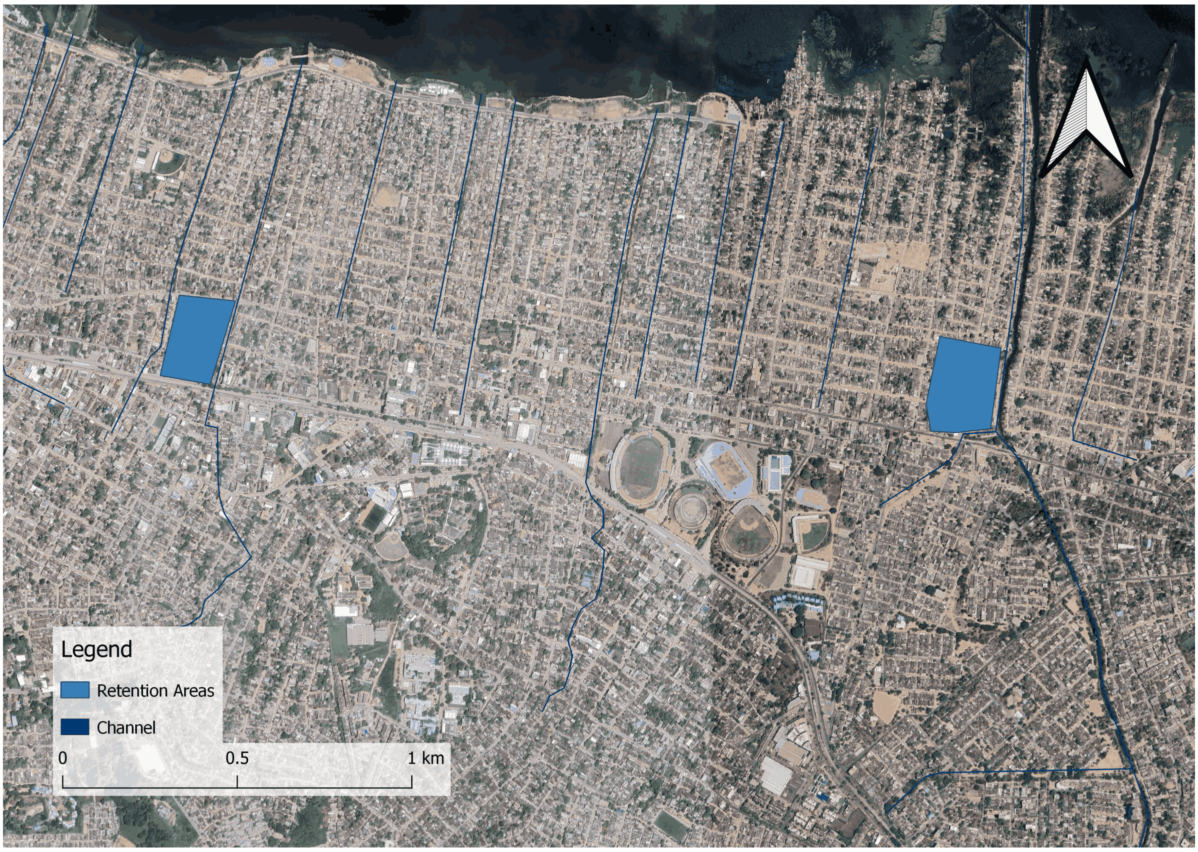

Figure 5.16: The two constructed retention areas

measures, this type of mitigation measure performs even better. The infiltration measures do not even reach such values of average level reduction. The increase in reduction becomes insignificant after a depth of 4 meters. The flood maps for the different depths in Appendix E.3 show that the eastern retention area is already satisfied at a depth of 2 meters. For the western retention area, the step from 2 to 4 meters significantly increases the reduction, but a further deepening of this area does not have a significant effect.

Mitigation Option 3
Considering the computational results, Mitigation Option 3 is to construct the two investigated areas with different depths. The depth of the eastern retention area is determined at 2 meters. The western retention area would be most functional if the depth was made 4 meters.

Mitigation Option 3 results in the following flood map and flood level reduction shown in Figure 5.17 and Figure 5.18.

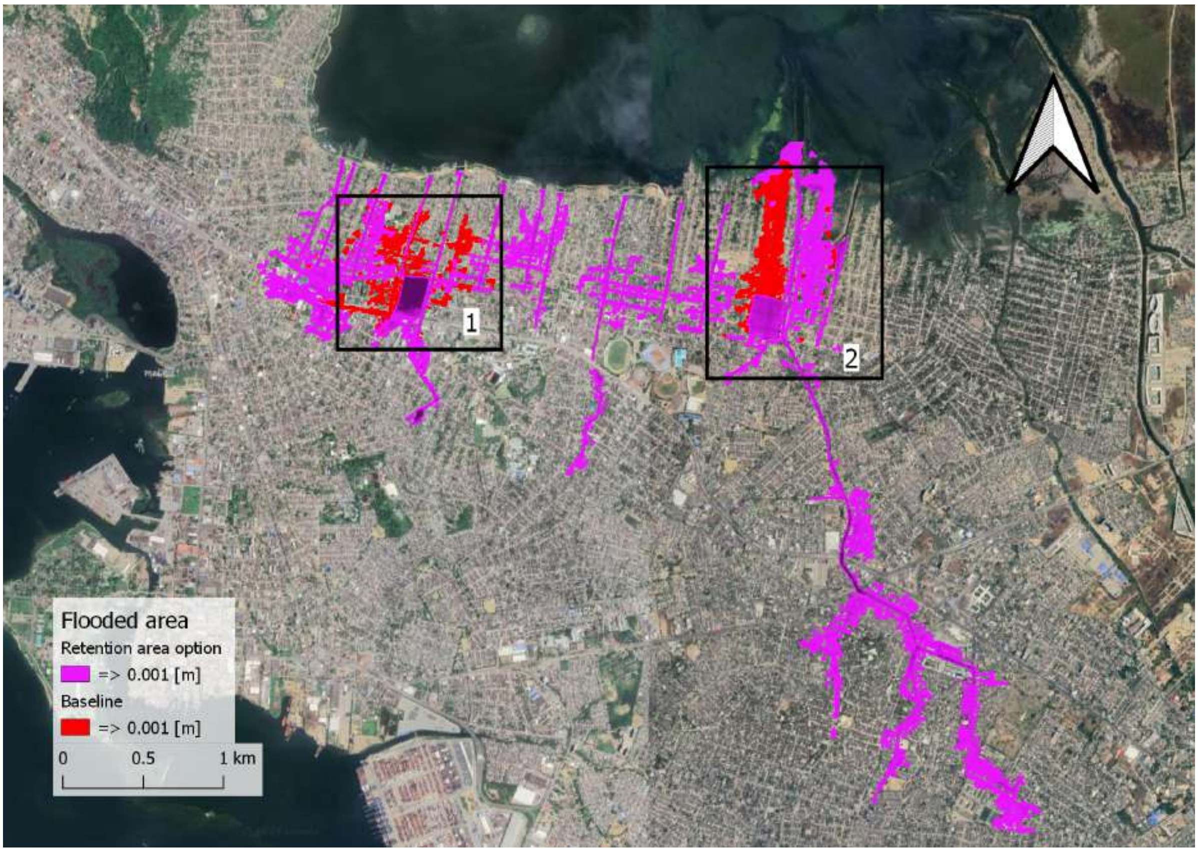

Figure 5.17: The comparison in the flood map for the construction of two retention areas, where the western area has a depth of 4 meters and the eastern area has a depth of 2 meters. The red area is the baseline flood map and the purple area is the flood for Mitigation Option 3.

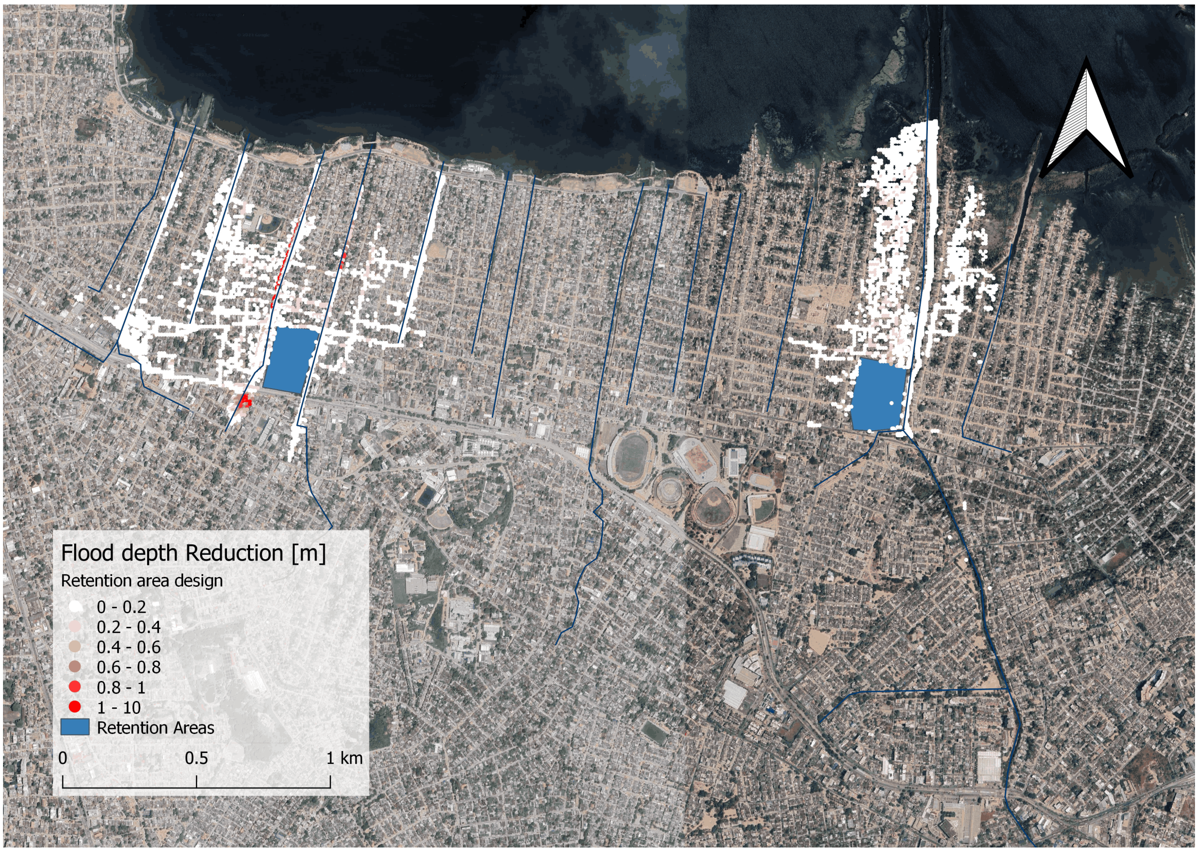

Figure 5.18: The reduced flood levels due to Mitigation Option 3. How redder the dots, how greater the reduction of flood levels.

Table 5.9: The calculated performance when constructing two retention areas. The reduction is expressed in flooded areas and the reduction in average flood level.

Retention area	Flooded Area [km^2]	% reduced	Average FL Reduction [cm]	% reduced
Option 3	0.85	13	8.7	29

The reduction in flooded areas is not as significant at only 13%, but the lower reduction in flooded areas was to be expected as it is a very local measure. Flood levels are reduced by almost 30%, which is significant. Two comments on the area marked in Figure 5.17 :

1. This marked section is a difficult area to tackle in terms of flood reduction. This option has a large impact on this area and it can be concluded that it is a highly effective option for this area. The Mitigation Option completely reduces flooding for large areas within this region.
2. The second marked section completely prevents the downstream area from flooding with a depth of only 2 meters. This eastern retention area is an effective option, also reducing flooding on the eastern side of the canal.

However, Mitigation Option 3 only reduces locally, this option shows that if it reduces flooding, it can also effectively reduce flood levels significantly. Furthermore, the option does not just retreat the boundaries of the floodplain, but also prevents whole areas from being flooded, even for a relatively small depth.

5.5. Conclusion

Different types of mitigation measures are investigated to what extent their impact would be on the hydraulic zone in the focus area. The analysis has deducted different types of mitigation measures that could be implemented. This deduction contained the possibility of creating a wetland area and evaporation. The construction of a wetland is not considered because the hydraulic zone has far more influence. The water level in the Ciénaga is not deemed an important factor in this focus area. Evaporation measures are also deducted as the floods are generated by extreme rainfall intensities over a short period. Evaporation will not be able to prevent floods for the investigated events.

Three types of mitigation measures are deemed useful for mitigating floods in the established Hydraulic zone. These three measures are:

1. Increase channel capacity
2. Enhancing infiltration
3. Retention areas

The impact of these three types is investigated with the D-Hydro model. The model is modified to get a better-detailed view of the impact of flooding. The reduced flooded area and an average reduction in flood levels are analyzed.

Increasing the channels' capacity, also called Mitigation Measure 1, would require widening and deepening the channel. The computational results show that increasing the channels by more than 30%, a significant reduction above 25% flooded area. With a channel dimension increase of 200%, the reduction would have the highest impact as could be expected. From Table 5.4 it became clear that the average increase needed is above 100%. Due to limited space, this is not possible for all channels. Rehousing is not considered allowable for this type of mitigation measure because a significant reduction could already be achieved without it. Therefore, Mitigation Option 1 is developed considering that will be feasible and would have an overall significant reduction. This ultimately concludes that Option 1 has a significant reduction. The reduction is 56% in flooded areas and the flood levels are reduced by 60 %.

To increase the infiltration, also called Mitigation Measure 2, in the area would require the construction of permeable pavement and green roofs. The computation results show that to achieve a significant reduction of over 25%, the percentage of infiltration should be increased by over 30%. As could be expected is the highest increasing percentage of 50%, corresponds also to the most effective reduction. Considering the area, the feasible increase in infiltration is set at a maximum of 20%. Furthermore, the literature about the kind of measures reveals that delay time should be included. Mitigation Option 2 therefore increases the infiltration by 20% and includes a delay time of 30 minutes. The computational results show a similar impact as the 20% infiltration on the flooded area. However, the average reduction in flood levels for Option 2 is significantly larger (+5.8 cm) than the investigated 20% increase in infiltration. This finding concludes that the average reduction in flood level delay time plays a big part reduction of flood levels.

The last Measure where the impact is tested is constructing retention areas also called Mitigation Measure 3. Due to the overall limited space available, the decision for rehousing was inevitable. The highest impact zones are investigated. Two are found, one on the west side upstream next to the channel that does not show reduction when investigating the Mitigation Measure 1. The second area is found on the east side of the focus area next to the biggest channel. The impact of different depths is investigated. The western retention area would work optimally for a depth of 4 meters. The reduction namely stagnates when the depth increases from 4 to 6 meters. For the eastern retention area, a depth of only 2 meters would suffice. No impact difference is seen for deeper retention areas. Mitigation Option 3 reduces the flooded area by 13% and almost achieves a reduction of 30 % for the flooded area.

Mitigation Option 1 has a great impact on the flooded area and also on the flooded area with a reduction higher than 50%. It is deemed a helpful measure regarding flood reduction. Mitigation Option 2 has a smaller impact on the flooded area but achieved a significant reduction in the average reduced flood level. Mitigation Option 2 showed that where the flooded area was reduced the levels there were reduced on average with almost 30%. This measure was deemed useful for the mitigation of floods in this area. Mitigation Option 3 reduces the flood level but does that very locally. This local reduction is why the flooded area itself does not reduce that significantly. The measure is deemed useful as a local measure.

6

Multi-criteria evaluation of the Mitigation Options

In Chapter 5 three types of mitigation options were explored for the focus area at the western side of the study area. The impact of the options was tested with the D-Hydro model. To evaluate the best preferred option, a MCA was prepared. This is a tool for weighing up criteria for the mitigation options to not let the recommendation solely depend on the technical impact but also consider other types of criteria. In Section 2.4 the full methodology of the MCA is explained. The conclusion that would follow from the evaluation, answers Sub-question 4: *Which mitigation option is best preferred in this study area?*

This chapter describes the setup, application and conclusions of the MCA assessment.

6.1. Set up MCA

The MCA involves a systematic approach to evaluate and compare the explored mitigation options to each other and the current situation. Six categories are identified:

1. Technical aspects
2. Future proofness
3. Adaptivity
4. Socio-economic aspects
5. Financial aspects
6. Environmental aspects

The above-mentioned categories correspond with categories within the main project. In this way, the results of the scores from this MCA can be more easily interpreted by the consortium and contribute to the decision-making process in the project. In Appendix D the extensive list of all the criteria that are used within the MCA framework of the consortium. Below the choices for these categories are explained related to the MCA framework of the consortium.

- Flood risk reduction and adaptability are chosen to assess the technical performance.
- Future proof adds to address the resilience.
- The category socio-economic assesses livability.
- The financial aspects covered investment costs.
- The environmental aspects are assessed separately from the livability objective.

The categories are assessed on their criteria. These scores for these criteria are on a scale from 1 to 5. This scale is also chosen concerning the MCA framework of the consortium. The criteria that can be scored based on a predetermined performance value are scored quantitatively. The rest of the criteria are scored based on qualitative analysis.

Weight factors (1-5) are applied within the categories to acknowledge the individual importance of a criterion within a category.

The same weight factors (1-5) are applied to the categories to acknowledge the individual importance of categories.

The MCA is established to ensure transparency and include more than one criterion for the recommendation. It should be emphasised that the MCA is a tool for discussion and not a guiding principle. Based on the MCA scores, logical reasoning can be used to make the final choice.

Category 1: Technical aspects

The technical aspects assess the mitigation options on the impact of their technical performance. The performance is based on a situation with a tidal sequence in the Ciénaga in combination with an extreme rainfall event with a return period of two years. The technical aspects are subdivided into two criteria that were scored separately.

Criterion 1.1 - The reduction in flooded areas:
This criterion assesses the impact of reducing the flooded area. This is expressed in the percentage of relative reduction to the base scenario. The scores are awarded regarding the following reductions:

1. 0% - 10 %
2. 10 % - 25 %
3. 25 % - 50 %
4. 50 % - 75 %
5. 75 % - 100 %

The weight of this criterion within Category 1 is set to 2 as the reduction of flood levels (Criterion 1-2) is deemed more important.

Criterion 1-2 - The average reduction in reduced flood level:
This criterion assesses the impact on the average flood level. This is expressed in cm and percentage reduction in the average reduced flood level. The scores are awarded regarding the following reductions:

1. 0% - 10 %
2. 10 % - 25 %
3. 25 % - 50 %
4. 50 % - 75 %
5. 75 % - 100 %

The weight of this criterion is set to 4 as the reduction of flood levels as the severity of the flood is seen as more important than the flooded area. The priority is given to reducing flood nuisance rather than total reduction. A significant reduction in flood levels could already potentially save properties from severe damage or even destruction.

Category 2: Future proofness

Future proofness refers to the ability of the options to withstand other projected challenges. In the context of extreme weather events and rising sea levels, future-proofing is essential to ensure the long-term resilience of the options. If the options do not perform well in future scenarios, then these would not be durable.

Criterion 2-1 - The reduction in flooded areas for a 100-year rainfall event:
In the first scenario, an extreme rainfall event with a return period of 100 years is considered. In Section 4.3.2 shows that the increase of rainfall intensity increased the flooded area significantly (>10% of the total study area). To assess the performance of the options under these new circumstances, the same aspects are used as mentioned, in Section 6.1. The results are generated with the modified

model from Section 5.3. Since the options are engineered for a less intense rainfall intensity (R=2 years), the goal of the aspects is lowered. Therefore, the scores are awarded regarding the following reductions:

1. 0% - 5 %
2. 5 % - 15 %
3. 15 % - 25 %
4. 25 % - 50 %
5. 50 % - 100 %

Criterion 2-2 - The average reduction in reduced flood level for a 100-year rainfall event:
The scores for this criterion are assessed the same as Criterion 2-1

1. 0% - 5 %
2. 5 % - 15 %
3. 15 % - 25 %
4. 25 % - 50 %
5. 50 % - 100 %

Criterion 2-3 - The reduction in flooded area for projected relative sea level rise:
In the second scenario, the impact of a 47 cm relative sea level rise is examined (see Section 3.2.6). In Section 4.3.3 the increase in impact of the relative sea level rise became clear. Since the water level does not have the same significant impact as the different rainfall intensities, the same reduction goal for the flooded area is set as in Section 6.1. The score tab resembles closer to the original design scenario. The scores awarded regarding the following reductions in flooded areas are again:

1. 0% - 10 %
2. 10 % - 25 %
3. 25 % - 50 %
4. 50 % - 75 %
5. 75 % - 100 %

Criterion 2-4 - The average reduction in reduced flood level for projected relative sea level rise:
The goal for reducing the average flood level is lowered. This goal is lowered as the water level in the Ciénaga will increase significantly and will permanently affect the water levels in the channels. The scores awarded regarding the average reduction in reduced flood level are:

1. 0% - 5 %
2. 5 % - 15 %
3. 15 % - 25 %
4. 25 % - 50 %
5. 50 % - 100 %

Category 3: Adaptivity
Criterion 3-1 - Feasibility for adaptation Adaptivity refers to the ability of an option to be easily modified or extended whenever necessary. In considering adaptivity, we evaluate the ease of modifying or expanding options. Options that are difficult to adapt receive a low score of 1, while those that are easy to adapt or expand receive the highest score of 5.

Category 4: Socio-economic aspects
Criterion 4-1 – Impact on livelihood:
The socio-economic criterion refers to the consideration of how the options can affect the local community. The assessment of this criterion looks at both the potential disadvantages and benefits that the social impact of the options could have on the area. A score of 1 is given if the option has only a

negative impact on the area in socio-economic terms. Examples of negative impacts are construction nuisance, the need to relocate residents and an unattractive streetscape. On the other hand, a score of 5 is given if the option has only positive effects. Examples of these positive effects are; improved quality of life, improved infrastructure and increased attractiveness.

Category 5: Financial aspects
Criterion 5-1 – Investment cost:
The financial criteria relate to the consideration of the costs associated with the options. A rough estimation of the construction costs is used to assess the options. The scores are awarded regarding the following costs:

1. $\geq$ 50 million $\$$
2. 30 million $\$$ - 50 million $\$$
3. 15 million $\$$ - 30 million $\$$
4. 5 million $\$$ - 15 million $\$$
5. $\leq$ 5 million $\$$

Category 6: Environmental aspects
The environmental criteria relate to the consideration of the impact of an option on biodiversity and water quality. Two key aspects are considered when assessing this criterion: enhancing biodiversity and improving water quality.

Criterion 6-1 – Improvement of biodiversity:
For biodiversity improvement, a score of 1 is given if there is no improvement in biodiversity. On the other hand, a score of 5 is awarded if significant areas are restored or returned to nature, resulting in a significant increase in biodiversity. The weight set for this aspect is set to three because it is important to strive for an option that would incorporate more nature in an urbanized area.

Criterion 6-2 – Improvement of water quality:
Similarly, for water quality, a score of 1 is given if there is no improvement in water quality, while a score of 5 is given if there is a significant improvement in water quality. Since the water in the drainage channels is very polluted, water quality is seen as the more important aspect of the environmental criteria.

6.2. Evaluation of criteria

The different mitigation options that are scored are the following:

0. The baseline scenario: In this scenario, nothing has been undertaken and is equal to the current situation
1. Mitigation Option 1 The increasing channel dimensions: This mitigation option extends the channels with the possible and/or required percentage.
2. Mitigation Option 2 Increasing the infiltration: This option increases the area's infiltration by 20$\%$ and introduces a delay time of 30 minutes.
3. Mitigation Option 3 Construction of two retention: In this option, a western retention area with a depth of 4 meters and an eastern retention area with a depth of 2 meters are constructed.

In Section 6.2.1 the scores and explanations are given for each of the different assessed criteria. In Section 6.3.2 the ultimate score of the evaluated options is given.

6.2.1. Scoring Explanation

In this section, the scores are explained per mitigation option. For each criterion, the scoring is clarified with a matrix per criteria. Additionally, the difference in scoring between them is clarified.

Category 1: Technical aspects
Computational results from the D-Hydro model (see Section 5.4) are used to evaluate the technical aspects of the mitigation options. As mentioned before, the simulation covers a tidal sequence and an

extreme rainfall event with a two-year return period (R=2 years). The performance of each mitigation option is listed below in Table 6.1.

Table 6.1: The computational results for the options regarding the technical aspects. This computational output consists of the flooded area in (m^2 and %) and an average reduced flood level. *Average flood level

#	Options	Flooded Area [km^2]	%	% reduced	Average reduced FL[cm]	% reduced
0	Baseline	0.98	10	0	30.0*	0
1	Channels	0.43	4	56	17.8	60
2	Infiltration	0.80	8	19	8.8	29
3	Retention	0.85	9	13	8.7	29

This results inTable 6.2 where the scores per mitigation option are depicted. The explanation for the scores is given in Table 6.3.

Table 6.2: The weights and scores for each criterion per specific option.

Technical aspects	Score 1	Score 5	weight (1-5)	0	1	2	3
Criterion			5	1.0	4.0	2.7	2.7
1-1	No reduction (0%)	Total reduction (75%)	2	1	4	2	2
1-2	No reduction (0%)	Significant reduction (+75%)	4	1	4	3	3

.

Table 6.3: The scores explanations given to the different mitigation options regarding technical aspects.

Criterion	**Baseline** **Doing nothing (baseline scenario)**	**Mitigation Option 1** **Increasing the channel dimensions**	**Mitigation Option 2** **Infiltration increase**	**Mitigation Option 3** **Construction Retention areas**
Technical aspects	**1.0**	**4.0**	**2.7**	**2.7**
Reduces flooded area	The scores were given based on the reduction rate. Since, this is the original scenario no reduction clearly observed.	Clear reduction over the whole area. There is no total reduction but the reduction consist of more than 50% reduction	This does not result in a significant reduction in flooded area. The reduction remains below 20 %	The construction of two retention areas does not result in a significant reduction in flooded area. The reduction remains below 20 %.
Reduction average flood level	The scores are given based on the reduction rate. Since this is the original scenario no reduction is observed.	An average reduction of 18 cm is achieved with is a bit above 50%. This a very high reduction to achieve and an indication that the measure works for flood level reduction	The average reduction in flood levels does achieve a significant reduction of almost 30 % but does not achieve by far the goal of 75%.	The average reduction of flood levels does achieve a significant reduction of almost 30 %.

Category 2: Future proofness

To assess the resilience of the options, the functioning of the options under two different extreme scenarios is investigated as discussed in Section 6.1. The results are derived from simulations from the D-Hydro model. The generated flood maps of each specific scenario can be consulted in Appendix F.1.

100-year rainfall

Table 6.4 shows the computational results of the model for the scenarios with an extremely high rainfall intensity event with a return period of 100 years (R=100Y). The flooded area for the baseline increased with 5% and the average flood level remained the same around approximately 30 cm. The mitigation options are tested based on their reduction to the new baseline scenario.

Table 6.4: The computational result for the scenarios using extreme rainfall with a return period of 100 years. These computational results consist of flooded areas in (m^2 and %) and average flood level. *This is the average flood level

#	Option	Flooded Area [km^2]	%	% reduced	Average reduced FL[cm]	% reduced
0	Baseline (100Y)	1.51	15	0	29.7*	0.00
1	Channels	0.90	9	41	16.2	55
2	Infiltration	1.41	14	7	8.2	28
3	Retention	1.49	15	2	4.0	14

The computational results correspond with scores in Table 6.5. The scores for the 100-year rainfall scenario are explained in Table 6.6.

Table 6.5: The weights and scores for the future proof criteria for a R= 100.

Future proof	Score 1	Score 5	weight (1-5)	0	1	2	3
Criterion			4	1.0	4.3	3.3	2.3
2-1	No reduction	Significant reduction (+50%)	2	1	4	2	1
2-2	No reduction	High reduction of FL (+50%)	4	1	5	4	2

Table 6.6: The scores explanations given to the different mitigation options regarding a future-proof scenario of R=100.

Criterion	**Baseline** **Doing nothing (baseline scenario)**	**Mitigation Option 1** **Increasing the channel dimensions**	**Mitigation Option 2** **Infiltration increase**	**Mitigation Option 3** **Construction Retention areas**
Future proof				
Reduction flooded area for R=100 Y	The flooded area increased with 5%	This option shows a relative reduction of just over 40%	This option does only show a reduction of less then 10% in flooded area during the peak drainage. The flood is delayed but not really prevented.	The option only shows a reduction of less than 2% in the flooded area. The volume that the retention areas can retain is too low for this scenario.
Reduction average flood level R=100 Y	The average flood level remains approximately the same	The flood level reduction is again very high and shows just a reduction under the 55%	Unlike the flooded area the flood level are reduced by 8.22 cm. Which is a relative reduction of approx 30%.	The average flood level is reduced by 4.02 cm. Which is a relative reduction of approx 13%

Relative sea level rise

Table 6.7 shows the results of the model for the sea level rise scenario in combination with a 2-year rainfall scenario. The flooded area increases with 1% and the average flood level increases to approximately 34 cm. Again, the mitigation options are tested based on the reduction compared to the baseline scenario with sea level rise.

Table 6.7: The result for the scenarios using relative sea level rise of 47 cm. This output consists of the flooded area in (m^2 and %) and the average reduced flood level. *This is the average flood level

#	Option	Flooded Area [km^2]	%	% reduced	Average reduced FL[cm]	% reduced
0	Baseline	1.05	11	0.00	33.9*	0.00
1	Channels	0.56	6	47	16.2	48
2	Infiltration	0.91	9	13	8.4	25
3	Retention	0.96	10	9	8.4	25

Table 6.8: The weights and scores for each criterion per specific option.

Future proof	Score 1	Score 5	weight (1-5)	0	1	2	3
Criterion			4	1.0	4.3	3.3	2.3
2-3	No reduction	Significant reduction (+75%)	2	1	4	2	1
2-4	No reduction	High reduction of FL (+50%)	4	1	4	4	4

Table 6.9: The scores explanations that are given to the different mitigation options regarding a future proof scenario of RSLR.

Criterion	Baseline Doing nothing (baseline scenario)	Mitigation Option 1 Increasing the channel dimensions	Mitigation Option 2 Infiltration increase	Mitigation Option 3 Construction Retention areas
Future proof				
Reduction flooded area for RLSR	The flooded area increases with 1%.	The option still achieves a reduction of just under 50%. This very good performance for such an extreme event.	The option achieves a relative reduction in the flooded area of just under 15%	The option achieves a relative reduction in the flooded area of 9%
Reduction average flood level RSLR	The average flood level increases to almost 34 cm.	High reduction of 16.24 cm is achieved. Almost reaching the goal of still an average reduction of just under 50%	The flood level are reduced by 8.4 cm which is a relative reduction of 25%	The flood level are reduced by 8.41 cm which is a relative reduction of 25%

Category 3: Adaptivity

The scores given in terms of adaptivity are shown in Table 6.10 and the scores are explained in Table 6.11.

Table 6.10: The weights and scores regarding the adaptivity

Adaptivity	Score 1	Score 5	weight (1-5)	0	1	2	3
Criterion			3	3.0	2.0	3.0	4.0
3-1	Not feasible	Easy to adapt		3	2	3	4

Table 6.11: The scores explanations given to the different mitigation options regarding the adaptivity.

Criterion	Baseline Doing nothing (baseline scenario)	Mitigation Option 1 Increasing the channel dimensions	Mitigation Option 2 Infiltration increase	Mitigation Option 3 Construction Retention areas
Adaptivity				
Feasibility of adaptivity	Because nothing is done this situation is easy to adapt.	The option already looks at the maximum allowable extension. For very few of the channels extra extension is possible without removing residents or infrastructure. Some of the channels could be further deepened but this would only help in upstream area above the tidal water level.	The option is drafted on what is maximally possible at the current state. If houses would to be reinforced over the coming years and the societal mindset would be changes by subsidising the construction of green roofs, the infiltration could be increased. Furthermore, during the study it became clear that the infiltration capacity increased over the years. With the help of new techniques and innovation of the future this could potentially advance the adaptivity of this option.	The construction of the two retention areas would be quite adaptable. The depths of the two areas could be increased if to be necessary for future scenarios. Although, the length and width of the retention areas would be remain fixed because an increase would mean the loss of more residents.

The possibility that more space will be available in the future for further extension is expected to be very low. This is why Option 2 scores higher relative to Option 1. Option 1 already considers the maximum possible increase without relocating the inhabitants. Further extension of the channel dimensions requires a lot more space that would not be immediately available. However, the possibility of upscale green roofs in the future with for example new techniques is assumed to be higher. Therefore the score of Option 2 is higher than Option 1.

Option 3 got a higher score than the other two options because the depth of the retention areas is very adjustable. The biggest struggle in adapting Option 3 is shifting the width of the retention areas. If more volume is required the depth is the adjustable parameter.

Category 4: Socio-economic aspects

The scores given to the socio-economic aspect are shown in Table 6.12 and the scores are explained in Table 6.13.

Table 6.12: The weights and scores regarding the socio-economic aspect.

Socio-economic aspects	Score 1	Score 5	weight (1-5)	0	1	2	3
Criterion			3	3.0	3.0	4.0	3.0
4-1	Disadvantages / less attractive	Benefits/more attractive		3	3	4	3

Table 6.13: The scores explanations given to the different mitigation options regarding the socio-economical aspects.

Criterion	Baseline Doing nothing (baseline scenario)	Mitigation Option 1 Increasing the channel dimensions	Mitigation Option 2 Infiltration increase	Mitigation Option 3 Construction Retention areas
Socio-economic				
Impact of livelyhood	No impact for the inhabitants other than still experiencing floodings (will not become more attractive).	The option takes into account that no rehousing has to take place. Increasing the dimension would be an intensive job with long construction times (over 5 years). The inhabitants that live in the area would experience nuisance from construction. Additionally this is a grey solution and not attractive to look at	The infiltration option is a very appealing measure since green roofs and infiltration strips would increase the attractiveness of the area. Furthermore, green roofs can also efficiently reducing the temperatures and the noise inside buildings. This option can reduce the cooling need up to 25% and reduce outside noise of around 40 decibels (Poleto & Tassi, 2012). The permeable pavement together with the green roofs introduced a delay time (see Section 5.4). The delay time has the advantage of allowing more evacuation time for residents. This is readily apparent for the 100-year rainfall situation. The increase in evacuation time is made clearly visible in Figure 6.1. However, the construction time of the roads would also be long and cause nuisance for traffic and residents.	Constructing 2 retention areas has advantages like providing a source of drinking water in regions with limited access to clean water and offering recreational spaces during dry periods. However, drawbacks include the need to relocate residents and the potential health risks associated with stagnant water attracting mosquitoes

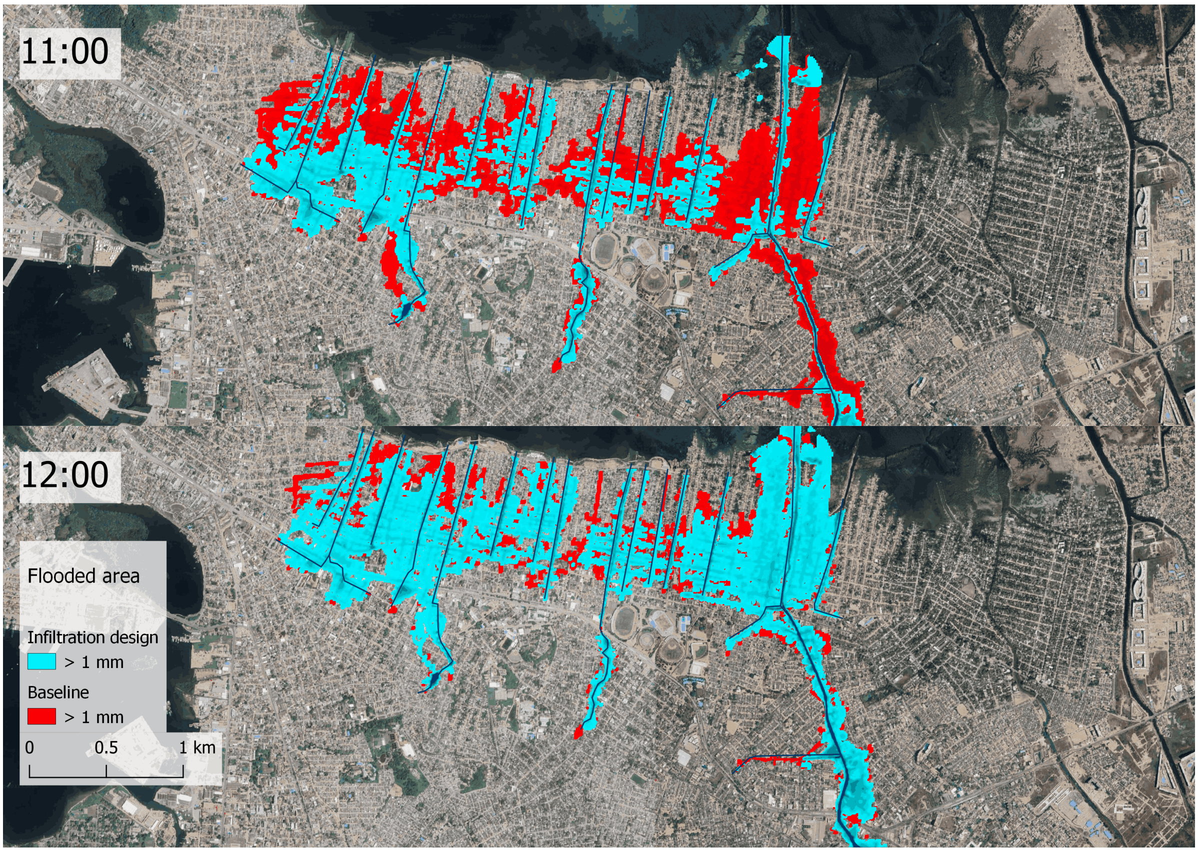

Figure 6.1: The response to the flooding due to the induced delay time. It creates more evacuation time.

Options 1 and 3 got the same score regarding criterion 4-1. This is because both options deal with some of the same drawbacks as construction nuisance. Option 1 does not need to relocate inhabitants which is a huge advantage regarding Option 3. On the other hand, Option 3 collects possible drinking water and creates recreational spaces at the expense of these houses. Therefore Options 1 and 3 are assumed in balance with each other.

Option 2 has a better score than the other two options. The reason is that the benefits that follow from this option weigh heavier than the disadvantages. The only disadvantage regarding criterion 4-1 is the construction nuisance. The infrastructural nuisance that follows from adapting the roads could potentially create gridlocks in the city. That is the reason this option did not receive a score of 5.

Category 5: Financial impact

The rough calculations are made to assess the construction costs. These cost assumptions per mitigation option can be found in Appendix G. The scores given in terms of costs are shown in Table 6.14 and the scores are explained in Table 6.15. These scores correspond with the cost tab given in Section 6.1.

Table 6.14: The weights and scores regarding the costs.

Financial impact	Score 1	Score 5	weight (1-5)	0	1	2	3
Criterion			2	5.0	4.0	1.0	4.0
5-1	High costs	No costs		5	4	1	4

Table 6.15: The scores explanations given to the different mitigation options regarding the financial aspects.

Criterion	Baseline Doing nothing (baseline scenario)	Mitigation Option 1 Increasing the channel dimensions	Mitigation Option 2 Infiltration increase	Mitigation Option 3 Construction Retention areas
Financial aspects				
Costs	No costs are attached to this plan	The option will costs approximately 10.5 million $.	This option would have a price over the 550 million $.	This option will cost approximately 6.5 million $.

Category 6: Environmental aspects

The scores given in terms of environmental aspects are shown in Table 6.16 and the scores are explained in Table 6.17.

Table 6.16: The weights and scores regarding the environmental aspects.

Environmental aspects	Score 1	Score 5	weight (1-5)	0	1	2	3
Criterion			3	1.0	2.6	4.0	4.0
6-1	No impact on biodiversity	Creating more natural areas	3	1	2	4	4
6-2	No impact on water quality	Water quality becomes significantly better	5	1	3	4	4

Table 6.17: The scores explanations given to the different mitigation options regarding the environmental aspects.

Criterion	Baseline Doing nothing (baseline scenario)	Mitigation Option 1 Increasing the channel dimensions	Mitigation Option 2 Infiltration increase	Mitigation Option 3 Construction Retention areas
Environmental				
Enhancing biodiversity	It is not enhancing the biodiversity.	The option results in more surface in the downstream areas for birds and other species. This expansion also leads to the construction of more grey structures, also removing more natural habitat. This is especially the case at the outlet mouths from the side of the Ciénaga. It also creates a more structural appearance overall.	Green roofs are creating more green areas for birds and other species. However, the option does not allocate any real areas for nature conservation but in general more green areas.	The retention areas can be made into a recreational park or something similar creating a more biodiverse habitat. Mainly the eastern retention area can be connected to the channel system to create an area for nature to thrive.
Improvement of water quality	More floods will bring in more and more domestic waste and pollution to the Ciénaga. This will deteriorate the lake further.	Less floodings will also reduce pollution. Lastly more fresh water can flow in the Ciénaga. However, this will only apply if maintenance dredging would be applied and the channels are structurally cleaned from domestic waste.	The infiltrated water is naturally treated within the soil, acting as a natural filter. Additionally, by reducing run-off water, there is a decrease in the amount of polluted water flowing from the surface into the drainage systems.	The rainwater can be collected and treated into clean (drinking) water and subsequently pour onto the Ciénaga.

Option 1 scores lower on criterion 6-1 than the other two options. The other two options have the potential to create new natural areas whereas Option 1 does not. Option 2 creates more natural areas on roofs and Option 3 can be used as a park or something similar. Also, the amount of sand that should be excavated for the retention areas can be used to nourish the eroding beaches. As this volume of Option 3 is more than double that for Option 1, it is also a reason for a higher score (for the excavated volumes see Appendix G). The reason for options 2 and 3 not achieving a score of 5 for this aspect is the size in which the options are enhancing the biodiversity since it operate on a very small scale.

In terms of criterion 6-2, Option 1 scores again lower than the other two options. The other two options have the potential to treat the rainwater whereas Option 1 does only increase the flow towards the Ciénaga, potentially improving the water quality on a small scale in the wetland through fresh water supply.

6.3. Best preferred mitigation option

After scoring the criteria and evaluating the individual scores the following steps are taken:

1. The weights of the categories
2. Total score results
3. The discussion of the ultimate results

6.3.1. The categories weights

In Section 6.3.1 the weightings between the categories are shown and the motivation behind them.

Table 6.18: The weights of the different categories and the motivation behind these weights.

Category	Weight (1-5)	%	Explaination
1	5	25	The technical criteria are seen as extreme importance because the options were created with flood reduction as objective. .
2	4	20	Since the option should be resilient to be seen as durable. .
3	3	15	Prioritising adaptability in the option will ensure that the Mitigation Option remains effective, resilient and sustainable in the face of future challenges. .
4	3	15	The options are invented to the benefits of residents. Due to the nature of the densely populated area, it may not be possible to completely avoid negative impacts. .
5	2	10	Although costs are considered, it is not the most important factor in the evaluation due to governmental support. The costs can however be a consideration to assess the effectiveness relative to requiring significant financial investment. .
6	3	15	Given the densely populated and increasingly urbanised nature of the area, environmental improvement is highly desirable. However, it is recognised that addressing the flooding problems and ensuring the safety of residents is a priority. .

6.3.2. Total score

After scoring the criteria and weighing the categories the results of the scores in the MCA can be calculated. These results are shown in Table 6.19.

Table 6.19: The performance of the mitigation options in the MCA. The retention area is receiving the highest overall score but the scores are close.

	Weight [%]	Option 0	Option 1	Option 2	Option 3
Criteria		Baseline scenario	Increasing the channel dimensions	Infiltration increase	Construction retention areas
Technical aspects	25	1.00	4.00	2.67	2.67
Future proof	20	1.00	4.33	3.33	2.33
Adaptivity	15	3.00	2.00	3.00	4.00
Socio-economic aspects	15	3.00	3.00	4.00	3.00
Financial impact	10	5.00	4.00	1.00	4.00
Environmental aspects	15	1.00	2.63	4.00	4.00
Total score	**100**	**2.00**	**3.41**	**3.08**	**3.18**

Option 0, where nothing is done scores by far the worst. None of the mitigation options would be worse than ultimately doing nothing. The best overall performing mitigation option was Mitigation Option 1 with an overall score of 3.41. Mitigation Option 1 outscores the other two by far. Mitigation Options 2 and 3 only receives an overall score of 3.08 and 3.18 respectively. Purely based on scores, the conclusion can be drawn Mitigation Option 1 is the best preferred to apply.

It must be emphasized that a MCA score is not a binding conclusion but the discussion that follows from the results of the MCA is more valuable for concluding.

6.3.3. Discussion results MCA

As was said above, the scores of the MCA are left open for interpretation. The agreement about the results has to be discussed to ultimately conclude the best preferred design.

Doing nothing would be the worst-case option. Although the high score is for the investment costs, the functional impact would be non-existent and the future proof indicates that the floods even will worsen.

Option 1 excels in technical performance and holds up for both future scenarios. This option has by far the best reduction values. Therefore, it was expected that Option 1 would outscore the other two for these two categories. Compared to the other options, Option 1 does not score very low on the rest of the categories. As the technical aspects are considered most important, it is, therefore, logical that this option comes out on top

Compared to Option 3, Option 2 is more resilient to future situations because Option 2 performs better in a 100-year rainfall event. Hence, Option 2 gets a better score for future proofness. Option 2 scores better predominantly in the socio-economic and environmental categories. However, these better scores cannot outweigh its high construction costs, making it not feasible as an option.

Despite the lowest technical performance of the three options, Option 3 has a high overall performance on the rest of the categories. The lowest technical performance is expected, given the fact that Option 3 is a very local measure. Option 3's impact on future-proof scenarios is not as high as desirable but the high score in adaptability makes sure that the option can be modified for a better technical performance. Even as it has a much lower overall score than Option 1, the adaptivity and relatively low costs of Option 3 make it a considerable option. Especially if you would deploy it locally where magnifications of the channels are not possible or make sense.

6.4. Conclusion

Considering the scores of the options in the MCA (see Section 6.3.2) and the discussion that followed from it (see Section 6.3.3) sub-question 4 can be answered. The best-preferred mitigation option that would be applicable in this focus area would be Mitigation Option 1, the extension of the channels due to the high technical performance and performance under heavier scenarios. Only Mitigation Option 1 is not able to resolve floods at the Amador Y Cortes channel (shown in the black rectangle in Figure 6.2). Therefore, the following adjustment is suggested to conclude an ultimate best-preferred mitigation option. This ultimate best preferred mitigation option would be to add the western retention area. This retention area will help to resolve floods locally around the area of Amador y Cortes channel.

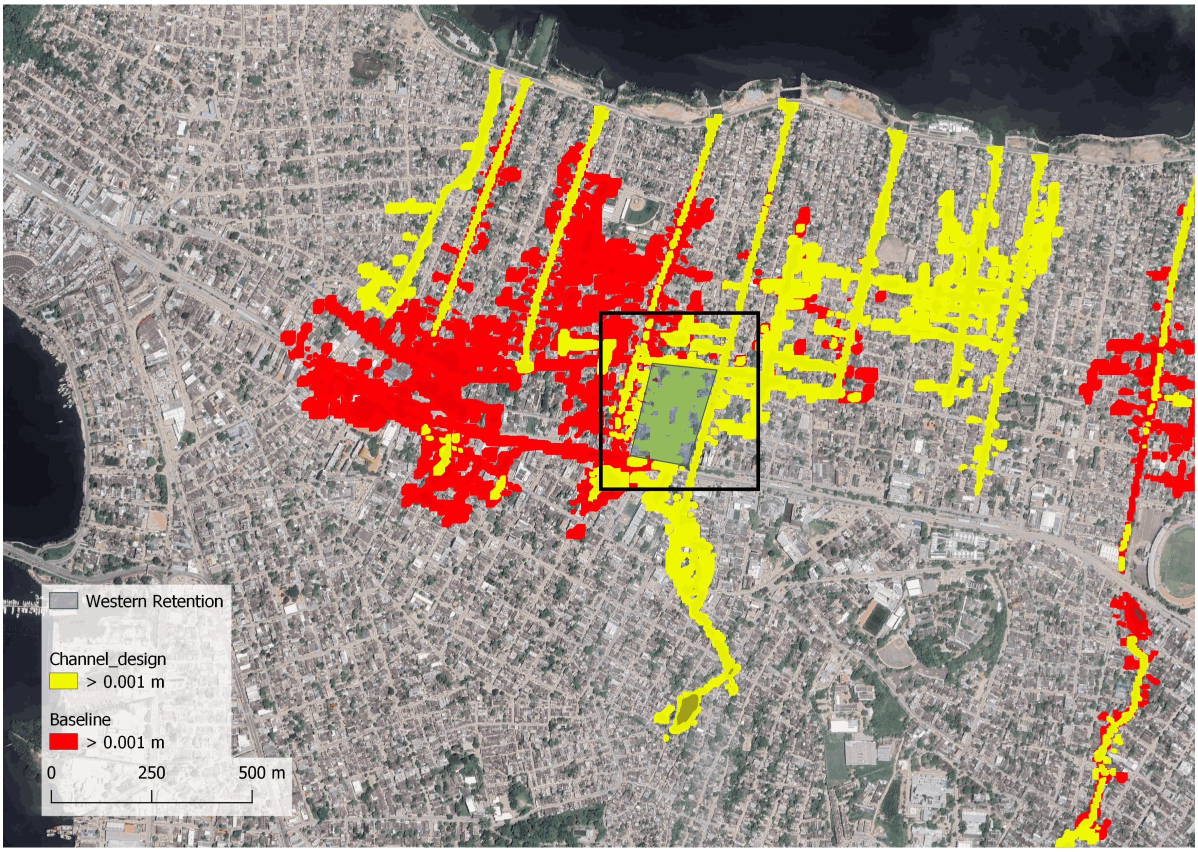

Figure 6.2: The adjustment to the best preferred mitigation option. The addition of the western retention area will resolve locally for this area.

The addition of this western area would, next to further reducing the floods, also add the talked about socio-economic and environmental benefits. Although rehousing has to be considered, sources within the project team indicated that most of the residents know that rehousing is inevitable.

7

Discussion

There are several questions about notable considerations, assumptions and limitations throughout the study that have to be discussed to understand their potential impact on the results and ultimately the conclusion. Below the following questions are stated and discussed:

In which way did data limitations influence the research?

Data limitations may influence the quality of research. Within this study, finding reliable and complete data was found a challenge. Below some of the data limitations and their influence on the quality of the research are discussed:

- The applied **data on channel dimensions** originates from 2009. More recent data is not found. Although official no renovation has taken place since, the unauthorised construction could for example have been narrowing channels without the authorities knowing. There is a fair chance that the channel dimensions in the model are not correct. With that, the model validation as well as simulations for design options are uncertain to a certain degree. The impact on the overall conclusions is however limited because the improvement as a result of increasing channel dimensions on flooding is judged relative to the baseline model instead of absolute.
- **Water levels in the Ciénaga** are not available. Tidal levels at sea are determined based on tidal constituents. The assumption is made that the water levels in the Ciénaga correspond with water levels at sea. This is a valid assumption because the Ciénaga has an open connection with the sea through La Bocana. Some water level differences can however be expected because the La Bocana is quite narrow (therefore the Ciénaga may not follow the tidal range at sea) and wind-driven water level variation may occur inside the Ciénaga. Also, the rural run-off water is not considered which can potentially increase the water level during storms. Based on simulations and observations it is concluded that flooding is mainly caused by rainfall and not tidal water levels. For that reason, the exact tidal levels are of less importance. For judging whether tidal flooding will also be limited in a situation with sea level rise, water levels in the Ciénaga should be known in more detail however.
- The **reference level** of topographic data (Digital Elevation Model) and water level data is missing. Based on an analysis of various data sources, an educated assumption is made concerning the applicable reference level. The impact on the study results is however considered to be limited. Based on simulations and observations, the conclusions hold that flooding is mainly caused by rainfall. Tidal flooding is expected to be limited, at least in the existing situation. For judging whether tidal flooding will also be limited in a situation with sea level rise, reference levels should be known, however.
- The found **short-term rainfall** (<mm/day) data is not deemed consistent enough. The rainfall distributions are therefore based on distributions from the Edurbe study. Simulations show the sensitivity of the model to peak rainfall intensities. The extreme rainfall intensity values calculated in this thesis correspond more with the intensity values of other older studies(Local authorities,

2009a) than from the Edurbe study. However, based on the literature, the found distributions with short duration of rainfall with high intensities, seem fairly reasonable (Arrieta-Pastrana et al., 2023). The impact of the uncertainty could be large on the simulations but there is a fair chance that these distributions do not much differ from the reality.

- The **spatial variability** of precipitation within the region is considerable. The average distance from the rainfall station, of which data has been used, to the study area is around 5 km. For a time frame larger than 12 hours, the correlation distance is around 7 km (Mouthon-Bello et al., 2023). So at the edges of the study area, small variations in rainfall intensities could emerge but these would be not so significant that these variations would change the overall conclusions.
- The **validation and calibration data** are limited. The validation is based on flood levels from a contextless community interview and recorded flooded neighbourhoods from new articles. Despite not knowing the conditions of the community interview, the model showed a strong correlation with the available flood levels. This suggested that the assumptions about the conditions of the community interview could be true. The model is validated as best as the data allows. However, new validations could improve the model in more areas and expose weaknesses.

Conclusively, although these data limitations introduced varying degrees of uncertainty and potential inaccuracy in the study, the overall conclusions were still supported by the available data and the assumptions made. More accurate and recent data could significantly improve the reliability of the results.

Did model assumptions influence the research?

The D-Hydro model is set up from scratch. To achieve a working model some assumptions are made. Below some of the assumptions are listed and discussed about their influence on the results:

- The drainage through a **single lateral inlet point** simplifies the real-world complexity of water distribution. This ensured the start of the water flow within the 1D model. The reason to do this was to schematize the worst-case scenario possible of all the water flowing through the whole channel. This could lead to an overestimation of the flooding in the upstream regions. On the other hand, using the 2D grid as an inlet point would otherwise lead the rainwater over the streets when draining towards the channel. These streets would nevertheless be indicated as flooded areas. Ultimately, this assumption checks capacity and ensures the usage of the channels' recorded cross-sections. Dividing the catchments and the inlet points of the larger channels helped to create realistic results.
- The channels are considered as **clean and unblocked**. The channels had to be assumed clean otherwise their functionality could not be tested. This is however not an accurate representation of the real-life situation. The actual channel conditions consist of sedimentation, vegetation and domestic waste throughout most downstream parts of the channels. This alters the hydraulic properties of channels. The capacity of the channels is further lowered. A slight allowance has been made by using a higher value of Manning's coefficient but nevertheless, the results of the simulation would be an underestimation.
- The **embedded linkage** can cause double storage within the model. The water would be stored in the 1D grid and the 2D grid. The storage on the 2D grid is shown on the flood map but the water is contained within the dimensions of the bed level. The reason for using embedded links was to reduce the set-up time and ultimately computational time. The double storage would underestimate the results of the simulations, mainly for the bigger channels. Although, downstream where the bed levels of the channels are lower than the water line, the channels are already filled as the initial water level imposed on the 1D and 2D grid is 0.00. Double storage of the run-off water would therefore not be possible for these sections of the channels. In the end, only the upstream parts of the channels would experience double storage.
- The **threshold of flooding** is defined as a grid cell containing a higher flood level than 1 mm. The reason for taking 1 mm into account is to cancel out the non-significant values. This threshold of 1 mm is defined as a wet surface. The difference between 1 and 1 cm was eventually checked and no significant change was seen. If the threshold is raised to an order of 10 cm, this change

would naturally have an impact on the total flooded area which would decrease. The threshold of 1 mm is therefore found to be logical.

- **Hydraulic structures** are not considered. It would have been a difficult and time-consuming process to exactly find out where the structures all are situated. The same assumption as for the consideration of clean channels applies here. The structures can be easily clogged by domestic waste and the results of the simulation would be an underestimation in areas where structures are present.

Conclusively, the discussed assumptions could have caused both over- and underestimations of the results. The underestimation of the results due to the embedded linkage is only the case for the upstream regions. In addition, these upstream regions are also the ones mainly affected by the over-prediction of the single lateral inlet points assumption. These two contradict each other and could make the errors negligible. The consideration of clean and unblocked channels will probably be more dominant in terms of underestimating the floods. The results of the validation, a very slight under-performance, support this statement.

How did the evaluation of the options influence the best-preferred mitigation option?

The Mitigation Options are evaluated to ultimately recommend a preferred mitigation option for the focus area. The remarks about the evaluation are listed below:

- The chosen **categories** in the MCA are the same as in the project of the consortium. This allows the evaluation to easily feed into the overall project. However, if other categories and criteria are evaluated then there could be a different ultimate recommendation.
- The **categories' weights** are justified, but this decision remains subjective. Another writer might have weighted the categories slightly differently. The weights have a direct impact on the overall score in the Multi Criteria Analysis, so changing the weights could result in a different overall score. This subjectivity underlines the importance of a transparent and inclusive approach to weighting and interpreting Multi-Criteria Analysis results. As Mitigation Option 1, increasing the channels, stands out by far, the same outcome with a slightly different weight would be expected.
- The **score scale** is set on the forehand of the evaluation. This causes the Multi-Criteria Analysis outcome to be transparent and carefully considered.
- The Multi-Criteria Analysis is used as a **tool for discussion** and the score was not binding. As a result, another objective look at the outcomes of the Multi-Criteria Analysis is taken into consideration and discussed. This ultimately ensures the best-preferred mitigation option is well considered.

Conclusively, all these above-mentioned elements ensured that the recommendation was not only the result of quantitative analysis but also of qualitative judgement and collective reflection.

How will the findings of this research contribute to the overall water system of Cartagena?

The research zoomed into the drainage channels of the water system of Cartagena. The drainage channels, however, are connected with the overall water system of Cartagena as stated in Section 1.2. To return to the whole system (shown in Figure 7.1), the following findings of the report are being discussed to understand their impact on the entire system:

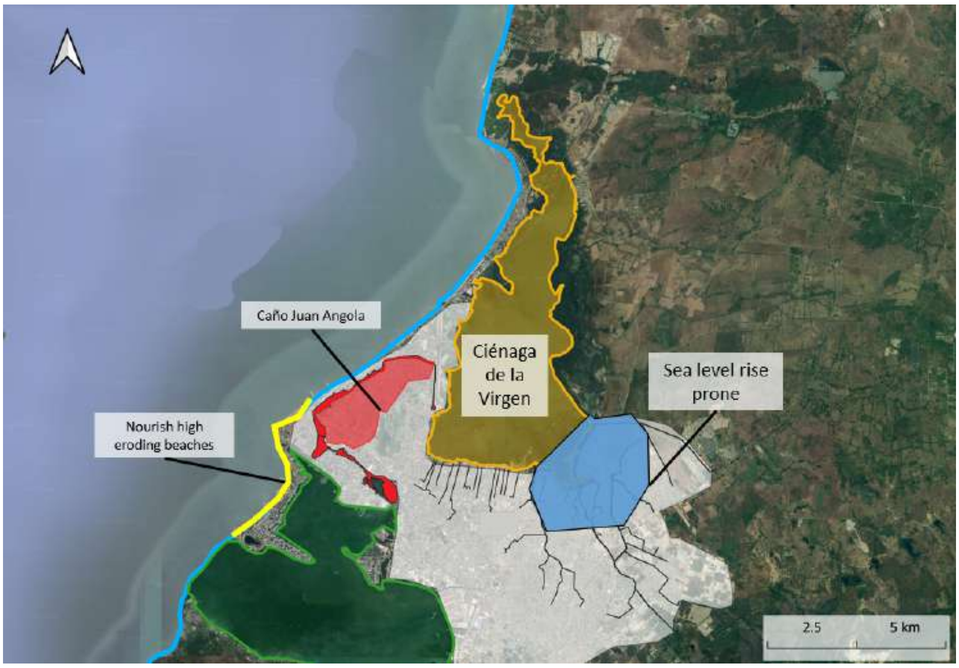

Figure 7.1: The overall water system of Cartagena with the points of interest in this research.

- The proposed best preferred mitigation option will cause fewer floods resulting in less domestic waste collected and transferred towards the Ciénaga. This will **improve the water quality of the Ciénaga de la Virgen** (see the orange area in Figure 7.1). The better water quality will improve the living conditions of the animals living in and onto the Ciénaga. This will make the eco-tourism more appealing. Enhancing water quality not only has positive effects on the environment but also benefits the fishing industry.
- **The approach used in this research can be applied to more areas in Cartagena**. For example, Arcadis is exploring the option of improving the Caño Juan Angola channel (see the red highlighted area in Figure 7.1). The Caño Juan Angola has the same uncertainties about the flood thriving influences in the area. The step-by-step approach used in this research could help explore the right types of mitigation measures.
- **The model's results can be used as input for (detailed) studies**. The drainage volume of the channels can for example be used as an input value in a detailed model of the Ciénaga.
- The **identification of areas vulnerable to sea level rise** (see the blue highlighted area in Figure 7.1) helps in conducting risk assessment and strategic planning within the broader water system. By highlighting areas vulnerable to sea level rise, this identification allows for the efficient targeting of further detailed research and the development of mitigation strategies. This approach serves to increase the resilience of coastal communities.
- The **excavated soil** that becomes available by implementing the best-preferred mitigation design (increasing the channels and a western retention area) can be used to **nourish the beaches** that are prone to erosion (this is highlighted with the yellow line in Figure 7.1 and corresponds with the information in Figure 3.17).

The research findings conclusively indicate that, while the primary focus lies on rainwater drainage, holds potential for enhancing Cartagena's entire water system. Not only can these results inform future studies, but the suggested mitigation design could also address other water-related challenges within Cartagena's infrastructure.

8

Conclusion

Cartagena de Indias, like many other coastal cities, faces an increased risk of flooding, exacerbated by heavy rainfall and rising sea levels. Over the last two decades, flooding has been established as the most severe disaster in Cartagena. Particularly vulnerable are the city's poorest residents, who live at the southern edge of Ciénaga de la Virgen, the city's wetland. The city's drainage system runs mainly through these residential areas to the Ciénaga de la Virgen. The seasonal extreme rainfall events and the projected relative sea level rise are threatening this group of residents with both types of flooding sources.

The ConAgua consortium, which Arcadis is part of, is in the design stages of exploring integral solutions to water-related issues for the city of Cartagena. This thesis supports the project by investigating urban flooding, as a part of the integral objective. The findings provide insights into the available data, indicate the flood-prone areas and ultimately recommend what types of mitigation would work and in what order of magnitude, these should be further explored. The main research question was stated as:

How can an integrated approach, after effectively investigating different types of flood sources along the edge of Ciénaga de la Virgen, recommend the best preferred mitigating design?

The answer to this main question is found by answering the following 4 sub-questions;

Sub-question 1: What are the key reasons for flooding which can be supported by available data?

The first sub-question highlights the significant challenges posed by the drainage capacity. The up-stream high slope variations and high rainfall intensity lead to flooding predominantly in downstream areas, as the water runs quickly off towards the areas with a milder slope. These areas lay mainly close to the banks of the Ciénaga de la Virgen. At these banks, most of the channel beds lay under the water line. The implication is therefore given that the water level would have an impact on the floods as the run-off water would be less likely to drain into the Ciénaga de la Virgen. The impact of relative sea-level rise, which would be around half a meter by 2050, should exacerbate the influence of the water level on floods in these lower-lying areas. This indicates the relationship between natural topography, drainage capacity, meteorological factors, and influences like sea-level rise.

Sub-question 2: How to quantify the impact on flooded areas for different meteorological conditions and or downstream water levels using a numerical model?

Addressing the second sub-question, the study employs a numerical model to simulate different types of flood scenarios. The D-Hydro model quantifies the indications regarding the first sub-question. The model's results revealed that rainfall intensity is a far more dominant factor in influencing flooded areas compared to downstream water level variations. A rainfall intensity with a return period of 2 years already shows a flooded area of 24%. The total influence of the downstream water level is found to be less than 1%. The results also point out the increasing influence of tidal conditions due to sea-level rise, marking a shift in the area's flood susceptibility profile. This increase is concentrated on the southeastern side of the Ciénaga de la Virgen, in areas with minimal residents. The western zone remains almost unaffected by the projected relative sea level rise scenario. This result is unexpected as the system description hypothesised that the relative sea level rise would increase the influence of the water level significantly. The overall results of the modelling study are crucial for exploring mitigation measures towards improving the more urgent hydraulic zone, especially for rainfall events with a 2-year return period.

Sub-question 3: What types of mitigation measures are possible to develop into a mitigation option to reduce floods in urgent zones?

In responding to the third sub-question, the study investigates different types of flood mitigation measures. Evaporation measures and creating a wetland are deducted. Evaporation is deducted as floods are generated by extreme rainfall intensities over a short period. Creating a wetland in the focus area is not deemed as a functional measure because the hydraulic zone has far more influence. In the end, the following three types of mitigation measures are ultimately considered the most viable types of mitigation measures:

- **Increasing channel capacity**: The impact of increasing channel dimensions by various percentages is investigated; 10%, 20%, 30%, 50%, 100% and 200%. The most impact is seen for an increase of 200%. Results show that significant reduction can already be achieved without relocation in most places. Therefore rehousing is not considered. This results in **Mitigation Option 1**, where the required increase is compared to the possible increase and implemented if possible without rehousing.
- **Enhancing infiltration**: The impact is investigated of increasing the infiltration by implementing green roofs and permeable pavement. The infiltration increase is pragmatically modelled by decreasing the catchments by various percentages; 10%, 20%, 30%, 40% and 50%. Considering the implementation of green roofs and permeable pavements a maximum infiltration increase of 20 % can be seen as feasible. These measures would apply a delay time of 30 minutes, which spreads out the peak discharges. The increase of infiltration by 20% in combination with the introduction of a 30-minute delay time results in **Mitigation Option 2**.
- **Constructing retention areas**: For the construction of two retention areas no suitable area can be found that would have an impact and would avoid rehousing. Therefore, two areas are chosen with the possible highest impact. The impact of these areas is investigated for various depths; 2, 4, 6 and 8 meters. The results of this investigation show that for the eastern area, a depth of 2 meters is most suitable and for the western area a depth of 4 meters suffices. A western retention area with a depth of 4 meters in combination with an eastern retention with a depth of 4 meters results ultimately in **Mitigation Option 3**.

Each of these options is assessed for their effectiveness in reducing flooded areas and flood levels. The understanding of their feasibility and technical functioning make the options the three most suitable mitigation options.

Sub-question 4: Which mitigating design is best preferred in this study area?

Finally, the study addresses the last sub-question by conducting a Multi-Criteria Analysis (MCA) to evaluate the best-preferred mitigation design. The MCA integrates various categories of criteria, including technical performance, future-proofness, adaptivity, socio-economic, financial and environmental aspects. The MCA concludes that Mitigation Option 1, focusing on increasing channel capacity, emerges as the best scoring option. This mitigation option demonstrated superior technical performance and resistance to extreme rainfall scenarios, despite scoring somewhat lower on categories like socio-economic and environmental benefits. Mitigation Option 2, enhancing the infiltration, is not deemed feasible due to the high costs. The ultimate best-preferred mitigation design is to apply Mitigation Option 1 and construct the western retention area. Mitigation Option 1 reduces the overall flood very well and the western retention area tackles the flood at the Amador y Cortes channel, for which Mitigation Option 1 is ineffective. Furthermore, the western retention area achieves high scores in non-technical performance. Therefore, the western retention areas are bringing along non-technical performing benefits despite only reducing flooding very locally.

To address the main question, this thesis concludes by presenting an integrated approach for selecting the best-preferred flood mitigation design for the area under study. System analysis plays a crucial role in understanding the prevailing conditions in the area. By testing and quantifying the formulated hypotheses, it becomes possible to pinpoint the primary factors driving flooding in the area, thus facilitating a more targeted investigation of appropriate mitigation options. This approach has proven to be an efficient means of arriving at a preferred mitigation design and can be recommended for use in areas where determining the principal influence of water levels and rainfall intensity on flooding is particularly challenging. Furthermore, this approach lays a robust foundation for a more comprehensive exploration of the best-preferred mitigation design.

9 Recommendations

In this chapter, recommendations are given based on the discussion and the conclusion. The recommendations are divided into recommendations for improving the system understanding and quality of the model input and recommendations regarding the next phase in the project.

9.1. Recommendations for improving system understanding and quality of model input

The data is critical for understanding the system and as an input parameter for a computation model. The following additional data gathering is recommended to increase system understanding and the reliability of the model:

- The constant monitoring of the **water level in the Ciénaga**. This would give clarity about the impact of the tidal range on the water level inside the Ciénaga. Furthermore, there is also an inflow of rural water to the Ciénaga. This could also potentially impact the water levels and the drainage capacity of the Ciénaga. Lastly, relative sea level rise was also indicated as a potential threat to the southeastern border of the Ciénaga. It would, therefore, be useful to know what the actual water level the Ciénaga has to deal with.
- As also recommended in Mouthon-Bello et al. (2023), **more rainfall stations** should be installed in the city within a range of 5 km and the data should cover **short-term data**. This would provide more insight into short extreme rainfall events and the distribution of rainfall events.
- **The flood levels** should be recorded in the neighbourhoods at the edge of the Ciénaga. This would allow for calibrating and validating numerical models more accurately. An option could be to install certain reference points with a specific height. These can be used when conducting community interviews after a flooding event to give more indication about flood levels. Also, overall more community interviews in more regions are recommended.
- The appropriate **soil content and green areas per catchment** should be determined. Then, the numerical model can include the correct infiltration capacity for each catchment. The catchments were assumed as uniformly paved and infiltration was disregarded. The schematising of the infiltration type of mitigation measure within the model was therefore to reduce the catchment areas in percentage steps. This assumption was made to investigate the overall performance of an infiltration increase within the study area. This is a very pragmatic representation. Ideally, for each catchment, its correct and current infiltration capacity was determined.

9.2. Recommendation for the next phase in the project

These recommendations are made to be implemented in the next phase of the project.

9.2.1. Improvements to the D-Hydro model

After gathering more calibration and validation data, the model should be improved. The following improvements are recommended:

- Correct for unequal bank height. A uniform cross-section is assumed but the bank height does vary for the channels.
- Use lateral links between the 1D and 2D grid to overcome the double storage in the upstream sections.
- Include hydraulic structures to evaluate their working.
- Assume clogged channels for simulations.

These improvements should improve the realism of the model and therefore will get better results.

9.2.2. Further assessment of mitigation options

The following recommendations are made for further development or assessment of mitigation options.

Channel increase

Mitigation Option 1 was based on what extension was possible without rehousing. Google Street View was used for the assessment of to which extent these channels were able to be extended or needed. The images in the upstream areas were fairly up to date as most were dated from 2022. The years of the images used downstream ranged from 2012 to 2019. For most of this downstream area, the images were taken from 2014. This means that the indication of the built-up area could be outdated. It is recommended that the possible enlargements should be verified with local parties.

Infiltration increase

It is assumed that a maximum increase in infiltration of 20% can be achieved. This is because the housing at the edge of the Ciénaga is in too bad shape for implementing green roofs. However, an innovative alternative could be explored. Because this project is funded by the municipalities, innovative options are more likely to be financially viable. This could eventually increase that extra infiltration capacity to get to that aimed significant increase of 30 %.

Retention areas

It could be considered to divide the proposed retention areas into smaller retention areas spread over parts that are vulnerable to flooding. It would then not be necessary to rehouse an entire neighbourhood but just smaller parts. Utilizing (new) vertical housing will make it possible to relocate affected people within their neighbourhood. This was not considered during the design process but would certainly be recommended to look at in a follow-up study.

Mitigation options for southeastern Ciénega border

In this report, the priority was shifted towards the hydraulic zone as these problems are of greater magnitude. However, the influence zones showed that the southeastern border is most influenced by the tidal levels of the Ciénaga. The influence of the water level will grow to land inward to the neighbourhoods more directly in the south part, due to relative sea level rise. For the residents living on the edge of the southeastern border, this relative sea level rise would pose a threat to their existence. It is recommended to also implement a study for mitigation options for this water level problem in the area.

9.2.3. Recommendations regarding public awareness

Some recommendations can be made for increasing public awareness about the following topics:

- **Clean channels and keeping them clean**: Doing so would require a lot of community participation but the drainage system or an increased variant of them would not work in case of blockage.
- **Consequences of building unauthorised settlements**: The high rate of sea level rise and building near the edge of the Ciénaga puts people at high risk of losing their property. People should be aware to stop building illegal settlements further to the water border.

- **Relocation may be inevitable**: The residents have to be made aware that rehousing could be inevitable. This would help them prepare to accept and a final solution can be considered together.

References

Aldridge, B. N., & Garrett, J. M. (1973). “Roughness coefficients for stream channels in arizona” (tech. rep. No. 87). U.S. Geological Survey.

Andrade, C. A., Thomas, Y. F., Lerma, A. N., Durand, P., & Anselme, B. (2013). “Coastal flooding hazard related to swell events in cartagena de indias, colombia”. “Journal of Coastal Research”, 290, 1126–1136. https://doi.org/10.2112/jcoastres-d-12-00028.1

Arcadis. (2022). “Water as leverage”. https://stswalcartagena.ireporting.nl/home

Arrieta-Pastrana, A., Saba, M., & Alcázar, A. P. (2023). “Analysis of climate variability and climate change in sub-daily maximum intensities: A case study in cartagena, colombia”. “Atmosphere”, 14(1), 146. https://doi.org/10.3390/atmos14010146

Barragán, J. M., & de Andrés, M. (2015). “Analysis and trends of the world’s coastal cities and agglomerations”. “Ocean and Coastal Management”, 114, 11–20. https://doi.org/10.1016/j.ocecoaman.2015.06.004

Bello, J. M., Badrán, N., & Basabe, B. (2021). “Formulación y adopción del plan integral de gestión del cambio climático territorial - pigcc-4c – del distrito de cartagena de indias, en el marco de lo dispuesto por la ley 1931 del 2018”.

Bharwani, S. (2020). “Cartagena de indias system description”. https://www.weadapt.org/knowledge-base/vulnerability/cartagena-de-indias-system-description

Brakel, L., Keyzer, L., Hasper, Y., Legene, M., Willemse, J., & van der Stap, E. (2017). “A study on reducing flood risk in cartagena de indias, colombia: Cartagena, it’s now or never”.

Brito, M. D., & Evers, M. (2016). “Multi-criteria decision-making for flood risk management: A survey of the current state of the art”. Natural Hazards; Earth System Sciences.

Camacho, J. J., & Rodríguez, A. F. C. (2021). “Floating symbiosis - centro ambiental ciénaga de la virgen, cartagena, colombia”. http://hdl.handle.net/10554/53232

Cañate, D. C., & Guzmán, M. P. (2017). “Proyección de los niveles de inundación actual y futura en el sistema de caños y lagos de la ciudad de cartagena”. Universidad de Cartagena.

Caracol Radio. (2020). “El 70 por ciento de la ciudad está inundada: Alcalde de cartagena”. https://caracol.com.co/emisora/2020/11/14/cartagena/1605371644_037684.html

Centre for Climate and Energy Solution. (2023). “Extreme Precipitation and Climate Change”. https://www.c2es.org/content/extreme-precipitation-and-climate-change

Cerón, W. L., Andreoli, R. V., Kayano, M. T., Canchala, T., Ocampo-Marulanda, C., Avila-Diaz, A., & Antunes, J. (2022). “Trend pattern of heavy and intense rainfall events in colombia from 1981–2018: A trend-EOF approach”. “Atmosphere”, 13(2), 156. https://doi.org/10.3390/atmos13020156

Cote, E. B., & Rodríguez, J. H. (2015). “Evaluación del drenaje pluvial existente con descarga al mar caribe frente a la alternativa solución con descarga sobre la bahía de cartagena, en el área comprendida entre las avenidas primera y san martín”. Universidad de Cartagena.

Davis, M., & Naumann, S. (2017). “Making the case for sustainable urban drainage systems as a nature-based solution to urban flooding”. In Nature-based solutions to climate change adaptation in urban areas (pp. 123–137). Springer International Publishing. https://doi.org/10.1007/978-3-319-56091-5_8

Deltares. (2023a). “D-hydro suite 1d2d”. https://www.deltares.nl/software-en-data/producten/d-hydro-suite-1d2d

Deltares. (2023b). “D-rainfall runoff technical reference manual” (tech. rep.).

Deltares. (2023c). “Rgfgrid user manual”. https://content.oss.deltares.nl/delft3dfm2d3d/RGFGRID_User_Manual.pdf

Deltares. (2023d). “Sobek and delft3d fm suite 1d2d”. https://www.deltares.nl/en/software-and-data/products/sobek-and-delft3d-fm-suite-1d2d

Díaz Cuadro, J. (2011). “Articulo evaluacion de la calidad del agua en la cienaga de la virgen (cartagena,colombia)”.

EDURBE. (2022). “Amenaza de inundación a partir de los análisis hidrológicos e hidráulicos de los cuerpos de agua principales de la zona urbana y expansión urbana del distrito de cartagena”.

Edurbe. (2022). “Flood hazard from hydrological and hydraulic analyses of the main watercourses in the urban area and urban expansion of the district of cartagena, colombia.”

Environment Agency. (2015). “Cost estimation for channel management - summary of evidence” [[Accessed 05-01-2024]]. https://assets.publishing.service.gov.uk/media/6034ed6ee90e0766047734a9/Cost_estimation_for_channel_management_-_summary_of_evidence.pdf

Establecimiento Publico Ambiental EPA Cartagena. (2023). “Arc gis map sig epa”. http://tinyurl.com/kfewj4z3

European Commission’s Joint Research Centre. (2015). “GHS-BUILT R2018A - GHS built-up grid, derived from Landsat, multitemporal (1975-1990-2000-2014) - OBSOLETE RELEASE”. %7Bhttps://data.jrc.ec.europa.eu/dataset/jrc-ghsl-10007%7D

Fan, Y., Ao, T., Yu, H., Huang, G., & Li, X. (2017). “A coupled 1d-2d hydrodynamic model for urban flood inundation”. “Advances in Meteorology”, 2017, 1–12. https://doi.org/10.1155/2017/2819308

Fischer, E. M., & Knutti, R. (2016). “Observed heavy precipitation increase confirms theory and early models”. “Nature Climate Change”, 6(11), 986–991. https://doi.org/10.1038/nclimate3110

Flórez, J. P. (2015). “Plan maestro de drenajes pluviales”.

Glavovic, B. (2022). “Ipcc report: Coastal cities are sentinels for climate change. it’s where our focus should be as we prepare for inevitable impacts”. https://theconversation.com/ipcc-report-coastal-cities-are-sentinels-for-climate-change-its-where-our-focus-should-be-as-we-prepare-for-inevitable-impacts-177726

Gowtham, S., & Das, G. K. (2023). “Block wise trend analysis and extreme events in raipur district, india”. “International Journal of Environment and Climate Change”, 13(10), 205–214. https://doi.org/10.9734/ijecc/2023/v13i102631

Hawkins, F. A., & Quintero Banda, I. D. (2022). “Capítulo levantamiento de la información primaria”.

IDEAM. (2023). “Consulta y descarga de datos hidrometeorológicos”. http://dhime.ideam.gov.co/atencionciudadano/

Insight, M. (2023). “Major ports in the caribbean”. https://www.marineinsight.com/know-more/major-ports-in-the-carribean/

Januta, A. (2021). “Explainer: The u.n. climate report’s five futures - decoded”. https://www.reuters.com/business/environment/un-climate-reports-five-futures-decoded-2021-08-09/

Latandret-Solana, S. A., Parra, R. R. T., & Moyano, D. P. H. (2023). “Ocean tides in the colombian basin and atmospheric contribution to s2”. “Dynamics of Atmospheres and Oceans”, 102, 101356. https://doi.org/10.1016/j.dynatmoce.2023.101356

Lee, Y.-T., Ho, M.-C., Chiou, Y.-S., & Huang, L.-L. (2023). “Assessing the performance of permeable pavement in mitigating flooding in urban areas”. “Water”, 15(20), 3551. https://doi.org/10.3390/w15203551

Local authorities. (2009a). “Estudios y diseños del plan maestro de drenajes pluviales del distrito de cartagena de indias” (tech. rep.).

Local authorities. (2009b). “Informe componente topografica 2009” (tech. rep.).

MIDAS. (2019). “Alcadia de cartagena”. https://midas.cartagena.gov.co/Content/Switcher

Mouthon-Bello, J. A., Quinones-Bolanos, E., Ortiz-Corrales, J. E., Mouthon-Barraza, N., Hernandez-Fuentes, M. D., & Caraballo-Meza, A. C. (2023). “Spatial variability study of rainfal lin cartagena de indias, colombia”. “Journal of Water and Land Development”. https://doi.org/10.24425/jwld.2022.142316

Munoz, D. F., Yin, D., Bakhtyar, R., Moftakhari, H., Xue, Z., Mandli, K., & Ferreira, C. (2021). “Intermodel comparison of delft3d-FM and 2d HEC-RAS for total water level prediction in coastal to inland transition zones”. “JAWRA Journal of the American Water Resources Association”, 58(1), 34–49. https://doi.org/10.1111/1752-1688.12952

NASA. (2023a). “Ipcc 6th assessment report sea level projections”. https://sealevel.nasa.gov/ipcc-ar6-sea-level-projection-tool

NASA. (2023b). “Is the rate of sea-level rise increasing?” https://tinyurl.com/NASASLR

National Oceanic and Atmospheric Administration. (2023). “Historical hurricane tracks”. https://tinyurl.com/Hurricane-iota

National River Flow Archive. (2023). “Peaks over threshold (pot)”. https://tinyurl.com/hf2h6npp

Northen Arizona University. (n.d.). “Costs construction retention area” [[Accessed 04-01-2024]]. https://www.ceias.nau.edu/capstone/projects/CENE/2020/FlagstaffDrywell/docs/budget.pdf

Omoregie, J. (n.d.). “How Much Does a Green Roof Cost in 2024?” [[Accessed 04-01-2024]]. https://roofgnome.com/blog/cost/green-roof-cost

Orejarena-Rondon, A. F., Sayol, J. M., Marcos, M., Otero, L., Restrepo, J. C., Hernandez-Carrasco, I., & Orfila, A. (2019). “Coastal impacts driven by sea-level rise in cartagena de indias”. “Frontiers in Marine Science”, 6. https://doi.org/10.3389/fmars.2019.00614

Poleto, C., & Tassi, R. (2012). “Sustainable urban drainage systems”. In Drainage systems. InTech. https://doi.org/10.5772/34491

Puello, A., & Martelo, N. (2021). “Remergencias de la historia reciente en el distrito de cartagena 1965 - 2020”. Salvermos Juntos a Cartagena.

Qin, Y. (2020). “Urban flooding mitigation techniques: A systematic review and future studies”. “Water”, 12(12), 3579. https://doi.org/10.3390/w12123579

Rangel-Buitrago, N. G., Anfuso, G., & Williams, A. T. (2015). “Coastal erosion along the caribbean coast of colombia: Magnitudes, causes and management”. “Ocean & mathsemicolon Coastal Management”, 114, 129–144. https://doi.org/10.1016/j.ocecoaman.2015.06.024

Restrepo-Angel, J. D., Mora-Paez, H., Diaz, F., Govorcin, M., Wdowinski, S., Giraldo-Londono, L., Tosic, M., Fernandez, I., Paniagua-Arroyave, J. F., & Duque-Trujillo, J. F. (2021). “Coastal subsidence increases vulnerability to sea level rise over twenty first century in cartagena, caribbean colombia”. “Scientific Reports”, 11(1). https://doi.org/10.1038/s41598-021-98428-4

Serna, Y., Correa-Metrio, A., Kenney, W. F., Curtis, J. H., Velez, M. I., Brenner, M., Hoyos, N., Restrepo, J. C., Cordero-Oviedo, C., Buck, D., Suarez, N., & Escobar, J. (2019). “Post-colonial pollution of the bay of cartagena, colombia”. “Journal of Paleolimnology”, 63(1), 21–35. https://doi.org/10.1007/s10933-019-00101-4

Shen, Y., Morsy, M. M., Huxley, C., Tahvildari, N., & Goodall, J. L. (2019). “Flood risk assessment and increased resilience for coastal urban watersheds under the combined impact of storm tide and heavy rainfall”. “Journal of Hydrology”, 579, 124159. https://doi.org/https://doi.org/10.1016/j.jhydrol.2019.124159

Susdrain. (2022). “Filter strips”. susdrain.org. https://www.susdrain.org/delivering-suds/using-suds/suds-components/filtration/filter-strips.html

Teng, J., Jakeman, A., Vaze, J., Croke, B., Dutta, D., & Kim, S. (2017). “Flood inundation modelling: A review of methods, recent advances and uncertainty analysis”. “Environmental Modelling and mathsemicolon Software”, 90, 201–216. https://doi.org/10.1016/j.envsoft.2017.01.006

Time and Data AS. (2023). “Past weather in cartagena, colombia — november 2020”. https://www.timeanddate.com/weather/colombia/cartagena/historic?month=11&year=2020

Tinoco Devia, J. (2006). “Análisis hidráulico y sedimentológico de la bocana de la ciénaga de la virgen-cartagena de indias”. Universidad de los Andes.

Tirpak, R. A., Winston, R. J., Feliciano, M., Dorsey, J. D., & Epps, T. H. (2021). “Impacts of permeable interlocking concrete pavement on the runoff hydrograph: Volume reduction, peak flow mitigation, and extension of lag times”. “Hydrological Processes”, 35(4). https://doi.org/10.1002/hyp.14167

Torres, R. R., & Tsimplis, M. N. (2012). “Seasonal sea level cycle in the caribbean sea”. “Journal of Geophysical Research: Oceans”, 117(C7). https://doi.org/10.1029/2012jc008159

TRUEGRID. (n.d.). “How Much do Pervious Pavers Cost?” [[Accessed 04-01-2024]]. https://www.truegridpaver.com/pervious-pavers-cost

Twigt, D. J., Goede, E. D. D., Zijl, F., Schwanenberg, D., & Chiu, A. Y. W. (2009). “Coupled 1d–3d hydrodynamic modelling, with application to the pearl river delta”. “Ocean Dynamics”, 59(6), 1077–1093. https://doi.org/10.1007/s10236-009-0229-y

United Nations Department of Economical and Socaial Affairs. (2018). “Population dynamics world urbanisation prospects 2018”. https://population.un.org/wup/Download/

University of Hawaii Sea Level Center. (2023). “Tide gauge data from the uhslc”. https://uhslc.soest.hawaii.edu/data/

Utria, A., Saba, M., & Quinones-Bolanos, E. (2017). “Analysis of the stormwater drainage of the historic walls of cartagena de indias between the bastions of san lucas, santa catalina and santa clara”. “Journal of Physics: Conference Series”, 935, 012043. https://doi.org/10.1088/1742-6596/935/1/012043

Villate Daza, D., Bolívar-Anillo, H., Anfuso, G., Manzolli, R., Portz, L., & Sanchez, H. (2020). “Mangrove forests evolution and threats in the caribbean sea of colombia”. “Water”, 12.

Yazdanfar, Z., & Sharma, A. (2015). “Urban drainage system planning and design – challenges with climate change and urbanization: A review”. “Water Science and Technology”, 72(2), 165–179. https://doi.org/10.2166/wst.2015.207

Yuca-Pelá. (2016). “La bocana: Un baile entre el mar y la ciénaga”. https://yuca-pela.webnode.com.co/la-bocana-oxigenacion-a-la-cienaga-de-la-virgen/

Zeleňáková, M., Diaconu, D. C., & Haarstad, K. (2017). “Urban water retention measures”. “Procedia Engineering”, 190, 419–426. https://doi.org/10.1016/j.proeng.2017.05.358

A

Channel dimensions

In this Appendix, the names and dimensions of all the different kinds of drainage channels are depicted. The numbers of the channels in Figure A.1 correspond with the dimensions in Table A.1.

A.1. Channel names

In Figure A.1 the names of all the different channels are given. The names corresponding with the location have been found through online GIS data (Establecimiento Publico Ambiental EPA Cartagena, 2023).

Figure A.1: 1) Canal Bolivar, 2) Canal Maria Auxiliadora,3) Canal San Pablo, 4) Canal Barcelona, 5) Canal Amardor Y Cortes,6) Canal San Martin,7) Canal Libano, 8)Salim Bechara, 9) Tabu, 10) Canal Villa, 11) Canal Papa Negro, 12) Canal Once de Noviembre, 13) Canal El Tigre, 14) Canal Ricaurte, 14a) Chepa + Ricaurte, 14b) Chiquinquirá, 14c) Las Gaviotas, 14d) Bias de Lazo, 14e) San Pedro, 15 Canal Maravilla, 16 Canal Playa Blanca, 17 Canal Arroyo Matute, 17a) Chapundun, 17b) Magdalena, 17c) Matute k3+800–k5+240, 17d) Canal simon Bolivar, 18) Canales de la Cuenca de Arroyo Fredonia, 18a) Calicanto Viejo, 18b) Ciudad Sevilla, 19) Arroyo Tomatal (Límon), 19a) Calicanto, 19b) Canal Limón, 19c) Canal La Carolina, 19d) Isla del León, 19e) San José de los Campanos, 20) Arroyo Chiamaría, 20a) Chiamaria, 20b) Flor de Campo, 20c) Canal Hormiga

A.2. Dimensions per section

In Table A.1 the different kinds of dimensions are shown per section per channel. With the help of (Local authorities, 2009a) these were compiled in an Excel file.

#	Name channel	name Sub channel	Section [m]	h [m]	B [m]	Shift [m	Btop [m	Section [m]	h [m]	B [m]	Shift [m	Btop [m	Section [m]	h [m]	B [m]	Shift [m	Btop [m	Section [m]	h [m]	B [m]	Shift [m	Btop [m
1	Canal Bolivar		300	0.37	4.7	1.11	5.90	675	0.73	3.5	2.4975	3.50										
2	Canal Maria Auxiliadora		250	0.74	11.41	4.55	12.71	750	1.41	5	13.65	5.00	930	1.44	3.5	16.926	3.50					
3	Canal San Pablo		430	0.24	2	1.806	4.00	670	0.8	3	2.814	3.00										
4	Canal Barcelona		330	0.8	2	4.224	4.47	510	1	3.4	6.528	3.40										
5	Canal Amardor Y Cortes		320	0.96	3.04	7.776	4.91	675	1.13	4.3	16.4025	4.30										
6	Canal San Martin		160	0.35	3.61	1.6	5.50	550	0.6	3.5	5.5	3.50										
7	Canal Libano		255	0.31	1.71	2.7285	2.93	670	0.92	2.76	7.169	2.76										
8	Salim Bechara		205	0.45	2.18	0.882	3.00	440	0.84	3.14	1.892	3.14	670	1.04	3.14	2.881	3.14					
9	Tabu		900	1.07	7.4	3.690	7.40	1690	1.09	2.7	6.929	4.30										
10	Canal Villa		300	1.77	1.85	2.310	1.85	840	1.09	1.3	6.468	1.30										
11	Canal Papa Negro																					
12	Canal Once de Noviembre		290	0.46	1.1	2.059	2.30	770	1.03	3.8	5.467	3.80										
13	Canal El Tigre		200	0.66	1.04	2.060	1.87	500	1.18	2.28	5.150	2.28	875	0.86	2.17	9.013	2.17					
14	Canal Ricaurte	14a) Chepa + Ricaurte	700	1.52	30	7.630	32.04	1200	1.74	9.3	13.080	15.00	2035	1.43	7.23	22.182	11.24	2570	0.52	7	28.013	9.00
		14b) Chiquinquirá	165	0.526	2.59	14.879	5.01	340	0.984	2.67	16.786	5.25	430	0.93	2.47	17.767	5.39					
		14c) Las Gaviotas	765	0.91	3.64	30.520	5.14															
		14d) Bias de Lazo	600	0.73	2.91	34.553	4.40	800	0.61	2.94	36.733	5.49	1000	0.46	2.28	38.913	4.40					
		14e) San Pedro	1525	0.89	3	44.636	5.00	2195	0.92	1.4	51.939	2.00										
15	Canal Maravila		200	0.81	4.4	0.460	5.19	510	0.81	2.5	1.173	2.59										
16	Canal Playa Blanca		195	0.41	2.16	3.237	2.79	530	0.58	2.75	8.798	2.75										
17	Canal Arroyo Matute	17c) Matute k3+800--k5+	3800	2.06	4.821	2.280	7.32	5240	2.06	4.821	7.896	7.32										
		17a) Chapundun	735	1.05	16.4	0.441	18.40	1575	1.02	7.26	0.945	10.30										
		17b) Magdalena	200	0.54	2.4	1.586	3.00	600	0.77	2.3	3.876	2.80	900	0.61	1.1	5.594	1.10	1230	0.61	1.1	7.483	1.10
		17d) Canal simon Bolivar	500	1.25	2.98	9.485	4.68	900	1.07	5.58	10.756	5.58	1200	0.84	4	11.709	4.89	1456	1.81	3.78	12.522	5.29
18	Canales de la Cuenca de Arroyo Fredonia	18a) Calicanto Viejo	325	1.69	10.5	0.748	11.85	1130	0.68	3.64	2.599	5.35										
		18b) Ciudad Sevilla	300	0.56	1.76	2.629	3.00															
19	Arroyo Tomatal (Límon)	19a) Calicanto	335	2.41	28.72	2.345	34.24	2300	1.02	14.79	16.100	22.00										
		19b) Canal Limón	800	1.24	32.6	3.145	40.30	1575	1.06	14.7	3.920	17.70										
		19c) Canal La Carolina	300	1.12	1.1	17.068	5.80	900	0.63	2.9	19.003	5.80	1500	0.89	2.2	20.938	6.00	1900	0.56	3.3	22.228	7.30
		19d) Isla del León	700	1.15	13.57	2.870	20.14	1530	0.45	1.76	3.493	3.16										
		19e) San José de los Campanos	300	1.44	5.8	18.196	9.80	800	0.92	4.6	20.076	10.80	1700	0.83	4	23.460	7.30	2100 2650	0.4 1.23	1.9 9.5	24.964 27.032	3.00 17.20
20	Arroyo Chiamaría	20a) Chiamaria	1500	2.15	20.2	2.400	24.60	2200	1.47	5.9	3.520	12.00										
		20b) Flor de Campo	3200	1.91	8.9	5.370	12.90	3900	2.87	7.1	6.665	13.10										
		20c) Canal Hormiga	800	1.3	7.9	5.440	11.87	1400	0.73	5.44	6.880	6.24										

Table A.1: The dimensions of the channels per section. Section indicates the start of the new section (upstream); h= height of cross-section in meters; B= width at the bed level of the cross-section in meters; shift=upwards shift of the cross-section in meters; Btop= width at the top of the cross-section in meters.

B

Rainfall analysis

In this Appendix, the meteorological analysis is extensively explained. The performed extreme value analysis is shown in steps. Additionally the rainfall distributions from Edurbe and the ultimate used rainfall distributions are depicted.

B.1. Extreme value analysis

In assessing the different types of rain events a peak over threshold (PoT) method was used. This method was chosen for individual extreme rainfall events. First, the daily data is plotted against the time seen in Figure B.1. A value of around peaks per year (N_s) of 5 is sought, as this is considered the average goal for a PoT (National River Flow Archive, 2023). The threshold is iteratively determined at 45 mm/day. This threshold caused that there are 294 peaks to be selected in 52 years of data. This corresponds with 5.44 peaks per year (N_s).

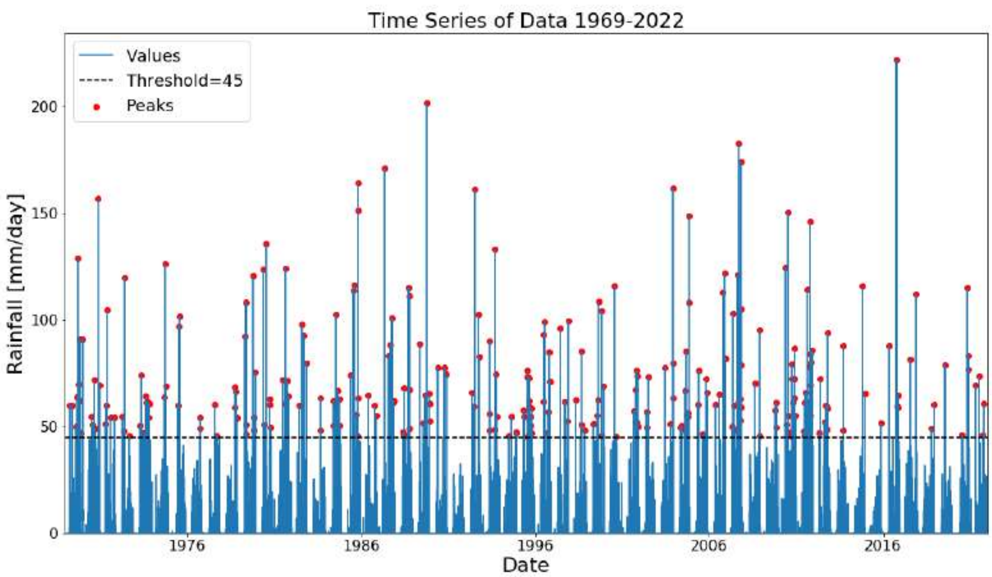

Figure B.1: The daily data plotted over time with the peaks and threshold (2009-2022)

After finding the peaks an extreme value fit is made for four types of distribution.

- Exponential Distribution

- Weibull Distribution
- Gumbel Distribution
- Generalized Pareto

A histogram made of all the peaks is made where the probability density functions of each distribution are fitted. Regarding Figure B.2 no clear answer can be given as to which fit will be the best.

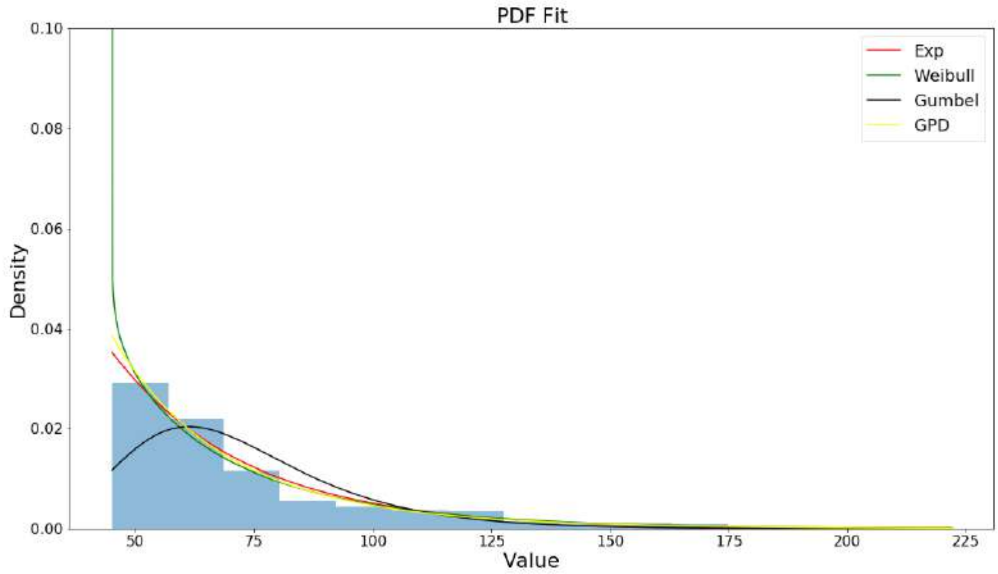

Figure B.2: Histogram of peaks with the different distribution fitted

Linear regressions are carried out for each of the distributions to look for the best fit. Linear regression is applied over maximum likelihood estimation due to it robustness to outliers and simplicity (Gowtham & Das, 2023).

First, the data is sorted from smallest to highest ratios. This is done for i= 1 to N, where N is the total number of peaks above the threshold value.

Table B.1: Sorted data

P_i[mm/hr]	i
45.1	1
45.4	2
45.5	3
45.6	4
45.6	5
45.6	6
...	...
201.8	294
222.0	295

For each data point, the probability of occurrence (P) and exceedance (Q) are calculated in the following way:

$$P_i = \frac{i}{N+1} \tag{B.1}$$

$$Q_i = 1 - P_i \tag{B.2}$$

The highest peaks get, therefore the lowest values of exceedance. The data points and their corresponding exceedance probabilities are plotted in Figure B.3.

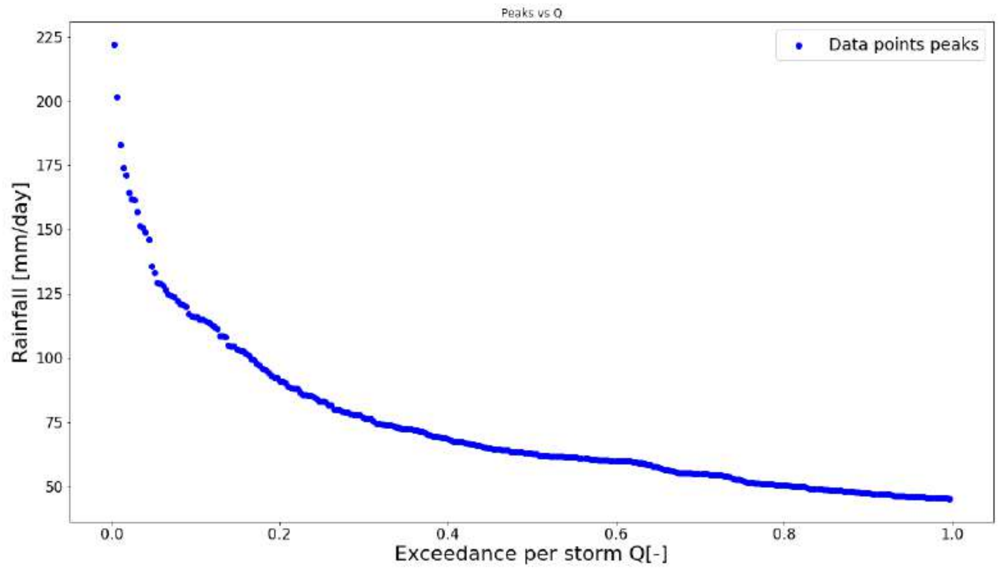

Figure B.3: Data point VS Q

A linear regression is made for the different distributions to fit the different types through the data points.

Exponential Distribution
The cumulative distribution function (CDF) of an exponential distribution can be described as follows:

$$P = 1 - exp(-(\frac{P_{rain} - \gamma}{\beta}) \quad \text{(B.3)}$$

$$Q = exp(-(\frac{P_{rain} - \gamma}{\beta})) \quad \text{(B.4)}$$

Here γ and β are used as linearization constants and correspond with the intersection and the slope respectively. After inverting Equation B.4 the following linearization of the x-axis must be made because fitting in logarithmic terms is difficult. This is done to define -ln(Q) as X_E.

$$P_{rain} = \gamma - \beta ln(Q) P_{rain} = A + BX_E \quad \text{(B.5)}$$

After linearization of the x-axis, the inverse can be fitted, and the coefficients are determined.

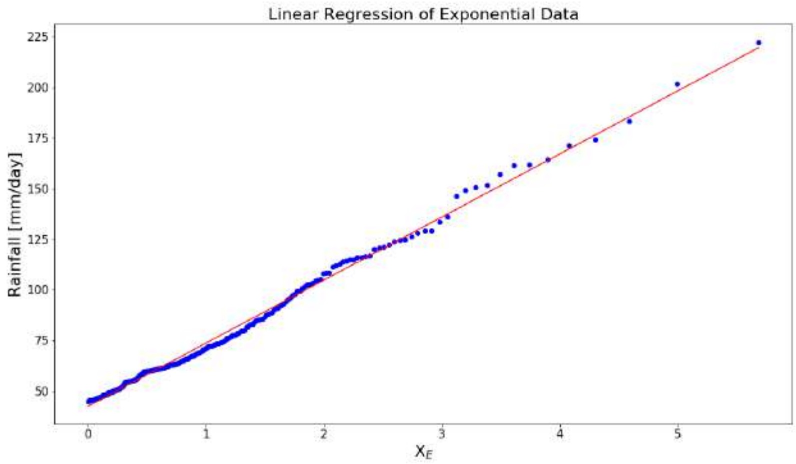

Figure B.4: The fitting of the inverse exponential distribution. γ=42.6 and β=31.1

Weibull Distribution

The cumulative distribution function (CDF) of a Weibull Distribution can be described as follows:

$$P = 1 - exp(-(\frac{P_{rain} - \gamma}{\beta})^{\alpha}) \tag{B.6}$$

$$Q = exp(-(\frac{P_{rain} - \gamma}{\beta})^{\alpha}) \tag{B.7}$$

Here γ and β are used as linearization constants and correspond with the intersection and the slope, respectively. After inverting Equation B.7 again, the x-axis must be linearized. This is done to define X_W=$(-ln(1/Q))^{1/\alpha}$. For α an optimum is found iteratively at 0.92.

$$P_{rain} = \gamma + \beta[-ln(Q)]^{1/\alpha} \tag{B.8}$$

$$P_{rain} = A + BX_W \tag{B.9}$$

After linearization of the x-axis, the inverse can be fitted and the coefficients are determined.

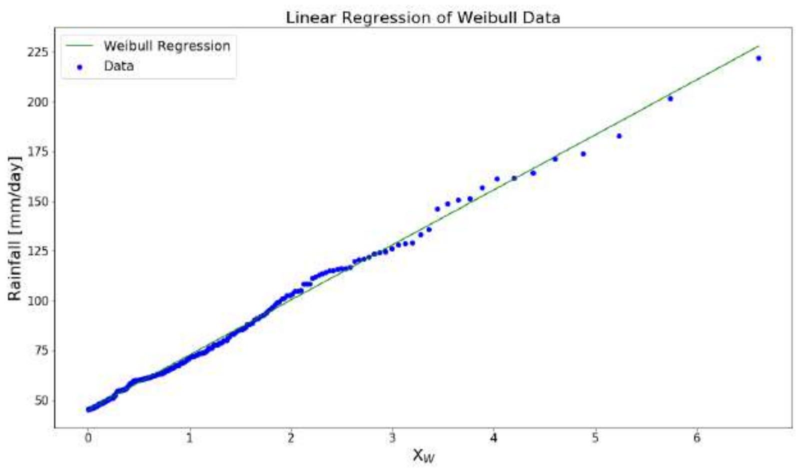

Figure B.5: The fitting of the inverse Weibull distribution. γ=42.6 and β=27.7 with α=0.92

Gumbel Distribution The cumulative distribution function (CDF) of a Gumbel Distribution can be described as follows:

$$P = exp[-exp(-(\frac{P_{rain} - \gamma}{\beta}))] \quad (B.10)$$

$$Q = 1 - exp[-exp(-(\frac{P_{rain} - \gamma}{\beta}))] \quad (B.11)$$

The linearization follows: $X_G = -ln(-ln(1-Q))$.

$$P_{rain} = \gamma - \beta ln(-ln(1-Q)) \quad (B.12)$$

$$P_{rain} = A + BX_G \quad (B.13)$$

After linearization of the x-axis, the inverse can be fitted and the coefficients are determined.

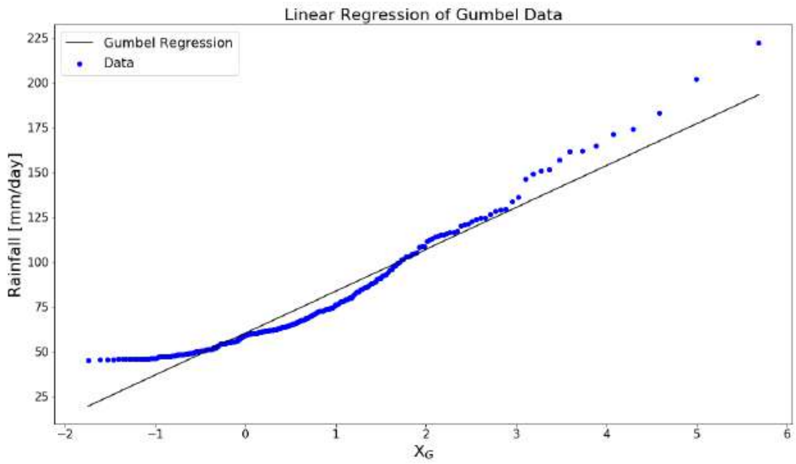

Figure B.6: The fitting of the inverse Gumbel distribution. γ=60.1 and β=23.4

Generalized Pareto Distribution The cumulative distribution function (CDF) of a Generalized Pareto Distribution (GPD) can be described as follows:

$$P = 1 - (1 + \alpha\frac{P_{rain} - \gamma}{\beta})^{-1/\alpha} \quad (B.14)$$

$$Q = (1 + \alpha\frac{P_{rain} - \gamma}{\beta})^{-1/\alpha} \quad (B.15)$$

The linearization is done following: $X_P = \frac{Q^{-\alpha}-1}{\alpha}$.

$$P_{rain} = \gamma + \beta(\frac{Q^{-\alpha} - 1}{\alpha}) \quad (B.16)$$

$$P_{rain} = A + BX_P \quad (B.17)$$

After linearization of the x-axis, the inverse can be fitted, and the coefficients are determined. For α an optimum is found iteratively at 0.05.

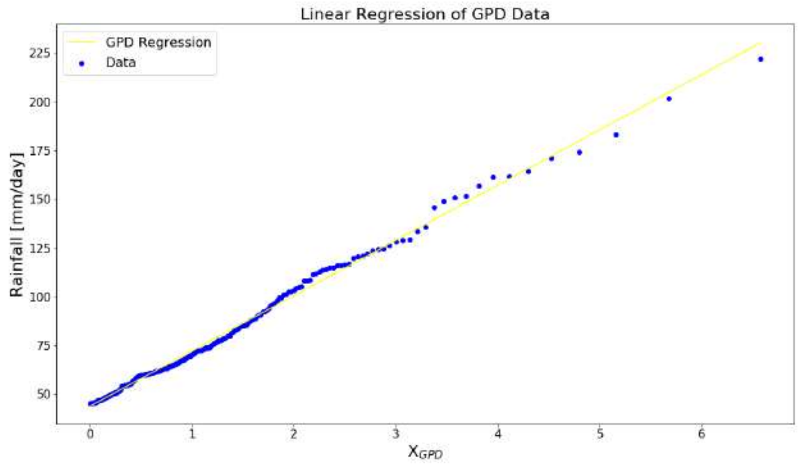

Figure B.7: The fitting of the inverse Generalized Pareto distribution. γ=43.9 and β=28.3 with α=0.05

After fitting the graphs are combined and transformed to return periods. This is shown in Figure B.8. The Gumbel under-predicts the extreme values. The rest of the fits are not far off.

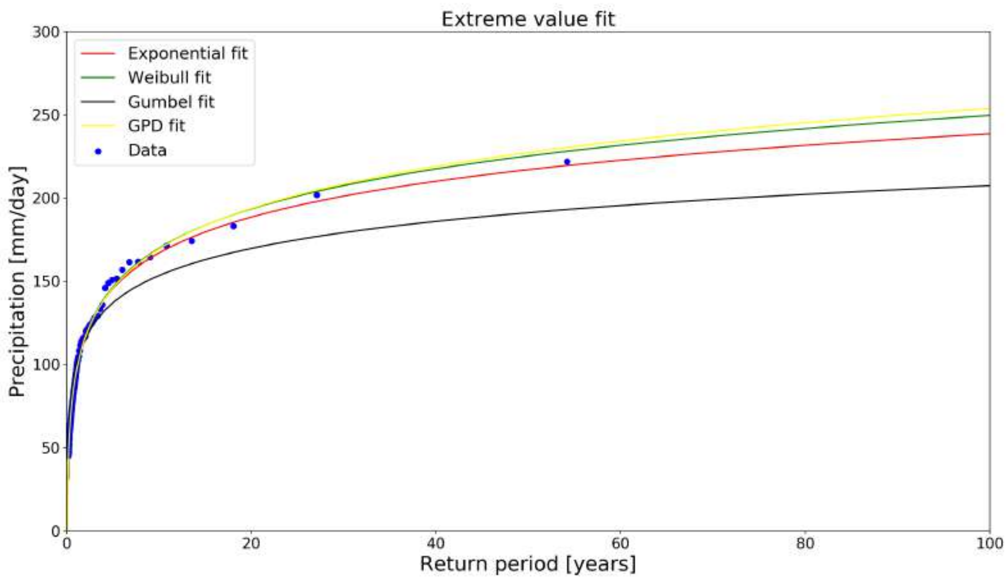

Figure B.8: The daily precipitation rates vs return periods for each distribution.

Table B.2: Precipitation values [mm/day] per return period for each distribution.

R [years]	1	2	5	10	20	50	75	100	
Q [-]	**1.92E-01**	**9.59E-02**	**3.84E-02**	**1.92E-02**	**9.59E-03**	**3.84E-03**	**2.56E-03**	**1.92E-03**	**RMSE**
Exp	95.33	116.89	145.39	166.95	188.51	217.01	229.62	238.57	2.17
Weibull	94.08	116.26	146.44	169.78	193.47	225.25	239.47	249.60	1.82
Gumbel	97.41	114.84	136.96	153.39	169.72	191.21	200.71	207.45	7.16
GPD	94.07	115.82	145.76	169.34	193.76	227.35	242.72	253.81	2.00

To determine the goodness of the fit the RMSE Equation B.18 for each distribution is calculated.

$$RMSE = \sqrt{\frac{1}{N}\sum_{i=1}^{n}(P_i - P_{pred,i})^2} \quad \text{(B.18)}$$

Regarding Table B.2 it can be concluded that the Weibull distribution and GPD are the most accurate for this data set. A reason can be the flexibility of the distributions as it allows us to find an optimum for the $alpha$ value. Another explanation can be the size of the data set as the Weibull and GPD could be more robust in this case. The last influence would be the number of peaks selected. For fewer peaks, so a higher threshold, the RMSE for all the fits becomes smaller but the robustness of the analysis will decrease as lesser peaks are selected.

Weibull distribution and GPD fits' uncertainty are examined and plotted. Given that they had the lowest Root Mean Squared Error (RMSE) among the four distributions, these two distributions were chosen for the uncertainty analysis. The uncertainty in the model's estimates is not captured by RMSE, despite it being a useful tool for evaluating the overall goodness of the fit. The certainty and dependability of the Weibull and GPD distributions are forecasted by performing an uncertainty analysis on them.

For both distributions, a bootstrap method is used to predict this uncertainty. The data is 10,000 times re-sampled and an extreme fit is made for each re-sampling. From all the fit the mean distribution and standard deviation can be calculated. This resulted in the following extreme value fits with 90$\%$ confidence interval. Seen in Figure B.9 the Weibull distribution over-predicts and has a larger confidence interval. The GPD will be used for interpreting the rainfall. This is because Arrieta-Pastrana et al. (2023) found that there was no clear indication of significant trends in the increase of intensities and daily maxima. So an over-prediction will demand a higher drainage capacity, which will likely never be reached in the chosen return period. As the 90$\%$ maximum confidence interval intersects the lower bound of the Weibull distribution, this intersection point could be seen as an indication of the fair value of the use. The final extreme rainfall values are shown in Table 3.1.

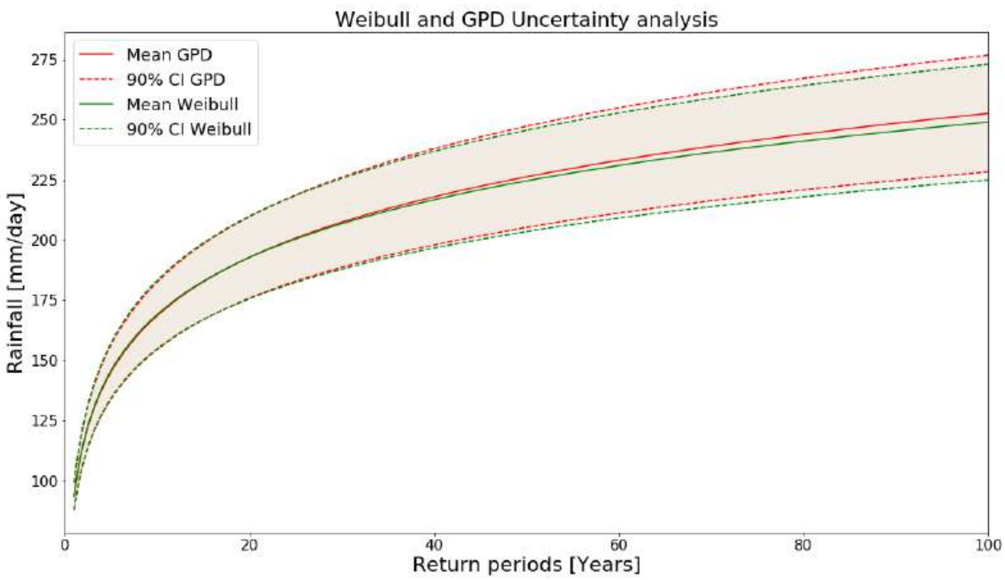

Figure B.9: The uncertainty of the Weibull and GP distributions using bootstrapping.

Table B.3: The return values for the GPD with the 90% confidence interval after bootstrapping

R [years]	1	2	5	10	20	50	75	100
GPD [mm/day]	93.82	115.45	145.23	168.69	192.96	226.38	241.66	252.69
σ_{gpd} [+/-]	3.38	4.73	6.79	8.49	10.27	12.75	13.88	14.71
Max P	99.38	123.23	156.41	182.65	209.86	247.35	264.50	276.89

Table B.4: The return values for the Weibull with the 90% confidence interval after bootstrapping

R [years]	1	2	5	10	20	50	75	100
Wei [mm/day]	93.62	115.70	145.82	169.15	192.85	224.68	238.92	249.07
σ_{gpd} [+/-]	3.45	4.83	6.92	8.61	10.35	12.72	13.78	14.54
Max P	99.31	123.64	157.20	183.31	209.88	245.60	261.59	273.00

B.2. Rainfall distribution

From the EDURBE (2022) the rainfall distribution per rainfall event are used to determine each imposed daily rainfall intensity. For this table, a temporal rainfall analysis is done with half-hourly data. Days with rainfall intensity of 30 mm/day were highlighted and their daily course was analysed. Based on this, the Table B.5 is generated. The percentage in the head row indicates how many of the 30 mm exceeding rain events finished within that specified time frame. It follows that 70 % of the showers are ready within eight hours. So this table is used in the following manners in this report. When the intensity of a rain event is available, a distribution curve by time can be generated. Further, when the duration of a specific shower is available, the distribution per unit time can be generated.

Table B.5: The distribution versus the duration of high-intensity rain events (EDURBE, 2022)

HORA	10%	20%	30%	40%	50%	60%	70%	80%	90%
0:00	0.0%	0.0%	0.0%	0.0%	0.0%	0.0%	0.0%	0.0%	0.0%
0:30	0.4%	1.0%	1.7%	5.3%	9.4%	14.3%	20.4%	28.9%	43.2%
1:00	1.0%	8.3%	17.8%	26.4%	34.8%	43.5%	53.2%	65.2%	82.7%
1:30	2.3%	17.6%	30.1%	40.8%	50.6%	60.5%	71.0%	83.3%	100.0%
2:00	3.1%	22.0%	35.2%	46.3%	56.4%	66.4%	76.8%	88.8%	100.0%
2:30	5.4%	25.5%	39.4%	50.9%	61.2%	71.2%	81.6%	93.4%	100.0%
3:00	8.0%	28.3%	42.2%	53.7%	63.8%	73.7%	83.8%	95.2%	100.0%
3:30	11.5%	32.4%	46.5%	57.9%	67.9%	77.5%	87.2%	97.8%	100.0%
4:00	13.4%	34.7%	49.0%	60.4%	70.3%	79.8%	89.2%	99.6%	100.0%
4:30	15.6%	37.4%	51.8%	63.2%	73.1%	82.4%	91.5%	100.0%	100.0%
5:00	18.3%	39.9%	54.1%	65.3%	75.0%	84.0%	92.9%	100.0%	100.0%
5:30	20.4%	42.2%	56.4%	67.5%	77.0%	85.8%	94.4%	100.0%	100.0%
6:00	22.6%	44.4%	58.5%	69.5%	78.8%	87.3%	95.6%	100.0%	100.0%
6:30	24.5%	46.7%	60.8%	71.7%	80.8%	89.2%	97.2%	100.0%	100.0%
7:00	27.0%	49.1%	63.1%	73.8%	82.7%	90.8%	98.4%	100.0%	100.0%
7:30	29.2%	51.4%	65.2%	75.7%	84.4%	92.2%	99.6%	100.0%	100.0%
8:00	33.6%	55.2%	68.6%	78.6%	86.8%	94.1%	100.0%	100.0%	100.0%
8:30	35.2%	57.0%	70.3%	80.3%	88.3%	95.4%	100.0%	100.0%	100.0%
9:00	36.1%	57.9%	71.2%	81.0%	89.0%	95.9%	100.0%	100.0%	100.0%
9:30	37.9%	59.5%	72.5%	82.1%	89.9%	96.6%	100.0%	100.0%	100.0%
10:00	39.8%	61.3%	74.2%	83.6%	91.1%	97.5%	100.0%	100.0%	100.0%
10:30	40.5%	62.2%	75.1%	84.5%	91.9%	98.2%	100.0%	100.0%	100.0%
11:00	42.9%	64.1%	76.7%	85.7%	92.8%	98.8%	100.0%	100.0%	100.0%
11:30	44.5%	65.5%	77.8%	86.6%	93.5%	99.3%	100.0%	100.0%	100.0%
12:00	48.2%	68.7%	80.4%	88.7%	95.0%	100.0%	100.0%	100.0%	100.0%
12:30	48.5%	69.0%	80.8%	89.0%	95.4%	100.0%	100.0%	100.0%	100.0%
13:00	48.9%	69.4%	81.2%	89.5%	95.8%	100.0%	100.0%	100.0%	100.0%
13:30	50.0%	70.5%	82.2%	90.3%	96.4%	100.0%	100.0%	100.0%	100.0%
14:00	50.5%	71.1%	82.7%	90.8%	96.9%	100.0%	100.0%	100.0%	100.0%
14:30	52.7%	72.9%	84.1%	91.9%	97.6%	100.0%	100.0%	100.0%	100.0%
15:00	57.0%	76.2%	86.7%	93.7%	98.8%	100.0%	100.0%	100.0%	100.0%
15:30	58.9%	77.8%	88.0%	94.7%	100.0%	100.0%	100.0%	100.0%	100.0%
16:00	60.7%	79.5%	89.4%	95.9%	100.0%	100.0%	100.0%	100.0%	100.0%
16:30	63.2%	81.1%	90.6%	96.7%	100.0%	100.0%	100.0%	100.0%	100.0%
17:00	64.0%	81.8%	91.1%	97.0%	100.0%	100.0%	100.0%	100.0%	100.0%
17:30	66.0%	83.1%	92.0%	97.5%	100.0%	100.0%	100.0%	100.0%	100.0%
18:00	67.0%	83.9%	92.5%	98.0%	100.0%	100.0%	100.0%	100.0%	100.0%
18:30	68.0%	84.8%	93.3%	98.6%	100.0%	100.0%	100.0%	100.0%	100.0%
19:00	69.9%	86.2%	94.3%	99.2%	100.0%	100.0%	100.0%	100.0%	100.0%
19:30	70.9%	86.7%	94.6%	99.4%	100.0%	100.0%	100.0%	100.0%	100.0%
20:00	71.0%	86.9%	94.7%	99.4%	100.0%	100.0%	100.0%	100.0%	100.0%
20:30	73.6%	88.4%	95.6%	100.0%	100.0%	100.0%	100.0%	100.0%	100.0%
21:00	81.7%	93.1%	98.2%	100.0%	100.0%	100.0%	100.0%	100.0%	100.0%
21:30	85.6%	94.8%	98.9%	100.0%	100.0%	100.0%	100.0%	100.0%	100.0%
22:00	92.3%	98.5%	100.0%	100.0%	100.0%	100.0%	100.0%	100.0%	100.0%
22:30	98.8%	100.0%	100.0%	100.0%	100.0%	100.0%	100.0%	100.0%	100.0%
23:00	100.0%	100.0%	100.0%	100.0%	100.0%	100.0%	100.0%	100.0%	100.0%
23:30	100.0%	100.0%	100.0%	100.0%	100.0%	100.0%	100.0%	100.0%	100.0%
24:00	100.0%	100.0%	100.0%	100.0%	100.0%	100.0%	100.0%	100.0%	100.0%

B.3. Rainfall sequences

As stated in the report, for the validation of the model three scenarios had been considered. Not much data is available to compare the model output to the data but, it is the only validation possible and will give guidance in wherever or not the outcome is realistic. The rainfall intensity distributions that were used as input are shown in Table B.6. These distributions are made concerning the Table B.5. The begin time for Table B.6a and Table B.6b is chosen so that the model has time to initialize. The end time of rainfall is chosen to allow for the observation of how the water gradually recedes and returns to a semi-dry equilibrium. The times for Table B.6c depended on recordings of rain from Time and Data AS (2023).

Table B.6: Rainfall distributions for the input for the numerical model.

(a) Edurbe study (100 year) P=185 mm/day

Time [h:m]	P[mm]
11:00	37.74
11:30	60.68
12:00	32.93
12:30	10.73
13:00	8.88
13:30	4.07
14:00	6.29
14:30	3.70
15:00	4.26
15:30	2.59
16:00	2.78
16:30	2.22
17:00	2.96
17:30	2.22
18:00	2.22
18:30	0.74
19:00	0.00

(b) Edurbe study (500 year) P=195 mm/day

Time [h:m]	P [mm]
11:00	39.58
11:30	63.63
12:00	34.53
12:30	11.25
13:00	9.31
13:30	4.27
14:00	6.60
14:30	3.88
15:00	4.46
15:30	2.72
16:00	2.91
16:30	2.33
17:00	3.10
17:30	2.33
18:00	2.33
18:30	0.78
19:00	0.00

(c) Tropical storm Iota P=83.18 mm/day

Time [h:mm]	P [mm]
6:00	11.90
6:30	24.29
7:00	14.14
7:30	4.91
8:00	3.99
8:30	2.08
9:00	3.16
9:30	1.91
10:00	2.16
10:30	1.33
11:00	1.50
11:30	1.25
12:00	1.58
12:30	1.33
13:00	1.16
13:30	1.58
14:00	1.08
14:30	0.42
15:00	0.58
15:30	0.75
16:00	0.58
16:30	0.50
17:00	0.42
17:30	0.58
18:00	0.00

C

Determining of tidal water levels

In this Appendix, the analysis of the water levels at the coasts of Santa Marta en Cartagena is considered.

C.1. Santa Marta

The closest station that had available water level data was located in Santa Marta, Colombia. It is located 170 km northeast of Cartagena. Figure C.1 shows the location of Santa Marta to Cartagena.

Figure C.1: The location of the Santa Marta water level station. (EPSG:3116[8634826.4,1031199.1: -8087663.7,1349183.7])

The data set contains water levels per hour from 01-10-2012 until 30-11-2022. In Figure C.2 the water level measured in Santa Marta for this period is shown. There are several outliers visible. These were filtered out and set to the mean. The mean was found to be 1.38 m above mean sea level as shown in Figure C.3. To calculate with a local sea level this mean is deducted from the set to set the base water level at zero.

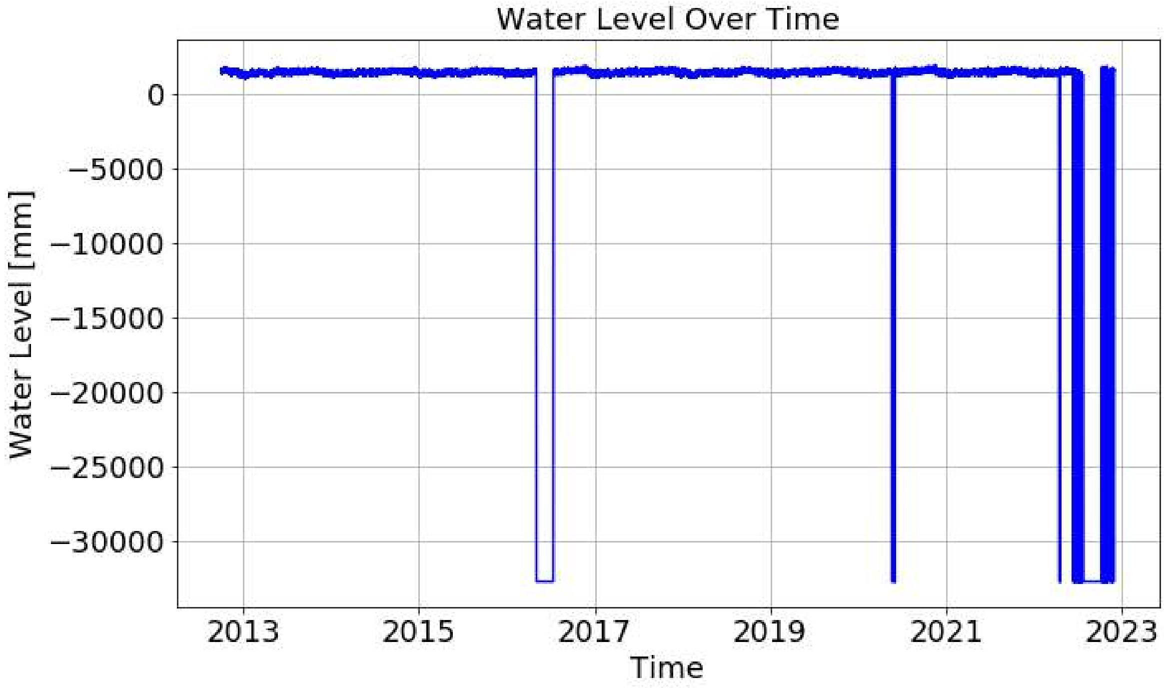

Figure C.2: The unfiltered dataset

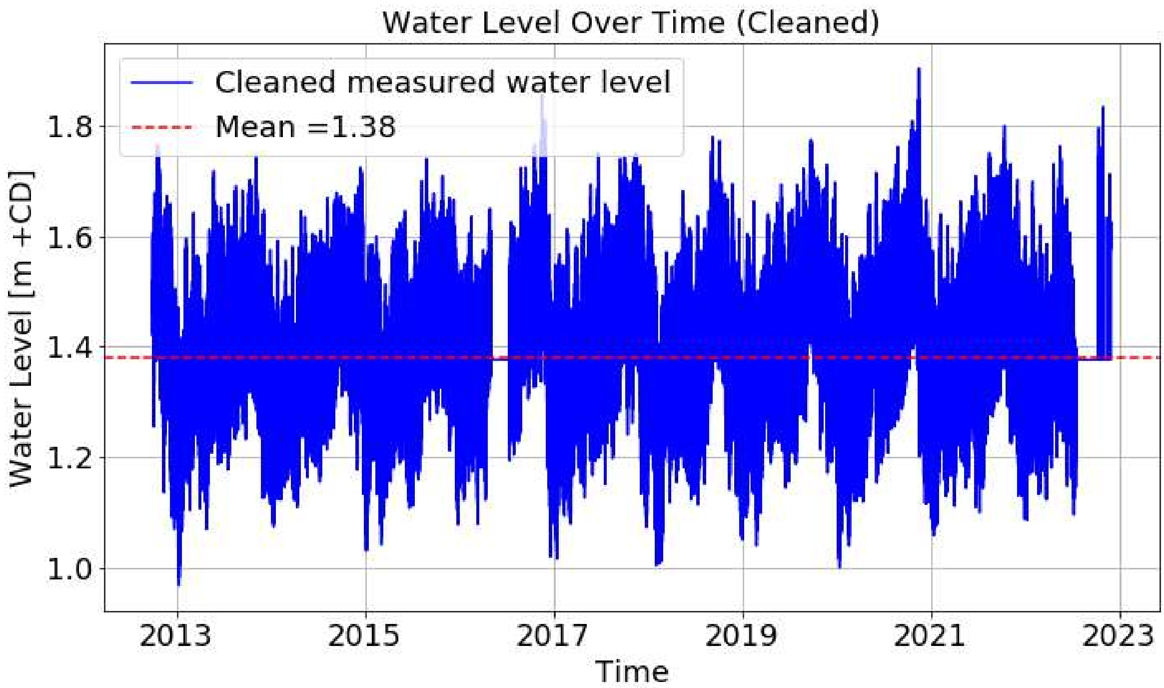

Figure C.3: The cleaned data set

Figure C.4: Water level measured in Santa Marta for the whole data set (University of Hawaii Sea Level Center, 2023)

C.2. 14 November 2020 water level

The tidal predictor is used to plot the tidal sequence per 10 minutes as input for the calibration run of the numerical model. A surge was seen as negligible as the tropical storm Iota was a long way from the coast shown in Figure C.5. The tidal sequence that was calculated by the tidal predictor can be seen in Figure C.6. Red marked area is the time frame of the rainfall during that day.

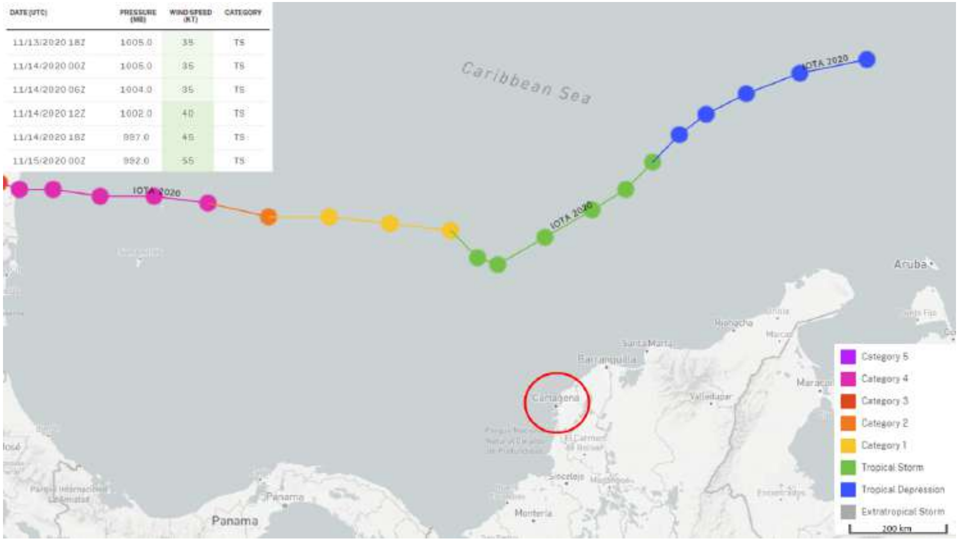

Figure C.5: The hurricane track of hurricane Iota (National Oceanic and Atmospheric Administration, 2023). The red circle indicates where Cartagena is located.

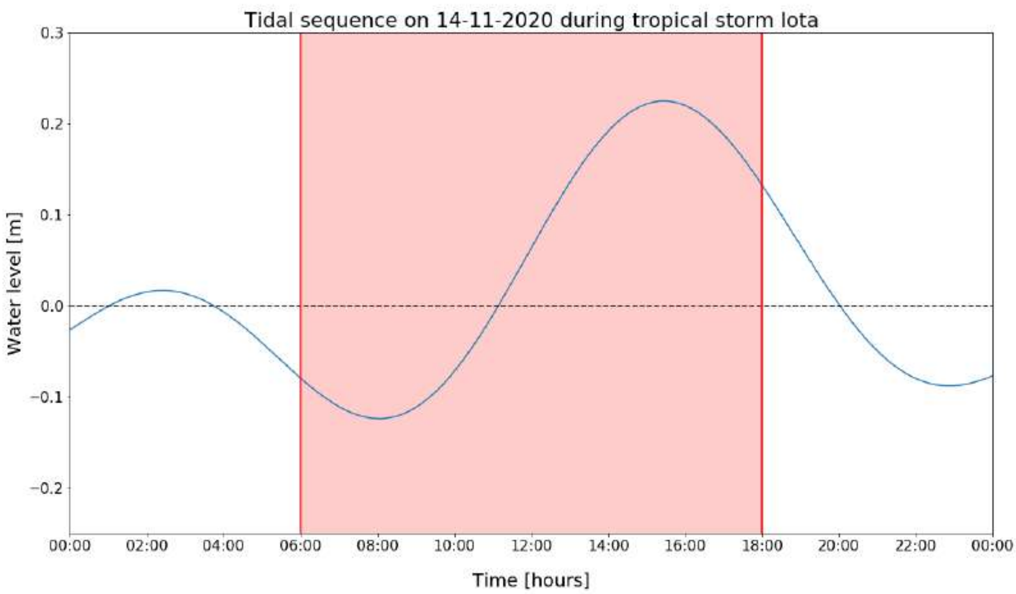

Figure C.6: The water level on the 14^{th} of November 2020 when Tropical Storm Iota was offshore Cartagena

C.3. Water level input scenarios

For the input of the scenarios, three types of water level boundaries were induced. The first is an extreme high and low tide and a tidal sequence. This tidal sequence was generated with the tidal predictor, using the Cartagena constituents. As October and November were analysed as the wettest period the same tidal sequence as for 14-11-2020 was used.

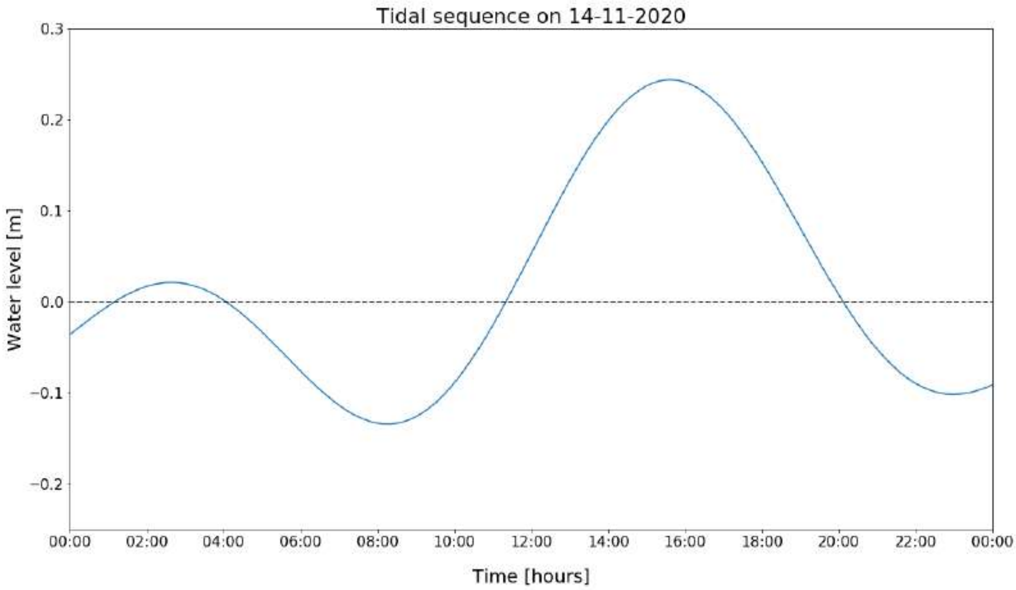

Figure C.7: The tidal sequence used in the input scenarios

D

Criteria ConAgua consortium

The ConAgua consortium developed a framework to compare and ultimately select preferable projects. The Multi Criteria analysis consists of so-called criteria, objectives and weighing factors.

The criteria are subdivided into more generic aspects:

1. **Finance**
    - Financing opportunities
    - Operation and maintenance
2. **Implementation**
    - Governance complexity
    - Technical complexity
    - Displacement
    - Replicability and scalability

For the objectives, the projects are more evaluated on the contribution benefits. Three main objectives that were stated to compare the different projects are:

1. **Performance:** to what extent can the project solve the water-related problems of the territory?
    - Flood Risk Reduction
    - Mitigation of other risks
    - Infrastructure protection & enhancement
    - Adaptability to change
    - Community evaluation
2. **Livability:** To what extent can the project contribute to solving environmental and health issues in the territory?
    - Human Health
    - Ecosystem health
    - Public Services
    - Community Evaluation
3. **Prosperity:** to what extent does the project have a positive socioeconomic impact?
    - Economic development
    - Community inclusiveness and social cohesion
    - Integration of cultural values and local practices

- Capacity building
- Community evaluation

All the criteria will be scored from 0 to 5. Where 0 is no improvement and 5 is the best possible solution.

E

Mitigation results

In this Appendix all the outcomes of analyzing the different mitigation measures with the established D-Hydro model. The flood maps together with their flood level reduction maps are given to give more context to the decisions made for the final designs from the thesis. The mitigation measures are divided into three groups:

1. Increasing the channel dimensions
2. Increase the infiltration
3. Establishing retention areas

These measures are subdivided into different kinds of simple pragmatic area-wide measures to see the impact of a measure on the area.

E.1. Increasing the channel dimensions

E.1.1. 10 percent channel increase

The height and width of all the cross-sections were increased with 10 %. This resulted in the following flood map (Figure E.1) that was which had been laid over the baseline scenario (red). The flooded area shows a relative decrease of 10.57 %. The only significant impact is seen at the right Ricaurte channel.

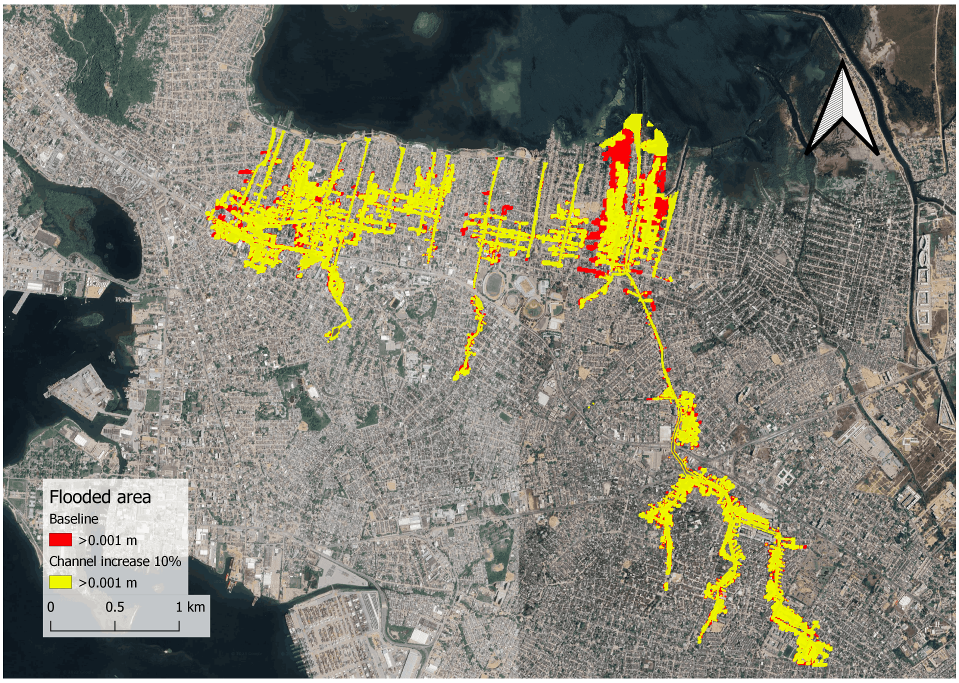

Figure E.1: The decrease in a flooded area with after the increase of 10 % channel width and height.

The flood level reduction is shown in Figure E.2. Most of the significant reduction is seen inside of the channels. The average flood level reduction is 3.55 cm. This is a reduction of 11.83 %. The area around Maria Auxiliadora (second channel from the left) the flooded area sees a reduction. Also, larger reductions can be seen in the area around the downstream section of the longest channel (Ricaurte channel).

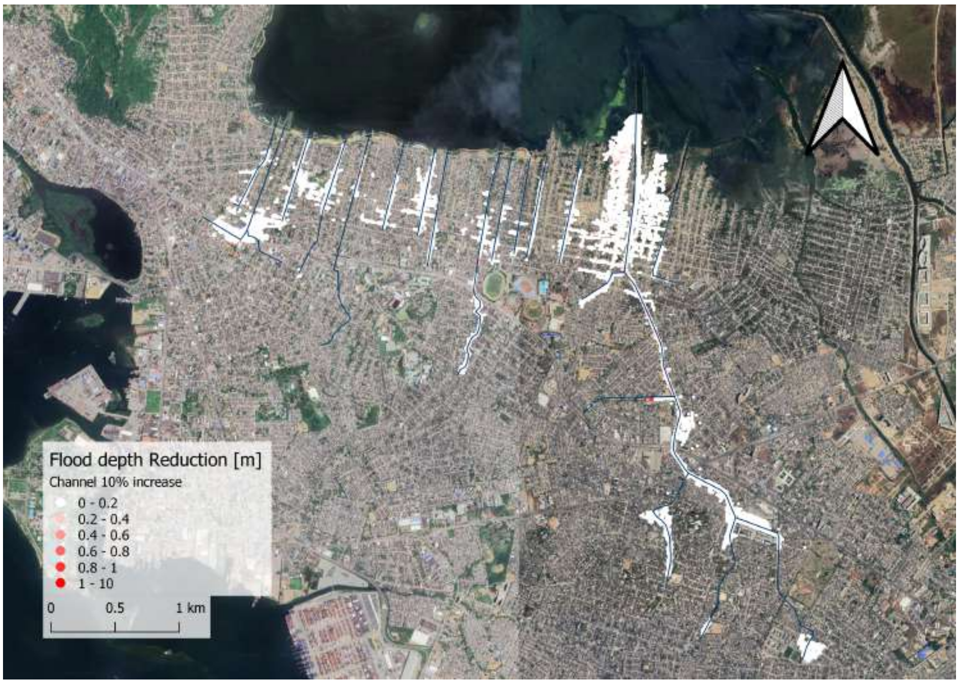

Figure E.2: The flood level reduction with after the increase of 10 % channel width and height.

E.1.2. 20 percent channel increase

The height and width of all the cross-sections were increased by 20 %. This resulted in the following flood map (Figure E.3) that was which had been laid over the baseline scenario (red). The flooded area shows a relative decrease of 19.09 %. Again the Ricaurte part of the channels shows a significant improvement but for the rest of the channels, no significant reduction can be observed regarding the flooded area.

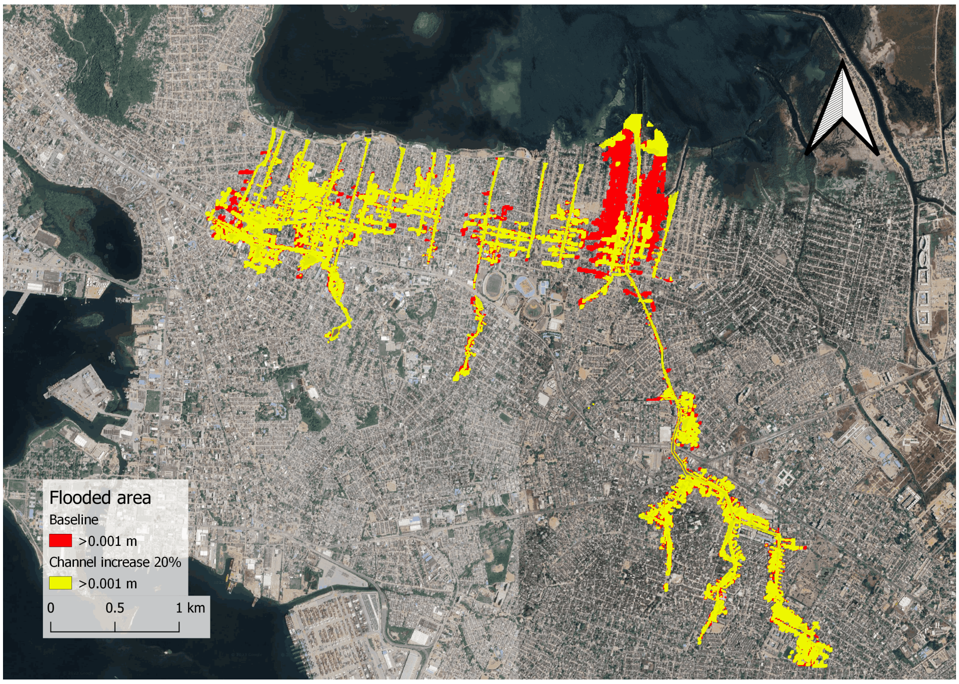

Figure E.3: The reduction in flooded area after the increase of 20 % channel width and height.

The flood level reduction is shown in Figure E.4. Most of the significant reduction is seen inside of the channels. The average flood level reduction is 6.10 cm. This is a reduction of 20.33 %. Less reduction can be seen in

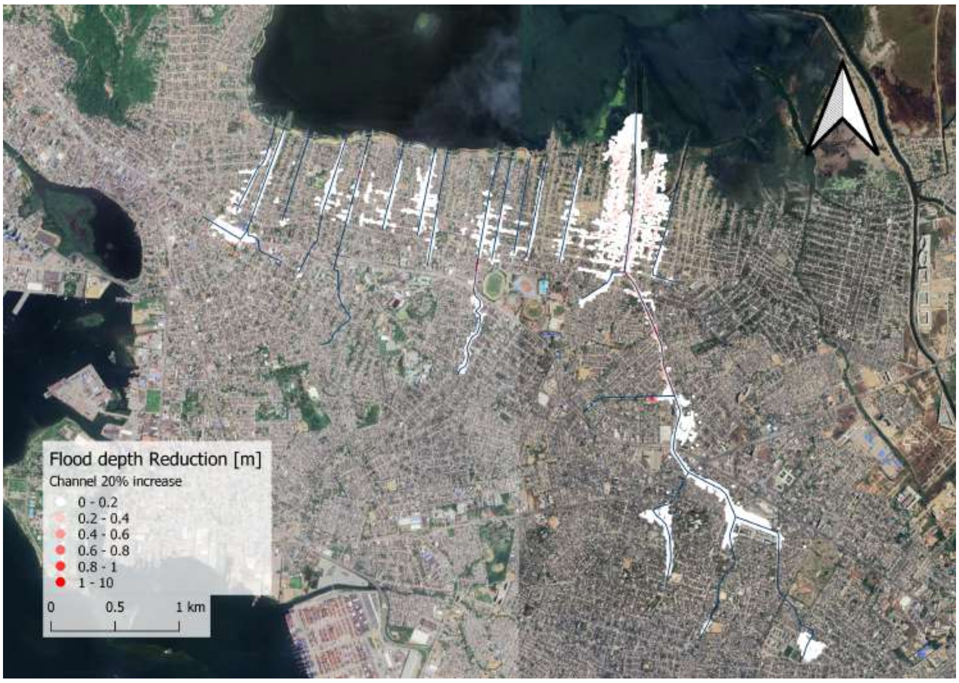

Figure E.4: The flood level reduction with after the increase of 20 % channel width and height.

E.1.3. 30 percent channel increase

The height and width of all the cross-sections were increased with 30 %. This resulted in the following flood map (Figure E.5) that was which had been laid over the baseline scenario (red). The flooded area shows a relative decrease of 26.98 %. The flood is almost completely reduced at the Ricaurte channel.

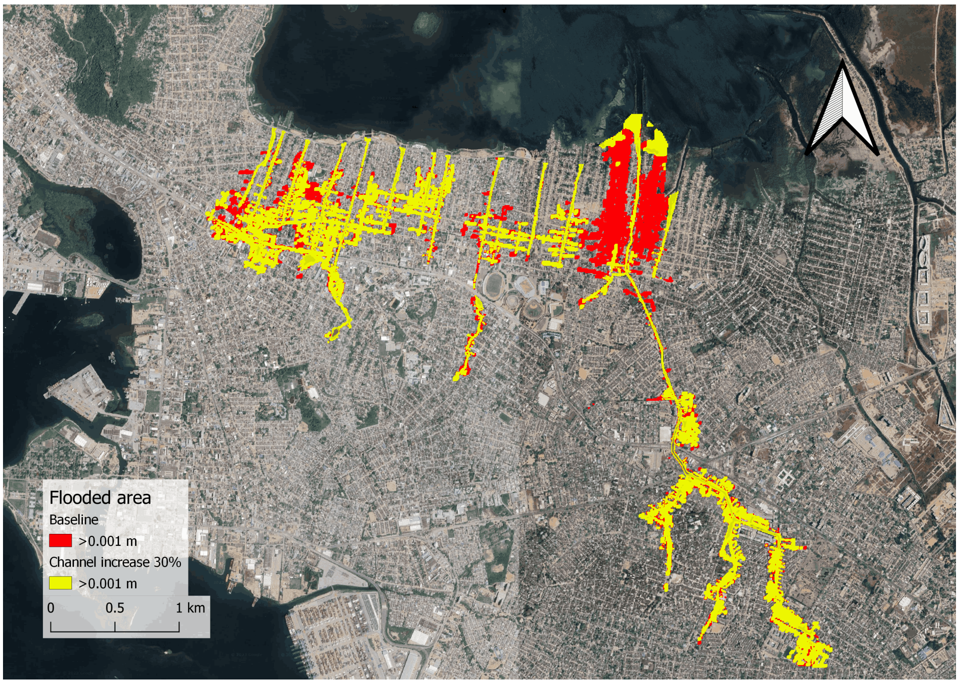

Figure E.5: The reduction flooded area with after the increase of 30 % channel width and height.

The flood level reduction is shown in Figure E.6. Most of the significant reduction is seen inside of the channels. The average flood level reduction is 7.62 cm. This is a reduction of 25.40 %.

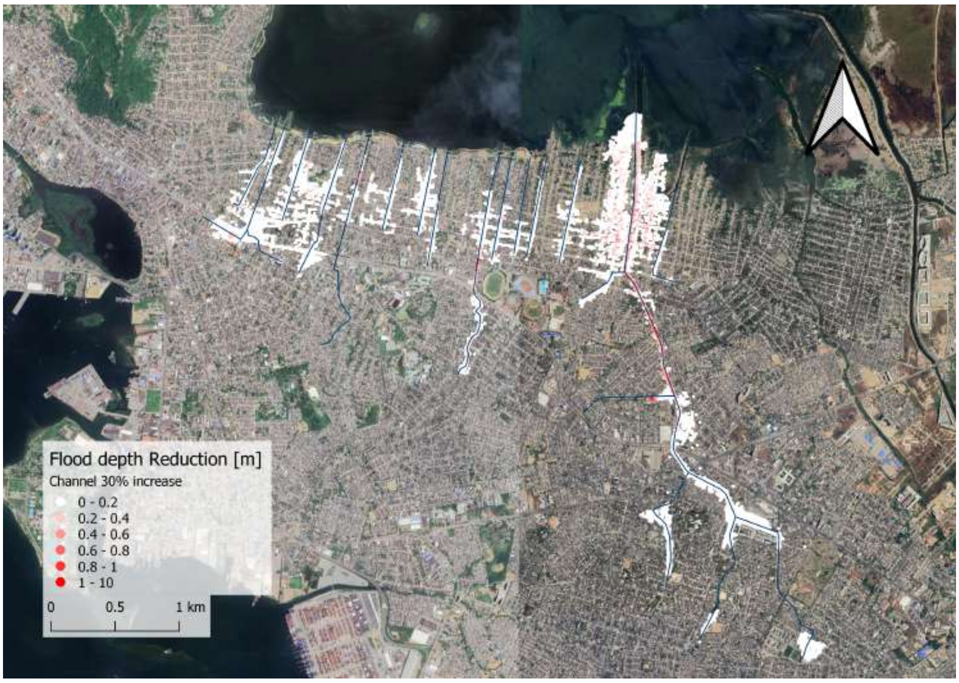

Figure E.6: The flood level reduction with after the increase of 30 % channel width and height.

E.1.4. 50 percent channel increase

The height and width of all the cross-sections were increased with 50 %. This resulted in the following flood map (Figure E.7) that was which had been laid over the baseline scenario (red). The flooded area shows a relative decrease of 35.14 %. Channel Tabu shows downstream now a reduction.

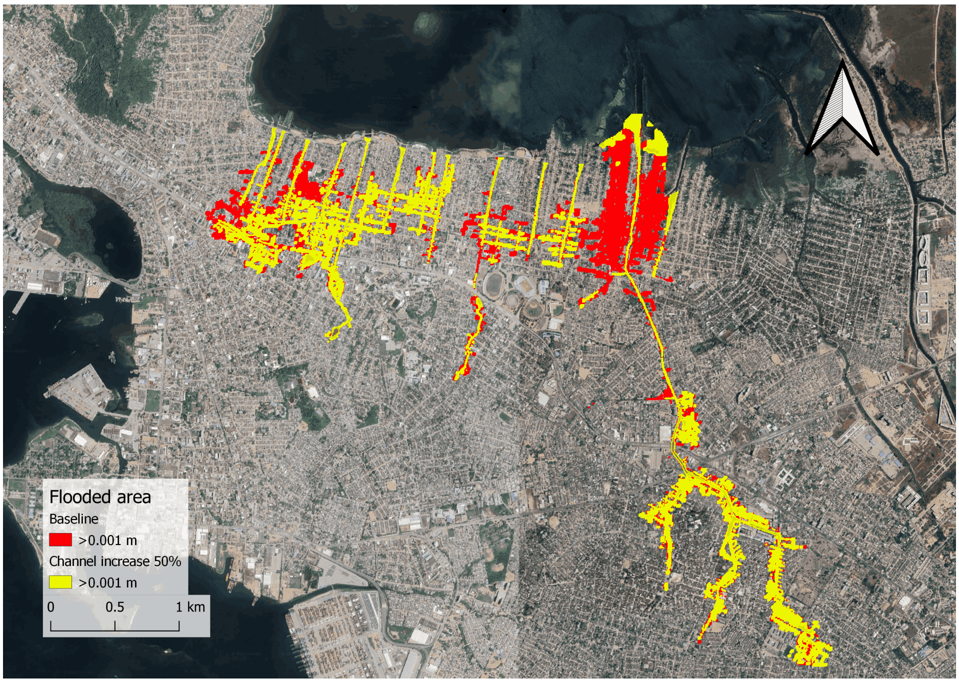

Figure E.7: The reduction in flooded area with after the increase of 50 % channel width and height.

The flood level reduction is shown in Figure E.8. Most of the significant reduction is seen inside of the channels. The average flood level reduction is 9.44 cm. This is a reduction of 31.47 %.

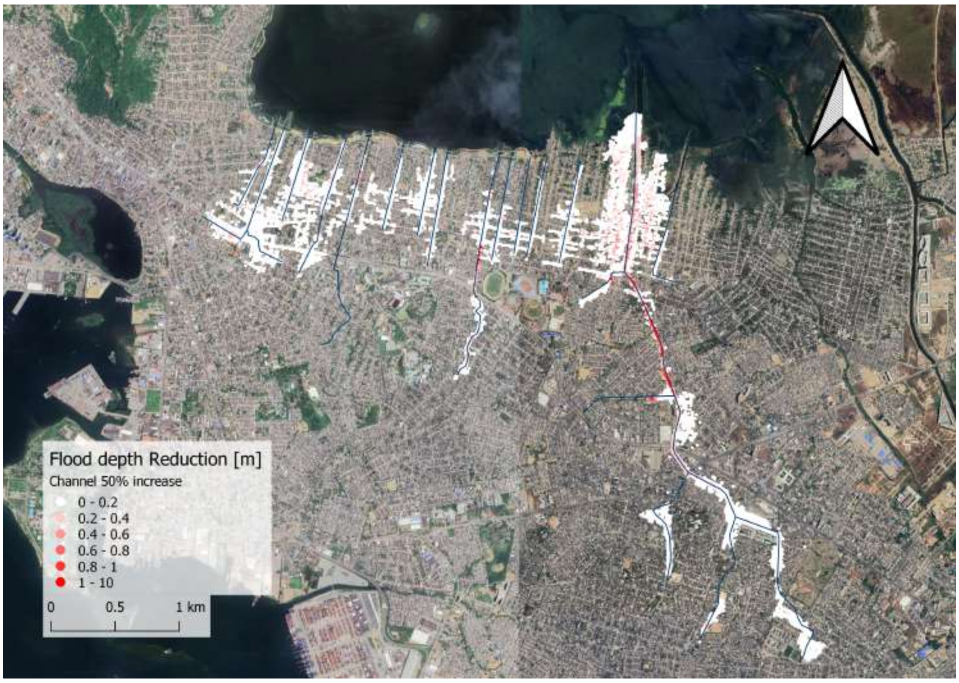

Figure E.8: The flood level reduction with after the increase of 50 % channel width and height.

E.1.5. 100 percent channel increase

The height and width of all the cross-sections were increased with 100 %. This resulted in the following flood map (Figure E.9) that was which had been laid over the baseline scenario (red). The flooded area shows a relative decrease of 52.29 %.

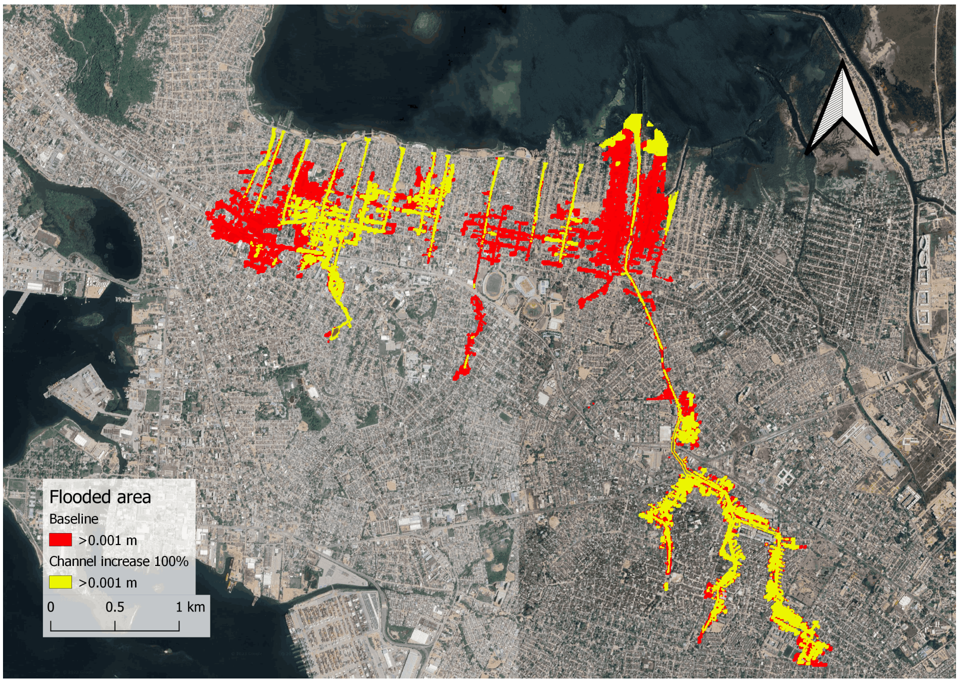

Figure E.9: The reduction in flooded area with after the increase of 100 % channel width and height.

The flood level reduction is shown in Figure E.10. Most of the significant reduction is seen inside of the channels. The average flood level reduction is 14.96 cm. This is a reduction of 49.87 %.

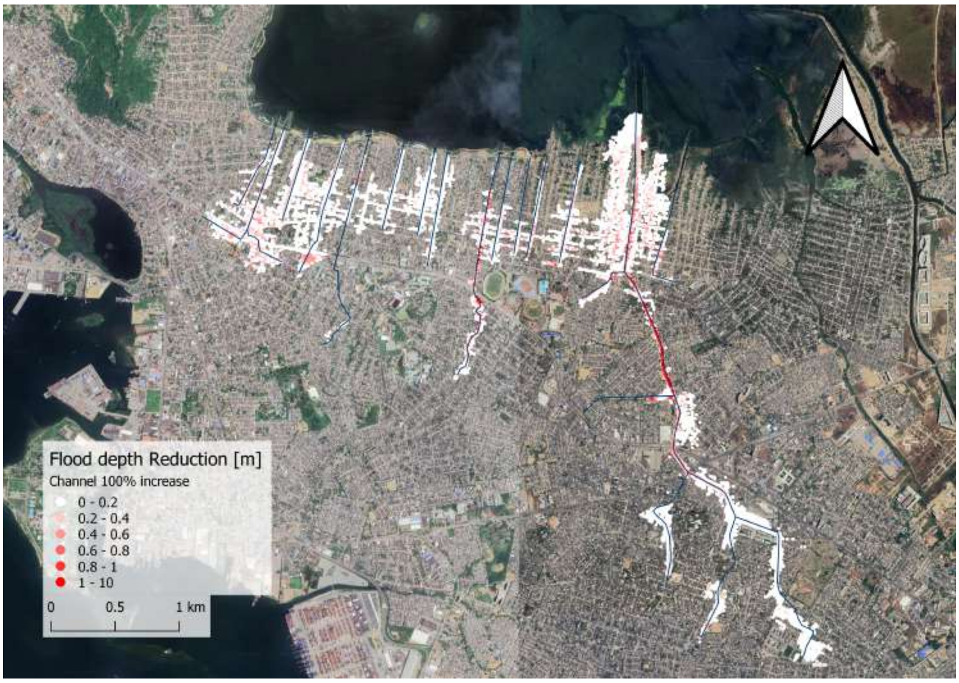

Figure E.10: The flood level reduction after the increase of 100 % channel width and height.

E.1.6. 200 percent channel increase

The height and width of all the cross-sections were increased with 200 %. This resulted in the following flood map (Figure E.11) that was which had been laid over the baseline scenario (red). The flooded area shows a relative decrease of 71.14 %.

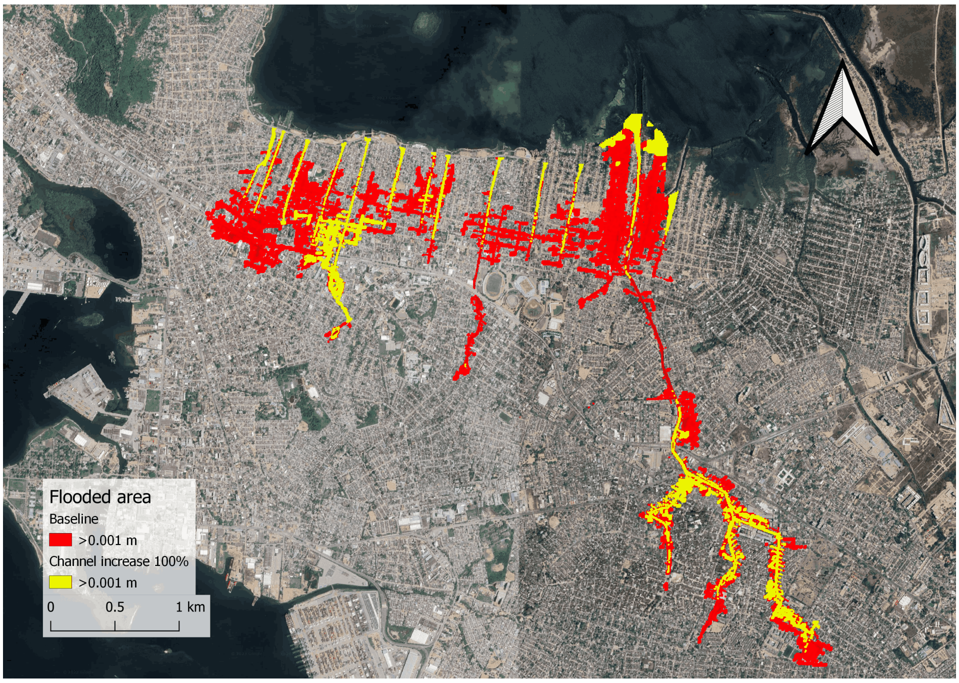

Figure E.11: The reduction in flooded area after the increase of 200 % channel width and height.

The flood level reduction is shown in Figure E.12. Most of the significant reduction is seen inside of the channels. The average flood level reduction is 20.01 cm. This is a reduction of 66.70 %.

Figure E.12: The flood level reduction after the increase of 200 % channel width and height.

E.2. Increase the infiltration

E.2.1. 10 percent infiltration increase

With the help of different kinds of infiltration measures the infiltration is simulated to increase with a total of 10%. This resulted in the following flood map (Figure E.13) that was which had been laid over the baseline scenario (red). The flooded area shows a relative decrease of 8.13 %.

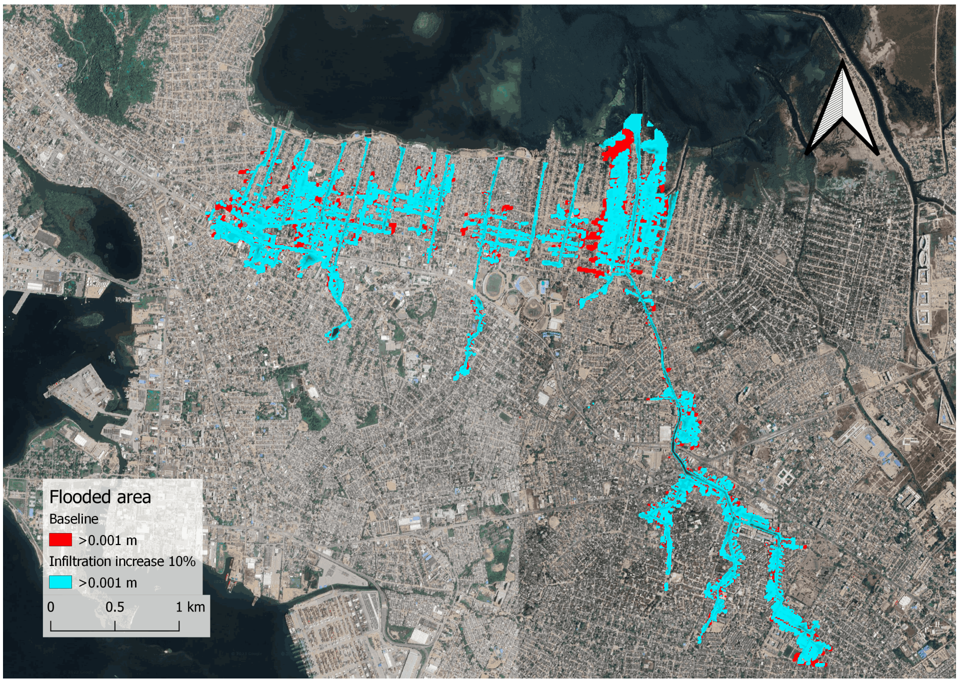

Figure E.13: The reduction in flooded area after the increase of 10 % of infiltration.

The flood level reduction is shown in Figure E.14. Most of the significant reduction is seen inside of the channels. The average flood level reduction is 1.53 cm. This is a reduction of 5.10 %.

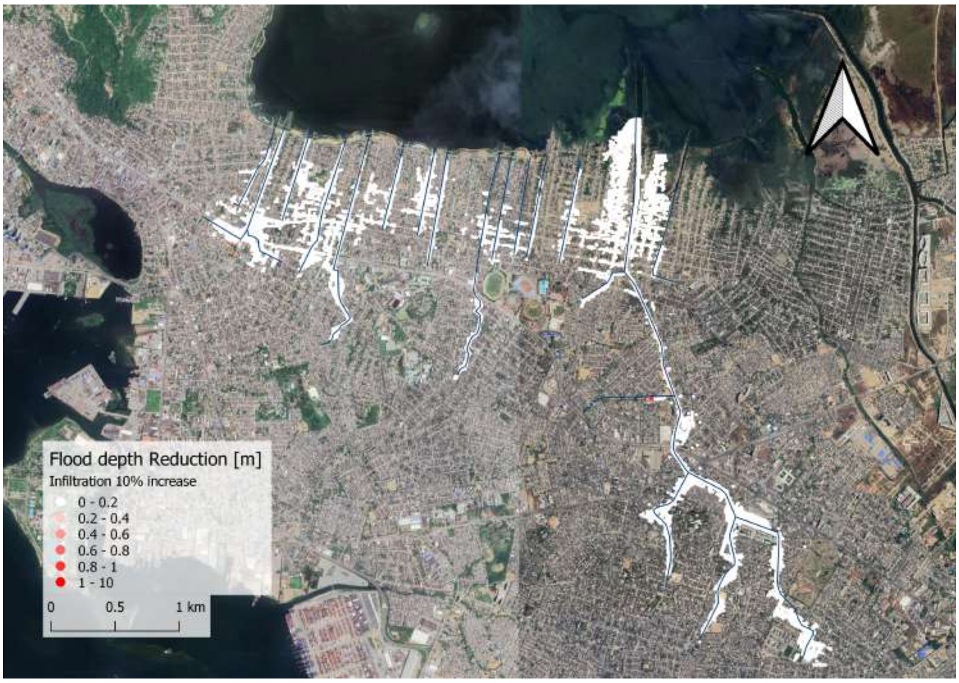

Figure E.14: The flood level reduction after the increase of 10 % of infiltration.

E.2.2. 20 percent infiltration increase

With the help of different kinds of infiltration measures the infiltration is simulated to increase with a total of 20%. This resulted in the following flood map (Figure E.15) that was which had been laid over the baseline scenario (red). The flooded area shows a relative decrease of 18.36 %.

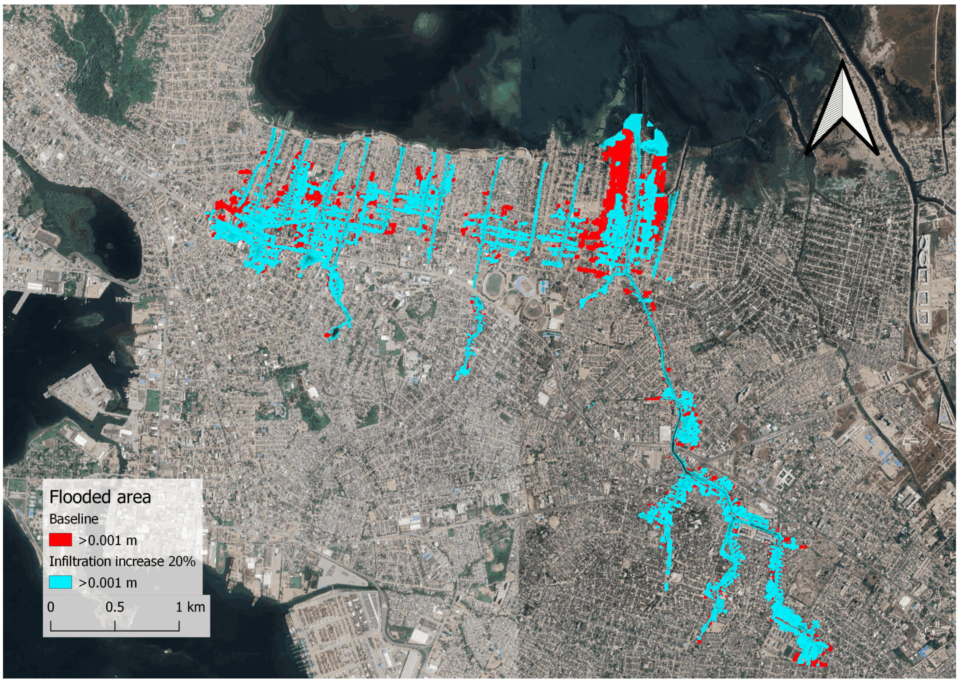

Figure E.15: The reduction in flooded area after the increase of 20 % of infiltration.

The flood level reduction is shown in Figure E.16. Most of the significant reduction is seen inside of the channels. The average flood level reduction is 2.91 cm. This is a reduction of 9.70 %.

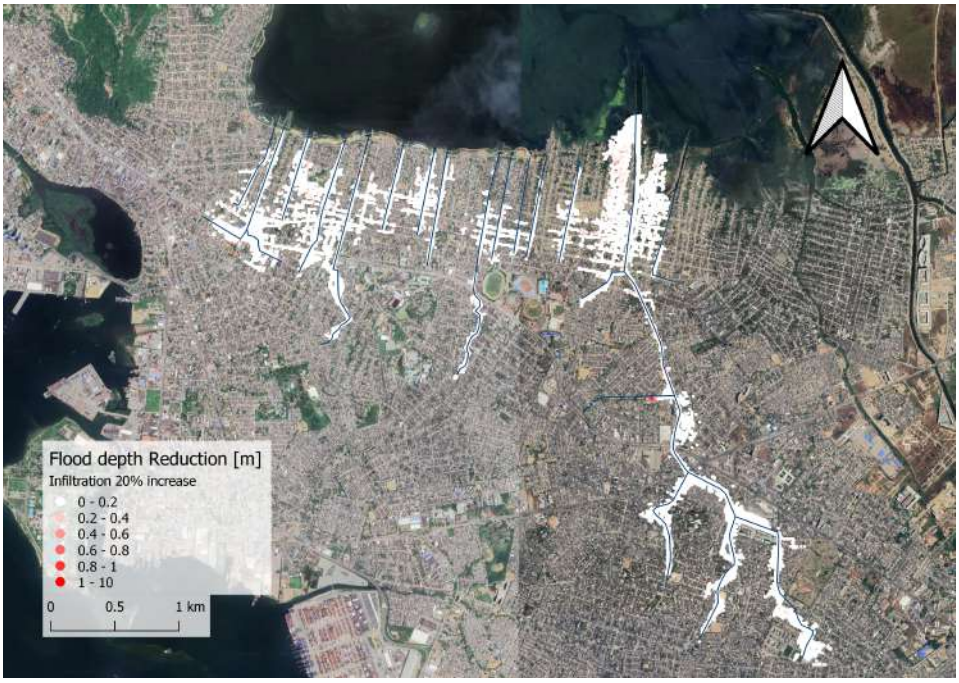

Figure E.16: The flood level reduction after the increase of 20 % of infiltration.

E.2.3. 30 percent infiltration increase

With the help of different kinds of infiltration measures the infiltration is simulated to increase with a total of 30%. This resulted in the following flood map (Figure E.17) that was which had been laid over the baseline scenario (red). The flooded area shows a relative decrease of 27.05 %.

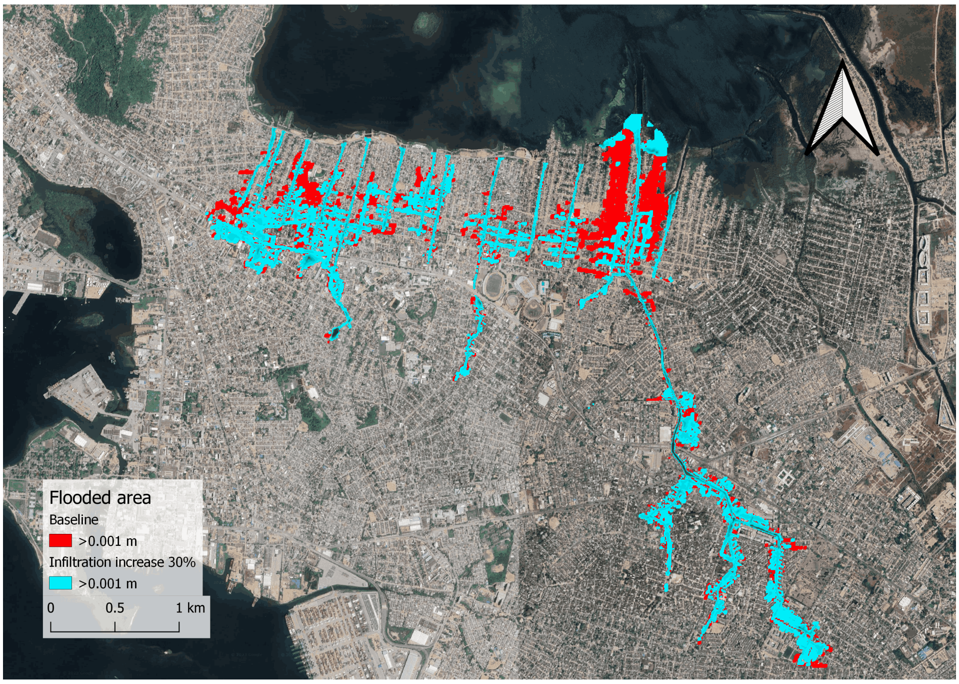

Figure E.17: The reduction in flooded area after the increase of 30 % of infiltration.

The flood level reduction is shown in Figure E.18. Most of the significant reduction is seen inside of the channels. The average flood level reduction is 4.31 cm. This is a reduction of 14.37 %.

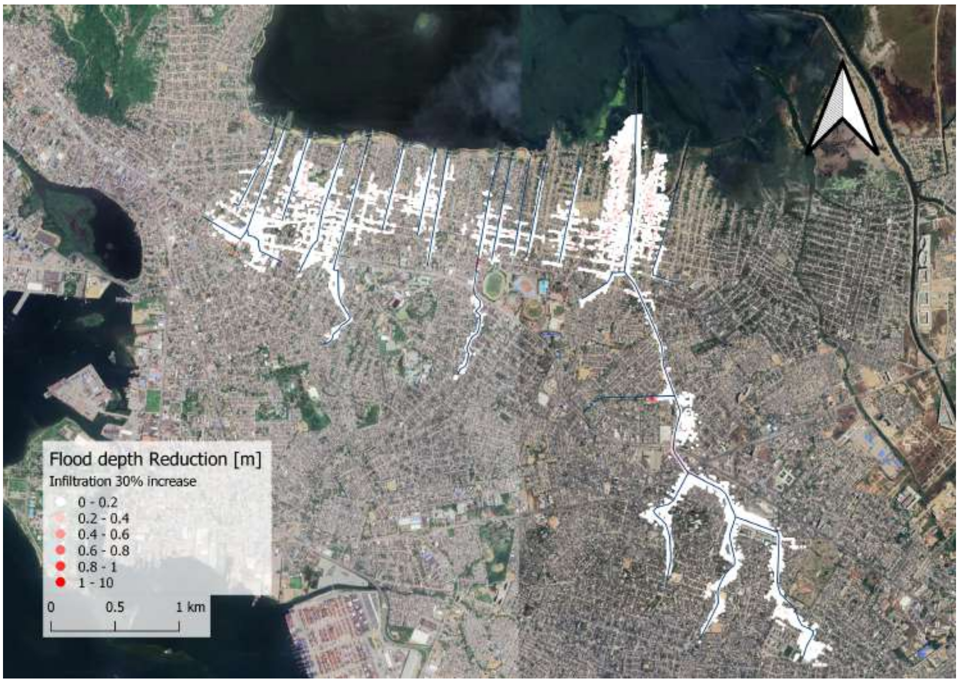

Figure E.18: The flood level reduction after the increase of 30 % of infiltration.

E.2.4. 40 percent infiltration increase

With the help of different kinds of infiltration measures the infiltration is simulated to increase with a total of 40%. This resulted in the following flood map (Figure E.19) that was which had been laid over the baseline scenario (red). The flooded area shows a relative decrease of 34.10 %.

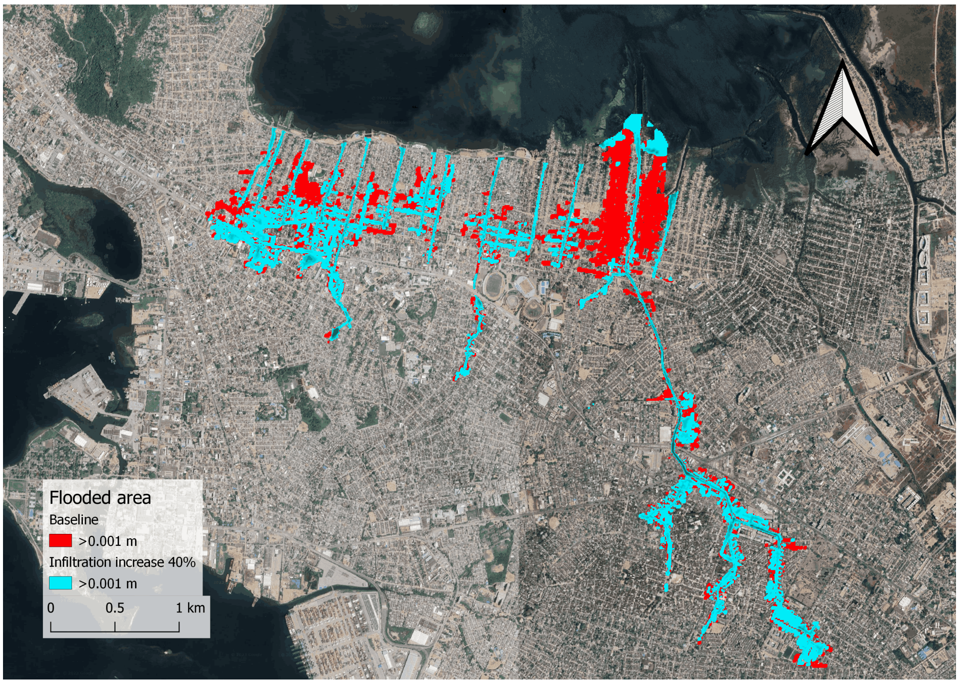

Figure E.19: The reduction in flooded area after the increase of 40 % of infiltration.

The flood level reduction is shown in Figure E.20. Most of the significant reduction is seen inside of the channels. The average flood level reduction is 5.66 cm. This is a reduction of 18.87 %.

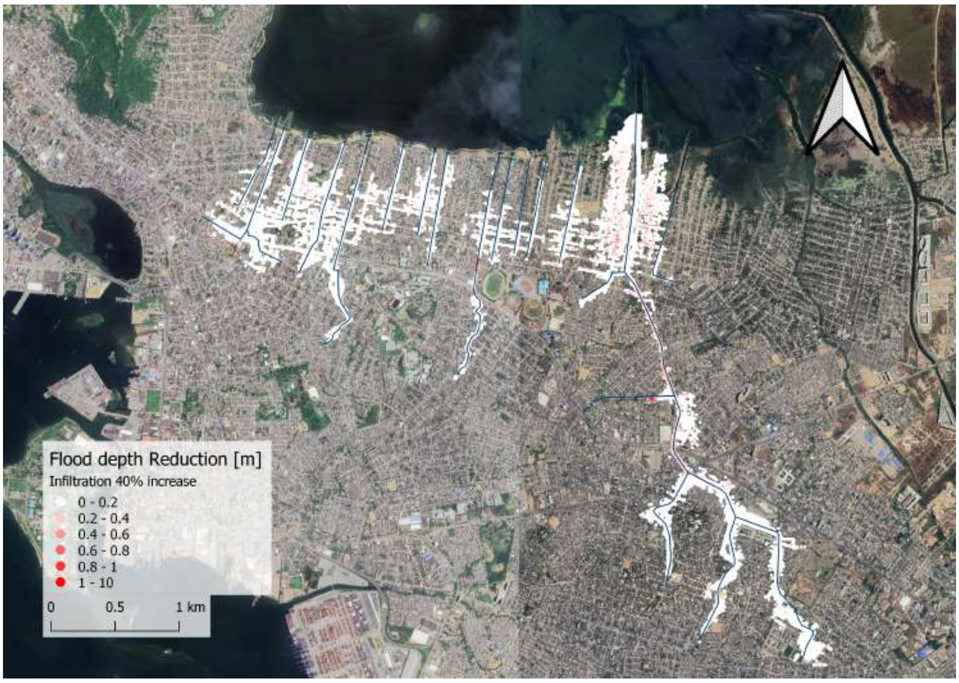

Figure E.20: The flood level reduction after the increase of 40 % of infiltration.

E.2.5. 50 percent infiltration increase

With the help of different kinds of infiltration measures the infiltration is simulated to increase with a total of 50%. This resulted in the following flood map (Figure E.21) that was which had been laid over the baseline scenario (red). The flooded area shows a relative decrease of 39.04 %.

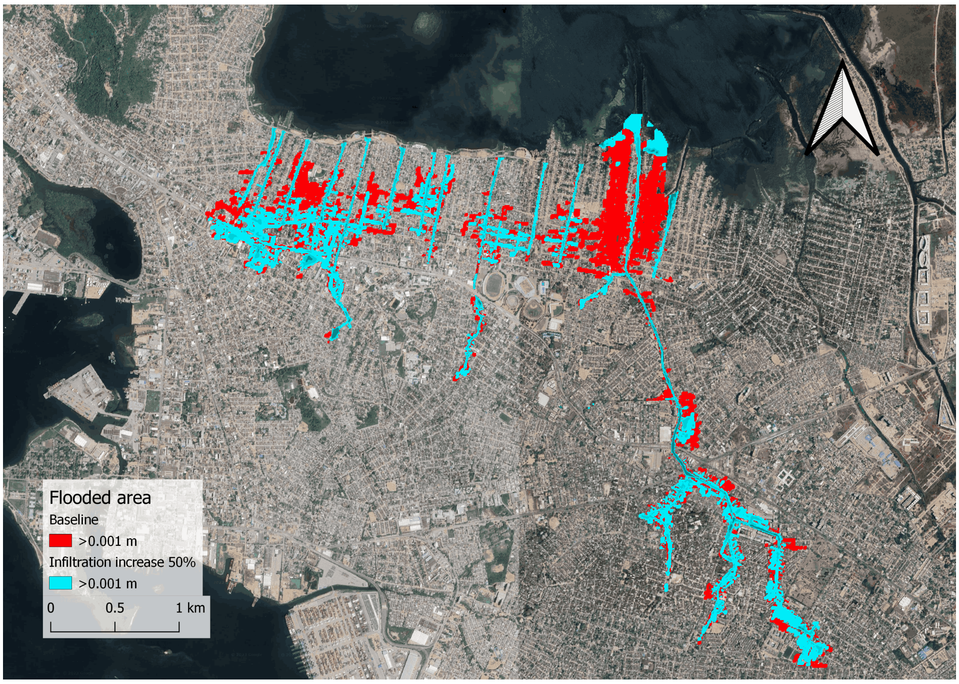

Figure E.21: The reduction in flooded area after the increase of 50 % of infiltration.

The flood level reduction is shown in Figure E.22. Most of the significant reduction is seen inside of the channels. The average flood level reduction is 6.87 cm. This is a reduction of 22.90 %.

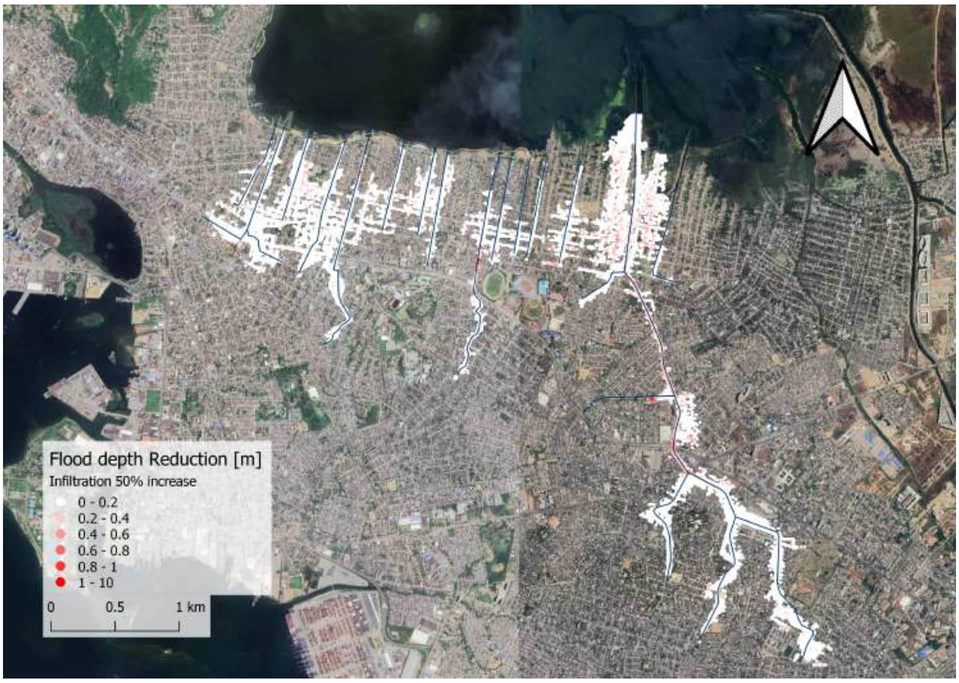

Figure E.22: The flood level reduction after the increase of 50 % of infiltration.

E.3. Establishing retention areas

E.3.1. Retention areas 2-meter depth

In two parts of the focus area, two retention areas are established. The depth of these retention areas is 2 meters. This resulted in the following flood map (Figure E.23) that was which had been laid over the baseline scenario (red). The flooded area shows a relative decrease of 9.45%.

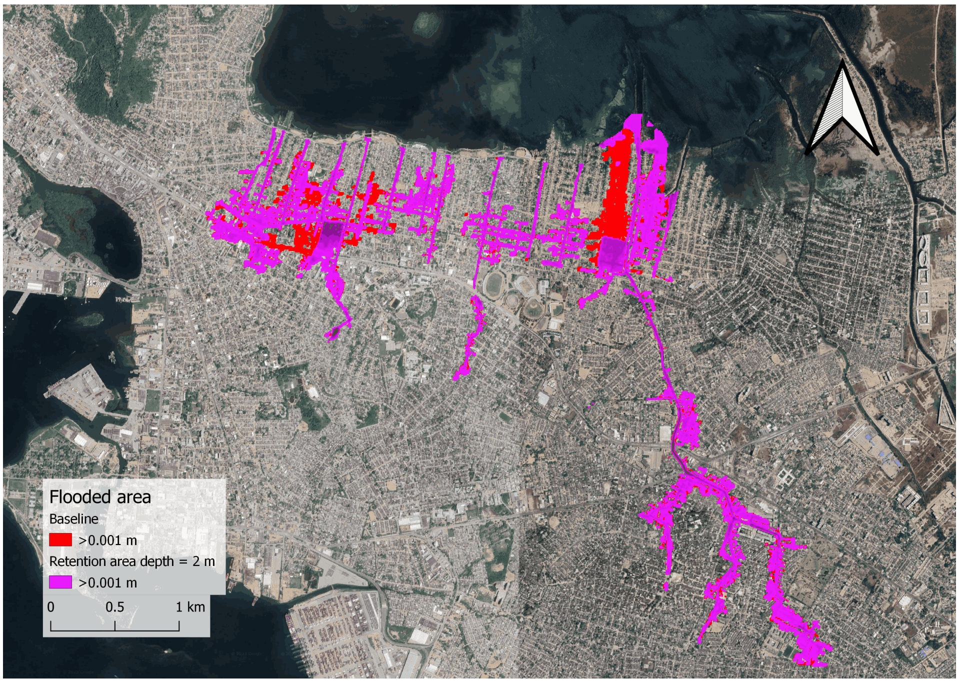

Figure E.23: The reduction in flooded area after the retention areas with a 2-meter depth

The flood level reduction is shown in Figure E.24. Most of the significant reduction is seen around the retention areas. The average flood level reduction is 6.37 cm. This is a reduction of 21.22 %.

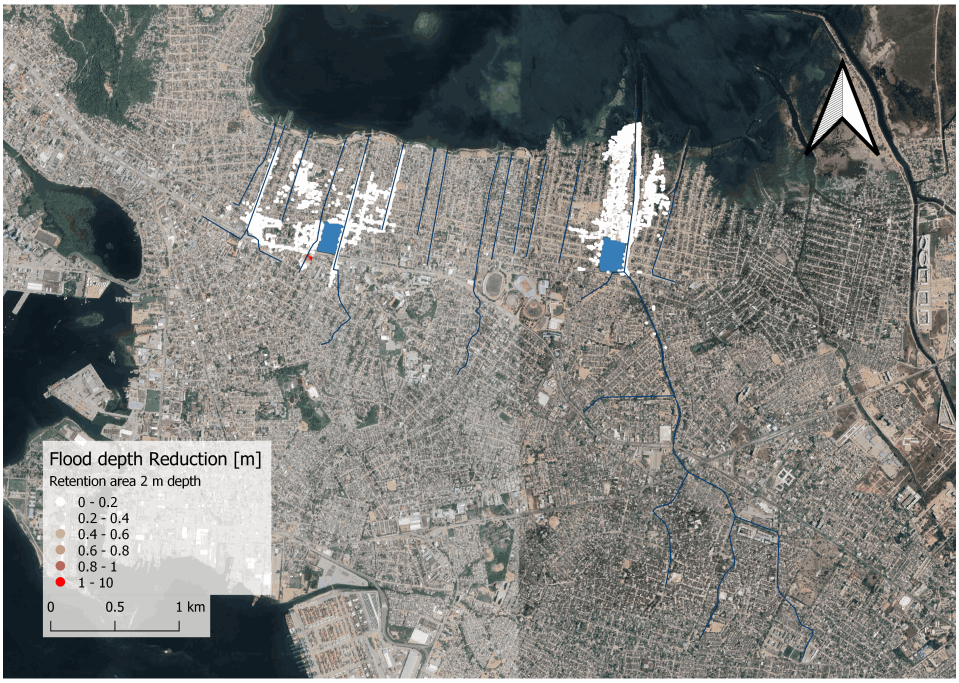

Figure E.24: The flood level reduction after the establishment of two retention areas with a 2-meter depth.

E.3.2. Retention areas 4-meter depth

In two parts of the focus area, two retention areas are established. The depth of these retention areas is 4 meters. This resulted in the following flood map (Figure E.25) that was which had been laid over the baseline scenario (red). The flooded area shows a relative decrease of 12.76 %.

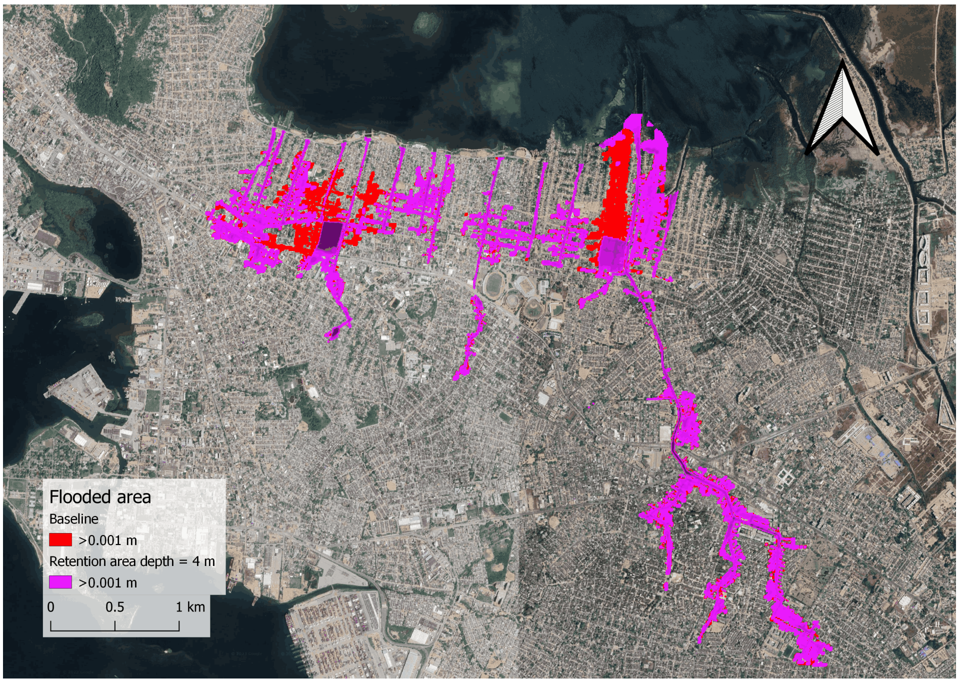

Figure E.25: The reduction in flooded area after the retention areas with a 4-meter depth

The flood level reduction is shown in Figure E.24. Most of the significant reduction is seen around the retention areas. The average flood level reduction is 8.72 cm. This is a reduction of 29.06 %.

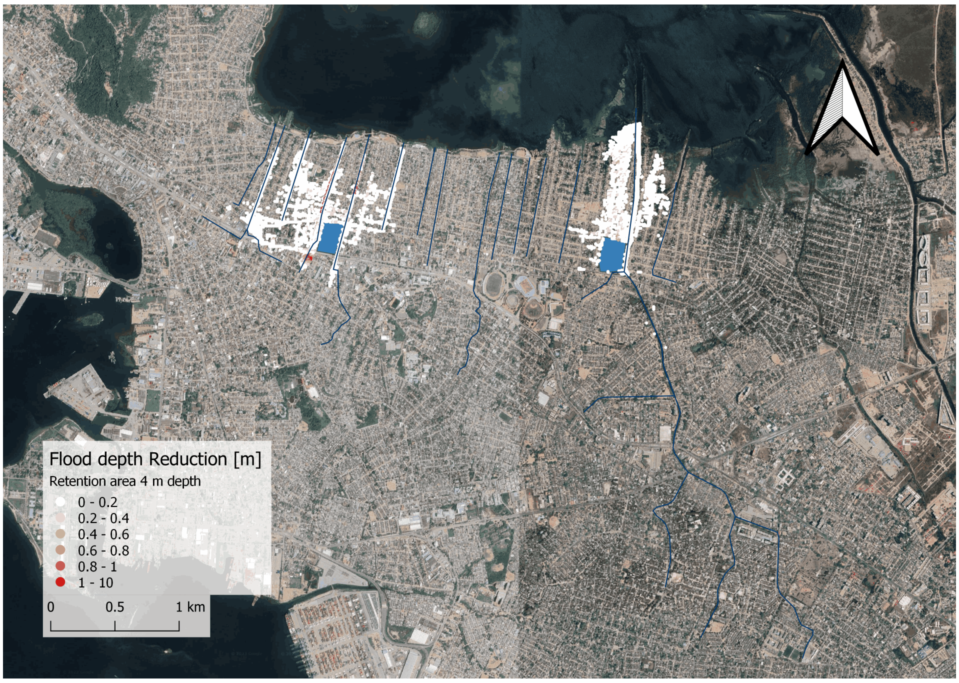

Figure E.26: The flood level reduction after the establishment of two retention areas with a 4-meter depth.

E.3.3. Retention areas 6-meter depth

In two parts of the focus area, two retention areas are established. The depth of these retention areas is 6 meters. This resulted in the following flood map (Figure E.27) that was which had been laid over the baseline scenario (red). The flooded area shows a relative decrease of 12.99 %.

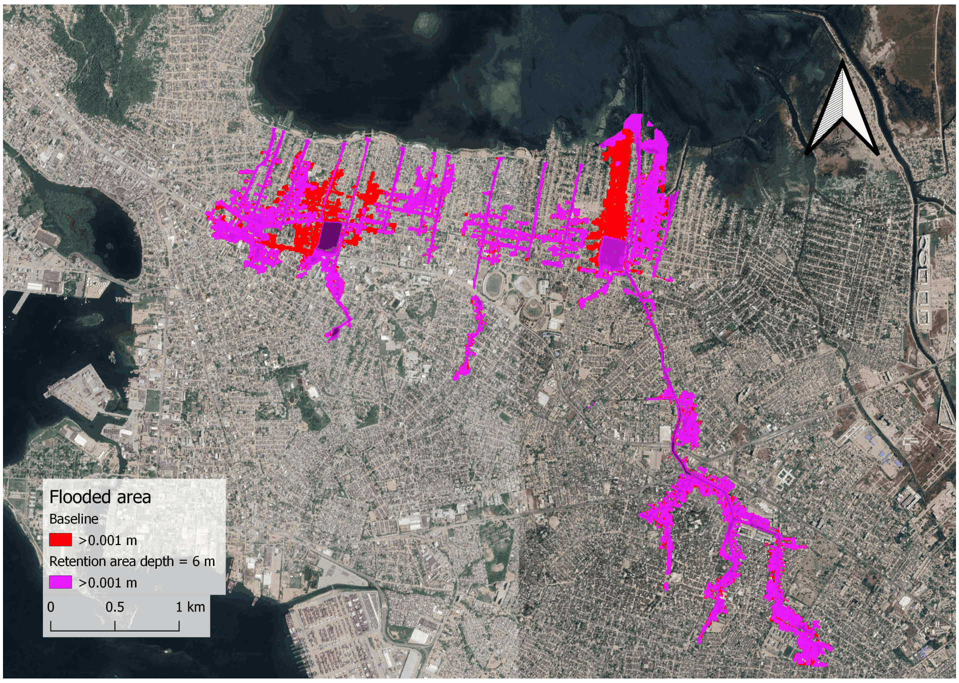

Figure E.27: The reduction in flooded area after the retention areas with a 6-meter depth

The flood level reduction is shown in Figure E.24. Most of the significant reduction is seen around the retention areas. The average flood level reduction is 8.74 cm. This is a reduction of 29.12 %.

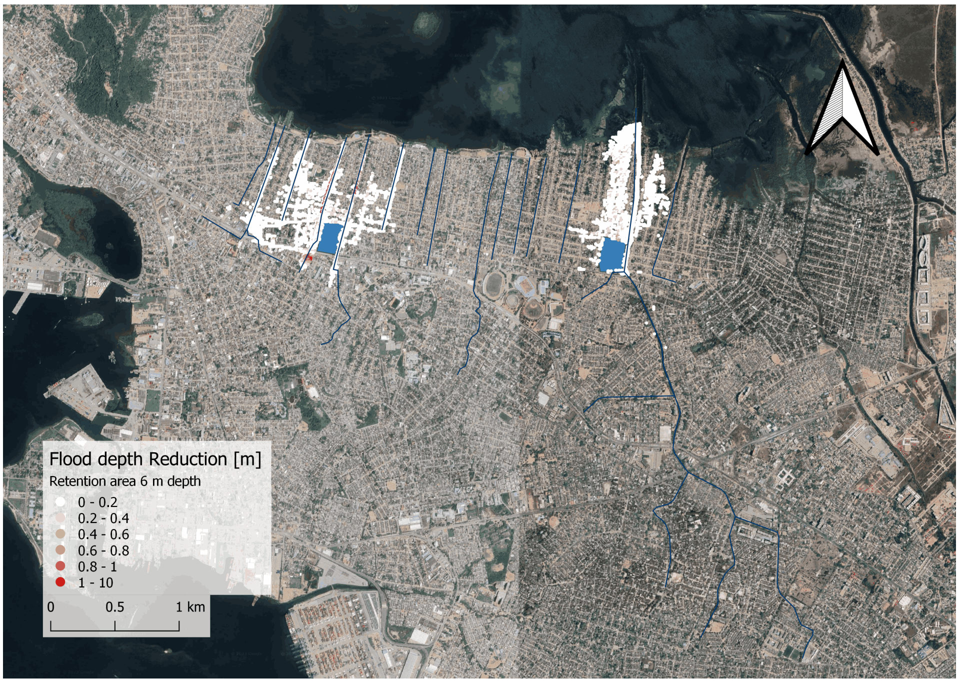

Figure E.28: The flood level reduction after the establishment of two retention areas with a 6-meter depth.

E.3.4. Retention areas 8-meter depth

In two parts of the focus area, two retention areas are established. The depth of these retention areas is 8 meters. This resulted in the following flood map (Figure E.29) that was which had been laid over the baseline scenario (red). The flooded area shows a relative decrease of 13.15 %.

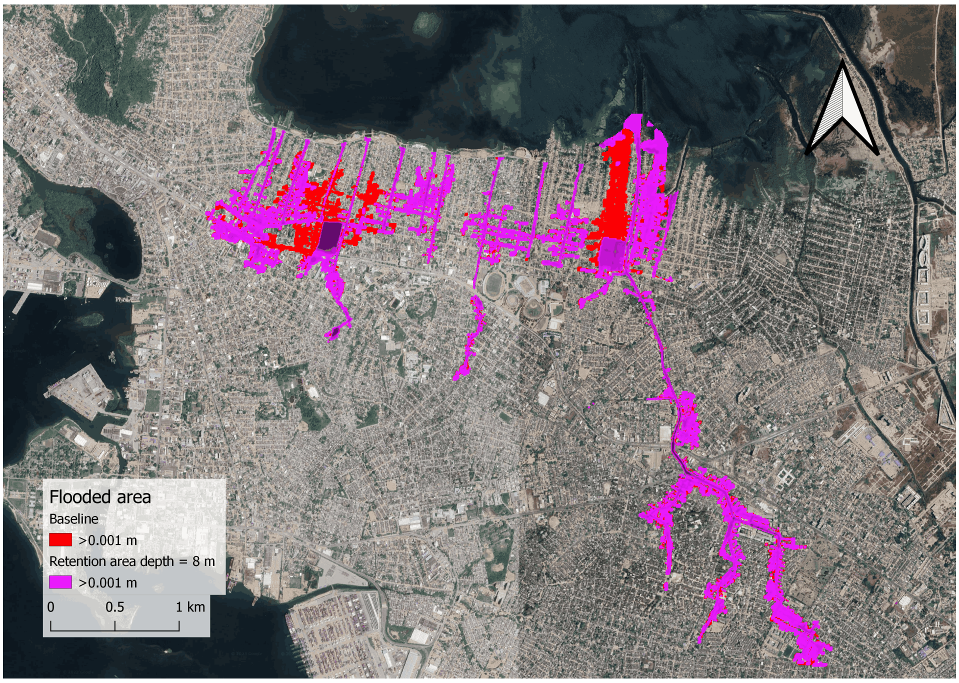

Figure E.29: The reduction in flooded area after the retention areas with an 8-meter depth

The flood level reduction is shown in Figure E.24. Most of the significant reduction is seen around the retention areas. The average flood level reduction is 8.75 cm. This is a reduction of 29.17 %.

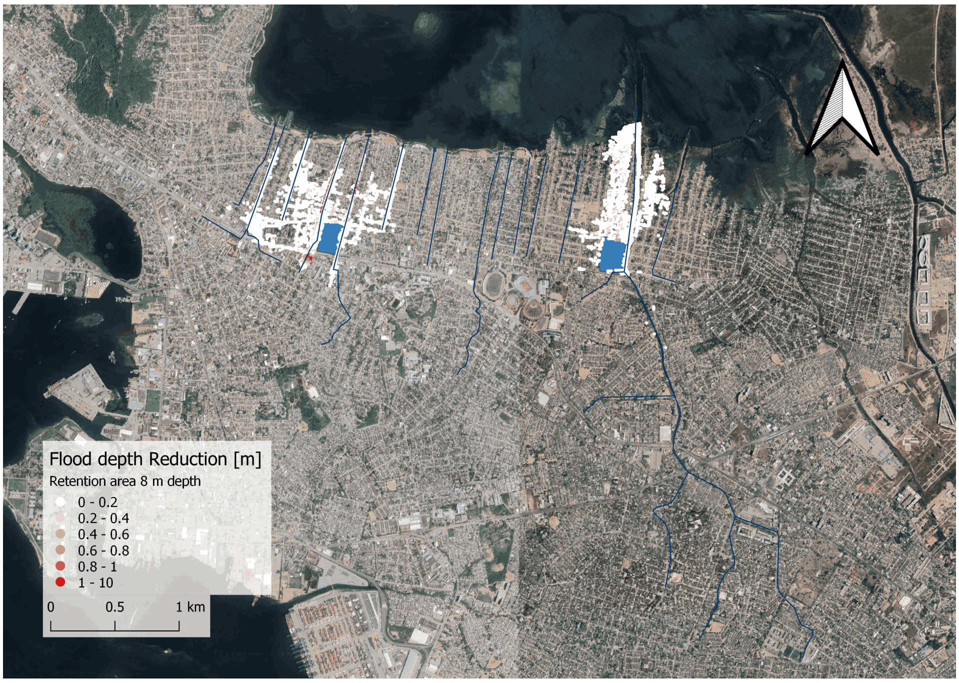

Figure E.30: The flood level reduction after the establishment of two retention areas with a 8-meter depth.

F

Future proof scenarios

In this Appendix, the computational results are given for the evaluation of future proofness of the Mitigating Options. The flood maps and the reduced flooded levels are shown for each of the options. The scenarios investigated were an extreme rainfall event with a return period of 100 years and a scenario with a projected relative sea level rise of 47 cm.

F.1. Extreme rainfall event R=100 years

In this segment, all the computational results regarding an extreme rainfall event with R=100 years (272 mm/day) are depicted.

F.1.1. Baseline R=100

The baseline flood map is shown in Figure F.1, the increase in flood levels is shown in Figure F.2 and the corresponding values are depicted in Table F.1. The flooded area increased with 5% and the average flood level decreased with 3 mm regarding the situation with a R=2y. The decrease in average flood level can be explained as more areas flooded but with the same severity in flooded level.

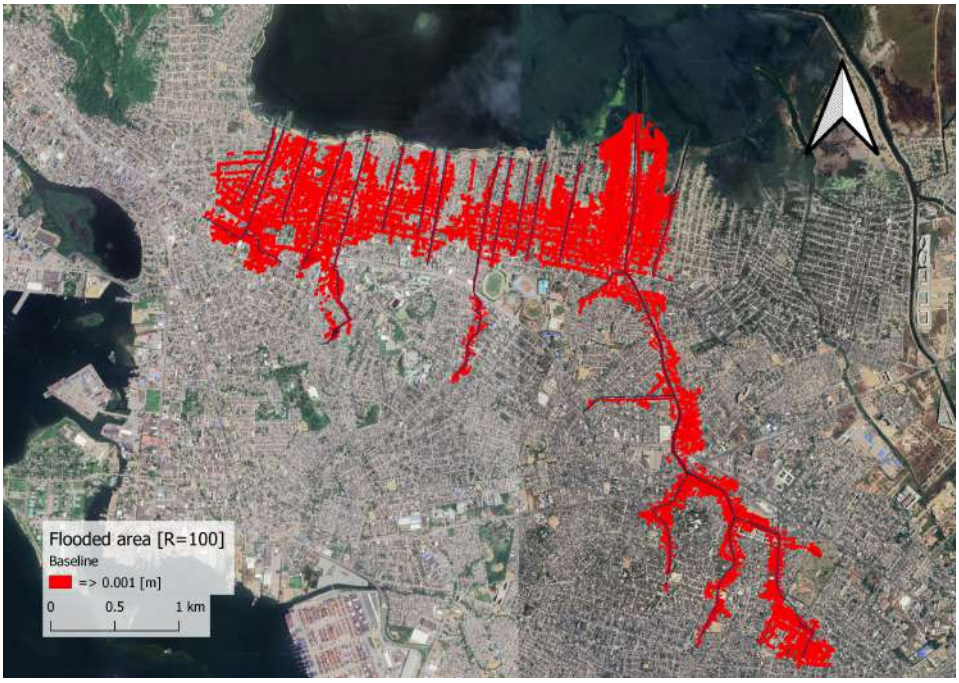

Figure F.1: The base flood map for an extreme rainfall R=100 years

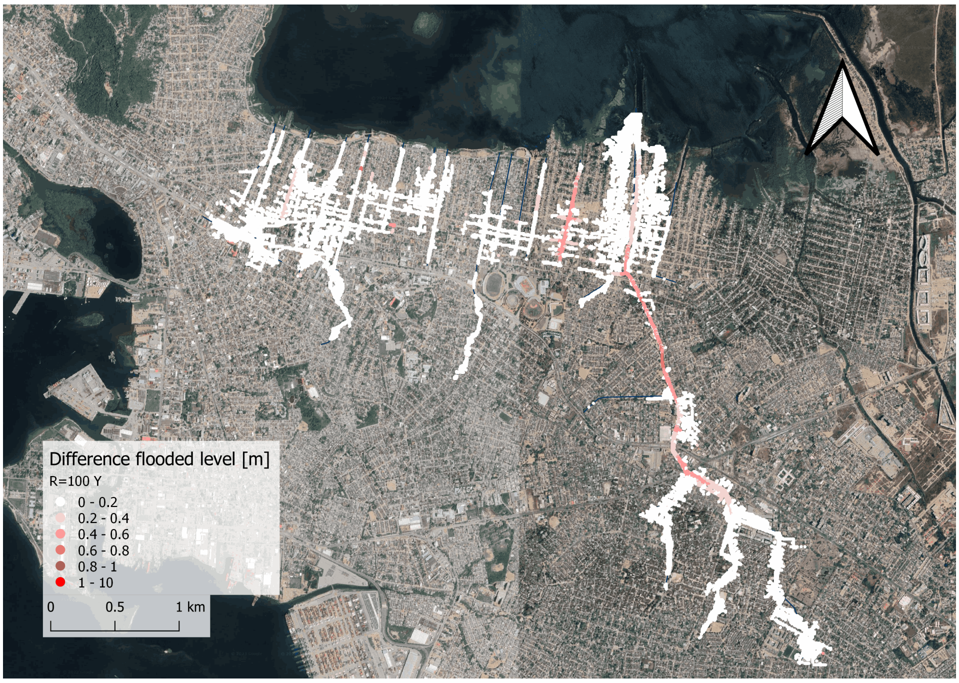

Figure F.2: The increase in flood levels (above 1 mm difference) due to the change of rainfall intensity from R=2 Y to R=100 Y.

Table F.1: The computational results for the baseline scenario for a R=100

R=100Y	Flooded Area [m^2]	%	% reduced	Average reduced FL[cm]
Baseline	1514181	15	0	29.7*

F.1.2. Mitigating Option 1 R=100

In Figure F.3 the reduction in flooded area is shown. Mainly the downstream eastern channels no longer show a reduction in flooded area compared to a scenario with a return period of 2 years. The western part still is showing a good reduction.

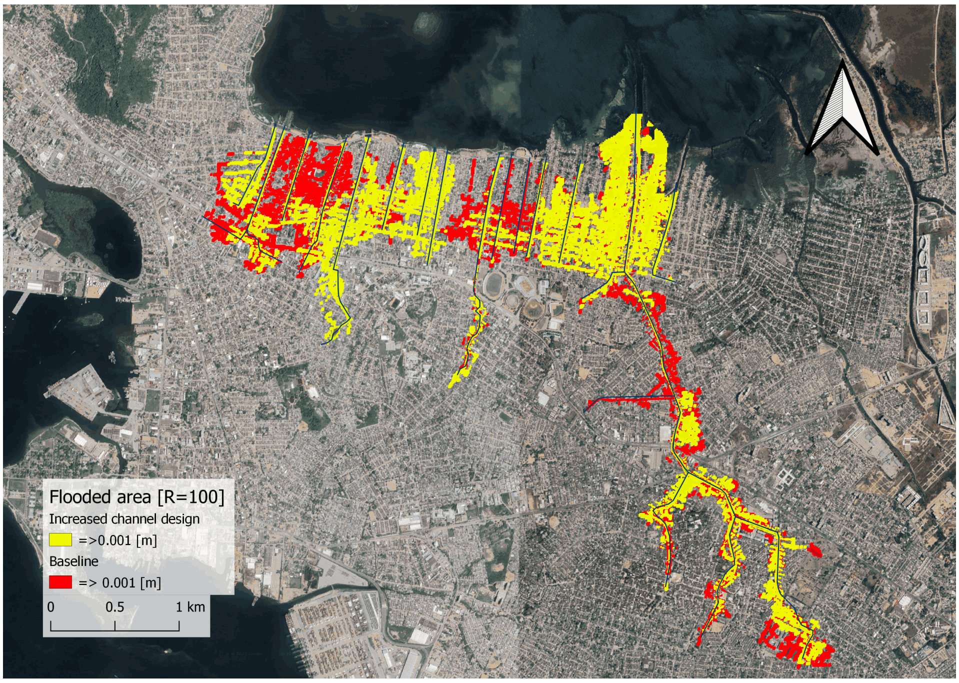

Figure F.3: The flood map for Mitigating Option 1 under an extreme rainfall (R=100 years)

RegardingFigure F.4, the reduced water level is depicted. The highest flood level reduction is in the western area where also the flooded area is largely reduced.

Figure F.4: The reduced flood levels due to Mitigating Option 1 for an extreme rainfall R=100 years

In Table F.2 the corresponding values regarding the results of Mitigating Option 1 are shown.

Table F.2: The computational result for Mitigating Option 1 for a scenario with a R=100.

R=100Y	Flooded Area [m^2]	%	% reduced	Average reduced FL[cm]	% reduced
Baseline	1514181	15	0	29.7*	0.00
Channels	897653	9	41	16.2	55

F.1.3. Mitigating Option 2 R=100

In Figure F.5 the reduction in flooded area is shown. Mainly the downstream channels no longer show a reduction in flooded area compared to a scenario with a return period of 2 years. The reduction is overall lower but not for a specific area.

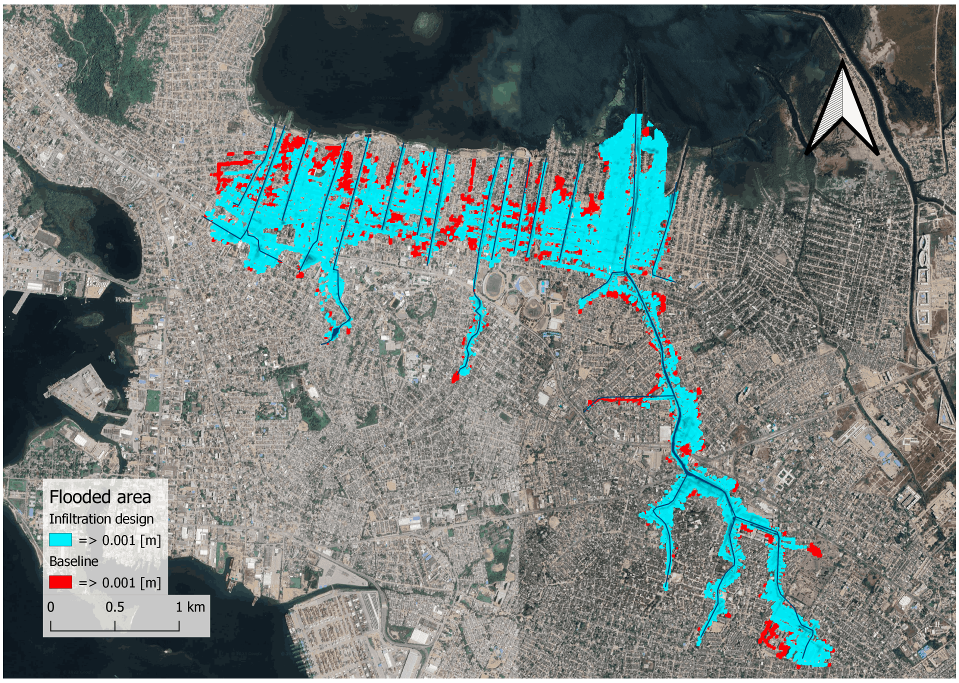

Figure F.5: The flood map for Mitigating Option 2 under an extreme rainfall (R=100 years)

Figure F.6 is showing the reduced water levels and it underlines the reduction seen in Figure F.6. The outer planes of the flooded area mainly got reduced. Again no water level reduction is seen within the channels, most likely because the leg time smears out the peak to a certain degree. So a longer time high water levels within the channel but less excess water leaving the channel.

Figure F.6: The reduced flood levels due to Mitigating Option 2 for an extreme rainfall R=100 years

In Table F.3 the corresponding values regarding the results of Mitigating Option 2 are shown.

Table F.3: The computational result for Mitigating Option 2 for a scenario with a R=100.

R=100Y	Flooded Area [m^2]	%	% reduced	Average reduced FL[cm]	% reduced
Baseline	1514181	15	0	29.7*	0.00
Infiltration	1407886	14	7	8.2	28

F.1.4. Mitigating Option 3 R=100

In Figure F.7 the reduction in flooded area is shown. Only the western side still shows a reduction in flooded area compared to a scenario with a return period of 2 years. The eastern retention area's capacity was too little to avoid flooded areas in the end.

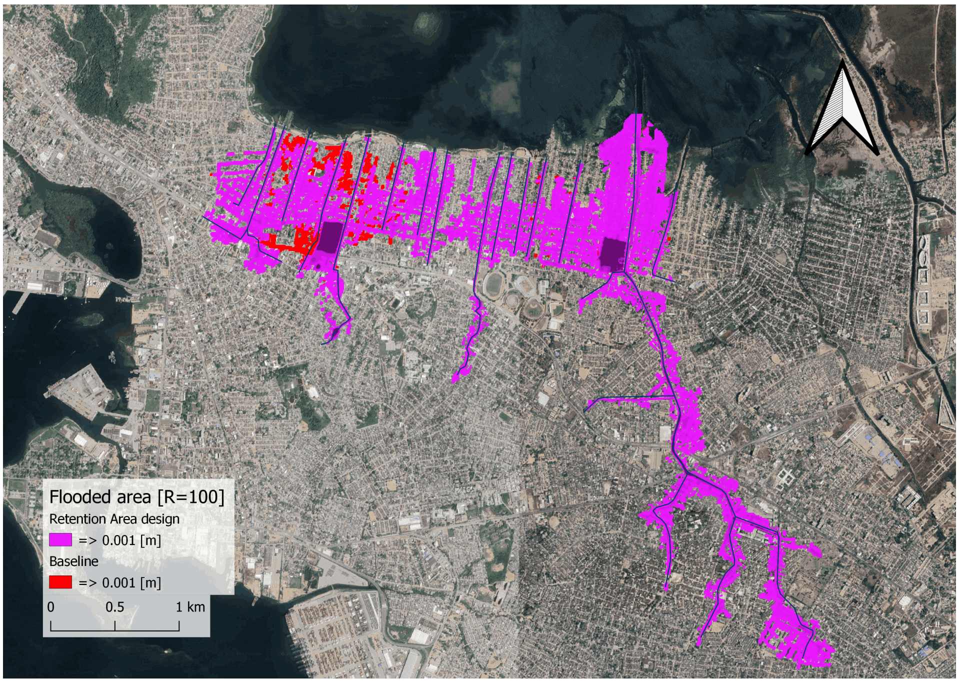

Figure F.7: The flood map for Mitigating Option 3 under an extreme rainfall (R=100 years)

The flooded levels are reduced around the retention areas as could be expected. Although the eastern retention area does not show any reduced flooded area in Figure F.7, Figure F.8 shows that there is flood level reduction around it.

Figure F.8: The reduced flood levels due to Mitigating Option 3 for an extreme rainfall R=100 years

In Table F.4 the corresponding values regarding the results of Mitigating Option 3 are shown.

Table F.4: The computational result for Mitigating Option 3 for a scenario with a R=100.

R=100Y	Flooded Area [m^2]	%	% reduced	Average reduced FL[cm]	% reduced
Baseline	1514181	15	0	29.7*	0.00
Retention	1487510	15	2	4.0	14

F.2. Relative sea level rise

In this segment, all the computational results regarding a 47 cm relative sea level rise are depicted.

F.2.1. Baseline Relative Sea Level Rise

In Figure F.9 the flood map and in Figure F.10 the increased flood levels of the baseline scenario are shown but with a projected relative sea level rise induced onto the southern border of the Ciénaga. The flood map shows a strong resemblance to the flood map of the investigated scenario without R=2. The difference is mainly seen at the end of the Rincaute channel, the most eastern channel, where small increases are shown for the flooded area. The values inTable F.5 made clear that the relative sea level rise increased 1% in flooded area but the average flood level increased significantly with 3 cm.

Figure F.9: The base flood map with an imposed relative sea level rise.

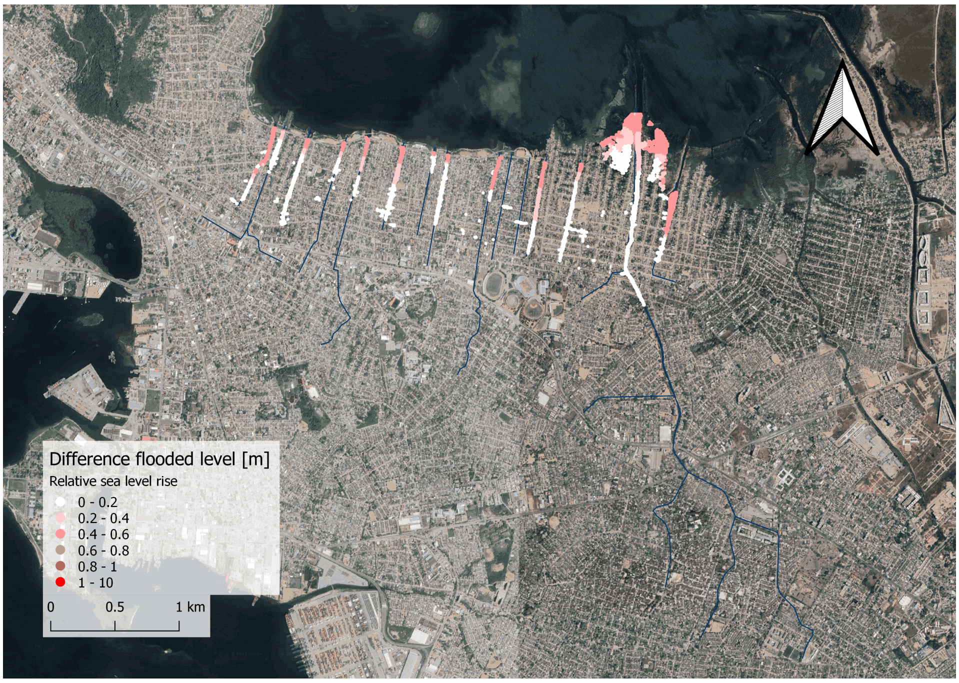

Figure F.10: The increase in flood levels (above 1 mm difference) due to the induced RSLR.

Table F.5: The computational results for the baseline with a relative sea level rise imposed.

RSLR	Flooded Area [m^2]	%	% reduced	Average reduced FL[cm]
Baseline	1051758	11	0.00	33.9

F.2.2. Mitigating Option 1 RSLR

In Figure F.12 the reduction in flooded area is shown. The downstream eastern side, as expected in the zones of influence, showed less reduction than before.

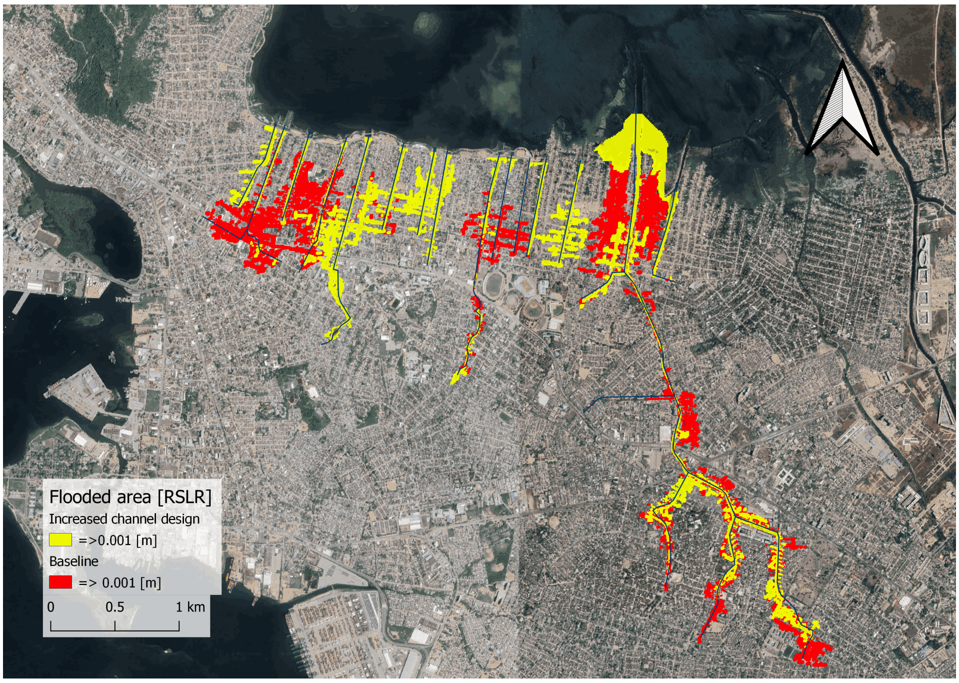

Figure F.11: The flood map for Mitigating Option 1 with a relative sea level rise imposed.

The significant difference compared to the situation without the RSLR is the reduction in the middle channels. No reduction in flood levels is seen in this area. Furthermore, not many differences are apparent.

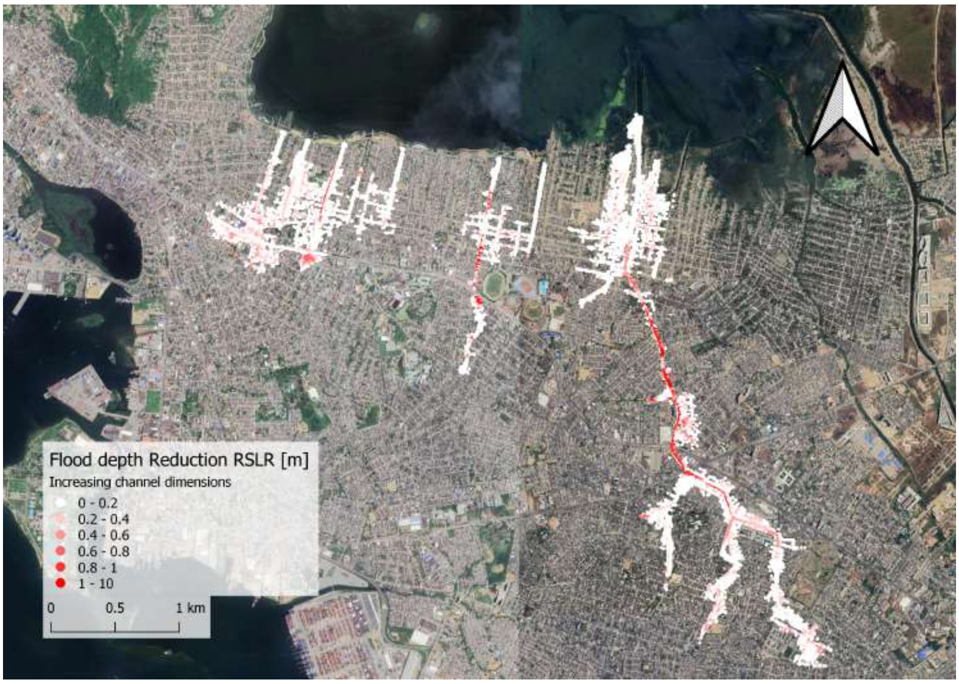

Figure F.12: The reduced flood levels due to Mitigating Option 1 with relative sea level rise imposed

InTable F.6, the corresponding values regarding the results of Mitigating Option 1 are shown.

Table F.6: The computational result for Mitigating Option 1 with a relative sea level rise imposed.

RSLR	Flooded Area [m^2]	%	% reduced	Average reduced FL[cm]	% reduced
Baseline	1051758	11	0.00	33.9	0.00
Channel	558811	6	47	16.2	48

F.2.3. Mitigating Option 2 RSLR

In Figure F.13 the reduction in flooded area is shown. The flooded area shifted further land-inwards on the eastern side of the focus area.

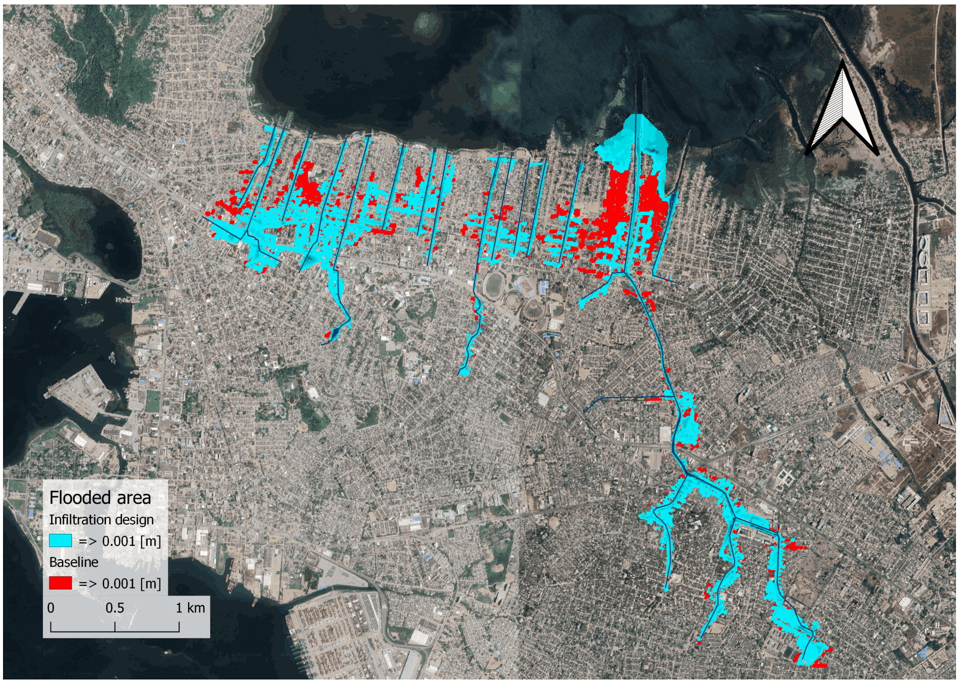

Figure F.13: The flood map for Mitigating Option 2 with a relative sea level rise imposed.

Overall, less reduction point can be seen at the downstream eastern side inFigure F.14 compared to the situation without RSLR. Otherwise, there is not much difference to be detected

Figure F.14: The reduced flood levels due to Mitigating Option 2 with relative sea level rise imposed.

InTable F.7, the corresponding values regarding the results of Mitigating Option 2 are shown.

Table F.7: The computational result for Mitigating Option 2 with a relative sea level rise imposed.

RSLR	Flooded Area [m^2]	%	% reduced	Average reduced FL[cm]	% reduced
Baseline	1051758	11	0.00	33.9	0.00
Infiltration	911104	9	13	8.4	25

F.2.4. Mitigating Option 3 RSLR

In Figure F.15 the reduction in flooded area is shown. The flooded area shifted further land-inwards on the eastern side of the focus area.

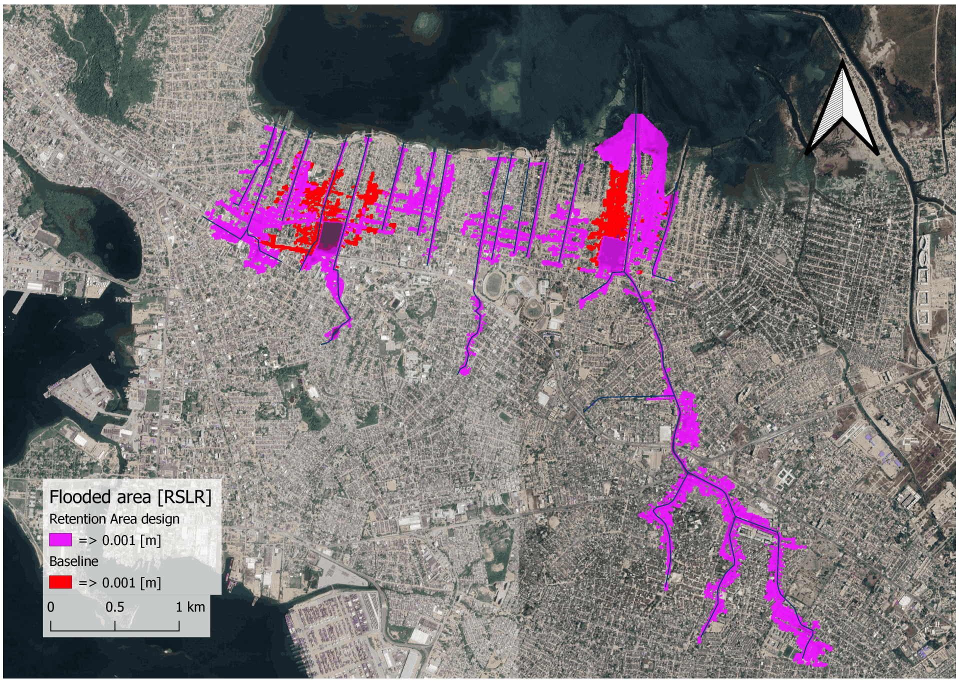

Figure F.15: The flood map for Mitigating Option 3 with a relative sea level rise imposed.

Very little difference can be seen compared with the reduced flood levels without RSLR.

Figure F.16: The reduced flood levels due to Mitigating Option 3 with relative sea level rise imposed.

InTable F.8, the corresponding values regarding the results of Mitigating Option 3 are shown.

Table F.8: The computational result for Mitigating Option 3 with a relative sea level rise imposed.

RSLR	Flooded Area [m^2]	%	% reduced	Average reduced FL[cm]	% reduced
Baseline	1051758	11	0.00	33.9	0.00
Retention	959710	10	9	8.4	25

G

Cost estimation

In this Appendix, the overview of the estimation of the cost per Mitigating Option is explained. The remark has to be made that these construction costs are very rough estimations as no site-specific costs could be found.

G.1. Mitigating Option 1: Extension of the channels

The costs regarding Mitigating Option 1 were determined with the help of the dimensions in Appendix A. This determined the average width (5.6 meters) and average depth (1.0 meters) of the channels. With the help of the cost estimation of Environment Agency (2015), the excavation costs were determined for all the channels. Since the average extension is around 100%, the ratio of 250 £/m is used. This amounts to an excavation of 5 meters wide and 1.5 meters in depth. The channels are assumed to become reinforced with a stone rip rap which amounts for 26 £/m. Together with all the installation costs (assumed medium costs for removal of existing material, riverbed restoration and re-profiling) will become around 3 million £. The exchange rate from £ to $ is assumed to be 1.25. In total Mitigating Option 1 will cost approximately 10.5 million $. The maintenance of the channel is disregarded since for all the options the channels are used and therefore will have on average the same maintenance costs. The calculation is shown in Figure G.1.

Variant 1

Average width		5	
average height		1	m
excavation costs		250	£/m
Average increase		100	%
Total length channels		21.582	km
Total excavated volume		107910	m^3
Costs excavation	£	5,395,500.00	£
stone reinforcement costs		26	£/m
Installation costs medium		115000	£/km
Total installation costs	£	3,043,062.00	
Exchange rate £ to $		1.25	
Mainanance costs		Do have all projects	
Totale kosten	**$**	**10,548,202.50**	

Figure G.1: The calculation of the construction costs for Mitigating Option 1.

G.2. Mitigating Option 2: Increasing infiltration

The area that has to be paved with concrete permeable pavement would be around 10% of the total area. This would mean that around 1 km^2 should be constructed. Taking into consideration an average price of 86 $/$m^2$ would result in construction costs of 86 million dollars (TRUEGRID, n.d.). Additionally, green roofs are also a very expensive measure. The price would be around a range of 150 and 500 $/$m^2$ (Omoregie, n.d.). Achieving a focus area with 30% of green roofs would then result in an additional price of at least 480 million dollars. This would result in Mitigating Option 2 having a price of over 550 million $. The calculation is shown in Figure G.2.

Variant 2

Total Area		10011200	m^2
Percentage Permeable pavement		10	%
Percentage green roofs		30	%
Permeable pavement area		1001120	m^2
Green roofs area		3003360.001	m^2
Ratio Costs permeable pavement		8	$/ft^2
Ratio Costs permeable pavement		86.11128333	$/m^2
Ratio Costs green roof		15	$/ft^2
Ratio Costs green roof		161.4586563	$/m^2
Cost permeable pavement	$	86,207,727.99	$
Cost Green roofs	$	484,918,469.96	$
Totale kosten	**$**	**571,126,197.95**	

Figure G.2: The calculation of the costs for Mitigating Option 2

G.3. Mitigating Option 3: Retention areas

The excavation costs are estimated at approx. 25 $/$m^3$ (Northen Arizona University, n.d.). The two areas combined would require an excavation volume of almost 250,000 m^3. This results in an estimation of construction costs of almost 6.5 million $. Excessive maintenance is required to prevent public health problems (Poleto & Tassi, 2012). The yearly maintenance is estimated at around 21.000 dollars. Resulting in a total cost of 6.5 million $. This would make it a relatively cheaper mitigating option compared to the other two options. The calculation is shown in Figure G.3.

Retention Basin and Drywell Construction Cost Estimate:

Excavation Volume	**54153**	**cubic feet**
Excavation Cost	$0.75	per cubic foot
	$40,614.75	
Grass-lined basin	43,096	square feet
Grass + Installation Cost	$1.50	per square foot
	$64,644.00	
Total Retention Basin Construction Cost		*$105,258.75*
# of Drywells	16	drywells
Cost per concrete drywell + Installation	$4,951.00	per drywell
Total Drywell Construction Cost		*$79,216*
Total Retention Basin and Drywell Construction Cost		***$184,475.00***

Retention Basin Annual Maintenance Cost Estimate:

Basin Grass Area	**0.989**	**acres**
Intensive Annual Maintenance	$1,000.00	per acre
Annual Maintenance Cost	***$989.00***	

Figure G.4: The costs recorded from a calculation of Northen Arizona University ()

Variant 3

Retetion depth left		4	m
Retetion area left		37016	m^2
Volume left		148064	m^3
Retetion depth right		2	m
Retetion area right		47313	m^2
Volume right		94626	m^3
Ratio excavation		0.75	$/ft^3
Ratio excavation metric		26.48600004	$/m^3
Total volume		242690	m^3
costs excavation		6427887.35	$
maintainance	$	1,000.00	$/acre
total acres		20.83806636	
yearly maintainance costs	$	20,838.07	/year
Totale kosten	**$**	**6,448,725.42**	

Figure G.3: The calculation of the costs for the retention area design

The costs are based on the values used in Figure G.4 of Northen Arizona University ().